

50L-625
SAN-1605-7(Vol.1)

SOLAR CENTRAL RECEIVER PROTOTYPE HELIOSTAT CDRL ITEM B.d

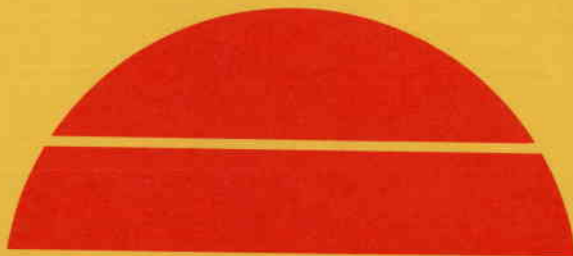
Final Technical Report, Volume 1

By
C. R. Easton

August 1978

Work Performed Under Contract No. EG-77-C-03-1605

McDonnell Douglas Astronautics Company
Huntington Beach, California



U.S. Department of Energy



Solar Energy

Cat No: 22.5105
VOL I

9

NOTICE

This report was prepared as an account of work sponsored by the United States Government. Neither the United States nor the United States Department of Energy, nor any of their employees, nor any of their contractors, subcontractors, or their employees, makes any warranty, express or implied, or assumes any legal liability or responsibility for the accuracy, completeness or usefulness of any information, apparatus, product or process disclosed, or represents that its use would not infringe privately owned rights.

This report has been reproduced directly from the best available copy.

Available from the National Technical Information Service, U. S. Department of Commerce, Springfield, Virginia 22161.

**Price: Paper Copy \$12.00
Microfiche \$3.00**

**SOLAR CENTRAL RECEIVER
PROTOTYPE HELIOSTAT CDRL ITEM B.d**

**Final Technical Report
Volume I**

AUGUST 1978

MDC G 7399

PREPARED BY:



**C. R. EASTON
PROJECT MANAGER
SOLAR CENTRAL RECEIVER
PROTOTYPE HELIOSTAT**

APPROVED BY:



**R. W. HALLET
PROGRAM MANAGER
SOLAR CENTRAL RECEIVER**

MCDONNELL DOUGLAS ASTRONAUTICS COMPANY-HUNTINGTON BEACH

5301 Bolsa Avenue, Huntington Beach, CA 92647

PREFACE

This report was prepared under DOE contract EG-77-C-03-1605. It presents the results of a 9-month study to define a low-cost approach to the production, installation, and operation of heliostats. The guidance and support of the program manager, R. W. Hughey, and the technical assistance of C. J. Pignolet and C. L. Marvis of the Sandia Laboratories were of immeasurable benefit in the conduct of this study and we wish to acknowledge their contributions.

CONTENTS

VOLUME I

| | Page |
|--|------|
| SECTION 1 INTRODUCTION AND SUMMARY | 1-1 |
| 1.1 Project Approach | 1-7 |
| 1.2 Collector Subsystem Description Summary | 1-7 |
| SECTION 2 COLLECTOR PRELIMINARY DESIGN | 2-1 |
| 2.1 Design Trade Studies | 2-1 |
| 2.2 Bench Model and Component Test Results | 2-20 |
| 2.3 Preliminary Design Description | 2-23 |
| 2.4 Design Change Summary | 2-76 |
| SECTION 3 MANUFACTURING, PROCESS CONCEPTUAL DESIGN | 3-1 |
| 3.1 Initial Baseline Manufacturing Process | 3-1 |
| 3.2 Manufacturing Trade Studies | 3-3 |
| 3.3 Manufacturing Plans | 3-23 |
| 3.4 Production Plant Concept | 3-52 |
| 3.5 Transportation Concept | 3-59 |
| 3.6 Production Concepts for 250,000 and 1,000,000 Heliostats Per Year | 3-66 |
| SECTION 4 INSTALLATION AND CHECKOUT CONCEPTUAL DESIGN | 4-1 |
| 4.1 Initial Baseline Process | 4-1 |
| 4.2 Installation and Checkout Trade Study Results | 4-2 |
| 4.3 Installation Concept Description | 4-5 |
| 4.4 Alignment and Checkout Concept Description | 4-13 |
| 4.5 Installation and Checkout Resource Utilization | 4-17 |
| 4.6 Installation and Checkout Summary | 4-22 |

| | Page |
|---|---------|
| SECTION 5 OPERATIONS AND MAINTENANCE CONCEPTUAL DESIGN | 5-1 |
| 5.1 Initial Baseline Process | 5-1 |
| 5.2 Operations and Maintenance Trade Study Results | 5-1 |
| 5.3 Operations and Maintenance Analyses | 5-10 |
| 5.4 Operations and Maintenance Change Summary | 5-20 |
| 5.5 References for Section 5 | 5-23 |
| SECTION 6 SPECIFICATION VERIFICATION AND OPTIMIZATION | 6-1 |
| 6.1 Optimization of Requirements | 6-1 |
| 6.2 System Performance | 6-14 |
| 6.3 Specification Verification Summary | 6-18 |
| APPENDIX A HELIOSTAT BASELINE DESIGN DESCRIPTION | A-1 |
| APPENDIX B PERFORMANCE AND DESIGN REQUIREMENTS SUMMARY | B-1 |
| APPENDIX C HELIOSTAT SIZING ANALYSES: FOCUSED VERSUS UNFOCUSED | C-1 |
| APPENDIX D SUMMARY OF SUPPORTING LABORATORY AND MANUFACTURING PROCESS TESTS | D-1 |
| APPENDIX E A LINEAR-ELASTIC METHOD TO CALCULATE THE THERMAL STRESSES AND DEFLECTIONS OF A THIN GLASS PLATE STIFFENED BY STEEL STRINGERS | E-1 |
| APPENDIX F EXAMPLE OF COMPUTERIZED OPTIMUM REPAIR LEVEL ANALYSIS | F-1 |
| APPENDIX G LOGISTIC SUPPORT ANALYSIS WORK SHEETS | G-1 |

Section 1

INTRODUCTION AND SUMMARY

In keeping with the nation's goal of achieving commercially viable solar electric power generation, the McDonnell Douglas Astronautics Company (MDAC) has conducted a study* for the U.S. Department of Energy (DOE) under the direction of the Sandia Laboratories, Livermore, California, to establish an improved, low-cost heliostat collector subsystem design for the central receiver solar thermal power system. The MDAC heliostat design selected by the DOE for the solar central receiver pilot plant has been used as an initial baseline design in this study. A concerted effort has been made to decrease the total costs of each element of the heliostat design, including material, manufacturing, assembly, installation, and maintenance costs. An improved version of the initial baseline design amenable to high-volume production rates has been established using conservative design practice. This approach significantly reduces capital and operating costs while meeting the necessary performance specifications. Additional major improvements in capital and operating costs are foreseen by conducting a short-term, low-cost research and development effort in key areas.

The objective of this study was to define a heliostat design, together with production, installation and checkout, and operations and maintenance plans, which will yield competitive electrical generation costs in high volume production. The cost goal for the installed field of heliostats and peripheral support hardware was set at $\$72/m^2R$ (cost per square meter adjusted by reflectivity). This cost leads to a cost of collecting solar thermal energy which is approximately equal to the current cost of imported oil, assuming the cost of the central receiver, tower and additional plant control hardware are approximately 25 percent of the total heliostat field cost. Hence, a heliostat available at $\$72/m^2R$ would allow the nation to install solar central receiver power plants without economic penalty and reduce dependence on foreign oil.

*Contract EG-77-C-03-1605

Employing baseline design perturbation, design-to-cost principles, cost reductions have been defined in all areas of the baseline heliostat concept resulting from the Solar Central Receiver 10 MWe Pilot Plant Phase I study. The cost reductions resulted in general from the following:

- Design optimizations to reduce materials quantities,
- Design changes to alter the types of materials used and to utilize more cost effective parts,
- Design changes to combine or eliminate parts,
- Production method changes to increase labor productivity, reduce material waste, and eliminate production steps.
- Optimization of the form and types of materials delivered to the factory.
- Optimization of the factory layout.
- Design changes to simplify installation and checkout.
- Equipment definition to increase installation and checkout labor productivity.
- Design changes and maintenance concepts to enhance reliability and reduce the difficulty of maintenance operations.
- Optimized repair levels for failed parts to minimize the cost of maintaining an adequate spares inventory.

Through these improvements, MDAC has developed a heliostat preliminary design which (1) projects to meet the DOE's goal of $\$72/m^2R$ at production volumes as low as 25,000 units per year and (2) reduces to less than $\$60/m^2R$ in very high volume production (~1,000,000 units per year).

MDAC elected to focus primary attention on a manufacturing facility with a nominal production rate of 25,000 heliostats per year with a flexible capability of expanding output to 100,000 heliostats per year with industrial robots. The primary reasons for this selection are:

- The introduction of new technology into the commercial market normally encounters market diffusion periods of the order of several years before full market acceptance is gained. This tends to limit production rate requirements in the first few years of market penetration.

- Unless collection of thermal energy by a collector field is economically competitive at 25,000 to 100,000 heliostats per year, high production rates may never be achieved.
- The installed electric power generation capacity in the six major southwestern states is approximately 100,000 MWe. Assuming a five percent growth rate, there would be a need for approximately 5,000 MWe additional generating capacity per year. Further, assuming that solar thermal central receiver systems can penetrate 3 to 25 percent of this market, a commensurate heliostat production level would be on the order of 25,000 to 225,000 heliostats per year.
- A moderate sized production facility will minimize the investment requirements and associated risk for the government and potential heliostat manufacturers, and therefore, may be the more likely manner in which solar thermal electric generation will be achieved.

The MDAC costs at 25,000 heliostats per year are based on a full resource loading analysis (i.e., a detailed analysis of the materials, production processes, and labor for each part produced). For higher production rate, net forming of parts (no material waste), material volume cost reductions, labor cost reductions through automation (e.g., industrial robots), and optimum location of production and form of parts and material delivered to the factory were assumed. The assembly factory itself was assumed to be replicated at locations close to the installation sites in order to minimize transportation costs of the bulkier heliostat subassemblies.

In addition, the actual costs of similar structural and mechanical hardware was determined both by direct comparison and by evaluating cost per unit weight for similar hardware. For the entire heliostat, the projected cost per unit weight is approximately 88¢/lb., which compares favorably with an intermediate size automobile costing 92¢/lb. Since heliostats are far simpler than automobiles, having approximately one-third the number of parts per unit weight and a high proportion of the weight (65%) in low cost structure and glass, actually achieving the projected costs appears feasible even at relatively low production rates.

*California, Arizona, New Mexico, Texas, Utah, and Nevada

Several scenarios exist for commercialization. As a commercial venture without market guarantees, the first plant would use a rather modest degree of automation. If the market were guaranteed, a substantially higher degree of automation would be used, even at this low production level. Figure 1-1 shows a composite cost reduction curve for production rate over the range from 2,500 to 1,000,000 per year. The upper curve represents a conservative approach to cost reduction with volume. The design is assumed to be essentially the same at all volumes. Automation is introduced rather slowly, such that extensive use of industrial robots is not introduced until the market grows to 250,000 heliostats per year. A conservative view of the effect of automation on overhead is also adopted. Moreover, the impact of further automation and process improvements in the basic industry is neglected. However, the larger volumes of production will surely drive the suppliers to greater economies of production when necessary to remain competitive.

The lower curve of Figure 1-1 shows a more optimistic assessment of the potential impact of production volume on costs. The cost reduction at 25,000 heliostats per year reflects the level of automation which is consistent with a guaranteed market. Some material quantity reductions are included at 25,000 which were previously incorporated at 250,000 heliostats per year. It is assumed that the additional cost reductions treated in Section 8 are implemented in the design by the time production reaches 250,000 per year (3.5×10^6 cumulative units produced).

At the opposite extreme, a large guaranteed market, or a combination of government incentives and investment could present the conditions amenable to a rapid startup at the 10^6 level. However, this level appears large for a single factory in the near term, even for the U.S. Southwest with its high electricity demand. High production rates may therefore require additional uses for heliostats, such as process heat.

Figure 1-1 shows that the potential for cost reduction by the millionth unit produced is such that heliostats can be installed for $\$65/m^2R$. For a 100 MWe plant, this cost is equivalent to energy collection costs of $\$2.11/MBtu$,

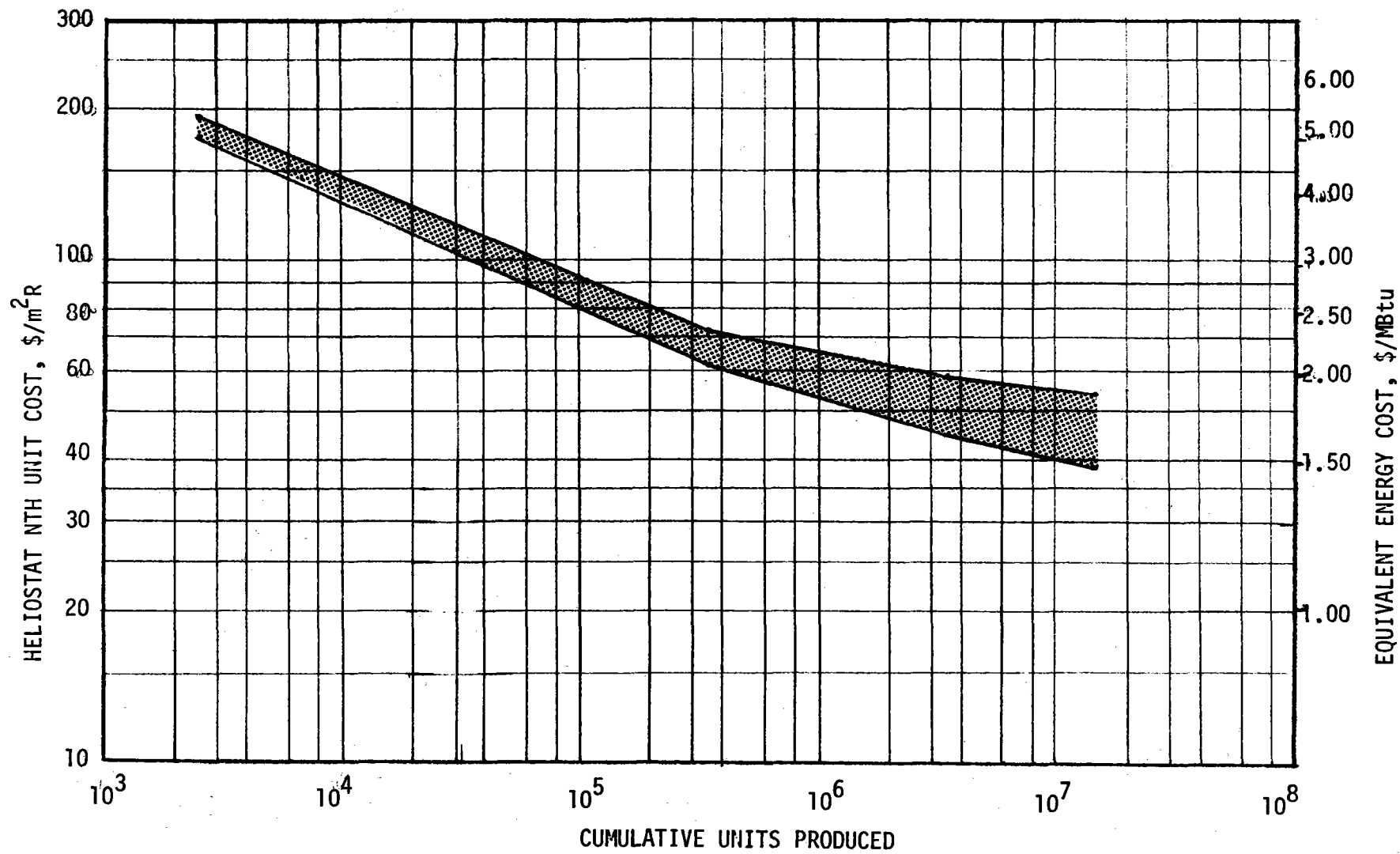


Figure 1-1. Expected Heliostat Cost Reduction

including a cost allocation of \$14M for the receiver subsystem.* Table 1-1 shows some current, comparative costs for energy from fossil fuel sources. The range of cumulative production volume at which heliostats can be competitive, as shown in Figure 1-1, is also indicated.

Table 1-1
ENERGY COST COMPARISONS

| FOSSIL FUEL ENERGY SOURCE | COST \$/MBtu | COMPETITIVE CUMULATIVE HELIOSTAT PRODUCTION VOLUME |
|------------------------------|-----------------|---|
| New Coal Contracts | 1 - 1.50 | 10,000,000 - Up |
| No. 2 Fuel Oil | 2.30 | 200,000 - 400,000 |
| No. 6 Fuel Oil | 1.90 | 500,000 - 3,500,000 |
| Imported Crude | 2.40 | 100,000 - 250,000 |
| Shale Oil (Estimated) | 3 - 5.00 | 3,000 - 40,000 |
| Imported LNG | 3 - 5.00 | 3,000 - 40,000 |
| Synthetic Gas | 3 - 6.00 | ~ 3,000 - 40,000 |

The table clearly indicates that solar energy can be competitive with other alternate energy sources such as synthetic gas and shale oil immediately, and with imported oil in the near term. However, it is essential to develop the technology associated with low cost heliostat production without delay in order to achieve these results.

Based on the results obtained to date, MDAC is confident that the project cost goal associated with the heliostat design resulting from this study is realistic, credible, and attainable, and that significant additional cost benefits can be achieved by further R&D efforts on this design.

The project approach, heliostat description, and summary of the study results are given in the remainder of this section.

*See Section 7 for energy collected. Assumptions include 330 days mean operation with field and daily average of 280 KWth Hr/heliostat/day, and 18,000 heliostats for a 100 MWe plant. Costs assume \$65/m²R, 49 m²/heliostat, 92 percent reflectivity and 18 percent levelized fixed charge.

1.1 PROJECT APPROACH

This study was conducted in accordance with a baseline design perturbation technique, as shown in Figure 1-2. Beginning with an initial baseline, trade studies between viable candidates were conducted for all project elements. Where necessary, promising candidates were subjected to minimum tests to ensure feasibility. Cost analyses were conducted to identify the areas which were most promising for cost reduction, establish and monitor progress toward cost goals, and resolve trade study issues. The resulting final baseline design was then defined to the preliminary design level. The design was verified to DOE Specification 001* by a combination of analysis, similarity, and operations and maintenance were developed. Cost estimates were made of the preliminary design. Key cost reduction issues were fed back into the design and plans. Finally, plans for Phase II testing were developed to demonstrate performance and compliance with the specifications.

The trade studies were presented in Table 1-2, grouped according to the lead project element. Table 1-2 also indicates the participation of other project elements in performing the trade study.

MDAC was assisted in this study by over fifteen major manufacturing concerns which provided specific design and cost inputs to the trade studies.

Additionally, production plans were prepared and reviewed by MDAC and Arthur D. Little, Inc., which is thoroughly experienced in planning for turn-key jobs. Stearns-Roger, Inc., a long-standing team member with MDAC on the central receiver solar thermal power program and a major architectural and engineering firm, developed foundation designs and installation procedures, and field wiring installation procedures and associated costs.

1.2 COLLECTOR SUBSYSTEM DESCRIPTION SUMMARY

The initial baseline heliostat design used in the trade studies is shown in

*Attachment 1 to Enclosure I, Statement of Work, Solar Central Receiver Prototype Heliostat, RFP No. EG-77-R-03-1468.

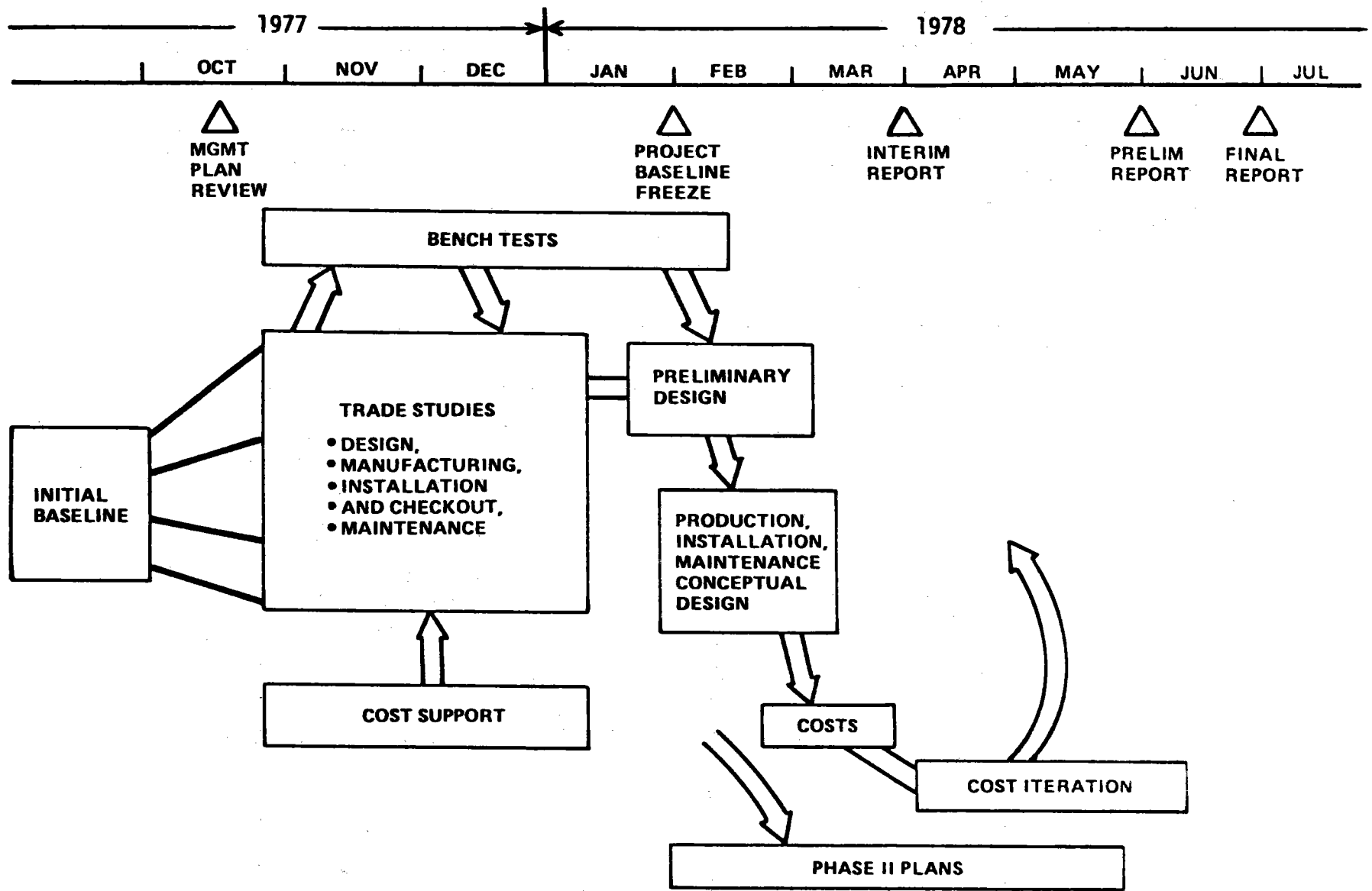


Figure 1-2. Study Flow Net

Table 1-2
PROJECT TRADE STUDY SUMMARY

| Lead Project Element | Trade Study Title | Project Elements Participating | | | | | |
|----------------------|---------------------------------------|--------------------------------|------|---------------|---------------------------|-------------|----------------------------|
| | | Design | Cost | Manufacturing | Installation and Checkout | Maintenance | Specification Verification |
| Design | D-1 Optimum Heliostat Size | X | X | X | X | X | X |
| | D-2 Low Cost Reflector | X | X | X | X | | X |
| | D-3 Drive Optimization | X | X | X | | | |
| | D-4 Control Optimization | X | | | X | X | |
| | D-5 Reflector Attachment | X | | X | X | | |
| | D-6 Reflector, Structure Optimization | X | | X | | | |
| Manufacturing | M-1 Integral Pedestal/ Foundation | X | X | X | X | | |
| | M-2 Drive Housing Materials Reduction | X | | X | | | |
| | M-3 Mirror Line Integration | | X | X | | | |
| | M-4 Float Glass Line Integration | | X | X | | | |
| | M-5 Foam Core Finishing | | | X | | | |
| | M-6 Foam Extrusion Integration | | X | X | | | |
| | M-7 Adhesive Application | X | | X | | | |
| | M-8 Site Factory Requirement | | X | X | | | |
| Installation | I-1 Optimum On-Site Transportation | | X | | X | | |
| | I-2 Collector Checkout | | X | | X | | |
| Maintenance | O-1 Reflector Cleaning | X | | | | X | |
| | O-2 Optimum Repair Levels | | | | | X | |

Figure 1-3. This design resulted from the DOE Phase I Pilot Plant study and is described in an earlier report.* A summary description is given in Appendix A.

The collector subsystem defined during this study is made up of three assemblies. The heliostat assembly of Figure 1-4 includes the reflective unit, the drive unit which orients the reflective unit, the foundation which supports the heliostat, and the heliostat electronics which control the drive unit.

The other assemblies are: (1) the collector controller which is collocated and interfaces with the system master control, and (2) field electronics consisting of primary and secondary power and data feeders, field transformers, distribution panels, and data distribution interfaces.

Table 1-3 shows a subsystem hardware tree down to the component level and indicates the correspondence of the hardware items to collector cost breakdown structure numbers.

1.2.1 Heliostat Summary Description (Section 2)**

The heliostat (Figure 1-4) is divided into four subassemblies, based on the physical pieces of hardware delivered to the field. These subassemblies are the reflector panel (one half of the reflective unit), the drive unit (including the pedestal), the foundation, and the heliostat electronics (including controllers and control sensors).

Reflector - Each reflector panel is composed of six mirror modules and a support frame. The mirror modules are 1.22 by 3.35 m (48 by 132 inches) and made of a 1.5 mm (0.060 inch) second surface mirror laminated to a 4.8 mm (0.1875 inch) glass back panel. The clean reflectivity is estimated to be from 0.92 to 0.95, depending on iron content and chemical state. The mirror modules are bonded to stringers which are, in turn, bolted to the cross beams. The outer cross beam is supported by two diagonal beams. All beams and stringers are made by continuous roll-forming from coiled sheet stock.

* R. W. Hallet, Jr. and R. L. Gervais. Central Receiver Solar Power System. SAN-1108-76-8, MDC G6776, October 1977.

**Denotes report section containing a complete description.

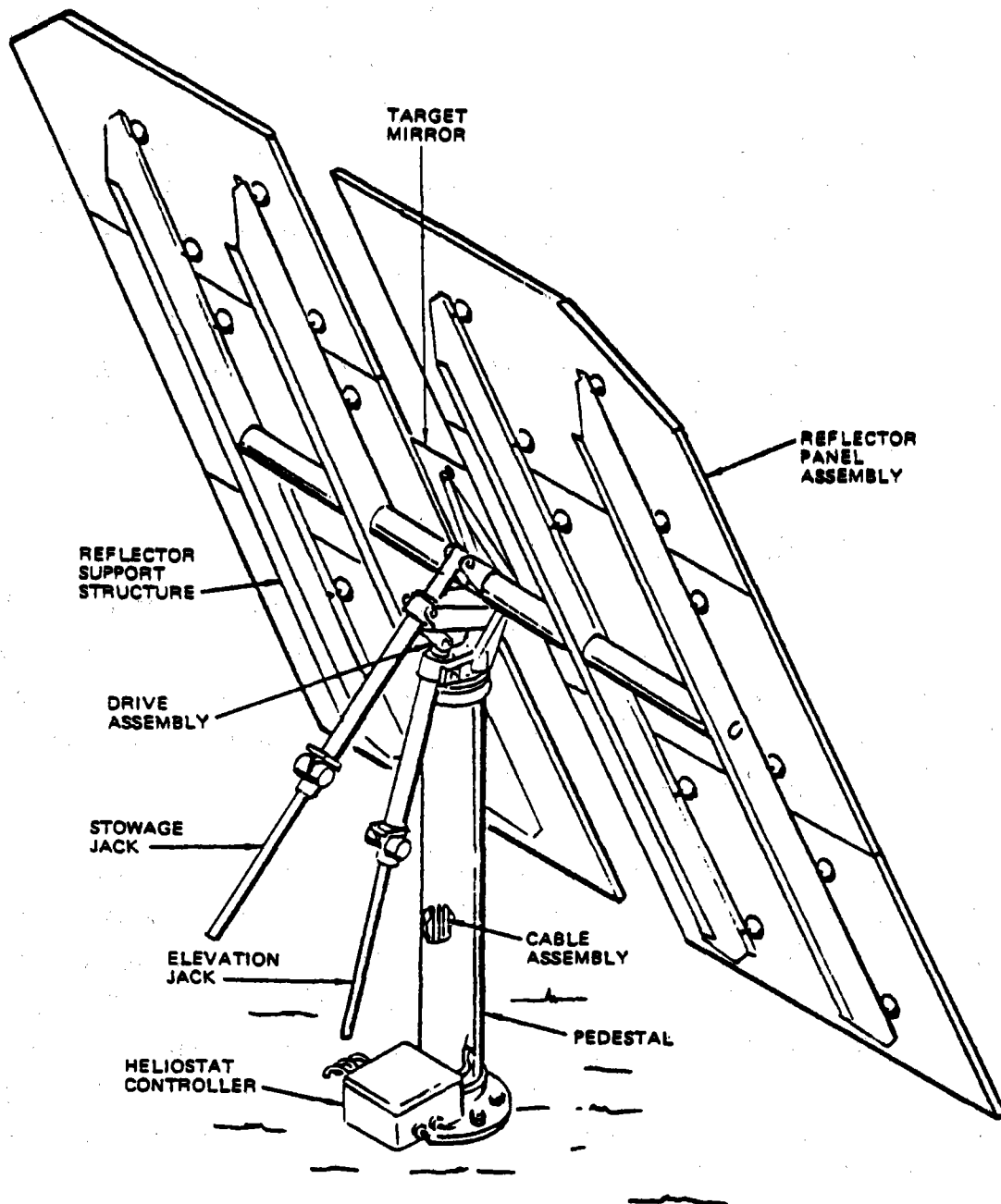


Figure 1-3. Heliostat Assembly – Initial Baseline Design

Table 1-3

(Page 1 of 2)

PROTOTYPE HELIOSTAT HARDWARE TREE

| SUBSYSTEM | ASSEMBLY | SUBASSEMBLY | COMPONENT | CORRESPONDING CBS NUMBER |
|-----------|-----------------------------------|-----------------------------------|--|-----------------------------|
| ● | Collector - (Field of Heliostats) | | | 4400 |
| | ● | Heliostat - (Includes Controller) | | - |
| | | ● | Reflector Panel - (Two Panels Make a Reflective Unit) | 4410 |
| | | | ● Mirror Module | 4411 |
| | | | ● Support Structure | 4412 |
| | | ● | Drive Unit | 4420 |
| | | | ● Azimuth Drive | 4421 & 4423 |
| | | | ● Elevation Drive | 4422 |
| | | | ● Pedestal | 4412 |
| | | ● | Foundation | 4440 |
| | | ● | Heliostat Electronics | 4430 |
| | | | ● Heliostat Controller | 4433 |
| | | | ● Motor | 4423 |
| | | | ● Pedestal Junction Box | 4425 |

PROTOTYPE HELIOSTAT HARDWARE TREE

| SUBSYSTEM | ASSEMBLY | SUBASSEMBLY | COMPONENT | CORRESPONDING CBS NUMBER |
|-----------|------------------------|----------------------|-------------------------------|-----------------------------|
| | • Collector Controller | | | 4430 |
| | | • Console | | |
| | | | • Key Board | |
| | | | • Cathode Ray Tube | |
| | | | • Control Panel | |
| | | • CPU | | |
| | | • Storage | | |
| | | • Field Interface | | |
| | | • MCS Interface | | |
| | | | • Mode | |
| | | • Time Pickup | | |
| | • Field Electronics | | | |
| | | • Power Distribution | | 4425 |
| | | | • Power Distribution Module | 4425 |
| | | • Data Distribution | | 4425 & 4433 |
| | | | • Data Distribution Interface | 4432 |

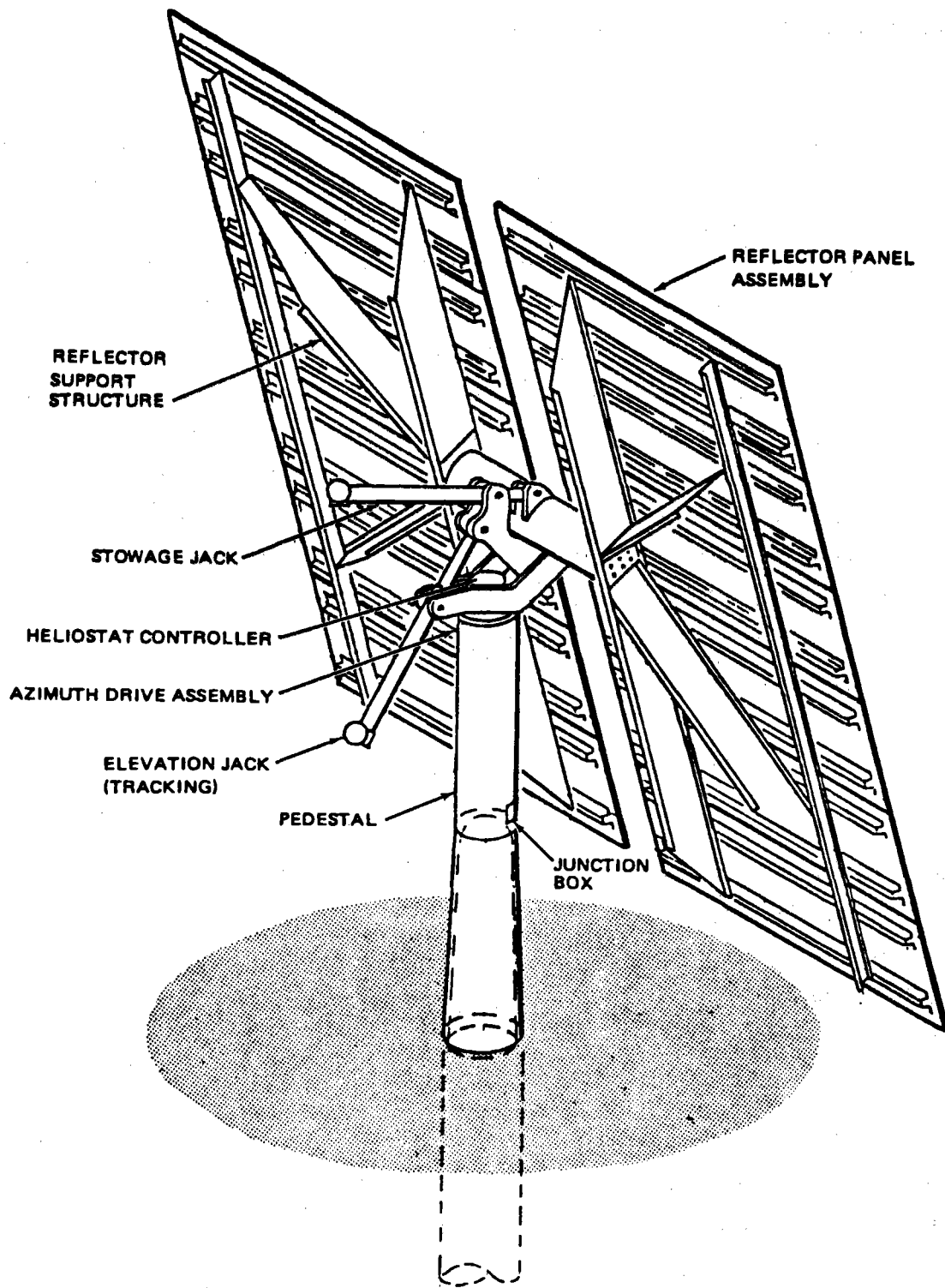


Figure 1-4. Primary Baseline Heliostat

This design achieves a direct production cost reduction compared to the initial baseline foam core, and provides an indirect cost reduction by use of a thinner glass with higher reflectivity. In addition, the total reflector area is increased commensurate with the drive unit loads.

Drive Unit - The drive unit is composed of a rotary azimuth drive, a double jack elevation drive, and a pedestal. All drive motors are three-phase, 480 VAC. A 162:1 Helicon input reducer provides the first azimuth stage reduction. The output is through a 242:1 Harmonic drive reducer. The elevation jacks utilize a Helicon input gear affixed to the shaft of a ball screw. The two jacks are connected by a drag link. One jack provides tracking motion while the other provides the additional motion required for stowage. The main beam is a 16-inch diameter tube with flange ends onto which the reflector panels are bolted. The tube has brackets which attach to a hinge line on one side and the tracking actuator on the opposite side, providing the final linkage of the elevation drive. The pedestal is a 24-inch diameter tube with a slight flare on the lower end which matches the tapered top of the foundation and provides a friction joint to the foundation. The top of the pedestal is closed by a dome which bolts to the circular spline of the Harmonic drive.

The drive unit is delivered to the field with the heliostat electronics installed.

This design incorporates a number of improvements, such as a lower-cost, more efficient jack design, lower-cost gears and bearings, and a pedestal design that allows simple field installation. The drive unit with its central main beam also allows a rapid and efficient field installation of the reflector panels in two pieces.

Heliostat Electronics - The heliostat controller is located in a housing on the top of the drive unit. The controller receives and transmits commands from the collector controller and responds to requests for data. A microprocessor calculates the motor revolutions required to maintain tracking and activates the motor controllers. The motor controllers switch the motor on and off to produce the required motion. The motor revolutions sensors detect motor revolution and direction, and the controller maintains a count of the accumulated revolutions. A nonvolatile memory retains motor counts

and alignment data in the event of a loss of power. The field wiring terminates at a junction box located on the pedestal. A "tee" junction provides the power to operate the heliostat. Data are routed to the heliostat controller, decoded, and relayed to the next heliostat in the link if not addressed to the receiving heliostat. Acknowledgment of receipt of a message and status are also transmitted.

The design of an integrated pedestal, drive, and electronics unit permits complete assembly and unit testing to be done in the factory.

Foundation - The foundation is a drilled pier, 0.6 m (24 in) in diameter. The pier extends about 1.2 m (4 ft) above grade and 6 m (20 ft) below. A tapered steel shell establishes the mounting surface to the pedestal and serves as a form for the protruding end of the pier. This design speeds field installation, reduces costs, and decreases the amount of steel required for the pedestal by over 272 kg (600 pounds).

1.2.2 Field Electronics Summary Description (Section 2)

The field electronics is a general term for the loops which distribute power and data to the heliostats. Those loops are illustrated in Figure 1-5.

A field distribution center is defined as the collocation of the field transformer and the data distribution interface. Its power handling function is to step down voltages and dispatch power to several "daisy chains" of heliostats; i.e., heliostats connected by a single cable which tap power off that cable. The data distribution function is to decode high baud rate messages, and address them to the correct heliostat in the correct chain.

The transformer interfaces with the electric power generation subsystem and receives 4160 V, three-phase power. The primary feeders link up to three transformers in a daisy chain.

The data distribution interface links into the master control through the collector controller. Data are transmitted from the collector controller concerning heliostat operating modes, time synchronization, and

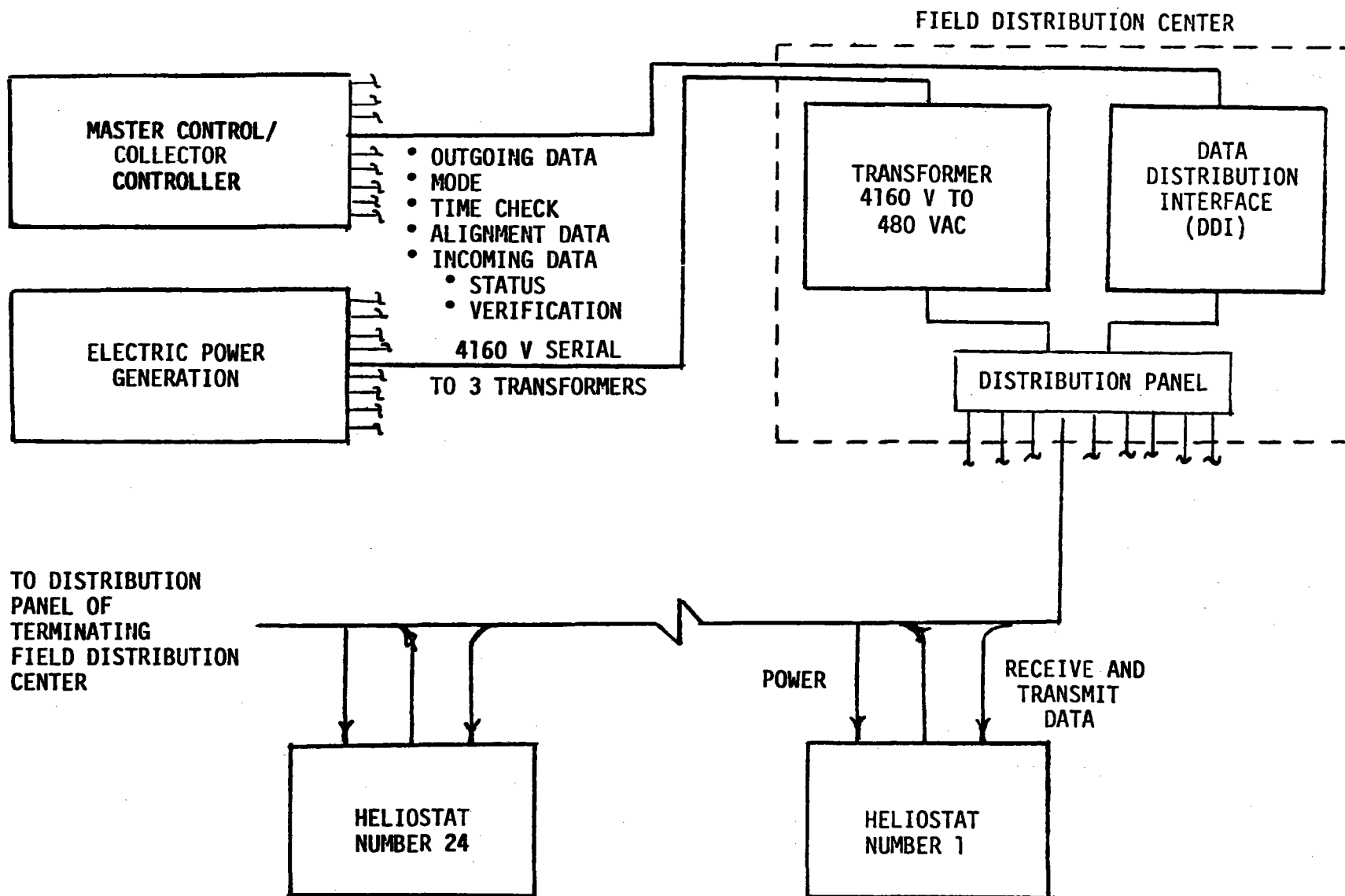


Figure 1-5. Collector Field Electronics

alignment/checkout parameters from the collector checkout sensors. Data received include heliostat status and verification of messages received. Again, serial connection of three data distribution interfaces is used.

All data are communicated by fiber optics to reduce cost and eliminate electromagnetic interference.

The data distribution interface receives data from the collector controller via either of two redundant lines and logic networks. The redundancy provided should prevent loss of control of more than a few heliostats at a time. The logic network decodes and addresses the data to the correct secondary data feeder and the intended heliostat.

Power and data are carried in the same cable from the distribution panel to the chain of heliostats. Each cable is terminated at another field distribution center. Hence, power may be fed either way on a cable if the cable fails open as in a break. A short circuit in a cable will, of course, trip the breaker in the distribution panel and cause the loss of power to all heliostats in the chain.

The control signals carried by the secondary feeder are all processed by the first heliostat in the chain. Those signals which are addressed to other heliostats are simply repeated, hence routed to the next heliostat. Signals addressed to the Nth heliostat are received by that heliostat and an acknowledgment signal is transmitted. The acknowledgment signal, which may include requested data on heliostat status, is relayed to the field distribution center at the end of the chain. From the center, data are relayed directly to the heliostat array controller.

Each heliostat has the capability to continue to operate autonomously in the event of a loss of data signals. If no data are received in a specified length of time, the heliostat will continue to track. The collector controller will monitor the signals received from the communications loops. The controller will notify the operator when an anomaly is detected.

1.2.3 Collector Production Summary Description (Section 3)

The heliostat is produced in a factory that can turn out 25,000 units per year. The two subassemblies produced in the factory, the drive/control unit and the reflector panel, are transportable by common carrier to essentially any field site. The drive/control unit is given a 100 percent functional inspection in an automated checkout facility and shipped to the field ready for installation. The reflector panels are also completely assembled in the factory and optically inspected by automated equipment prior to shipment. To meet higher volume production rates, the same type of factory is replicated at different locations. Sources of parts and materials are expanded to service the greater volume. The form of the receiver materials and parts may be altered to centralize some of the fabrication operations.

Figure 1-6 shows the production steps for the reflector panels, indicating the assembly sequence without considering where the glass, beams, and attach fittings are made. These decisions may vary with production volume.

The front glass panel (or "lite") is cleaned, sensitized, and mirrored. Adhesive is applied in lieu of backing paint. The back glass panel is cleaned, dried, and mated with the front panel. The resulting mirror module is rolled to ensure good adhesion and cured on a conveyor belt.

The frame is assembled from its parts by automatic spot welding in a jig. The holes for the attach bolts are jig-bored. The stringers are bolted to the cross beams.

The mirror modules are loaded into a bonding fixture at the appropriate cant angle and curvature. Adhesive is extruded onto the back surface of the mirror modules. The frame is joined to the mirror modules to form the reflector panel. The bonding fixture contains reference surfaces to ensure that the mirror surfaces are correctly aligned with the bolted interface to the drive unit.

After curing, the assembled panel is inspected by automatic optics analyzing a reflected test pattern. The reflector panel is then loaded onto a reusable shipping fixture.

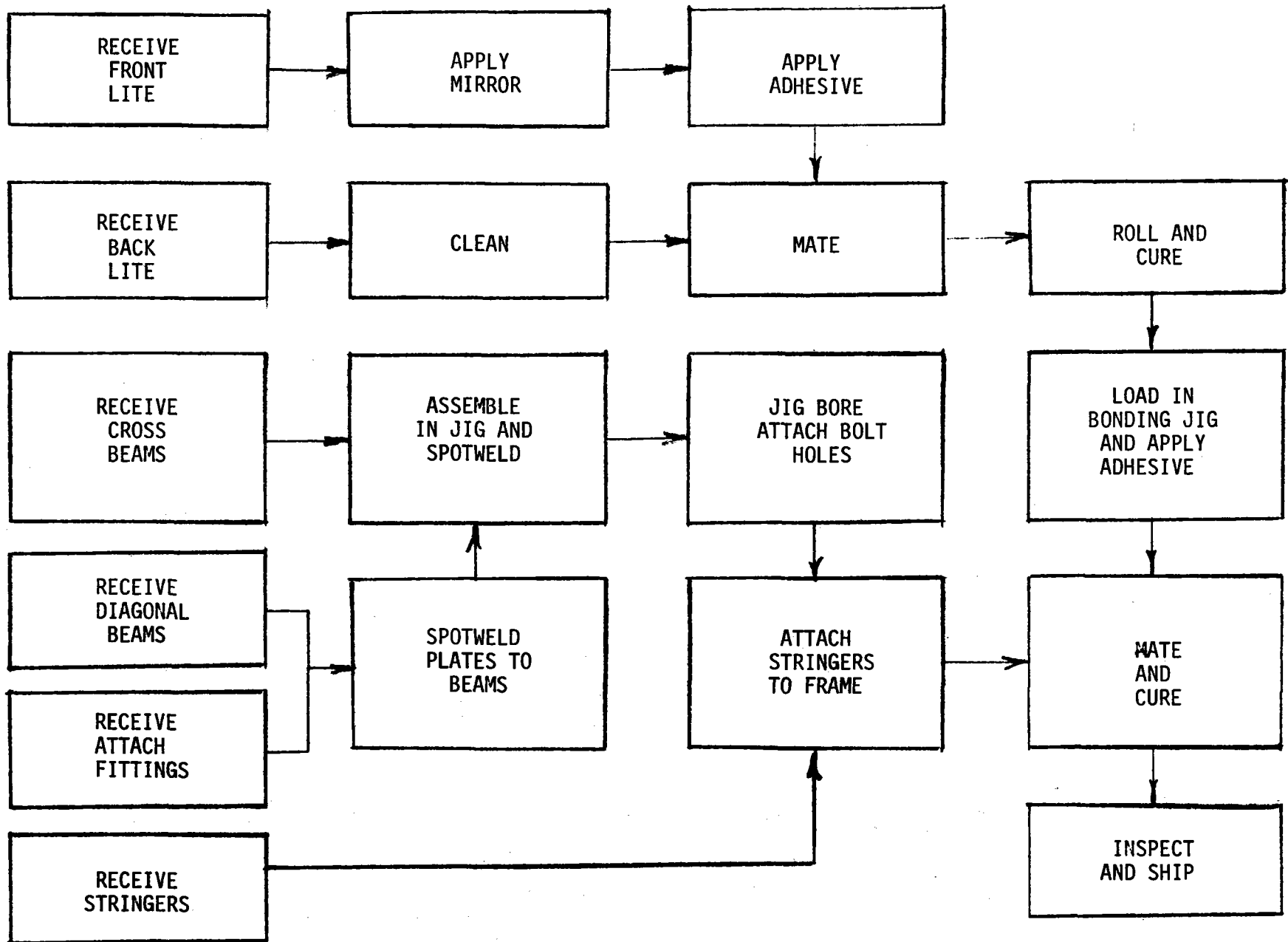


Figure 1-6. Panel Assembly – Initial Baseline Design

The azimuth drive unit assembly is illustrated in Figure 1-7. There are many steps to the assembly of the azimuth drive, most of which are in-line installations of parts or subcomponents whose assembly can be completed off-line and stockpiled. Hence, the process is amenable to a very simple assembly line such as an overhead conveyor or monorail.

The completion of the drive unit assembly is illustrated in Figure 1-8. Again, the simple assembly line approach appears to be suitable.

On completion of assembly, the drive/control unit is loaded into a computer-operated fixture and given a complete functional checkout. In addition, alignment data are stored in the controller and key characteristics of the assembly are automatically measured to provide data on the production process.

After inspection, the drive unit/control assembly is loaded onto a shipping fixture ready for delivery to the field.

Collector production techniques have been optimized by the generation of cost-effective component designs and manufacturer approaches which are compatible with current related industry trends.

1.2.4 Installation and Checkout Summary (Section 4)

The installation process flow is shown in Figure 1-9. Site preparation includes rough grading and surveying. The foundation hole is drilled, the rebar installed, and the foundation is poured. A thin sheet metal cone serves as a form for the mating surface to the pedestal.

The drive/control unit is held vertical and oriented south by the installation equipment. After mating to the foundation, the drive/control unit is loaded and vibrated to ensure adequate seating.

The secondary feeder cable is brought to the field with the ends terminated and rolled on spools. The cable is plowed into the ground and the terminations left above ground. Each cable requires bolting on three lugs, terminating one optic fiber and making electrical contact with the ground at each end. A weatherproof cover seals the junction box.

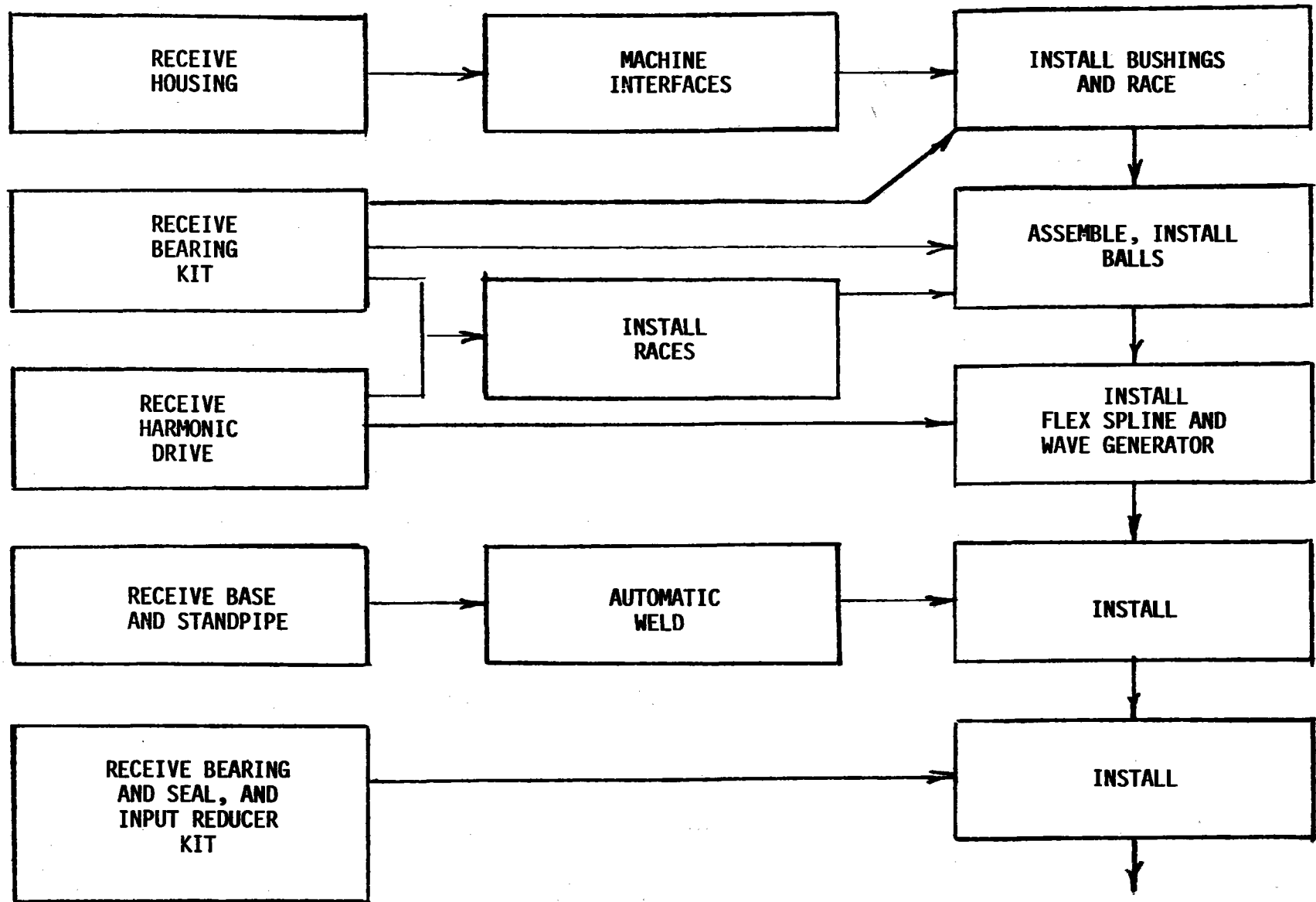


Figure 1-7. Azimuth Drive Assembly

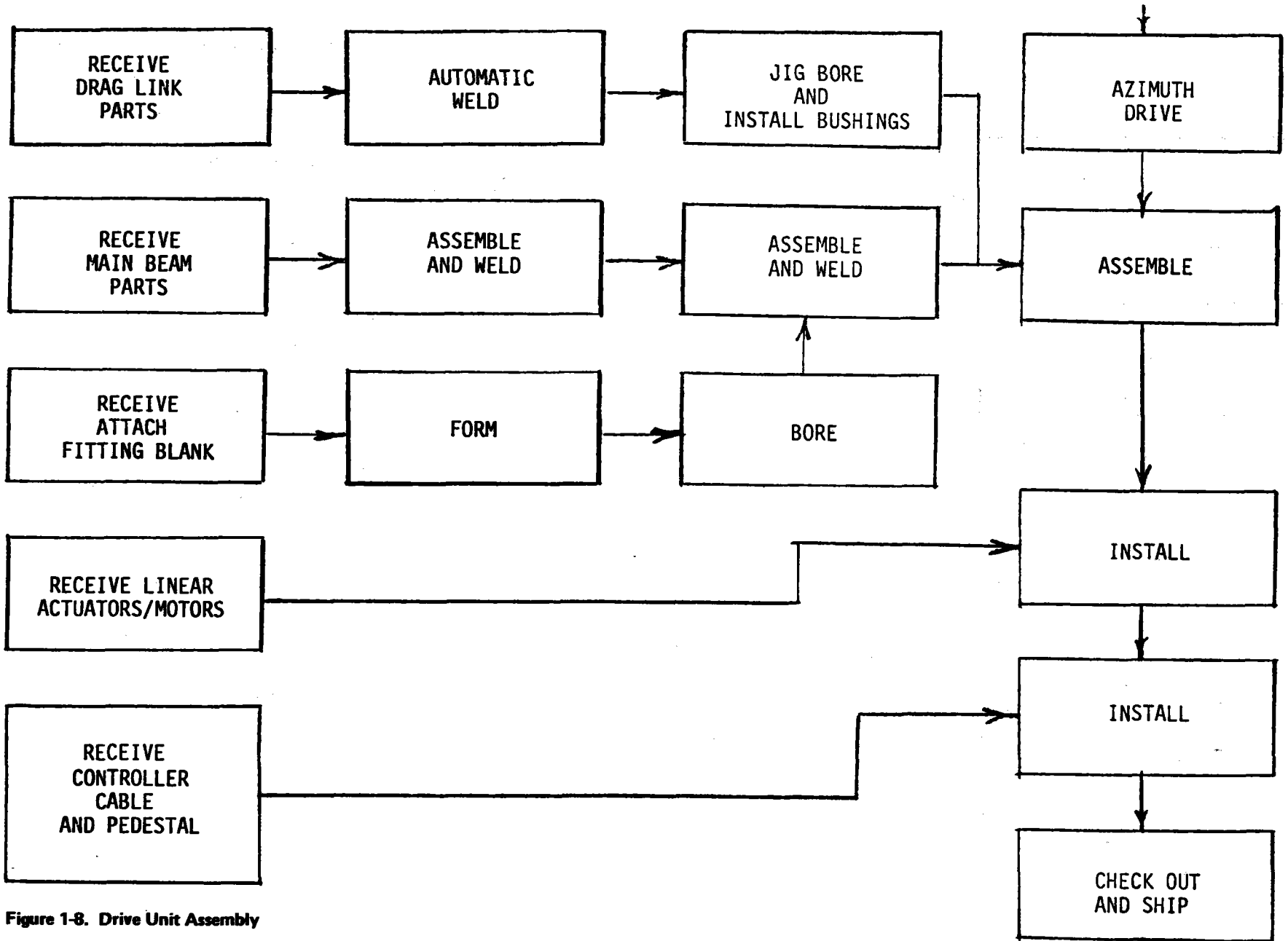
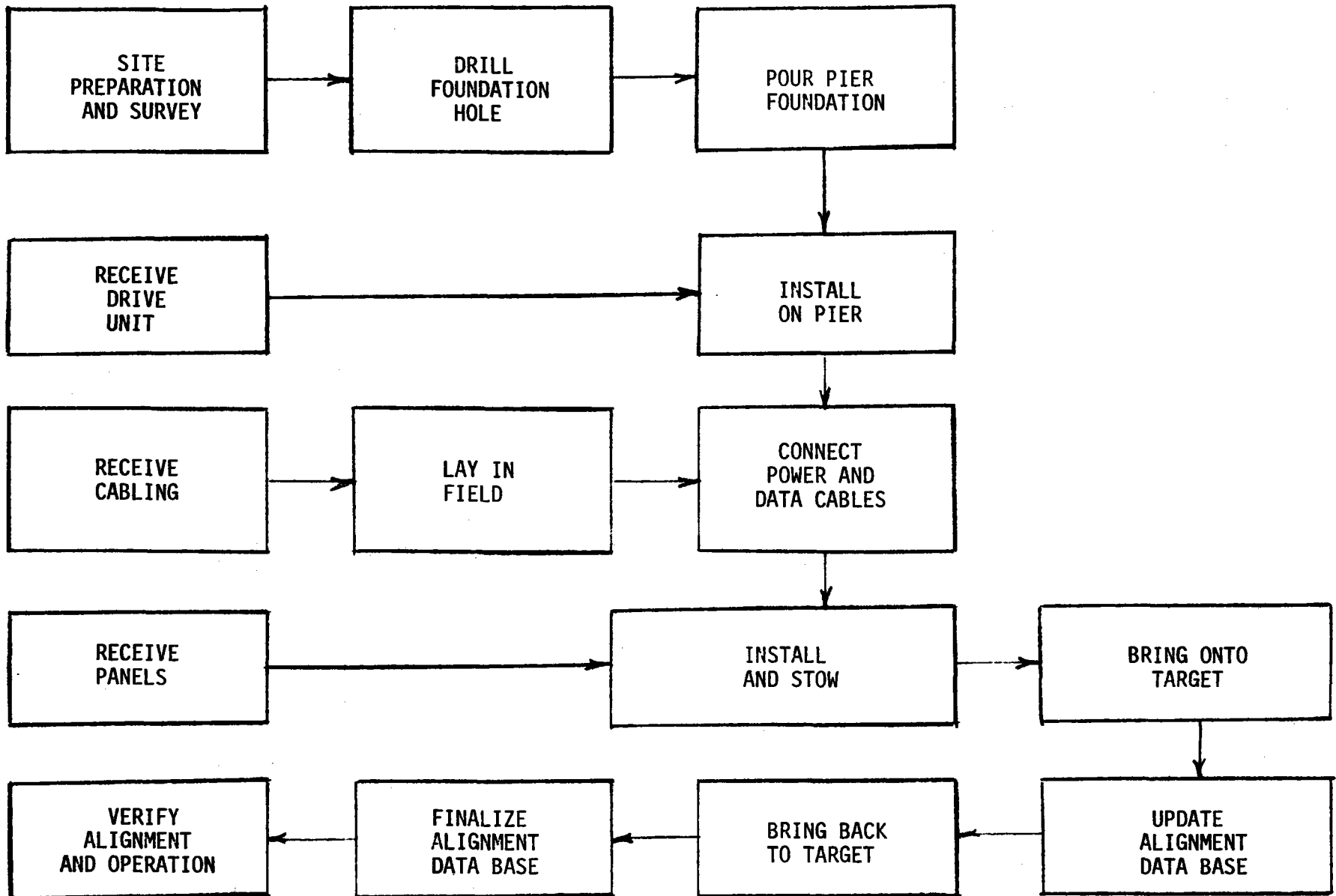


Figure 1-8. Drive Unit Assembly



1-24

Figure 1-9. Installation and Checkout Processes

The reflector panels are installed, and the heliostat is stowed until the time for alignment and checkout.

To align, the heliostat is centered on a passive target. The motor counters are set and the heliostat is removed to standby. After the elapse of at least two hours, during which time additional heliostats undergo initial alignment, the heliostat is returned to target and recentered. Vertical errors are computed and added to the data base. The alignment and tracking capabilities are then verified.

A cost-effective approach to installation and checkout activities has been achieved by means of simple and efficient procedures.

1.2.5 Operations and Maintenance Summary (Section 5)

Operations and maintenance includes the areas of reflector cleaning, routine inspection, scheduled maintenance, repair of failed heliostats and field electronics, spares inventory, repair and replacement of failed parts, and maintenance of the support equipment.

Reflector Cleaning - Methods of reflector cleaning were compared. Mechanized equipment which sprays on washing solution followed by equipment which rinses with deionized water projects the lowest cost. The trade did not consider the efficacy of the methods and should be revised when data on the "as-cleaned" reflectivity become available.

Routine Inspection - Maintenance personnel will inspect each heliostat once a year. The inspectors will look for such things as lubricant leaks, corrosion, and mirror module damage.

Scheduled Maintenance - There will be no scheduled maintenance on the collector equipment in the field. However, the collector controller will require weekly maintenance.

Repair of Failed Equipment - The heliostats and field electronics will be repaired by substitution of line-replaceable units (LRU's) from the spares inventory. Typical LRU's are mirror modules, motors, linear actuators,

azimuth drive rivets, controller cards, and transformers. Almost all repairs on the LRU's will be performed in the maintenance shop at the field. Few, if any, repair operations will be centralized. The location of the repair operations will vary only slightly with the production volume.

Spares Inventories - LRU spares will be stocked at the field so that a spare part will be on hand when needed. Additional spares will be counted for LRU's which are to be repaired to account for the time elapsed between failure and return to inventory.

Repair/Replace LRU's - The decision of whether to repair or replace failed LRU's is based on economics for the individual LRU. These decisions are affected by production volume. The derived costs should be conservative, as they do not account for the salvage value of the LRU.

Maintenance of Support Equipment - The equipment used for maintenance must, itself, be maintained. Actions include repair and routine maintenance of the equipment and scheduled maintenance actions such as proof of testing of hoisting slings.

A smaller number of hardware parts and a reduction in complexity have improved reliability, and as a result, there will be fewer maintenance actions, requiring less elapsed time per task.

1.2.6 Specification Optimization and Verification Summary (Section 6)

The corners on the reflective unit shown in Figure 1-2 were clipped to provide clearance for a pole supporting the beam sensor for closed-loop tracking. With the change to open loop tracking, clipped corners are no longer required. A study of the impact of clipped and square corners on field layout showed that squared corners were more cost-effective. A second study considered the impact of elevation actuator backlash and allowed for the selection of the ball screw jacks. A third study determined the optimum curvature for the mirror modules to minimize defocusing from thermal warping.

Error analyses were conducted to ensure that the individual heliostats will meet beam pointing and beam quality requirements.

The heliostat design was verified to Specification 001 by analysis, similarity, and laboratory tests. Additional verification by component and assembly level tests is required to complete verification to Specification 001.

1.2.7 Performance Analysis Summary (Section 7)

MDAC has generated performance characteristics for heliostats in the locations (northeast and southeast of the tower) described in Specification 001. These locations are all extreme with respect to some characteristic of performance loss (i.e., slant range and cosine factor). The specified points are not necessarily representative of the characteristics of the field. To illustrate this point, MDAC selected a fourth point, directly north of the tower, representative of the best annual performance. To further illustrate, an approximation of the field average performance characteristics was generated. The results of all of these data indicate that an average heliostat will deliver to the receiver about 33 KW average over the year.

1.2.8 Critical R&D (Section 8)

MDAC identified five areas of critical R&D which may lead to further significant cost reductions. These areas are: (1) eliminating the requirement for inverted stowage; (2) optimizing designs to minimize wind loads; (3) deleting power and communications wiring; (4) developing alternate motor and drive unit concepts; and (5) optimizing the frequency, efficacy, and cost of washing.

1.2.9 Cost Analysis Summary (Section 9)

Cost analyses were generated first for a production rate of 25,000 heliostats per year. The analyses utilized vendor cost estimates for purchased parts and materials and detailed resource loading for labor and equipment costs.

The analysis showed that $\$72/m^2R$ (cost per unit area normalized to reflectivity) is feasible at the production rate of 25,000 heliostats per year.

Additional analyses were conducted at a rate of 2,500 heliostats. One analysis used cost reduction curves projected from the 25,000 heliostat per year production rate. Another analysis used a detailed resource load initial baseline at 2,500 heliostats per year and ratios of material, parts, and labor costs representing changes from the initial to the final baselines. Both analyses agree and indicate about $\$170/\text{m}^2\text{R}$ for a one-time 2,500 unit run.

Additional analyses were conducted at production rates of 250,000 and 1,000,000 heliostats per year. Those analyses were performed with a combination of cost reduction curves and detailed spot checks of predictions from the curves. The ultimate cost of the Prototype Heliostat design (arbitrarily set at the 10^7 unit) is estimated at about $\$55/\text{m}^2\text{R}$ for a projected reflectivity of 0.95.

First-year and average subsequent-year operations and maintenance costs were estimated from detailed failure rates, maintenance manhour to repair, and costs of spares and replacement parts. The O&M costs are estimated at about $\$1.15/\text{m}^2$ for the first year of operation and $\$0.60/\text{m}^2$ for subsequent years, which is a steady state rate of 1.2 mils/KWH.

Section 2

COLLECTOR PRELIMINARY DESIGN

The initial baseline design described in Section 1 has been investigated by performing a series of design trade studies, supported by preliminary laboratory tests, to achieve cost reductions while maintaining compliance with the performance and design requirements of RFP EG-77-R-03-1468, Specification 001. Performance and design requirements are summarized in Appendix B.

2.1 DESIGN TRADE STUDIES

The major design trade studies conducted by MDAC are summarized in Table 2-1. These studies encompass material cost reductions, improvement of manufacturing techniques by design modifications, simplification of assembly and site operations, and use of emerging technology.

The following design improvements resulted from these studies: an improved reflector configuration; a new actuator type; a low-cost, noise-free fiber optic control system data link; a low-cost foundation/pedestal; and a design configuration which minimizes both site assembly and installation activities and capital investment in on-site assembly facilities. Additional design effort has been conducted on manufacturing, installation/checkout, and maintenance trade studies.

2.1.1 D-1 Optimum Heliostat Size

This trade study was conducted to optimize the reflective unit area to reduce costs while maintaining appropriate cost-effective power interception at the receiver. Previous studies had shown the existing drive unit to have excess load capability for the 38 m² reflector. Hence, this effort was directed first to enlarge the reflector to match drive unit capability. The receiver size and field geometry were assumed to be fixed. The structural strength/deflection requirement was met, as will be discussed. This approach led to a first-order cost reduction of 15 percent with an insignificant difference in

Table 2-1
DESIGN TRADE STUDIES

| <u>Trade Study</u> | <u>Objective</u> |
|--------------------------------------|--|
| D-1 Optimum Heliostat Design | Optimize reflector area for minimum cost |
| D-2 Low-Cost Reflector | Evaluate panel designs to reduce material and fabrication costs |
| D-3 Drive Optimization | Integrate drive elements, reduce parts, reconfigure design |
| D-4 Control Optimization | Reduce cost by incorporating emerging technology in electronic components |
| D-5 Reflector Attachment | Reconfigure main beam to optimize on-site assembly and transportation and reduce costs |
| D-6 Reflector Structure Optimization | Optimize support structure for minimum weight within design constraints |
| D-7 Low-Cost Motors | Optimize motor configuration and voltage |

energy spillage at the receiver for the baseline area of 38 m² (408 ft²) compared to the optimized area of 49 m² (528 ft²).

Additional changes in the reflective unit configuration include: (1) new mirror modules which require less gap between mirrors than the baseline foam core, (2) the clipped mirror module corner was eliminated, (3) the mirror width became 1.22 m (48 inches) a practical dimension which matches well to nominal material stock sizes.

The optical interception at the receiver was determined for a sufficient variety of conditions to verify that power loss differences between the two areas were not a constraining factor. Results are summarized in Appendix C.

2.1.2 D-2 Low-Cost Reflector

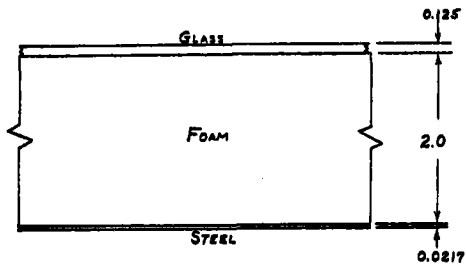
This study was conducted to lower the mirror module cost by reducing material and fabrication costs and increasing performance. Figure 2-1 shows the various configurations considered. Preliminary cost analyses performed by Manufacturing Engineering are summarized in Table 2-2. The lowest-cost approaches were the corrugated-stiffened reflector (configuration No. 3), the hat-stiffened reflector (No. 4) and the low-cost laminated (No. 7). Stress analyses were performed on all of the candidates using the methods described in Appendix C. Conditions include survival temperatures, survival wind, gravity, operating wind and temperature, and combined stresses.

These three candidates were then tested in a salt spray environment and subjected to hail impact tests. Results of the salt spray tests (see Section 2.2) showed all three candidates have an excellent probability of survival. However, the laminated edges must be sealed. A gray mirror-backing paint appears adequate for the exposed second-surface mirrors.

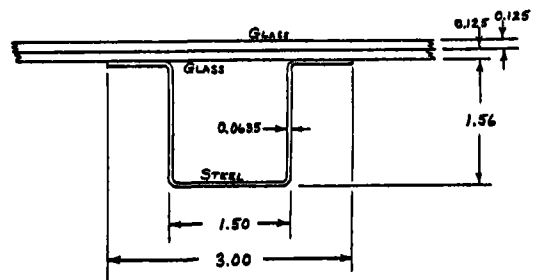
Results of the hail tests (see Section 2.2) showed that:

- 1) The 3.2 mm (1/8 inch) hat stiffened configuration (No. 4) is marginal to unsatisfactory for hail impact of 19 mm (0.75 inch) at 20 m/sec (65 ft/sec).
- 2) The 3.2 mm (1/8 inch) corrugated-stiffened configuration (No. 3) would survive the hail impact of 19 mm (0.75 inch) at 20 m/sec (65 ft/sec), but was marginal for 25 mm (1 inch) at 23 m/sec (75 ft/sec).
- 3) The hat-stiffened 3.2 mm plus 3.2 mm (1/8 plus 1/8 inch) low-cost laminate (No. 7) could survive both 19 m (0.75 inch) and 25 mm (1 inch) hail impacts.

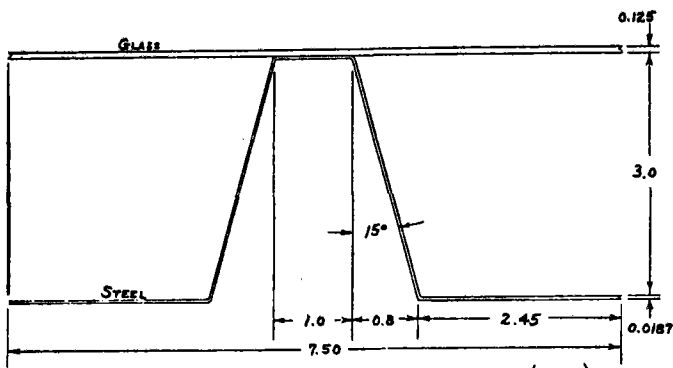
The low-cost laminate configuration can utilize a thin (1.5 mm or 0.060 inch) second-surface mirror (Configuration No. 8) for increased performance, but the



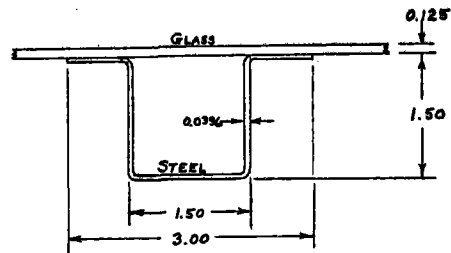
BASELINE REFLECTOR
(NUMBER 1)



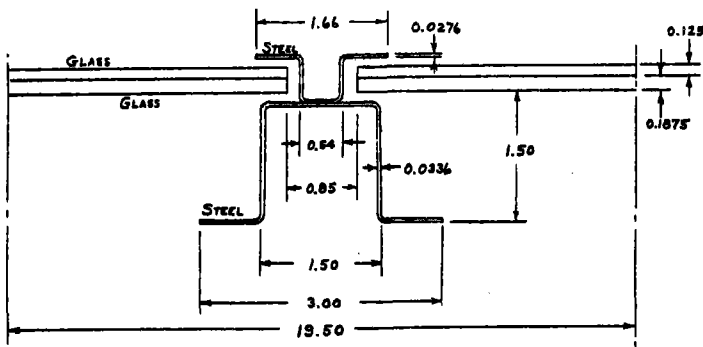
SRE LAMINATED REFLECTOR
(NUMBER 2)



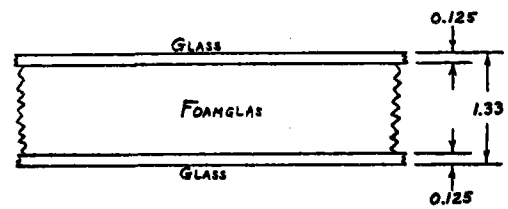
CORRUGATION-STIFFENED REFLECTOR (No. 3)



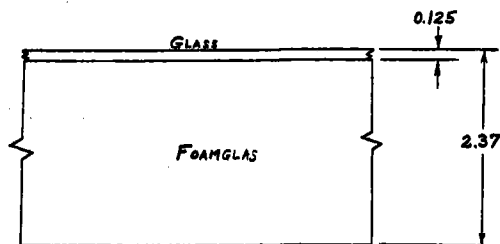
HAT-STIFFENED 1/8" REFLECTOR
(NUMBER 4)



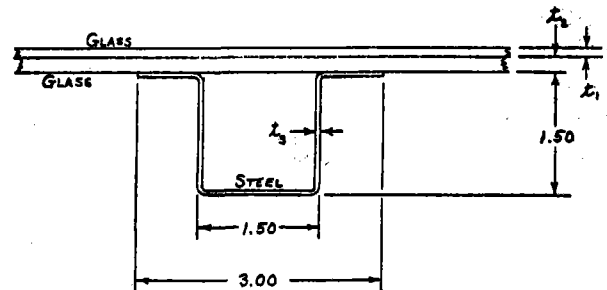
LAMINATED REFLECTOR, EDGE-CLAMPED
(NUMBER 5)



GLASS/FOAMGLAS SANDWICH
(NUMBER 6)



FOAMGLAS-SUPPORTED REFLECTOR
(NUMBER 7)



LOW-COST LAMINATED REFLECTOR, HAT STIFFENED
No. 8 $t_1 = 0.125$, $t_2 = 0.125$, $t_3 = 0.0516$
No. 9 $t_1 = 0.040$, $t_2 = 0.1875$, $t_3 = 0.0635$

NOTE: ALL DIMENSIONS
ARE IN INCHES

Figure 2-1. Candidate Reflector Designs

Table 2-2

COMPARISON OF LOW-COST REFLECTORS

| PARAMETER | REFLECTOR CONFIGURATION | | | | | | | |
|--|---|--|--|--|---|---|---|---|
| | 1 | 2 | 3 | 4 | 5 | 6 | 7 | 8 |
| | BASILINE SANDWICH REFLECTOR 0.125" Glass 2.0" Foam Core 26 Ga. Steel | SRE LAMINATED REFLECTOR 0.125" + 0.125" Glass 3 Hats of 16 Ga. Steel 85" Wide | CORRUGATION-STIFFENED REFLECTOR 0.125" Glass 28 Ga. Corrugation Steel | HAT-STIFFENED 1/8" REFLECTOR 0.125" Glass 4 20 Ga. Steel Hat Sections | LAMINATED REFLECTOR Edges Clamped 0.125" + 0.1875" Glass 22 Ga. Steel Hats | GLASS/FOAMGLAS SANDWICH REFLECTOR 0.125" Glass Faces 1.08" Thick Core | LOW-COST HAT-STIFF. LAMINATED REFLECTOR 0.125" + 0.125" Glass 2 18 Ga. Steel Hats | LOW-COST LAMINATED FUSION GLASS HAT-STIFF. REFLECTOR 0.060" + 0.1875" Glass 2 16 Ga. Steel Hats |
| WEIGHT (psf) | | | | | | | | |
| Glass | 1.692 | 3.384 | 1.692 | 1.692 | 4.046 | 3.384 | 3.350 | 3.350 |
| Steel | 0.906 | 0.548 | 1.219 | 0.798 | 0.568 | - | 0.517 | 0.637 |
| Other | 0.333 | - | - | - | 0.070 | 0.765 | - | - |
| TOTAL | 2.931 | 3.932 | 2.911 | 2.490 | 4.684 | 4.149 | 3.867 | 3.987 |
| MAXIMUM SLOPE (mrad) | | | | | | | | |
| Temp ($\Delta T = +50^\circ F$) | 3.705 | 5.579 | 1.816 | 5.505 | 0 | 0 | 5.743 | 5.751 |
| Gravity | 0.428 | 0.598 | 0.089 | 0.520 | 2.048 | 0.024 | 0.933 | 0.619 |
| Wind (26 mph $\alpha = 30^\circ$) | 0.390 | 0.384 | 0.077 | 0.527 | 1.104 | 0.015 | 0.609 | 0.519 |
| MAXIMUM GLASS TENSILE STRESS (psi) | | | | | | | | |
| Temp ($\Delta T = +70^\circ F$ $-92^\circ F$) | 132 | 228 | 357 | 290 | 0 | 38 | 227 | 244 |
| Gravity | 65 | 84 | 34 | 75 | 75 | 8 | 103 | 99 |
| Wind (90 mph $\alpha = 10^\circ$) | 401 | 642 | 354 | 905 | 562 | 57 | 803 | 749 |
| OPER. GLASS TENSILE STRESS (psi) | | | | | | | | |
| Temp ($\Delta T = +50^\circ F$) | 94 | 163 | 253 | 207 | 0 | 27 | 162 | 174 |
| Gravity | 61 | 79 | 32 | 70 | 70 | 8 | 97 | 93 |
| Wind (26 mph $\alpha = 30^\circ$) | 52 | 54 | 30 | 76 | 50 | 5 | 67 | 63 |
| HAIL IMPACT RESISTANCE | >1 in. | >1 in. | >3/4 in. | <3/4 in. | - | - | >1 in. | >1 in.* |
| RELATIVE COST (MATL + LABOR) | 1.0 | 1.2 | 0.87 | 0.75 | High | High | 0.93 | 0.93 (0.73**) |

*Not tested - but inferred from hail test results of Configuration 2.

**Including benefits from increased reflectivity.

↑
SELECTED

corrugated configuration (No. 3) must use a second-surface mirror of at least 3.2 mm (1/8 inch) thickness to withstand hail. When reflective efficiency is included in the cost estimates, the relative cost ratio of Configuration No. 8 is 0.73. In addition, Configuration No. 8 can use a lower-cost bolted attachment to the cross beams where Configuration No. 3 must be bonded to the cross beams because of the very thin corrugated steel. These low-cost features, coupled with an operating thermal stress less than 1.4 MPa (200 psi), were the primary reasons for the selection of Configuration No. 3 as the baseline.

A composite hat stiffener was investigated as a replacement for the steel stiffener because of the desirability of matching the thermal expansion coefficient of the glass. The difference in thermal expansion between glass and steel causes the mirror module to change shape as a function of the temperature, thereby resulting in possible energy spillage. This effect could be eliminated with identical thermal expansion coefficients. A 60 percent E glass and graphite epoxy resin combination with all fibers oriented along the length of the stiffener was found to match the glass coefficient of expansion very closely. A hat section with identical bending stiffness to the steel hat was designed. A fabrication technique of pultrusion was determined to be feasible and cost estimates were obtained. These cost estimates showed this composite stiffener to be noncompetitive with steel at this time. Further investigation and development considering higher production rates is required to determine if the composite stiffener can be made cost effective.

Having selected a baseline approach of the low-cost laminate, a further study was conducted to determine the best approach to the mirror. Results are summarized in Table 2-3. Both the direct cost of the glass and the cost adjustment for performance (based on $\$72/\text{m}^2\text{R}$) were considered. Low- and very-low iron float glass should have a distinct cost benefit. However, these glasses are not presently available, the cost basis is not verified, and there is a tendency for waviness in float glass to increase with decreasing thickness. By contrast, Corning is willing to make fusion glass in low to very low iron content at the present time. The samples of fusion glass examined by MDAC in the 1.5 mm (0.060 inch) thickness show exceptional flatness and smoothness. Hence, the choice is fusion glass, pending further developments in float glass.

COMPARISON CHART OF VARIOUS LAMINATED GLASS CONFIGURATIONS

| CONFIGURATION | Fe CONTENT (%) | COST (\$FT ²) | REFLECTIVITY + OR - FACTOR | EFFECTIVE COST (\$ FT ²) | RELATIVE COST RELATIONSHIP |
|---|----------------|---------------------------|----------------------------|--------------------------------------|----------------------------|
| 1. .060 Fusion .1875 Float | .05 | .32 .36 | .92 (Base) | .68 | 1.0 |
| 2. .060 Fusion .1875 Float | .01 | .40 .36 | .945 \$-.20 | .56 | .82 |
| 3. .085 Fusion .1875 Float | .05 | .45 .36 | .91 \$+.08 | .89 | 1.3 |
| 4. .085 Fusion .1875 Float | .01 | .57 .36 | .94 \$-.16 | .77 | 1.1 |
| 5. .070 Clear Float .1875 Float | .07 | .17 .36 | .90 \$+.16 | .69 | 1.0 |
| 6. .070 Low Iron Float .1875 Float | .05 | .19 .36 | .915 \$+.04 | .59 | .87 |
| 7. .070 Very Low Iron Float .1875 Float | .01 | .23 .36 | .943 \$-.18 | .41 | .60 |
| 8. .085 Clear Float .1875 Float | .07 | .18 .36 | .89 \$+.24 | .78 | 1.1 |
| 9. .085 Low Iron Float .1875 Float | .05 | .20 .36 | .91 \$+.08 | .64 | .94 |
| 10. .085 Very Low Iron Float .1875 Float | .01 | .25 .36 | .94 \$-.16 | .45 | .66 |

27

ASSUMPTIONS:

.05% Fe content cost 10% more than .07%

.01% Fe content cost 25% more than .05%

2.1.3 D-3 Drive Optimization

Drive cost optimization was effected by component integration and design changes made to reduce the number of parts and thus minimize related material and labor. Areas optimized included the azimuth turret bearing, harmonic drive wave generator, input gear reducers in both azimuth and elevation, and the elevation linear actuators.

Azimuth Turret Bearing

This bearing supports the reflector assembly and transfers the system overturning moment from the azimuth housing into the pedestal. The baseline design is a four-point contact ball bearing with the inner and outer races partially contained by precision bores in the bearing retainers. The Subsystem Research Experiment units used this design. The alternative designs which were studied are shown in Table 2-4. The modification of the baseline bearing retainers is a simple change, and does result in some cost savings. It retains the design integrity and confidence obtained during the SRE Test program, and thus has been included in the Pilot Plant program. Increased cost savings, ease of assembly, and effective design integration can be obtained with the wire race bearing, and so it was recommended for the prototype design.

Harmonic Drive Wave Generator

The baseline design incorporates an Oldham coupling to compensate for misalignments between the rigidly supported input drive shaft and the circular spline. An alternative design is to attach the drive shaft rigidly to the wave generator plug (no Oldham coupling) and support this assembly by a small bearing at one end and by the wave generator bearing at the other end. The runout of the shaft at the wave generator bearing is larger than would be achieved by a conventional bearing installation, but it is not excessive and can be accommodated by a very slight increase in backlash in the input helicon gear stage. The alternative design eliminates the coupling and is therefore more cost-effective than the baseline design.

Table 2-4

AZIMUTH TURRET BEARING TRADES

| Design | Description | Comment |
|--|--|--|
| 1. Baseline bearing with modified retainers | Bearing races completely contained and supported by the azimuth housing (outer) and by the harmonic drive circular spline (inner). | Eliminates precision bores in the bearing race retainers. |
| 2. Baseline bearing with extra thick races (inner and outer) | Attaching bolts will be able to pass through holes in the races and thus clamp the bearing into the proper position. | Eliminates the bearing race retainers but overall assembly is not cost-effective. |
| 3. Baseline bearing with integral inner race | The harmonic drive circular spline will act as the inner race for the bearing. | Eliminates the bearing inner race; however, practical integration problems were encountered which would probably nullify its cost-effectiveness. |
| 4. Wire race bearing | Four-point contact ball bearing utilizing wire rings as races. The circular spline and split housing act as integral retainers. | Low-cost bearing with relatively simple assembly procedure. |

Input Gear Reducers

The input gear reductions in both azimuth and elevation incorporate a gear box integral with the drive motor and a worm/worm gear combination. An alternative approach which has proven to be cost-effective is to substitute a single-stage helicon gear set reducer. This eliminates one stage of reduction and allows the use of a simple drive motor rather than a more expensive gear motor. Reduction ratios must be carefully selected, however, to obtain a reasonable tooth size.

Elevation Linear Actuators

In the initial evaluations, cost studies indicated that it would be advantageous to use a machine screw jack for the stowage actuator and a ball screw jack for the tracking actuator. Due to lower efficiencies of the machine screw unit, however, it was found that a larger drive motor would be required, thus reducing its cost-effectiveness. Continued studies revealed increased cost savings based upon ball screw commonality, and so it became apparent that the best approach would be to use ball screw jacks for both tracking and stowage.

2.1.4 D-4 Control Optimization

Advances in microcomputers and optical fiber transmission have enabled the heliostat controls to be modified to improve reliability and lower costs. The prototype control system consists of a master control, a heliostat array controller, a data distribution interface, and a heliostat controller. The master control and the heliostat array controller are designed to coordinate the activities of the individual heliostats. They are located in the central control building along with peripheral equipment.

The heliostat array controller communicates with a series of data distribution interfaces, which distribute information to the heliostat controllers. Each interface receives control commands from the heliostat array controller and distributes them to its 300 assigned heliostats. The data distribution interfaces are collocated throughout the field with the transformers.

No control calculations are made by the master control or the heliostat array controller. New developments in the microcomputers enable each heliostat controller (at the top of the pedestal) to make appropriate calculations and

carry out the necessary readjustments. To make these calculations, the heliostat controller receives base information from the master control and position information from encoders mounted in the motor housing.

This control decreases the overall system cost, and makes it possible to eliminate the field controllers which once handled calculations and command jobs in the baseline design. The microcomputers used in the heliostat controller will be capable of receiving serial information from the master control and returning serial reply information without the need for external circuitry. The microcomputers will contain a nonvolatile random access memory, so that absolute encoders will not be needed for position indicators. Incremental, magnetic encoders will be designed into the motors with short data lines transmitting position information to the memory elements in the heliostat controller.

The drive interface was also revised so that the drive components would be located in the motor housing. This would alleviate the alternating current noise problems in the heliostat controller and reduce the size of the wire interfacing the controller and the motors. This concept prevents close contact between the microcomputer and the three-phase power observed in earlier designs.

All components will operate from a 5-volt modular power supply instead of from the earlier discrete multivoltage units.

The data communication links also reflect changes resulting from new technology. The links are designed using an optical transmission medium. The unique advantage of optical transmission over electrical hardwire transmission makes its use attractive in performance and cost. Optical fiber transmission offers a wider bandwidth and smaller cable cross section than previously possible. In addition, since cables employing optical transmission neither pick up nor emit electromagnetic radiation and offer total electrical isolation, the problems of radiofrequency interference, electromagnetic interference, electromagnetic pulse, ground loops, and sparking associated with electrical cables can be eliminated. In addition, fiber optics communication links eliminate the requirements for relays and line drivers and receivers in the communication lines. This also allows the data communication lines to be housed in the same cables with the power being delivered to the heliostats.

Two types of power distribution systems layouts, radial and secondary network, were considered for the 100 MW Pilot Plant (Figure 2-2). Both systems feature high-voltage primary feeders to transformers located throughout the heliostat field to avoid the need for long, low-voltage lines (600 V) requiring large-gauge cable. Distribution systems consisting solely of low-voltage distribution lines were not found to be cost effective in the 10 MW plant study. Since the greater distances involved in the 100 MW plant would only aggravate this problem, low-voltage distribution was not considered.

The radial distribution layout is proposed for the 10 MW Pilot Plant. It consists of a high-voltage primary feeder from the central power distribution point to the transformers located throughout the field. Short-length, low-voltage branch circuits run radially from the transformers to the heliostats. The network distribution layout consists of a grid of low-voltage cable covering the field area with transformers located at the intersections of the grid. The heliostat branch circuits are then run off the grid to the heliostats.

The network distribution system is highly desirable from a reliability standpoint since the loss of a primary feeder or transformer does not cause the loss of any of the heliostats. Since each segment of the secondary mains is supplied by at least two circuits, the loss of any transformer or primary feeder does not cause a loss of power to any section of the secondary mains. Power continues to be supplied to the secondary mains by the remaining transformers and feeders. In the radial system, however, the loss of a transformer or primary feeder causes the loss of all heliostats fed by that transformer or feeder.

The network system is not at all desirable from a cost standpoint, however. The secondary mains require large-gauge, high-amperage cable without reducing the requirements of the branch circuit cable. This large increase in cable requirements along with increased trenching and installation costs makes the network system more than twice as costly as an entirely radial distribution system and therefore not cost-effective even with the increased reliability. Since the transformers and primary feeders have among the lowest failure rates of any of the components in the power plant system, the cost-to-reliability factor of the network system is reduced even more.

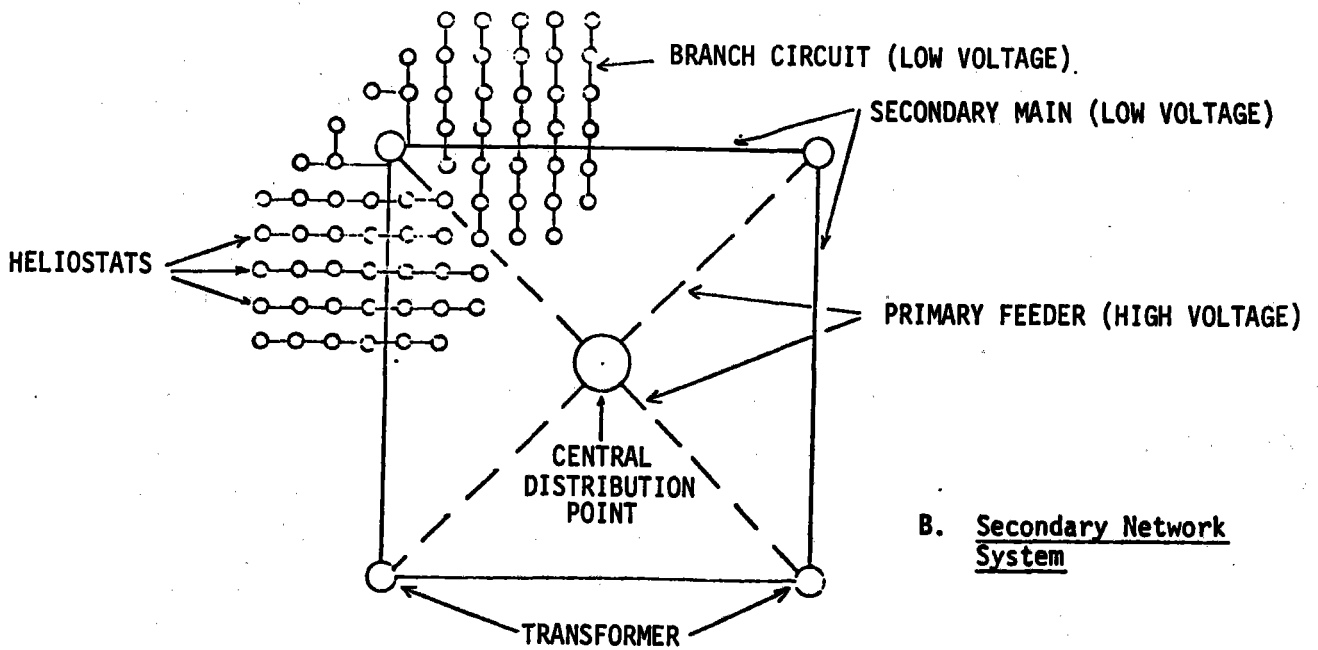
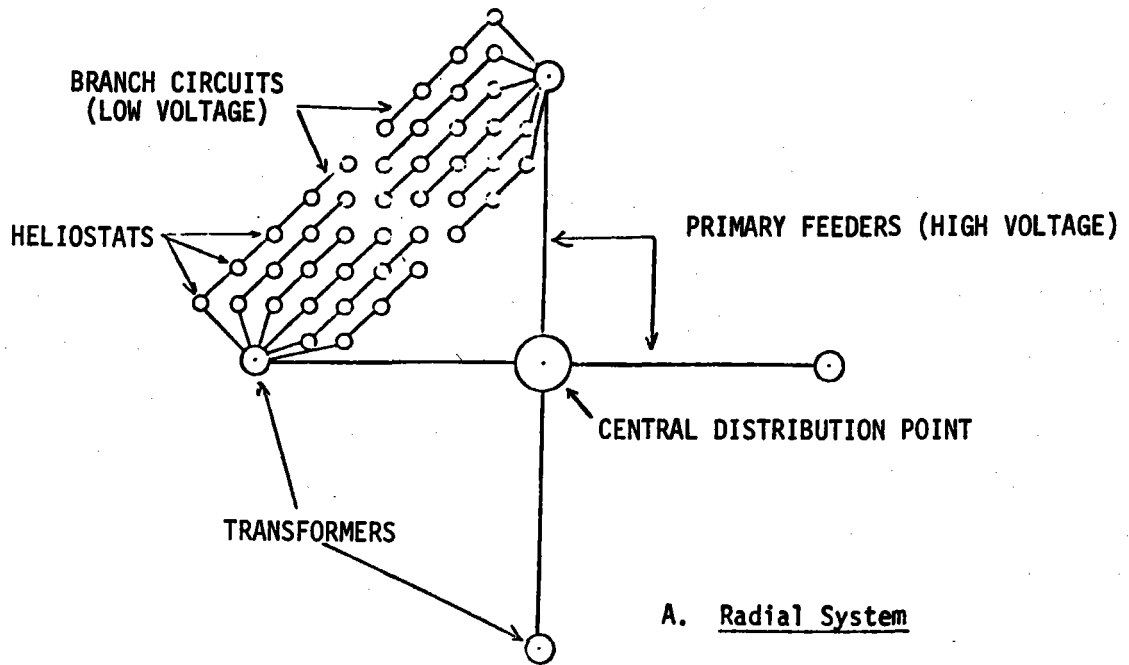


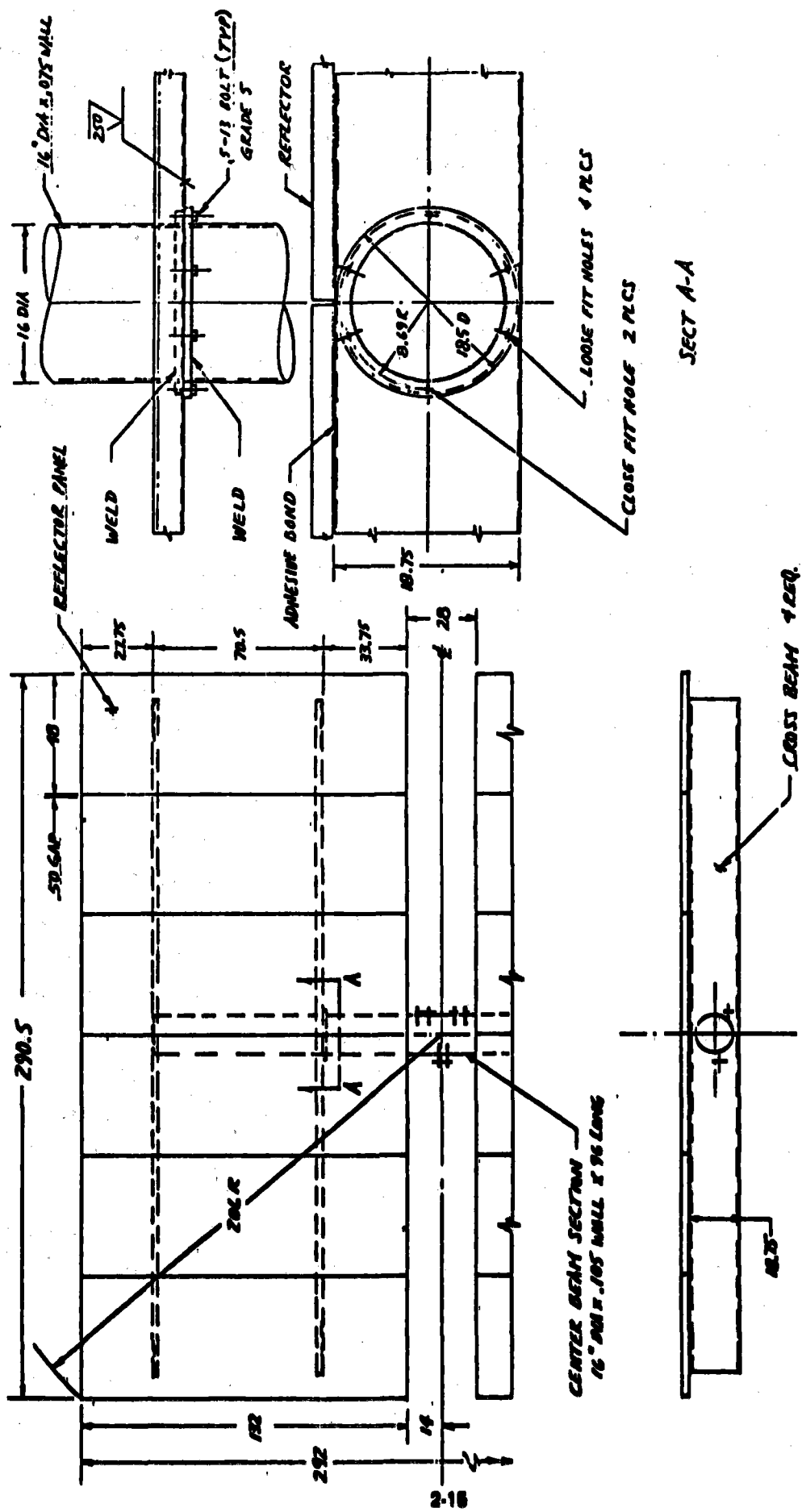
Figure 2-2. Reflector Panel to Torque Tube Joint

It is possible, however, to incorporate part of the reliability of the network system into the radial distribution system without increasing cost. This can be accomplished by making the branch circuits a continuous cable run from transformer to transformer rather than a strictly radial system. This hybrid radial system (see Section 2.3.5) is not totally redundant, but would provide redundancy in the form of emergency operation to approximately 90 percent of the transformers in the field. With the hybrid system, the heliostats normally supplied by a transformer which has failed are not supplied sufficiently for complete operation, as in the network distribution system, but can be operated in a stowage mode or other emergency procedures, which increases the operating safety of the field.

2.1.5 D-5 Reflector Attachment

This trade study was conducted to design joints along the main beam (torque tube). Joints in the main beam allow a reduction in tube size or wall thickness in the outboard section, which reduces material requirements. Joints that divide the reflective unit in half provide a manufacturing and shipping advantage since they allow the reflector to be preassembled in a size that can be transported over highways by common carrier. Preassembly eliminates the need for an assembly facility at the field site and reduces labor costs. In the field, the panels are merely located on the ends of the drive unit main beam section and bolted in place. Normally, no field adjustment would be required. The cost savings which can result from the elimination of the site assembly facility are very large compared to the cost savings in the structure. The initial baseline design had a continuous one-piece main beam made from 0.25-m (10 inches) diameter by 6.35-mm (0.25 inch) thick wall pipe. Placing a main beam at each side of the drive unit was originally considered, but since this required a large hole in the inboard cross beam, it was found more advantageous to make the joint at the inboard cross beam (see Figure 2-3). This design eliminates the large hole in the cross beam, which reduces the manufacturing cost, and also increases the strength and stiffness of the beam. Further, with the joint at this location, the bending moment is less and the joint can be lighter.

A reduction in diameter of the outboard main beam was studied, but it was found to be better to reduce the wall thickness and leave the tube diameter the same



NOTE: ALL DIMENSIONS IN INCHES.

Figure 2-3. Two Segment Reflector - Three Piece Tube

as the center section. The constant tube diameter design is lighter and makes a simpler, more efficient joint since the loads can be carried straight through the joint.

A slightly different joint was devised for a structural arrangement which had two diagonal channel beams outboard of the joint instead of the tube, as shown in Figure 2-4. In this joint, the eight attach-bolts are located four above and four below the structural centerline since the bending reactions from the diagonal beams are reacted more efficiently at the deepest section of the beam.

2.1.6 D-6 Reflector Support Structure Optimization

The trade study was conducted to reduce structural materials by optimizing beam sections. The effects of varying the size of the main beam (torque tube) were investigated, and it was found that larger-diameter tubes having thinner walls gave lower weights for equivalent stiffness. The results are given in Table 2-5. The main beam requires a moment of inertia of at least $68.7 \times 10^6 \text{ mm}^4$ (165 inches⁴). The table shows this to be provided by an 0.40-m (16-inch) diameter tube of 2.66 mm (0.1046 inch) wall thickness. The effects of increasing the depth of the cross beams and reducing the gage thickness were also investigated. Results are shown in Table 2-6. The deeper beams have lower weights, but as the gage thickness decreases, the lateral stability of the beam decreases. The cross beam selected is 0.976-m (18.75 inches) deep and 1.9-mm (0.0747 inch) thick.

The sizes selected for the tube and channel beams are near the optimum thickness to provide for minimum weight, while stiffening beads are included in the web to enhance the structural stability. Changes in structural geometry would be necessary to improve the stability for any further decrease in gage thickness.

Another approach to material reduction is to reconfigure the outboard section of the main beam so that it is divided into two beams which run diagonally toward the corners of the reflector (see Figure 2-4). With this arrangement, the outboard beam is supported at two points with overhang on each end. This configuration allows the depth of the outboard beam to be considerably reduced since the overhang lengths and bending moments are reduced. The weight saved by this configuration relative to the tubular main beam and deep outer cross beam is 187 kg (426 pounds).

Table 2-5
MAIN BEAM DESIGN COMPARISONS

| Configuration | O.D. (In) | Wall Thickness (In) | Length (In) | Area (In²) | MOI (In⁴) | Bare Weight (Lb) | Galv. Weight (Lb) |
|---|----------------------|------------------------------------|------------------------|----------------------------------|---------------------------------|---------------------------------|----------------------------------|
| PDR Baseline (408 Ft²) | 10.25 | 0.250 | 206 | 7.854 | 98.2 | 458 | 469 |
| | 10.25 | 0.250 | 234 | 7.854 | 98.2 | 520 | 533 |
| | 14.0 | 0.1046 | 206 | 4.566 | 110.2 | 266 | 275 |
| Enlarged Inverted (528 Ft²) | 14.0 | 0.1046 | 234 | 4.566 | 110.2 | 302 | 320 |
| | 14.0 | 0.1196 | 234 | 5.215 | 125.6 | 345 | 363 |
| | 14.0 | 0.1345 | 234 | 5.859 | 140.8 | 388 | 406 |
| | 14.0 | 0.1495 | 234 | 6.505 | 156.0 | 431 | 448 |
| | 14.0 | 0.1644 | 234 | 7.146 | 171.0 | 473 | 491 |
| | 14.0 | 0.1875 | 234 | 8.136 | 194.1 | 539 | 556 |
| Prototype Heliostat (528 Ft²) | 16.0 | 0.1046 | 234 | 5.223 | 165.0 | 346 | 366 |
| | 16.0 | 0.1345 | 234 | 6.704 | 211.0 | 444 | 464 |
| Selected Design | 16.0 | 0.1046 | 83* | 5.223 | 165.0 | 123 | 130 |

*The selected design is terminated at the inboard crossbeams of the reflector panels.

Table 2-6

CROSS BEAM DESIGN COMPARISONS

| Configuration | Depth (In) | Width (In) | Thickness (In) | Length (In) | Area (In²) | MOI (In⁴) | Bare Weight-4 Beams (Lb) | Galv. Weight-4 Beams (Lb) |
|---|-----------------------|-----------------------|---------------------------|------------------------|----------------------------------|---------------------------------|---|--|
| PDR Baseline (408 Ft²) | 14.0 | 2.5 | 0.1196 | 240 | 2.39 | 62.0 | 510 | 526 |
| | 16.5 | 2.5 | 0.0897 | 240 | 2.004 | 68.12 | 530 | 552 |
| | 14.0 | 2.5 | 0.1196 | 272 | 2.39 | 62.0 | 735 | 758 |
| Enlarged Inverted (528 Ft²) | | | 0.0747 | 272 | 1.669 | 56.73 | 500 | 525 |
| | 16.5 | 2.5 | 0.0897 | 272 | 2.004 | 68.12 | 600 | 625 |
| | | | 0.1046 | 272 | 2.337 | 79.43 | 700 | 725 |
| Prototype Heliostat (528 Ft²) | 16.5 | 2.5 | 0.1046 | 272 | 2.337 | 79.43 | 700 | 725 |
| | | | 0.0747 | 272 | 1.837 | 78.35 | 548 | 575 |
| | 18.75 | 2.5 | 0.0897 | 272 | 2.206 | 94.08 | 658 | 685 |
| | | | 0.1046 | 272 | 2.572 | 109.71 | 767 | 794 |
| Selected Design | 18.75 | 3.0 | 0.0747 | 272 | 1.928 | 87.00 | 575 | 603 |

A trussed beam concept for reducing the cross beam material requirement is shown in Figure 2-5. A sizable weight reduction can be achieved for the cross beams by this design, but the fabrication costs increase and mostly cancel the savings resulting from reduced material. This design is therefore not considered economical.

2.1.7 D7 Low-Cost Motors

In the interest of designing a more efficient motor drive system, alternative motors were studied for the prototype heliostat array. A major portion of the study involved the alternatives available in supply voltage for the three-phase drive motors. The baseline configuration was designed to operate at 240 volts. At this voltage, a starting current of 124,000 amperes would be required for a 17,700-heliostat field. This poses the need for heavy-gauge wire for the distribution network. As an alternative, a 480-volt system was studied. The motors showed a slight decrease in manufacturing cost and require a smaller-gauge cable for power distribution.

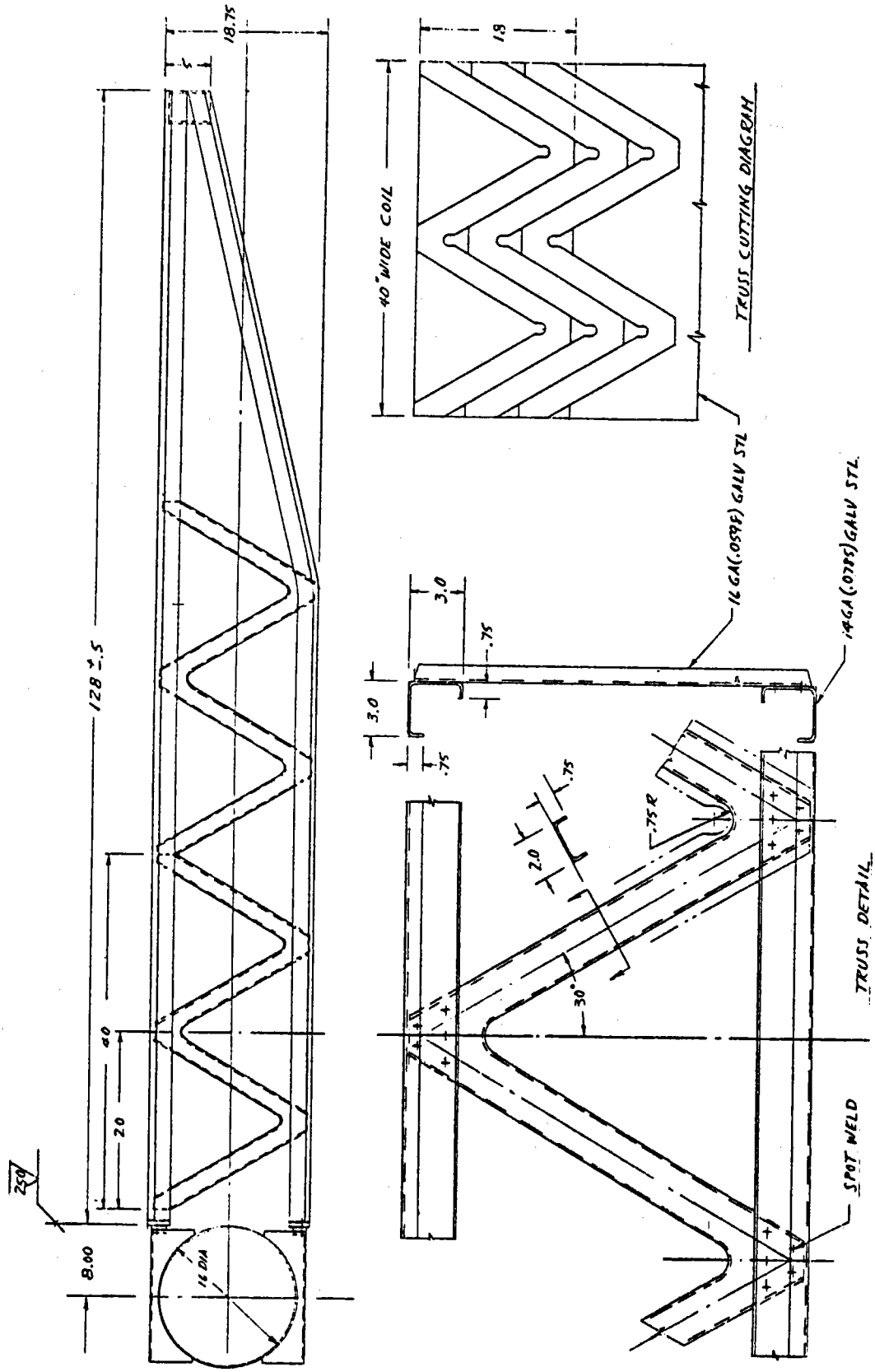
The asynchronous brushless motors studied also provided some promising characteristics. The DC motors proved to be high-torque motors with a stall torque of 0.47 kg-m (650 oz-inch), approximately twice that required for gimbal drive. The motors possessed smooth and fast acceleration and were capable of operating at very high speeds. Additional testing and study is necessary before the incorporation of these motors is considered.

2.2 BENCH MODEL AND COMPONENT TEST RESULTS

Two types of tests were conducted to support the trade studies and preliminary design: environmental tests and manufacturing techniques tests. Results are summarized below and presented in detail in Appendix D.

The environmental tests included:

- Salt spray test of candidate mirror module specimens, especially of the mirror silvering and protective coatings, to investigate accelerated, simulated weathering processes.



NOTE : ALL DIMENSIONS IN INCHES.

Figure 2-5. Trussed Cross Beam Design

- Hailstone impact tests to evaluate integrity of the mirror module designs for severe hail storms.
- Thermal cycling tests to evaluate thermal stresses and deformation of the reflector, including degree of permanent deformation.
- Backlighting tests to investigate the effects of mirror module back-side heating on the stresses and deformations in the glass due to differential expansion, caused when the reflector is in the inverted stowage position or backlit by adjacent heliostats.

The manufacturing tests included:

- Simulated procedures for bonding a mirrored panel to a glass panel to produce a laminated mirror module.
- Fabrication of relatively large modules of a size approaching that of the baseline mirror module, and measuring performance.

Significant results and conclusions are:

- A. Standard gray alkyd melamine mirror backing paint provides excellent protection for the mirror in the salt spray environment.
- B. A finish paint coating may enhance mirror survival.
- C. The polyurethane adhesive selected for the low-cost laminated mirror provides good mirror protection when the coating is continuous and seals the edges.
- D. The low-cost laminated mirror without backing paint must have the edges sealed.
- E. Both the low-cost laminated configuration and the corrugated-support configuration showed satisfactory hail performance.
- F. The stringer-supported configurations showed adequate resistance to thermal cycling. Thermal stresses were somewhat higher for the corrugated-support configuration.

2.3 PRELIMINARY DESIGN DESCRIPTION

The heliostat configuration resulting from the trade studies is shown in Figure 2-6. The configuration embodies improvements over the initial baseline design in a number of key areas including mirror module design, elevation actuator type, simplified azimuth drive, an open-loop control system based on emerging technology, and a tapered slip joint between the foundation and pedestal. A key feature of the configuration is its adaptability to low-cost assembly, transportation, and installation without a site factory operation.

The laminated mirror modules, each of which measures 1.22 by 3.35 m (48 by 132 inches), are assembled in groups of six on their respective support structure assembly to produce a reflector assembly which is 3.35 by 7.38 m (132 by 290.5 inches) in size (Figure 2-6). Two of these reflector assemblies are bolted to the main beam on each side of the drive unit to produce overall dimensions of 7.38 by 7.42 m (290.5 by 292 inches) with a slot 0.71 m (28 inches) wide down the middle. This gives a reflecting area of 49 m^2 (528 square feet). Each of the 12 laminated mirror modules is made by bonding a mirrored pane of 1.52-mm (0.060-inch) thick fusion glass to a pane of 4.76-mm (3/16-inch) thick float glass.

Each of the laminated mirror modules is stiffened with a pair of hat-section stringers, which are part of the support structure assembly and are bonded to the glass when the reflector assembly is fabricated. Each of the 12 stiffeners is attached to the two cross beams which run the long distance of the reflector assembly. Two diagonal, tapered beams attach the shallow outboard cross beam to the deep inboard cross beam where they attach to the tubular main beam. The diagonal beams tie into the outboard cross beam at two points 4.26 m (167.9 inches) apart. Each reflector assembly is bolted to a flange at each end of the main beam, which is a part of the drive unit.

The drive unit consists of an azimuth drive assembly, two linear actuator assemblies, a drag link, a short main beam, and the pedestal. Maximum rotation in elevation is 190 degrees, obtained with a double-jack system which is motor-driven. Maximum azimuth rotation is 540 degrees, obtained with a motor-driven helicon gear and harmonic drive mechanism.

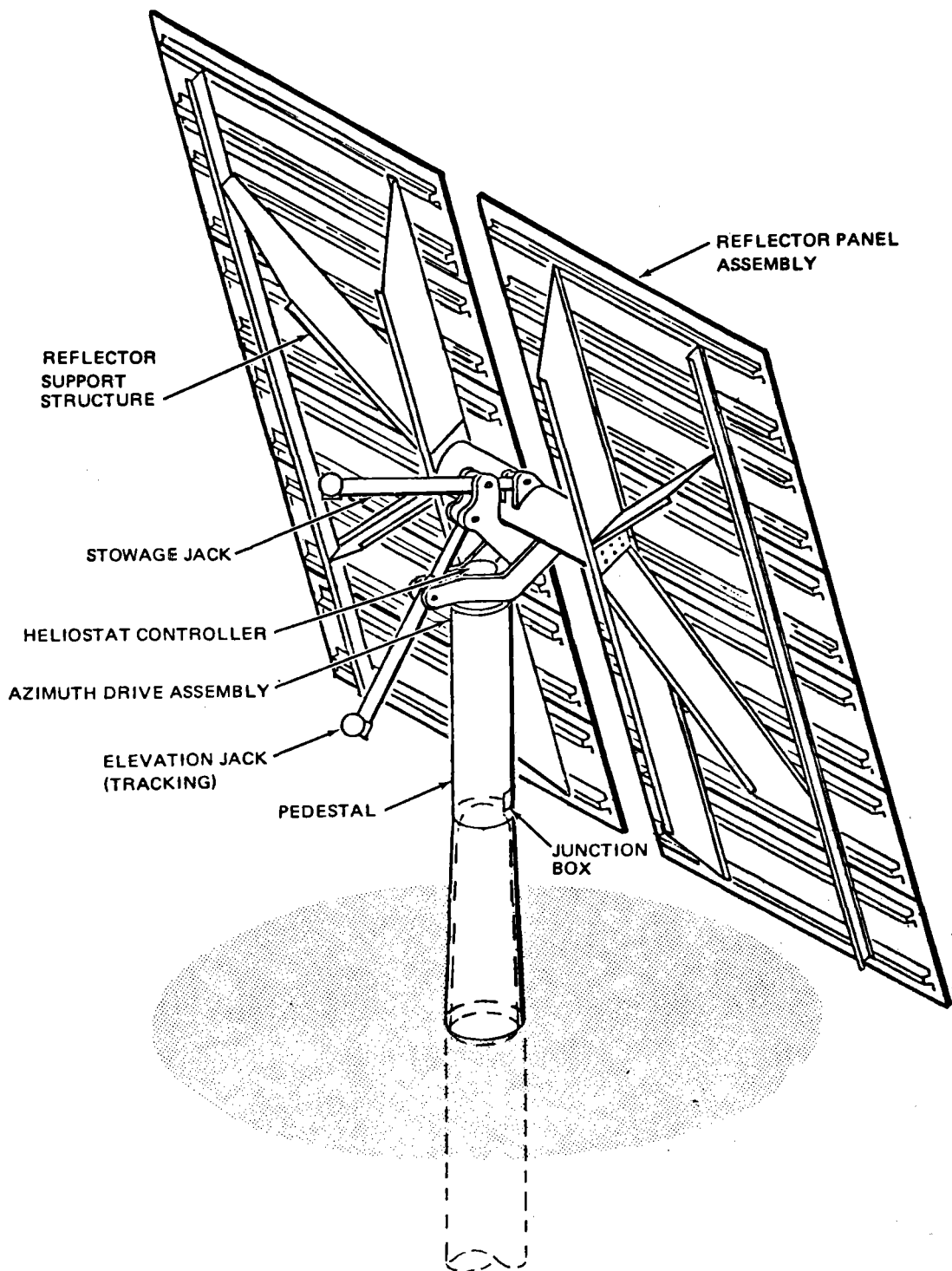


Figure 2-6. Primary Baseline Heliostat

The pedestal is a vertical tube 3.18 m (125 inches) high. At the top, the drive unit is welded to the pedestal; at the bottom, the lower 1.12 m (44 inches) is expanded to give a slight taper for slip-joint attachment to the rigid foundation. A weight summary for the heliostat is given in Table 2-7.

The heliostat electronics interfaces with the secondary power and data feeders at a junction box located on the side of the pedestal. The power and data cables interface with heliostat cabling through connectors and a circuit breaker. The cabling is routed through the hollow harmonic drive shaft to the heliostat controller located on the top of the azimuth drive unit. The heliostat controller makes all calculations necessary to operate the heliostat and execute tracking and stowage algorithms. The power cable is routed directly to the motor controllers located on each motor. The heliostat controller switches the motors on and off to execute the required number of motor revolutions. Motor revolution feedback is provided by Hall-effect sensors on the motors.

The field electronics interfaces with the system master control and the electric power generation subsystem. A schematic (Figure 2-7) of the data network illustrates the general flow of both networks. A collector controller may be used as a separate controller, or its functions may be incorporated into the master control. The collector controller commands operating modes, transmits and coordinates the reference time, and requests and receives data from the field on heliostat status.

The collector controller communicates with the heliostats through a series of data distribution interfaces. These interfaces provide a radial arrangement to minimize cable runs and data rates in the cables feeding the heliostats. Data from the collector controller are received and routed to one of 15 to 20 parallel data feeders, along which nominally are located 24 heliostats.

All of the data links utilize fiberoptics. The fiberoptics data link provides a nearly noise-free environment, eliminates the need for line drivers/receivers, and takes advantage of major cost reductions which can be reliably projected for the near future.

Table 2-7

WEIGHT OF HELIOSTAT

| | | |
|--|----------------------|---|
| Reflector Assembly | | 1256 Kg (2768 lbs) |
| Mirror Module (Lam. Glass only) | 787 Kg (1734 lbs) | |
| Steel Hat Sections | 152 Kg (336 lbs) | |
| Support Structure Assembly (Less Hats) | 317 Kg (698 lbs) | |
| Drive Unit Assembly | | 578 Kg (1273 lbs) |
| Center Main Beam | | 122 Kg (268 lbs) |
| Elevation Drive | | 102 Kg (225 lbs) |
| Jacks | 63 Kg (139 lbs) | |
| Motors | 9.5 Kg (21 lbs) | |
| Drag Link | 29.4 Kg (65 lbs) | |
| Azimuth Drive | | 185 Kg (407 lbs) |
| Housing | 108 Kg (238 lbs) | |
| Harmonic Drive Kit | 51.5 Kg (113.5 lbs) | |
| Motor | 8.6 Kg (19 lbs) | |
| Turret Bearing Retainer | 13.3 Kg (29.3 lbs) | |
| Turret Bearing | 3.2 Kg (7 lbs) | |
| Pedestal | | 169 Kg (373 lbs) |
| Total Heliostat Weight | | 1834 Kg (4041 lbs) |
| Total Heliostat Weight/Unit Area | | 37.39 Kg/m ² (7.65 lb/ft ²) |
| Foundation | | 5706 Kg (12,579 lbs) |
| Concrete | 5478 Kg (12,076 lbs) | |
| Steel Reinforcement | 194 Kg (428 lbs) | |
| Steel Form | 34 Kg (75 lbs) | |
| Heliostat Controller | TBD | |
| Field Wiring | Not applicable | |

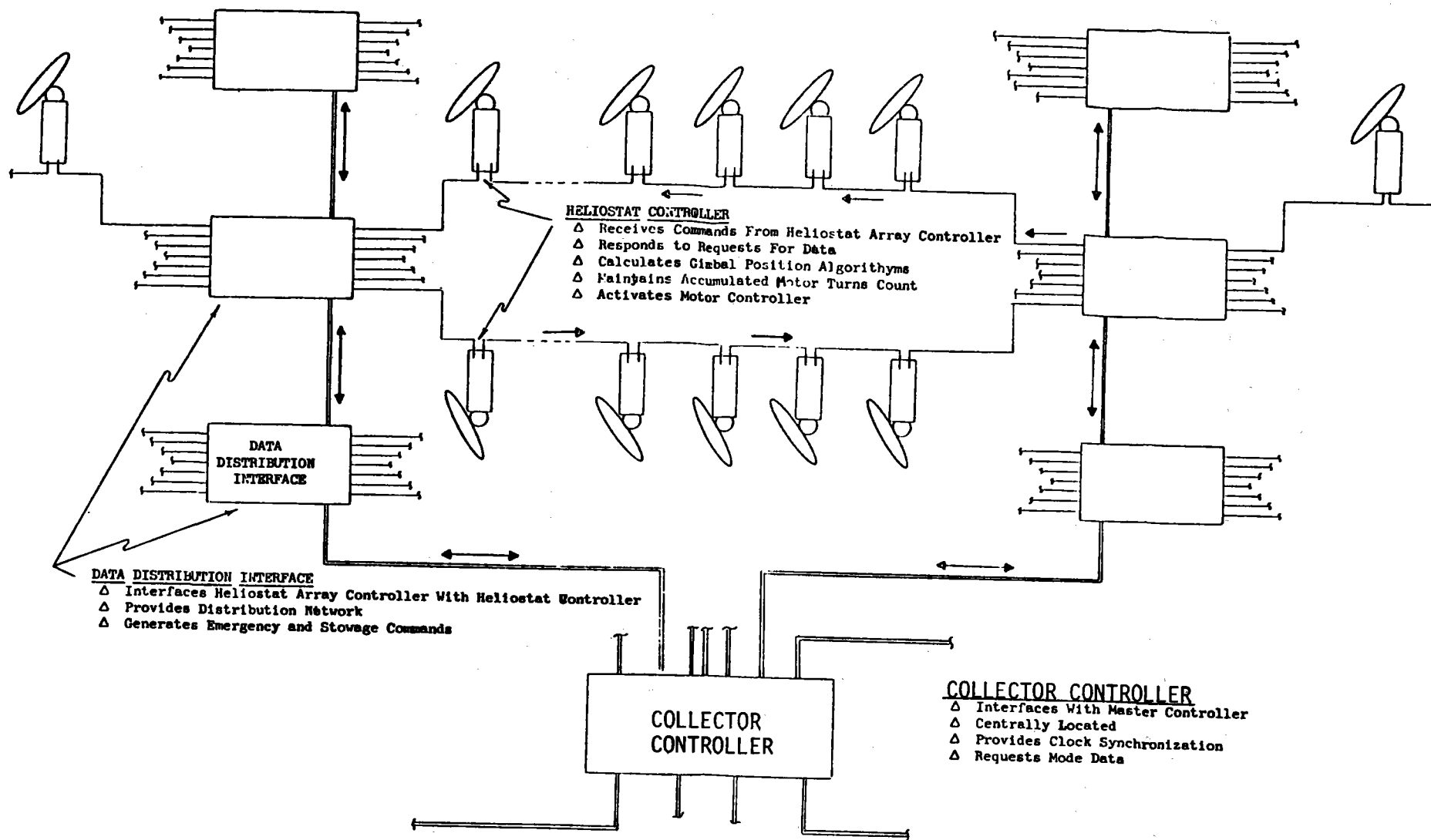


Figure 2-7. Data Distribution Network

The secondary data feeder connects each heliostat on the line in a series hookup. Data received by a heliostat controller are decoded and, if addressed to the heliostat, the data are retained and a message relayed onto the next heliostat, and hence to a data distribution interface at the end of the line. If the data are not addressed to the heliostat, the message is relayed to the next heliostat.

Power is distributed in a manner similar to that of the data. Power from the electric power generation subsystem is transmitted in a radial net to field transformers. Two to three transformers are located on each primary power feeder. The transformers are collocated with the data distribution interfaces. The transformers reduce the 4160-volt primary power to the 480-volt secondary feeder voltage.

The secondary feeders connect the heliostats in a daisy chain (through wiring with power tapped off for each heliostat). The chain is connected on each end to a transformer so that a failure of a transformer does not result in complete loss of power to any heliostat. The fiberoptics secondary feeders and the secondary power feeders are in the same cable.

The heliostats are capable of operating independent of the data network, except for commanding operating modes and updating time calculations. Hence, a failure of the data network would not result in the immediate shutdown of the affected portion of the heliostat field.

2.3.1 Reflector Panel Design Description

To facilitate the shipment of large assemblies from the manufacturing facility to the installation site, the reflector has been designed so that it can be built in two parts. Each identical reflector panel assembly is 7.38 by 3.35 m (290.5 by 132 inches) in its long directions and measures 0.524 m (20.65 inches) in maximum thickness. Two assemblies are connected together by the main beam at the installation area. This connection is made with bolts, and alignment is obtained with tapered close-tolerance holes and proper bolt placement and torquing. A detailed weight breakdown of this assembly is presented in Table 2-8.

Table 2-8

Detailed Weight Breakdown of Reflector Panel Assembly

| Part Name | Size and Material (Inches) | Wt. Per Unit (Lb) | No. Per Heliostat | Total Weight (lb) |
|------------------------------------|---|-------------------------|----------------------|----------------------|
| Mirror Front Sheet | 0.060 x 48 x 132, Fusion Glass | 35.74 | 12 | 428.82 |
| Mirror Back Sheet | 3/16 x 48 x 132, Float Glass | 111.67 | 12 | 1340.06 |
| Adhesive for Glass | t = 0.005, A = 48 x 132, 3M 1XA3504 | 1.36 | 12 | 16.35 |
| TOTAL for Mirror Module | | | | 1785.23 • |
| Hat-Section Stringers | A = 0.352, L = 130, 16 Ga. Galv. Steel Sheet | 13.76 | 24 | 330.20 |
| Outboard Cross Beam | A = 0.517, L = 285, 18 Ga. Galv. Steel Sheet | | | |
| Inboard Cross Beam | A = 1.928, L = 285, 14 Ga. Galv. Steel Sheet | 44.92 | 2 | 89.84 |
| Diagonal Beam | A = $\frac{1.864}{0.911}$, L = 110, 14 Ga. Galv. Steel Sheet | 163.25 | 2 | 326.50 |
| Joint Fitting | 1/4 x 12 x 32.1, Galv. Steel Sheet | 45.52 | 4 | 182.10 |
| TOTAL for Support Structure | | 41.45 | 2 | 82.90 |
| | | | | 1011.54 • |
| Adhesive for Assembly | t = 0.150, A = 1.5 x 130, 3M EC3532 | 1.26 | 24 | 30.19 • |
| TOTAL for Reflector Assy. | | | | 2826.96 ← |

2.3.1.1 Mirror Module

Each mirror module is made up of laminated glass, as shown in Figure 2-8. The front sheet is a 1.52-mm (0.060-inch)-thick pane of Corning fusion glass which is mirrored on its inner face. The mirror surface consists of chemically deposited silver, over which copper is flash-deposited. The sheet weighs 16.2 kg (35.7 pounds).

The back sheet is 4.76-mm (3/16-inch)-thick float glass. It weighs 50.7 kg (111.7 pounds). The two glass sheets are bonded together with a polyurethane adhesive (3M 1XA 3504) which weighs approximately 0.62 kg (1.36 pounds) per mirror module. The bonding technique must ensure edge sealing.

Each mirror module is supported by two sheet-steel hat-section stiffeners, which are actually part of the support structure and are bonded to the glass laminates at assembly. The thermal stresses and deflections (rotations) have been calculated by using the technique described in Appendix E. A summary of the maximums for the design is presented in Table 2-2, Column 8. The weight of each item making up the mirror module is shown in Table 2-8.

The mirror modules are assembled in groups of six, with a gap of 12.7 mm (0.50 inch) between each to produce a reflector assembly. Two reflector assemblies are subsequently joined by bolting to the center main beam, giving a reflector surface of 49.0 m² (528 square feet). A mirror surface in the central slot area, between the two reflector assemblies, may be cost-effective, but is not included in the present design, pending evaluation of wind tunnel test data showing the effect of the additional mirror area on heliostat loads.

- Glass Type Selection - In order to achieve high performance at low cost, glass with a high degree of flatness and with high transmission properties over the solar spectrum is required. Because of its high absorption characteristics, iron oxide content must be low and predominately Fe⁺⁺⁺. For these reasons, Corning fusion sheet glass (< 0.05 wt.% Fe), low-iron float glass (~ 0.05 wt.% Fe), and clear float glass (~ 0.08 wt.% Fe) were investigated. Corning fusion glass was selected because of its high reflectance properties (Table 2-9), its adequate flatness (Table 2-10), and reasonable costs. Although low-iron float may be flatter and the extrapolated value of reflectance

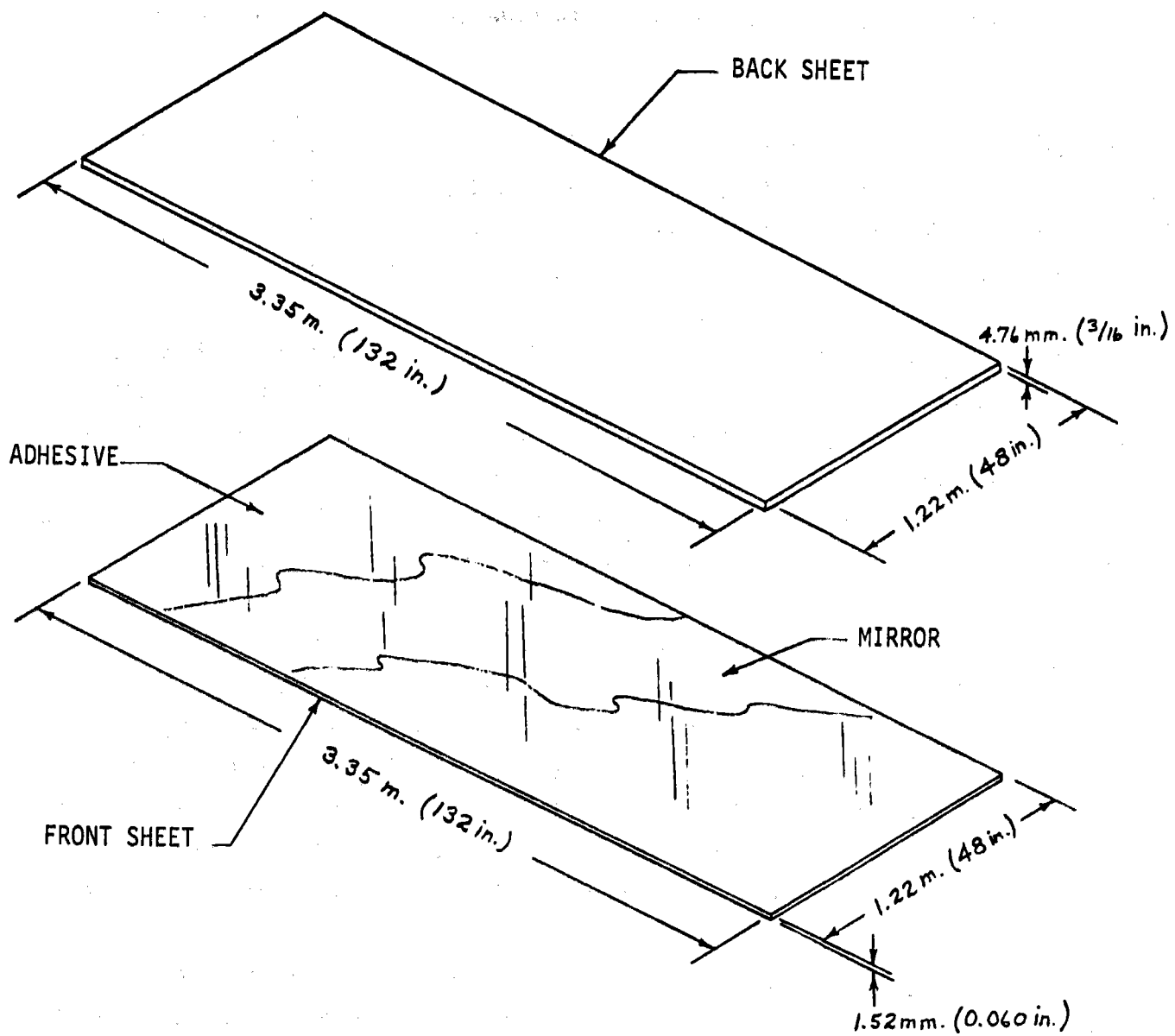


Figure 2-8. Mirror Module

Table 2-9
TOTAL REFLECTANCE EFFICIENCY OF MIRRORS
MADE FROM SELECTED GLASSES

| Specimen No. | Glass Type | Reflectance Efficiency at Selected Thickness | | | |
|--------------|----------------------|--|-------------|-------------|-------------|
| | | 1.5(0.060") | 2.1(0.083") | 2.4(0.043") | 3.2(0.125") |
| | Corning Fusion Glass | 95% ^(1,3) | | | |
| 1 | Low Fe Float | 94% ⁽²⁾ | | | 92% |
| 2 | Low Fe Float | 94% ⁽²⁾ | | | 92% |
| 3 | Low Fe Float | 94% ⁽²⁾ | | | 92% |
| 120-1 | Ford Clear Float | 90% ⁽²⁾ | 89% | | |
| 120-2 | Ford Clear Float | 91% ⁽²⁾ | 90% | | |
| 120-3 | Ford Clear Float | 91% ⁽²⁾ | 90% | | |
| 111-1 | PPG Clear Float | 91% ⁽²⁾ | | 88% | |
| 111-2 | PPG Clear Float | 91% ⁽²⁾ | | 88% | |

- NOTES: (1) Paper presented at ERDA Concentrating Solar Collector Conference, Georgia Institute of Technology, Atlanta, Georgia, Sept 26-28, 1977
- (2) Extrapolated data using curve in Paper presented at 1977 Annual Meeting of American Section of the International Solar Energy Society, Orlando, Florida, June 6-10, 1977.
- (3) MDAC measurements indicate a reflectivity of 98 percent for type 0317 Corning fusion glass.

Table 2-10

FLATNESS MEASUREMENTS OF VARIOUS GLASSES AND MIRRORS
 USING SCATTEROMETER APPARATUS

| <u>GLASS TYPE</u> | <u>MIRROR OR GLASS</u> | <u>THICKNESS MM (IN.)</u> | <u>RMS SLOPE ERROR (MRAD)</u> |
|--|----------------------------|-------------------------------|-----------------------------------|
| EDMONDS $\lambda/10$ OPTICAL FLAT | GLASS | | 0.059 |
| PPG CLEAR FLOAT | MIRROR | 3.2 (0.125 in.) | 0.074 |
| PPG LOW IRON FLOAT | MIRROR | 3.2 (0.125 in.) | 0.085 |
| PPG CLEAR FLOAT | GLASS | 3.2 (0.125 in.) | 0.144 |
| FORD CLEAR FLOAT | GLASS | 3.2 (0.125 in.) | 0.146 |
| PILKINGTON FLOAT NO. 3 | GLASS | 3.2 (0.125 in.) | 0.188 |
| FORD CLEAR FLOAT | MIRROR | 3.2 (0.125 in.) | 0.191 |
| CHEM-CORE SHEET (CORNING TYPE 0313 GLASS) | GLASS | 1.5 (0.060 in.) | 0.230 |
| SCHOTT B270 SHEET | GLASS | 3.0 (0.188 in.) | 0.290 |
| PILKINGTON FLOAT NO. 2 | GLASS | 3.2 (0.125 in.) | 0.315 |
| PILKINGTON FLOAT NO. 1 | GLASS | 3.2 (0.125 in.) | 0.350 |
| LOF SOLAR 90 SHEET | MIRROR | 3.2 (0.125 in.) | 0.560 |
| LOF SOLAR 90 SHEET | GLASS | 3.2 (0.125 in.) | 1.300 |

efficiency after silvering at a glass thickness of 1.5 mm (0.060 inches) approaches fusion glass, it cannot be made in that thickness. Currently, the thinnest float glass available is 2.1 mm (0.083 inch) thick, which would lower the extrapolated reflectance efficiency to 92 percent. In addition, float glass manufacturers are reluctant to produce low-iron float.

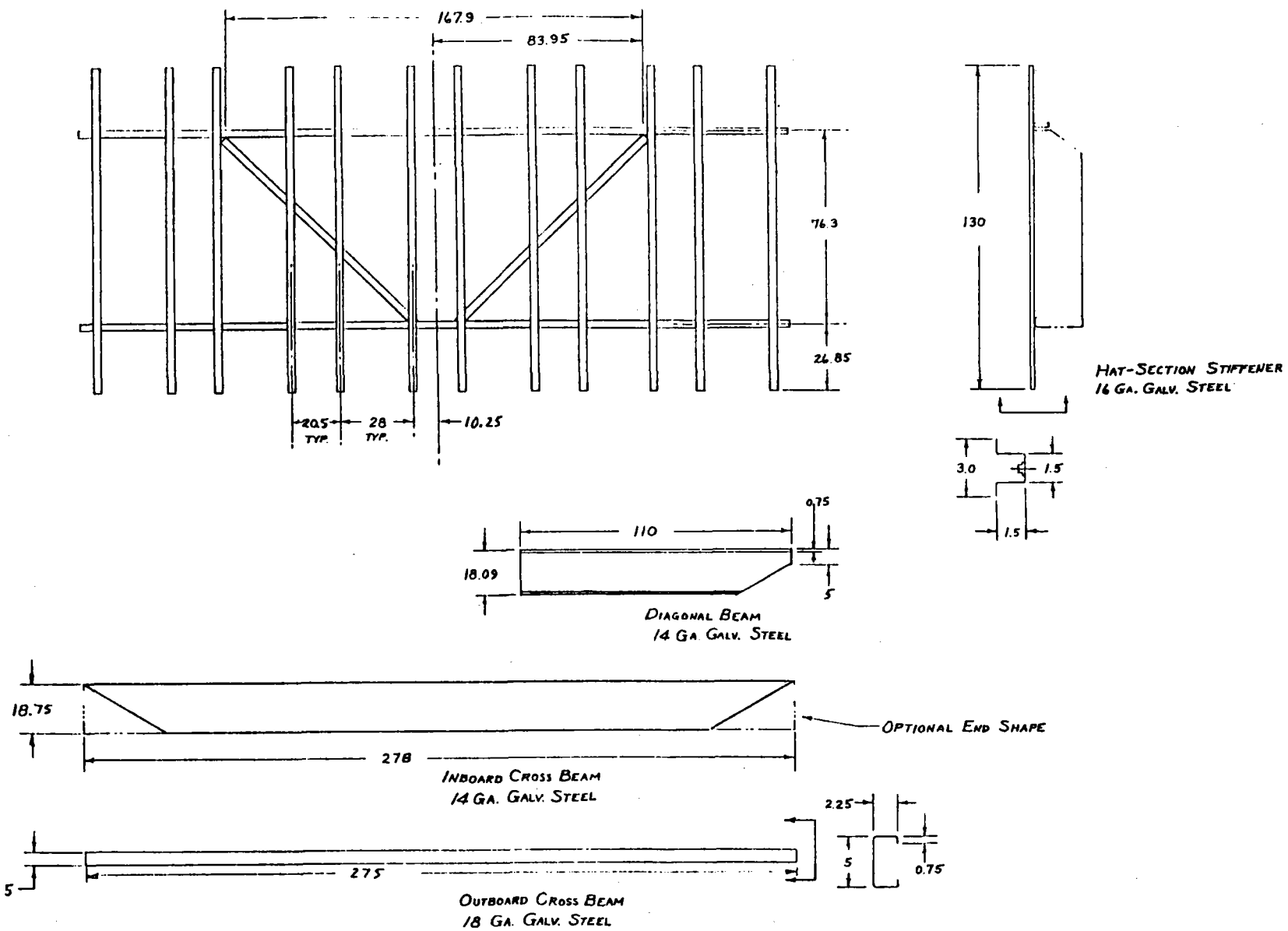
- Glass Thickness Selection - Although Corning sheet glass per pound is more expensive than float, the cost per square foot is lowered by producing the sheet as thin as possible for increased performance but still maintaining adequate hail resistance, handling capabilities, and stiffness under wind and thermal loads.

- Protection - Laminated mirrors traditionally have been thought of as offering the maximum protection for mirrors by putting glass on both sides. The recommended configuration does not use a mirror backing paint. The urethane adhesive appears to give good protection to the mirror. However, the salt spray tests showed that it is important to ensure that there is an edge seal. Where the adhesive extrudes from the mating surfaces and accumulates at the edges, it appears to provide an adequate seal. The production process must either ensure the adhesive extrusion or provide an edge seal of another form.

2.3.1.2 Support Structure

The reflector support structure must have sufficient strength to withstand combined wind, temperature, and gravity loads under all operating and stowed conditions. The stiffness in bending and torsion must be sufficient to limit the angular deflections of the reflector panels attached to the structure to the specified maximum. Throughout its life, the structure must resist environmental effects such as rain, snow, temperature changes, dust, humidity, and hail which occur in the field. Manufacturing and assembly costs must be low and the subassemblies of the structure must be easily transported from factory site to field location. The configuration of the structure should provide for inverting the reflector during plant shutdown periods.

The reflector support structure selected to meet these conditions is illustrated in Figure 2-9. Each of the laminated mirror modules is stiffened with



Note: All dimensions in inches

Figure 2-9. Reflector Support Structure Assembly

a pair of hat-section stringers which are part of the support structure assembly and are bonded to the glass when the reflector is assembled.

The two hat-section stiffeners are 7.62 cm (3.0 inches) wide and 3.81 cm (1-1/2 inches) high. They are rolled from 16-gage galvanized steel sheet and are 3.30 m (130 inches) long. The two legs are bonded to the glass back sheet along their full length. If necessary, the entire back surface of the reflector assembly may be painted white to reduce heat absorption during inverted stowage. Each stringer weighs 6.24 kg (13.8 pounds).

The twelve hat-section stiffeners are attached to the two cross beams which run the long distance of the reflector assembly. The deep, inboard cross beam is a rolled C-channel of 14-gage galvanized steel sheet, 0.476 m (18-3/4 inches) deep and 7.62 cm (3.0 inches) wide, with 1.59 cm-(5/8 inch)-wide return flanges, as shown in Figure 2-10. Two beads are rolled into the web of the channel to give it stability. The channel serves to transfer the wind and dead weight loads on the mirror panels into the main beam. This beam weighs 74.1 kg (163.3 pounds).

The shallow outboard cross beam is a rolled channel of 18-gage galvanized steel sheet, 12.7 cm (5.0 inches) deep and 5.72 cm (2-1/4 inches) wide, with 1.91 cm-(3/4 inch)-wide return flanges. This cross beam is attached to the main beam by diagonal frames (beams) which tie into this cross beam at two points 4.26 m (167.9 inches) apart. The outboard cross beam weighs 20.4 kg (44.9 pounds).

The diagonal outer beams which connect the outboard cross beam into the main beam are formed of 14-gage galvanized steel sheet. They are constant-section channel beams 0.476 m (18-3/4 inches) deep for most of their length. The outer 0.5 m (20 inches) are scarfed at an angle of 30 degrees. These diagonal beams are 6.35 cm (2.5 inches) wide with 1.91 cm (3/4 inch) return flanges.

The shear force exerted on the outboard cross beam is carried through the structure by shear in the beam webs and appropriate angle connections at the ends of the diagonal main beams, as shown in Figure 2-11. The angles are spot-welded to the beams, and the flanges of the diagonal beams are also spot-welded to the flanges of the inboard cross beam.

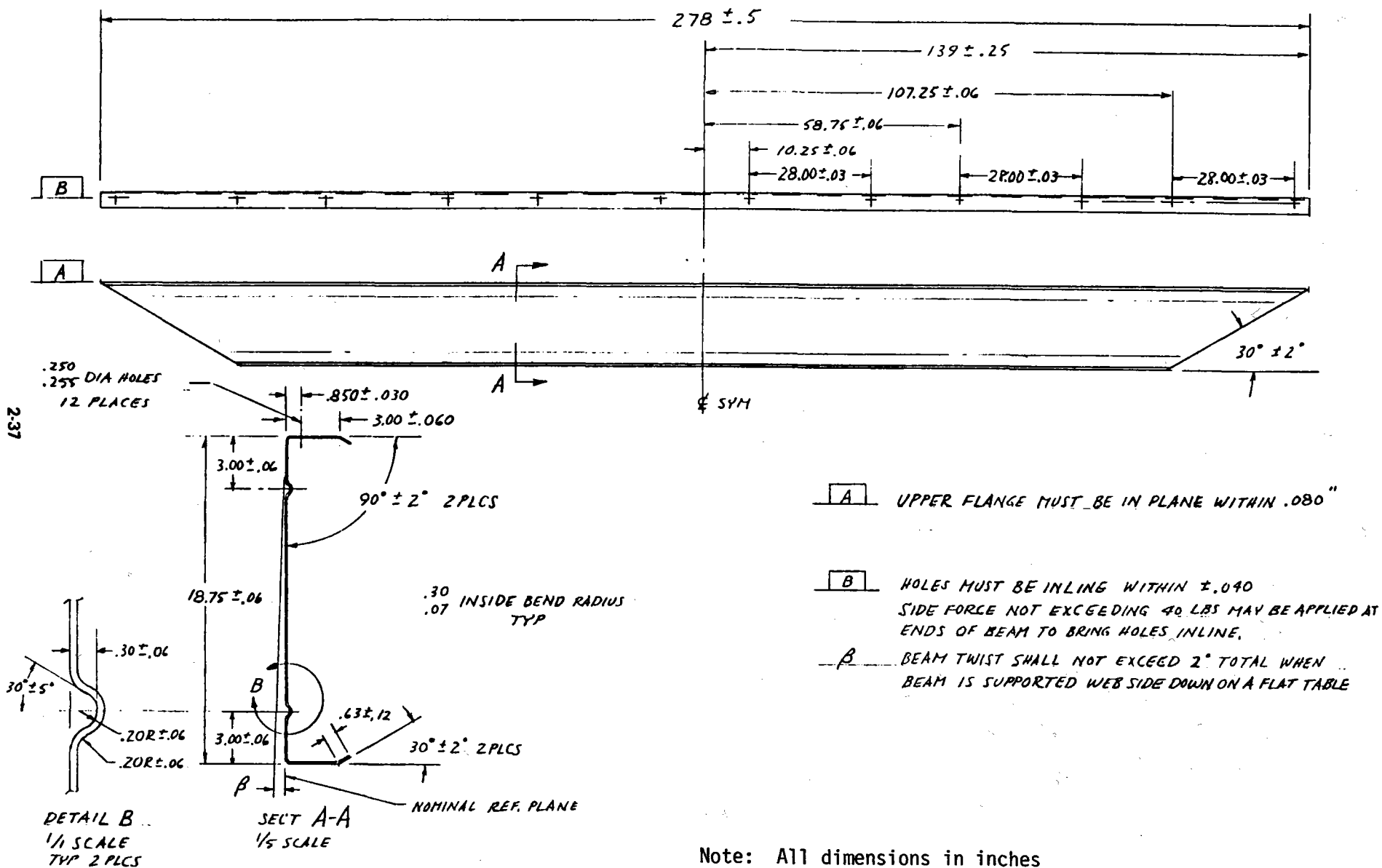


Figure 2-10. Cross Beam - Low Cost Heliostat

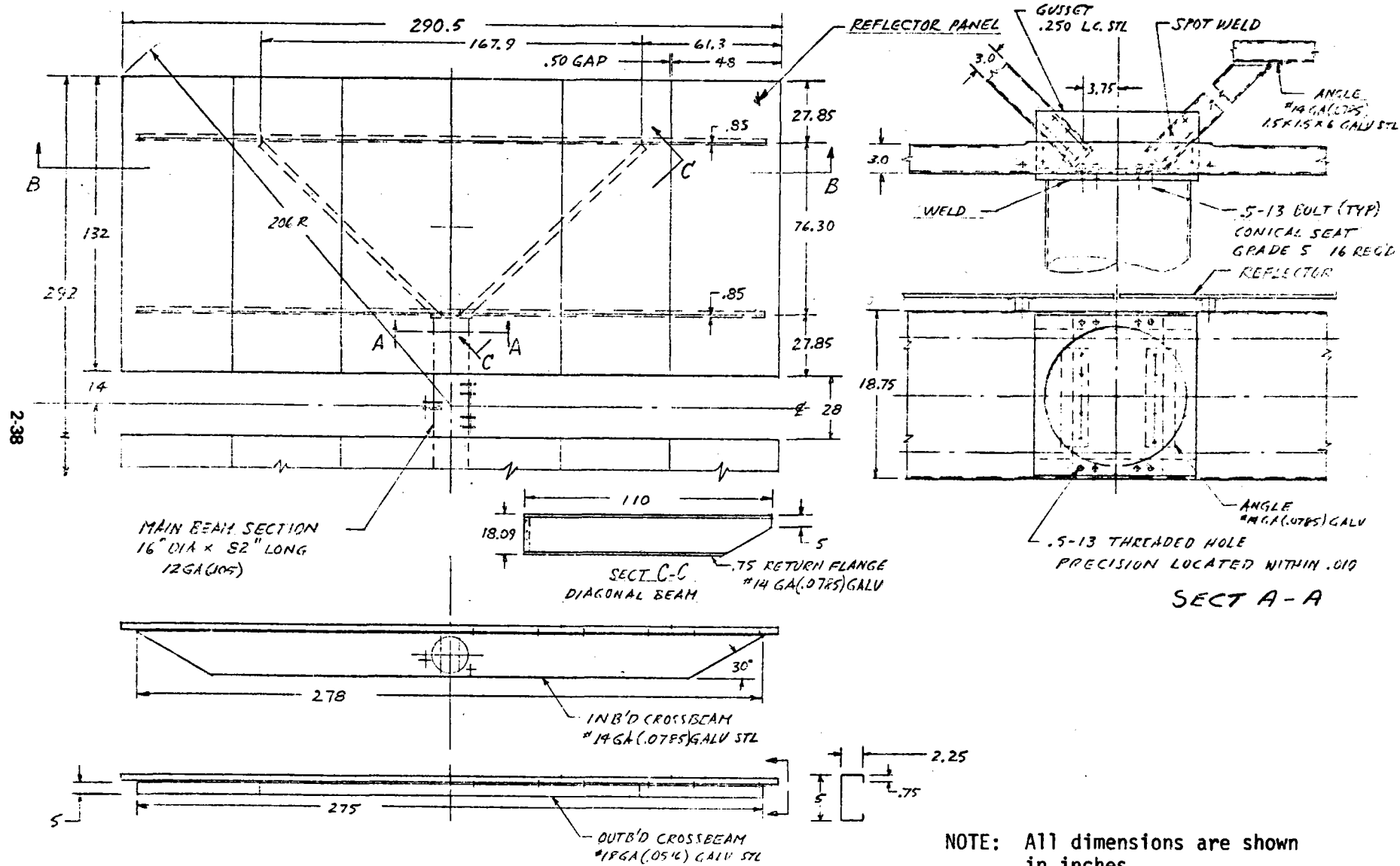


Figure 2-11. Tubular Center Beam - Channel Outer Beam

The weight of each item of the support structure is given in Table 2-8. The stress analysis of the support structure uses the airload distributions of MDAC Report MDC G6477, dated September 1976, Page 19, to calculate the airloads on the panels and support structure. Regular engineering procedures, as stated in the latest issue of the Uniform Building Code, have been used to calculate the stresses in each structural item and its allowable stresses.

The accuracy of the surface formed by the hat stiffeners will be held within 2.0 mm (0.080 inch) to limit the adhesive bond thickness to a maximum of 3.0 mm (0.12 inch) during assembly.

The following table summarizes the adhesives used for the prototype heliostat low cost laminated mirror module. Both the adhesives are a two part polyurethane containing the silicone additive and manufactured by the 3M Company.

| <u>Bonded Part</u> | <u>Adhesive No.</u> | <u>Adhesive Application</u> | | <u>Pressure Application</u> | |
|-------------------------------|---------------------|-----------------------------|------------------------------|-----------------------------|-----------------------------|
| | | <u>Method</u> | <u>Rate</u> | <u>Method</u> | <u>Amount</u> |
| Mirror to Glass Substrate | 1XA3504-2 | Spray | .04 lb/ft ² | Nip Roller | 25-50 lb/in Width of Roller |
| Laminated Mirror to Stringers | EC3532 | Extrude | .08 lb/ft Length of Stringer | N/A | |

2.3.1.3 Reflector Panel Assembly

The reflector panel assembly is made by bonding six mirror modules to the steel support structure (see Figure 2-11). The mirror modules are supported in position on a fixture, adhesive is applied, and the support structure is positioned over the mirrors so that the hat stiffeners contact the adhesive. The polyurethane adhesive 3M EC 3532 forms a thick bond which levels out structural tolerances and cushions the glass. After the adhesive cures, the assembly is ready for shipping. The overall size of the completed panel is 3.35 m (132 inches) by 7.38 m (290.5 inches). The joint to the main beam is accurately controlled so that the panel assembly is positioned within 0.5 mrad when the bolts are tightened. Rotational position is also controlled within 0.5 mrad by tapered holes in the frame which are indexed by conical bolts in the main beam assembly.

The completed reflector panel will be held to an angular deflection error of 1.0 mrad over 90 percent of the reflector. Past experience with bonded glass/steel structures shows that 1.0 mrad is achievable.

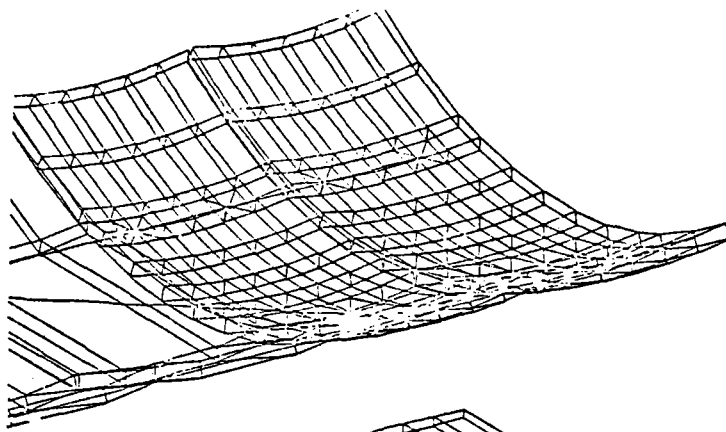
The structural analysis of the reflector panel assembly used the NASTRAN (NASA Structural Analysis) computer program, a finite-element program developed for general structural analysis of complicated structures. A mathematical model of the reflector panel assembly was formulated and physical properties assigned to each of the 502 elements and 3238 connections. Loading conditions included wind, gravity, and temperature changes and combinations of these. The output of this program includes internal forces, stresses, deflections, and rotations for each element. In addition, plots of the deformed shape of the structure under each loading condition can be obtained. Typical plots are shown in Figure 2-12.

2.3.2 Drive Unit Assembly

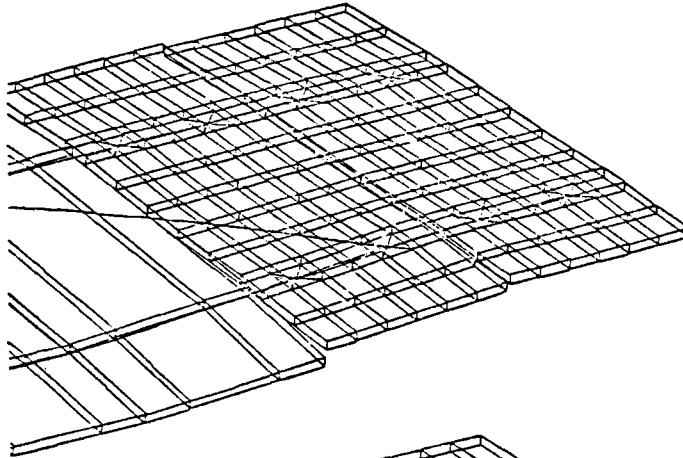
The function of the drive unit assembly is to rotate the heliostat mirror about the azimuth and elevation axes. The drive unit will be operated for solar tracking, emergency slewing, stowage, and maintenance activities. The major performance requirements are given in Table 2-11.

With the azimuth travel capacity of ± 270 degrees, there is no need to configure the drive unit as a function of position in the field. The 180 degrees of travel about the elevation axis is required to permit the mirror to be stored in an inverted position. Excessive operating loads are avoided because the mirror can be stowed in less than 15 minutes in rising wind conditions. This rate capability, with respect to the South field singularity, coupled with appropriate control algorithms, will maintain the necessary beam accuracy during turnaround of the heliostat at the azimuth.

The design life of the drive unit is 30 years. Every day the drive unit will move the mirror from a stowed position to acquire the sun, track the sun during the day, and then return the mirror to its stowed position at the end of the day. This life will be achieved without any scheduled maintenance activity.

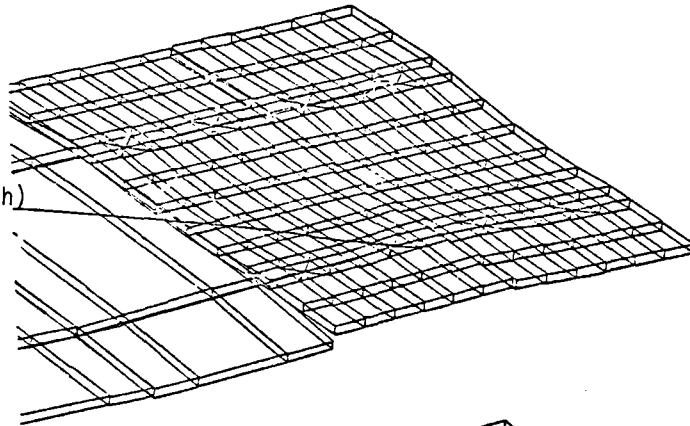


TEMPERATURE - WARMUP
 $T = 50^{\circ}\text{C} (120^{\circ}\text{F})$



GRAVITY
 $\alpha = 30^{\circ}$

WIND - $\alpha = 30^{\circ}$
 $V = 14 \text{ m/sec (26 mph)}$



COMBINED = TEMP + GRAVITY
 + WIND
 $\alpha = 30^{\circ}$

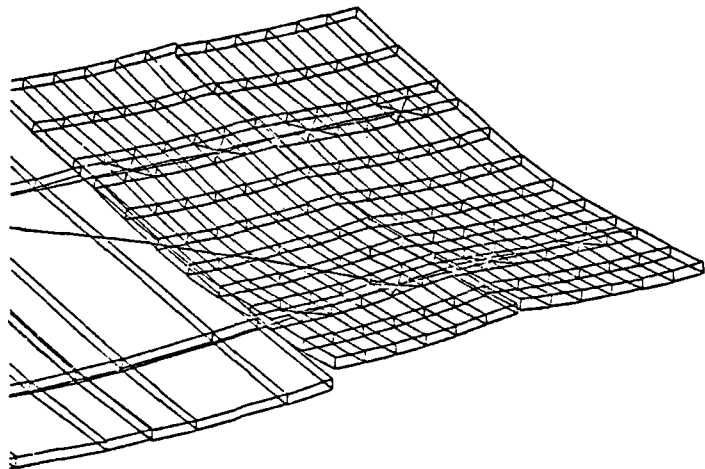


Figure 2-12. Typical NASTRAN Mirror Module Deformed Plots for Operational Conditions

Table 2-11
DRIVE UNIT REQUIREMENTS

| <u>Requirement</u> | <u>Azimuth</u> | <u>Elevation</u> |
|----------------------------------|--|---|
| ● Travel | ± 270° | 0 to -180° |
| ● Maximum Travel Time Under Load | 180° in 15 minutes | |
| ● Maximum Static Load | 9830 N-m (87,000 in-lbs) | -32,650 N-m (-289,000 in-lbs) @ α = 0° |
| ● Maximum Starting Load | 10,050 N-m (89,000 in-lbs) | ± 13,890 N-m (± 122,900 in-lbs) @ α = -50° |
| ● Maximum Running Load | 10,050 N-m (89,000 in-lbs) | ± 26,790 N-m (± 237,100 in-lbs) @ α = -50° |
| ● Maximum Overturning Moment | 42,140 N-m (373,000 in-lbs) | |
| ● Backlash/Hysteresis | 1 mrad | 1.6 mrad |
| ● Back Drive | None | None |
| ● Life | 30 Years | 30 Years |
| ● Minimum Stiffness | 1.13×10^6 N-m/rad (1.0×10^7 in-lb/rad) | 1.516×10^6 N-m/rad (1.342×10^7 in-lb/rad) |

The drive unit assembly has been designed to meet these general requirements as well as those of Specification 001. The design is shown in Figure 2-13. The major components of the drive unit are an azimuth drive assembly, two linear actuator assemblies, a drag link, a torque tube, and the pedestal. Details of these components are discussed below.

2.3.2.1 Elevation Actuators

Two identical linear ball screw actuators acting in conjunction with the drag link cause the main beam assembly to rotate about the elevation axis. Each actuator (one for tracking and one for stowage) must have the capacity to rotate the torque tube 90 degrees to satisfy the requirement for a maximum

travel of 180 degrees. The stowing actuator is preloaded into a structural stop when the sun is being tracked, to eliminate its backlash from the system.

The jack is a translating type in which the ball nut and attached output rod translate as the jack's screw is rotated by the drive motor. Speed is reduced by a single input helicon gear stage (106:1) and when combined with the lead of the jack screw (6.35 mm [0.25 in]), results in an actuator travel of 0.06 mm (0.00236 inch) per motor shaft revolution. Related performance requirements are given in Table 2-12.

The jack incorporates an integral motor mount so that, with the pinion mounted on the motor shaft, the jack screw is completely housed and all the joints sealed for protection of the rotating parts from the external environment. A support tube extending from the trunnion fitting to the main housing provides a sealed cavity for the screw shaft and ball nut assembly. The actuation rod made from a corrosion resistant material is sealed with a cartridge containing a dual seal configuration. A scraper seal removes any solid contaminate on the rod and a wiper seal protects against entry of water or other liquid contaminate. The external scraper seal has a convex shape, thus preventing water puddling. Also, the jack attitude is normally at a sufficient angle to prevent collection of water in the seal area.

Reversing the jack mounting arrangement to allow the rod seal to be in a down position is not necessary or practical since this would necessitate a very long extension of the trunnion clevis attachments on the drive housing and drag link. The jack is grease-lubricated and no scheduled maintenance is planned during the 30-year life.

In order to meet this life requirement, a total of 10,000 cycles, as defined in Figure 2-14, must not cause the combined actuator backlash/hysteresis to increase more than 0.125 mm (0.005 inch), including wear in the actuator trunnion bushings and rod end bushing.

The jack assembly does not include position sensing equipment since the control system incorporates the necessary logic to provide complete limit protection.

Table 2-12
ACTUATOR REQUIREMENTS

| | |
|----------------------------------|---|
| ● Travel | 679.5 mm (26.75 in) |
| ● Maximum Travel Time Under Load | 679.5 mm (26.75 in) in 7.5 min. |
| ● Maximum Static Load | 96,100 N (21,610 lbs) |
| ● Maximum Starting Load | 30,300 N (6810 lbs) |
| ● Maximum Running Load | 58,450 N (13,140 lbs) |
| ● Backlash/Hysteresis | .261 mm (.0085 in) |
| ● Backdrive | None |
| ● Life | 30 Years |
| ● Fatigue Life | 322 cycles under 28,000 N (6300 lbs) |
| ● Minimum Stiffness | 1.313×10^7 N/m (75,000 lbs/in) |

During the various tracking scenarios, the reflector assembly gravity moment coupled with the wind loads will cause a reversal of moments about the elevation pivot. As a result, the tolerances associated with the jack and related attachments will affect the heliostat pointing accuracy. This effect is minimized by the following considerations:

- a) During tracking the gravity loads are predominate, thus negating any adverse affect of tolerance at the elevation pivot.
- b) During tracking, the stowage jack will be positioned into the stops, thus eliminating any adverse affect of its related tolerance.
- c) Machinable self lubricating bushings are used at each joint, thus permitting low tolerance designs. For example, at the jack trunnion fitting, the tolerance between the bushing and pivot pin is between 0.0005 and 0.0015 inch.
- d) Each joint configuration will be designed to maximize heliostat pointing accuracy while maintaining cost effective manufacturing and assembly procedures.

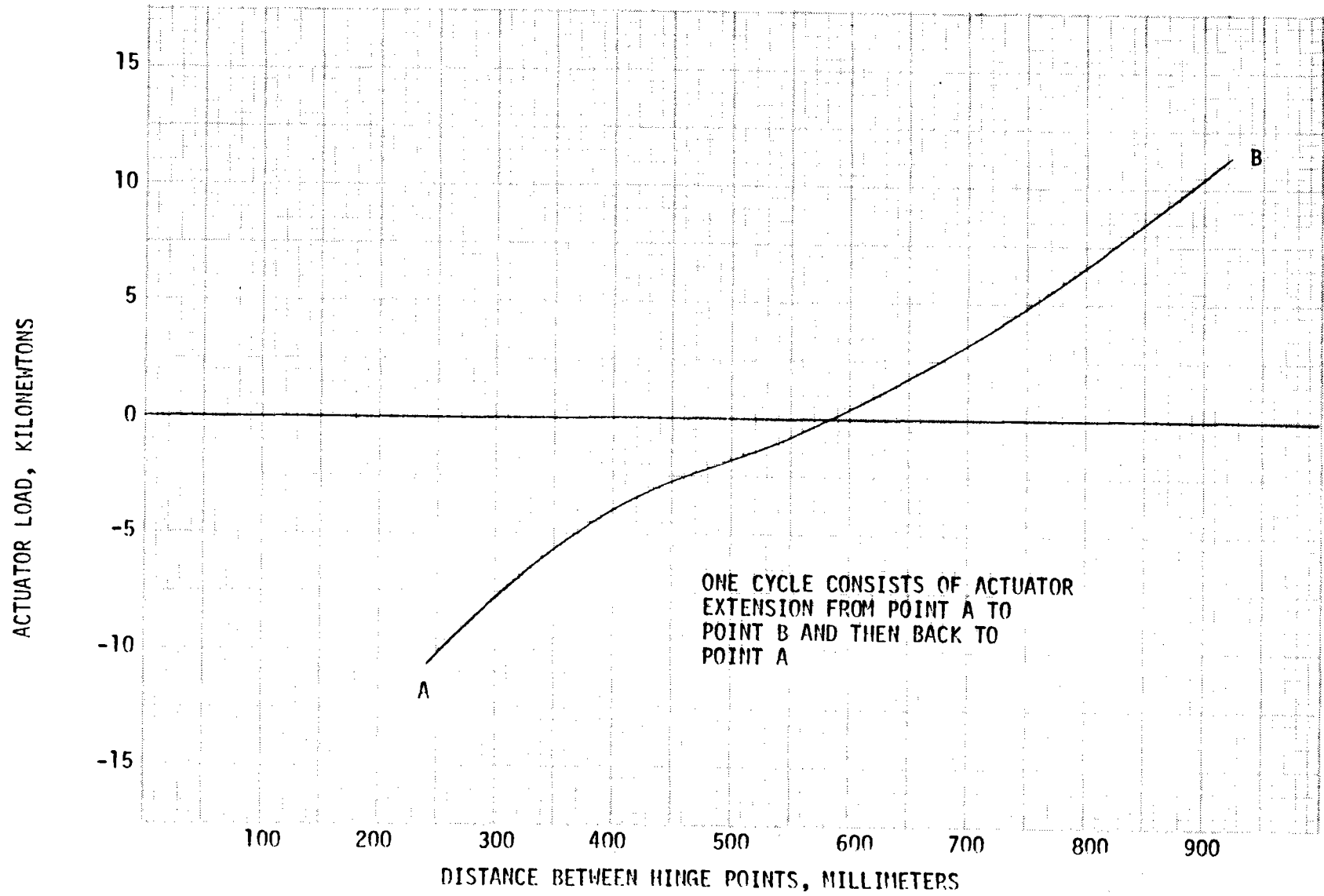


Figure 2-14. Duty Cycle for Actuator Wear Test

2.3.2.2 Azimuth Drive

The azimuth drive requirements were given in Table 2-11, and the azimuth drive is illustrated in Figure 2-15. The azimuth drive provides support for the tracking actuator trunnion hinge pins and the torque tube and drag link hinge. Drive components include the drive motor (see Section 2.3.2.5), input gear reducer, Harmonic drive (wave generator, flexspline, circular spline), housing, and turret bearing.

The input reduction stage is a helicon gear set (162:1) mounted integral with the motor shaft. It is self-locking, so the azimuth drive cannot be back-driven. The Harmonic Drive is essentially the same as the baseline with a 242:1 reduction, thus providing an overall azimuth reduction of 38,200:1. The Harmonic drive shaft is supported by the wave generator bearing at one end and a small ball bearing at the other, so an Oldham coupling is not required as part of the wave generator.

The azimuth housing which supports the torque tube assembly is machined from a low-carbon steel weldment and is zinc-plated for protection against corrosion.

The turret bearing, upon which the azimuth drive housing rotates, is made up of two outer wire races, two inner wire races, and a set of bearing balls. One of the outer races is contained in a counterbore in the housing, and the other in a counterbore in the bearing retainer. The inner races are supported in grooves in the circular spline. The bearing is preloaded by tightening the retainer attach bolts.

A standpipe extends up into the hollow Harmonic drive shaft. It is welded to a flat plate which covers the bottom of the circular spline. This arrangement allows the electrical cable to be routed through the Harmonic drive shaft. It also allows the wave generator bearing, circular spline teeth, and flexspline teeth to be lubricated by filling the cavity created by the inner diameter of the circular spline with oil. All other moving components in the drive are grease-lubricated.

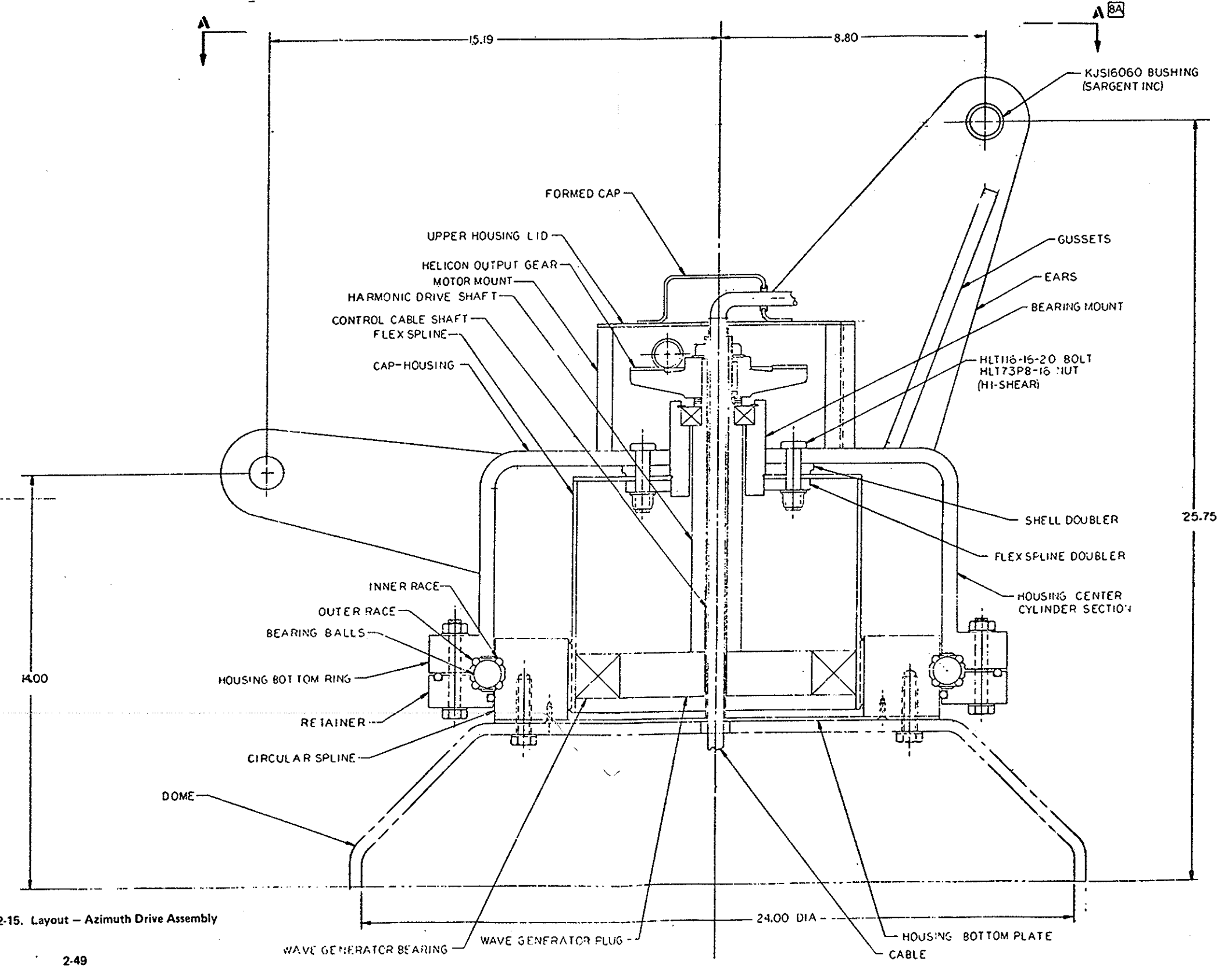
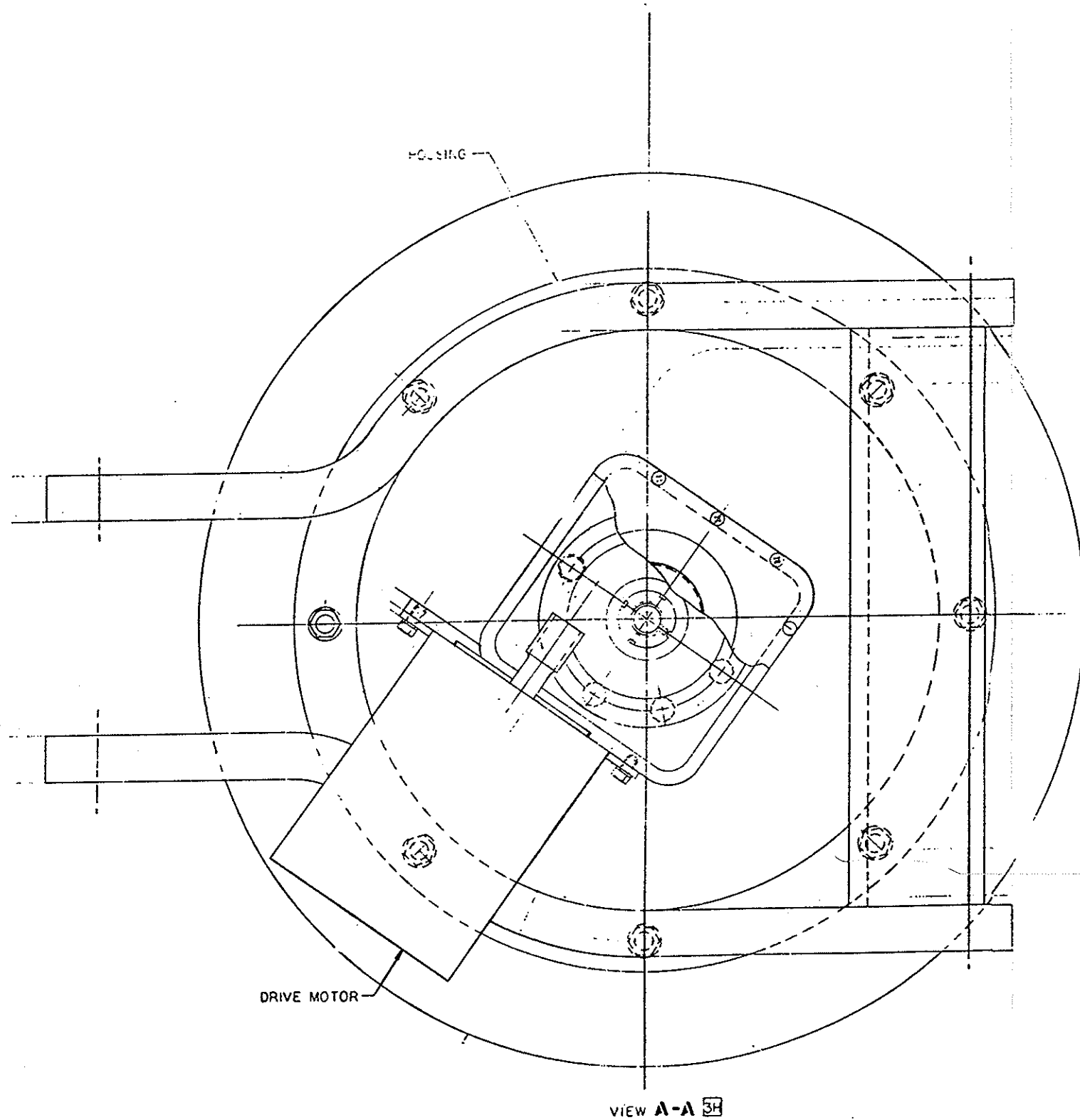


Figure 2-15. Layout - Azimuth Drive Assembly

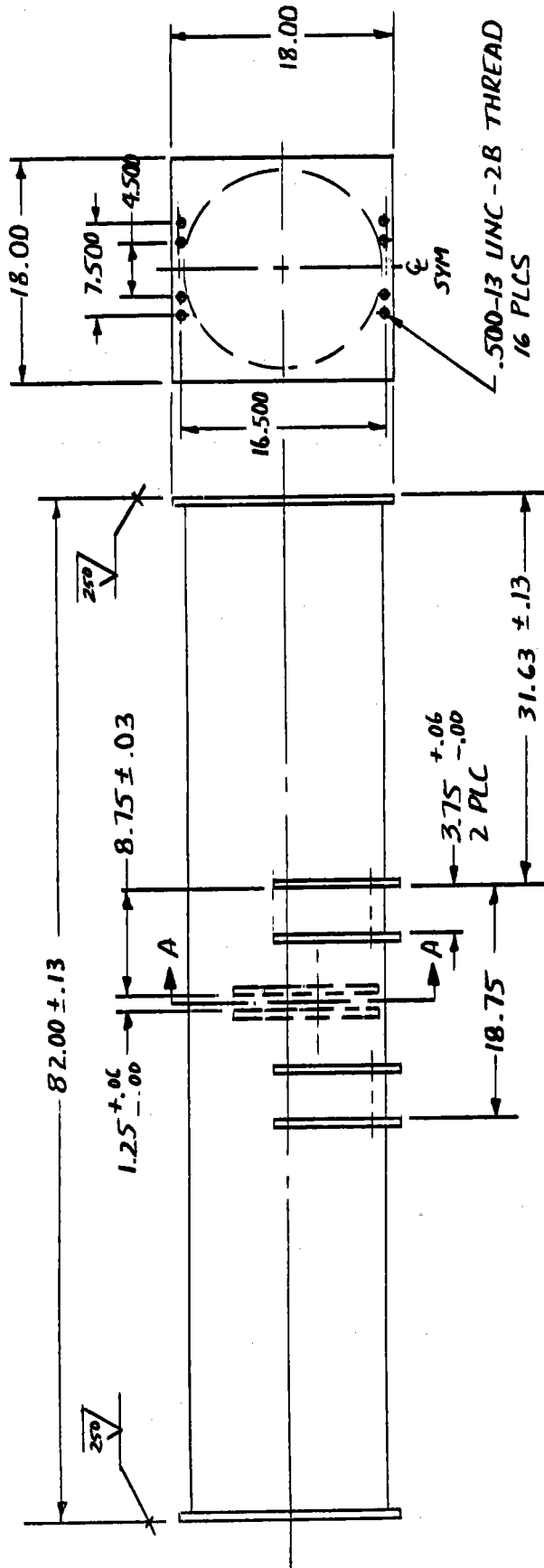
Performance and life specifications require that the combination of backlash and hysteresis shall not increase more than 0.5 mrad by the application of 10,000 cycles under no load. For purposes of this requirement, a cycle consists of rotating the drive 180 degrees in one direction and then back 180 degrees to the starting point. Accelerated gear life tests for a similar design indicated that the performance and life specifications would be met.

2.3.2.3 Main Beam

The central torque tube main beam connects the two reflector panels (the reflective unit) together and ties the reflector to the elevation hinge and the elevating jacks at the top of the drive unit assembly. The main beam, illustrated in Figure 2-16, carries all the airloads and dead weight loads from the reflector to the pedestal as bending, torsion, and shear. It is 2.08 m (82.0 inches) long, of circular cross section, 0.406 m (16 inches) in diameter (outside), formed of 12-gage steel sheet, and hot-dip galvanized after fabrication. End plates 15.9 mm (0.625 inch) thick are fusion-welded to each end and machined flat and parallel to provide accurate location for the reflector assemblies. Tapered holes in the reflector panels and conical bolts provide accurate angular location of the reflector panels relative to each other.

The end plates connect the main beam to each of the inboard cross beams and to each pair of diagonal beams with 12.7 mm (0.5 inch) diameter conical bolts through the web of the inboard cross beam and through the joint fitting at the end of the diagonal beams.

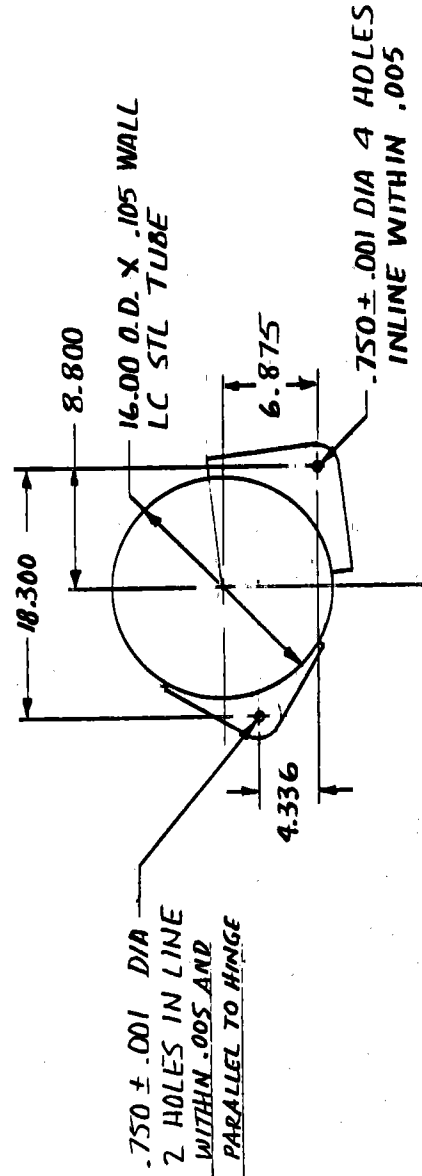
In the slot between the two six-panel reflector assemblies, the main beam has six lugs of steel plate welded to it. Four of these lugs, in line, serve as the support of the elevation hinge line. They are attached to the drive housing at the top of the drive unit assembly with two bolt-type pins. The other two lugs are the mount for the stowage jack through which the elevation rotational forces are applied.



NOTES:

1. HOT DIP GALVANIZE AFTER WELDING
2. MACHINE ENDS PARALLEL WITHIN .010

NOTE: ALL DIMENSIONS ARE IN INCHES



SECTION A-A

Figure 2-16. Heliostat Main Beam Assembly

2.3.2.4 Drag Link

The function of the drag link is to connect the tracking actuator and the stowage actuator in such a way that they can provide 180 degrees of heliostat rotation about the elevation axis. The drag link consists of a finish-machined, low-carbon steel weldment and a pair of bushings. Although the raw stock for the weldment weighs 68 kg (150 pounds), the finished part weighs 29 kg (65 pounds). The design is shown in Figure 2-13.

An alternative to the design described above uses a ductile iron casting in place of the weldment. The weight of the casting would be 38.5 kg (84.9 pounds).

For stowage, the stowage jack is retracted into the vicinity of a mechanical stop, and then the motor pulsed incrementally until a pulse command produces no change in the stowage motor's incremental encoder. This signifies complete retraction, and eliminates backlash. The encoder count is automatically accumulated and the position data used to correct the tracking equation output. In the event stowage is prevented by inadvertent obstruction, an error flag will be used to stop the stowage motion and alert the master control.

2.3.2.5 Drive Motors

The motors described in this section provide power to the azimuth drive and the elevation actuators during tracking and slewing operations. The motors operate on 480 VAC \pm 10 percent, 60 Hz, three-phase electrical power, and the motor windings are delta-connected. The method of control is triac switching (bang-bang) of the three-phase AC line; switching durations can vary from one three-phase sinusoidal pulse to continuous three-phase sinusoid. The motors operate bidirectionally.

The life of the motors must exceed 30 years with no scheduled maintenance. The motors must be able to operate 365 days per year, where a typical daily duty cycle is 15 minutes of continuous running, 7.5 hours at one three-phase sinusoidal pulse every two seconds, and then 15 more minutes of continuous running. The maximum duty cycle is 20 minutes of continuous running, then 60 minutes off. The minimum duty cycle is one three-phase sinusoidal pulse every 10 seconds.

The motors are totally enclosed and able to operate in any attitude. The motor shaft will be supported by permanently lubricated ball bearings. At the fan end, 25.4 mm (1 inch) of shaft will be provided for mounting an MDAC-installed shaft turn transducer. The output shaft will have provisions and load capacity for mounting the helicon pinions described in Sections 2.3.2.1 and 2.3.2.2.

The elevation drive motors have a torque requirement greater than 2.00 N-m (17.7 in-lb) at 0 rpm and 1.41 N-m (12.5 in-lb) at 1500 rpm. The azimuth drive motor has a torque requirement greater than 2.85 N-m (25.2 in-lb) at 0 rpm and 1.08 N-m (9.54 in-lb) at 1300 rpm.

It is estimated that the elevation drive motor requirements can be met by a 1/4 hp 42-frame motor which has NEMA C torque-speed characteristics and weighs less than 4.76 kg (10.5 lb). It is estimated that the azimuth drive motor requirements can be met by a 1/3 hp 48-frame motor which has NEMA D torque-speed characteristics and weighs less than 8.62 kg (19 lb). The motor external shaft can be extended, if necessary, to provide for manual slew using common hand held drill motors.

2.3.2.6 Control Sensors

Incremental encoders are mounted at the base of each of the three drive motors to provide control feedback data. The encoder is designed to provide the processor with information concerning the direction and the number of revolutions of each motor.

The incremental encoder is designed with two Hall-effect transducers. A ferrous metal vane mounted on the motor shaft produces an interrupt in each of the transducer's magnetic fields at slightly out-of-phase intervals, depending on the direction of rotation. The sensor exhibits a level shift which latches either of two flip-flops. The latched signals are transmitted to the processor and simultaneously an interrupt signal is provided to inform the processor that one motor revolution has occurred.

The encoder sensors are environmentally sealed in durable plastic casing. Dust and dirty atmospheric conditions produce no damage or inaccuracy due to the magnetic operation of the units.

The encoder has an accuracy to within one motor revolution. This is equivalent to a deflection of 0.144 mrad in heliostat azimuth and approximately 0.144 mrad in elevation.

2.3.2.7 Pedestal

The support for the heliostat is provided by the pedestal. The pedestal is 3.18 m (125 inches) high to provide ground clearance when the reflector is elevated. It is fabricated of 0.61 m (24 inches) diameter spiral-welded steel pipe with a wall thickness of 2.66 mm (0.1046 inch). The pedestal is hot-dip galvanized after fabrication. The lower 1.12 m (44 inches) of the length is expanded to produce a slight taper of 11.7 mm diameter per meter of length (0.14 inch per foot) to obtain a wedged, slip-joint attachment with the foundation on installation. A recessed junction box is located in the pedestal 1.37 m (4.5 feet) above its lower end. Underground electrical lines are routed externally from the ground to the box, then through the box and up the inside of the pedestal. The drive unit housing is welded to the top of the pedestal. A draw-pressed dome is fusion-welded to the top of the pedestal. A bolt circle in the dome provides a bolted interface to the circular spline in the azimuth drive unit. The dome is made of 9.53 mm (0.375 inch) low-carbon steel.

2.3.3 Foundation Assembly

To properly anchor the heliostat to the ground, a rigid foundation is required. Stearns-Roger Engineering Company of Denver, Colorado designed a low-cost foundation which would meet the strength and rigidity requirements imposed by the heliostat performance. The design had to be capable of resisting an overturning moment of 7630 kg-m (662,000 inch-pounds) and show a rotation not to exceed 1.3 mrad at the ground line under a twisting moment of 1003 kg-m (87,000 inch-pounds). The low-cost aspect included a novel slip-joint attachment of the pedestal.

Several types of foundations were considered in this study, and a pile-type foundation with a slip-joint pedestal attachment was recommended, as shown in Figure 2-17. An 0.61-m (24-inch) diameter hole, 6.7 m (22 feet) deep, is drilled into the ground. A prefabricated, circular rebar cage is located in that hole. This rebar cage extends 1.22 m (4 feet) above the ground. A tapered form, of 15-gage galvanized steel sheet and 1.22 m (4 feet) long, is slipped over the rebar extension, and then the hole and form are filled with concrete. The taper on the form matches the taper at the bottom of the pedestal, 11.7 mm per meter of length (0.14 inch per foot).

2.3.4 Heliostat Electronics

The heliostat electronics subassembly includes:

- Pedestal Junction/Circuit Breaker Box - Located on the pedestal, and interfaces with the field secondary power and data network.
- Cabling - A single cable takes power to and data to/from the heliostat controller box on the drive unit from the junction box. A second set of cables run from the controller box to the motors/sensors.
- Heliostat Controller - A microprocessor in the heliostat controller makes all command calculations. The microprocessor interfaces directly with motor switching network, sensor, and communications link.
- Motors/Sensors - Incremental encoders and switching networks are mounted on the motor shaft.

The heliostat electronics receive signals from the data network and relay messages to the next heliostat in the chain. Open-loop tracking algorithms are used to determine the required heliostat position. The difference between the calculated position and actual position is used as an error signal for turning the motors on and off. The signal from the incremental encoder is used to determine the actual position by counting motor turns. The accumulated turns are stored in nonvolatile electrically erasable memory (EEROM); therefore, if power should be lost, the position reference of the heliostat will not be lost.

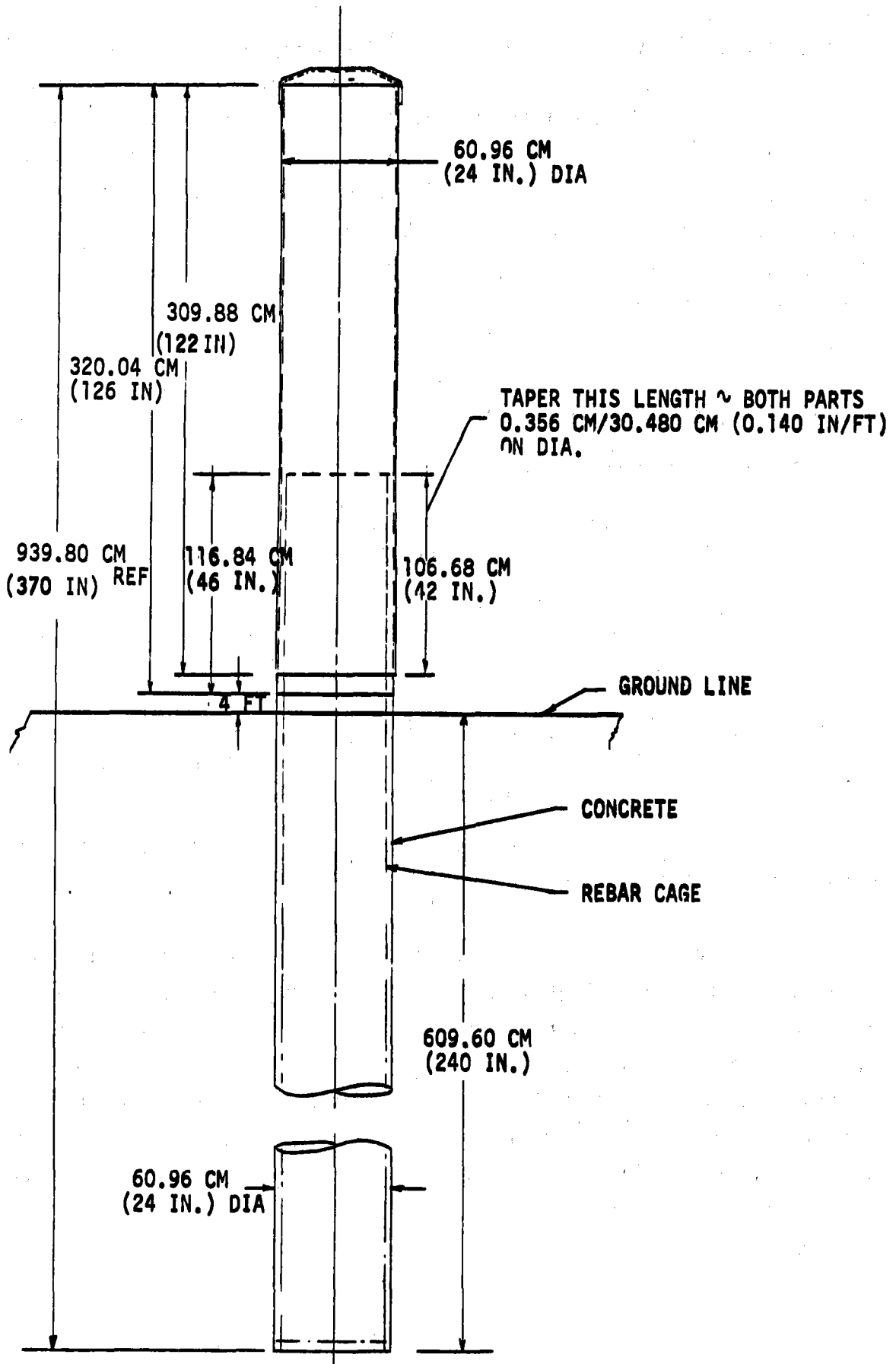


Figure 2-17. Pedestal - Pile Type I

2.3.4.1 Pedestal Junction/Circuit Breaker Box

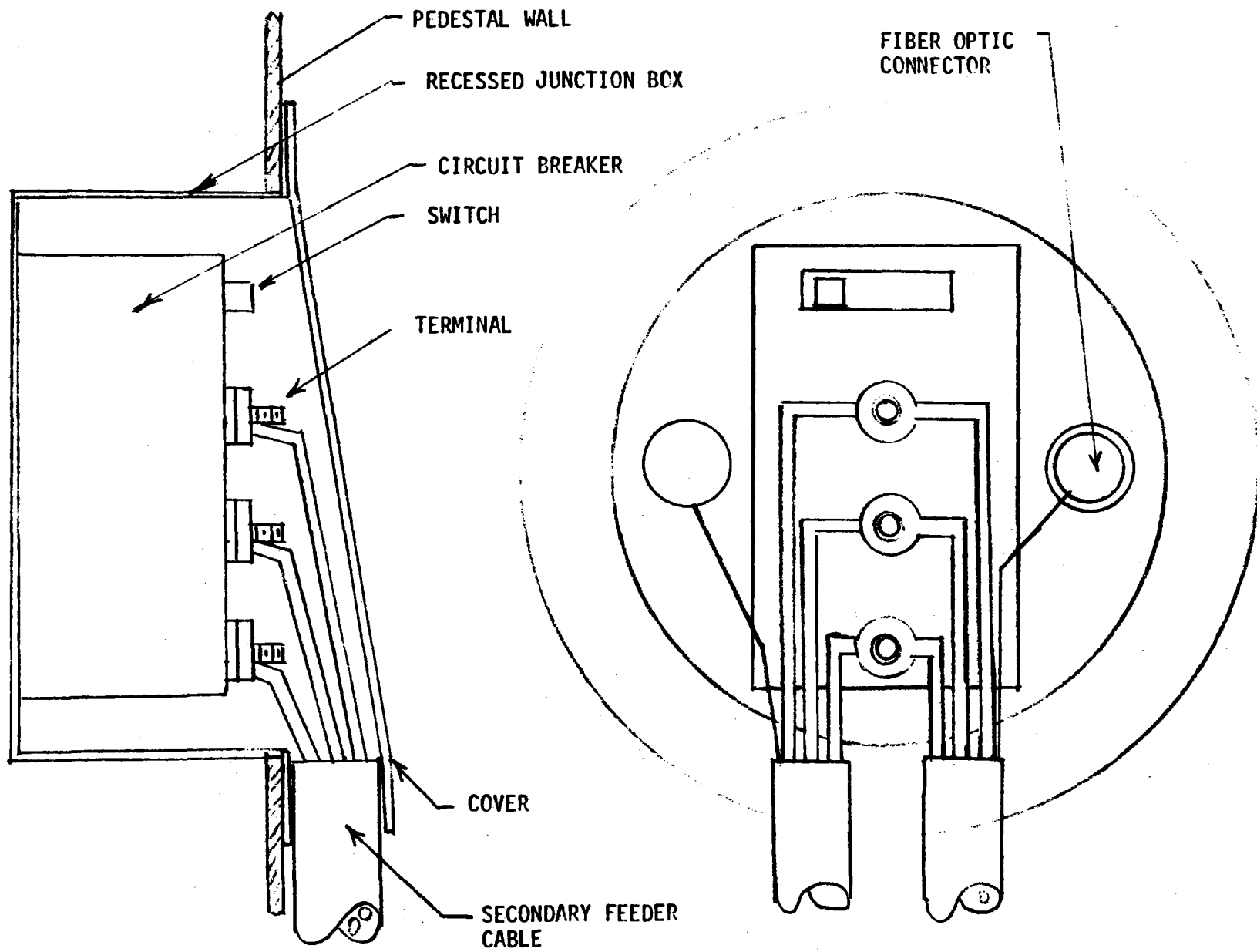
The secondary feeder cable enters the pedestal and terminates in a junction box located on the side of the pedestal. The junction box is illustrated in Figure 2-18. The recessed box contains a circuit breaker which joins the incoming and outgoing cables and noninterchangeable fiber optic connectors. On the inside of the pedestal, the circuit breaker is wired directly into the cable leading to the heliostat controller. An internal protective cover will be required to provide personnel protection from the 480-volt terminations after the wire installations are made. The cutout will also contain a cover for environmental protection. The cover will be protected against moisture, dust, and ice.

Proper phasing must be maintained in the power distribution network. Therefore, cables will be terminated in the factory with crimp or ring terminals which will only connect in one manner (Figure 2-18). Also, the fiber optic connectors will be male and female, with the male used for the incoming signal and the female for the outgoing signal to prevent any possibility of reversing.

2.3.4.2 Cabling

The heliostat pedestal wiring consists of 3-conductor, No. 16 AWG, 480-volt, copper wire with aluminum sheath for power distribution and twin-lead optical fiber cable for data transmission. The cable runs from the junction box in the pedestal to the heliostat controller mounted on the drive unit. In order to route the cable past the gimbal axis, a hollow shaft has been designed into the center of the azimuth axis. The cable will be routed through the shaft, thus allowing for rotation and elevation of the heliostat without putting stress on the power cable. To allow for 270 degree rotation of the azimuth gimbal, a section of cable is left slack inside the pedestal. The cable and other components are completely wired in the factory; hence, the only field wiring required is to connect the secondary feeder to the junction box. The connectors at the heliostat controller end of the cable are single-fiber connectors designed to mate with terminals located on the printed circuit board of the heliostat controller. The two connectors have irreversible connectors to prevent accidental misconnection.

Figure 2-18. Pedestal Junction Box



2.3.4.3 Helioostat Controller

The helioostat controller is a microprocessor-based unit which interfaces with the helioostat array controller and the motor/sensor system. The main functions of the helioostat controller are to respond to the commands from the collector controller, send information to the collector controller, calculate commands for moving the helioostat from one position to another, and keep track of helioostat orientation. Helioostat orientation is determined by counting the number of turns the motor makes. The microprocessor contains a nonvolatile memory (EEROM) where the motor counts are kept. Even if the power should fail, the helioostat will not lose the number of motor turns or its reference position.

It is estimated that in 1984, the required capabilities of the helioostat controller will easily be available in a single-chip microprocessor. The current trend and demand also indicate that microprocessors will be available with electrically erasable read-only memories (EEROM) within the next year or two. The microprocessor and interfaces of the helioostat controller are shown in Figure 2-19. Analysis has indicated that it is cost-effective to use commercial grade parts in these components. See Section 9 for related cost data.

The communications interface consists of an optical receiver, an optical transmitter and a data shift register. Received serial data is shifted into the shift register and transferred in parallel to the data processor. The address bits are decoded in the processor. If an address match is obtained, the remaining message is decoded and executed. If not, the shift register is enabled and the data transferred to the next helioostat in the chain.

Equations for control of the helioostats are calculated in the helioostat controller with inputs from the helioostat array controller. Using a transmitted time signal, the helioostat controller updates its clock, calculates the sun angles, the gimbal angle required for reflecting the beam onto the target, the error signal between the actual gimbal angles and the commanded gimbal angles, and the motor command for reducing the error signal.

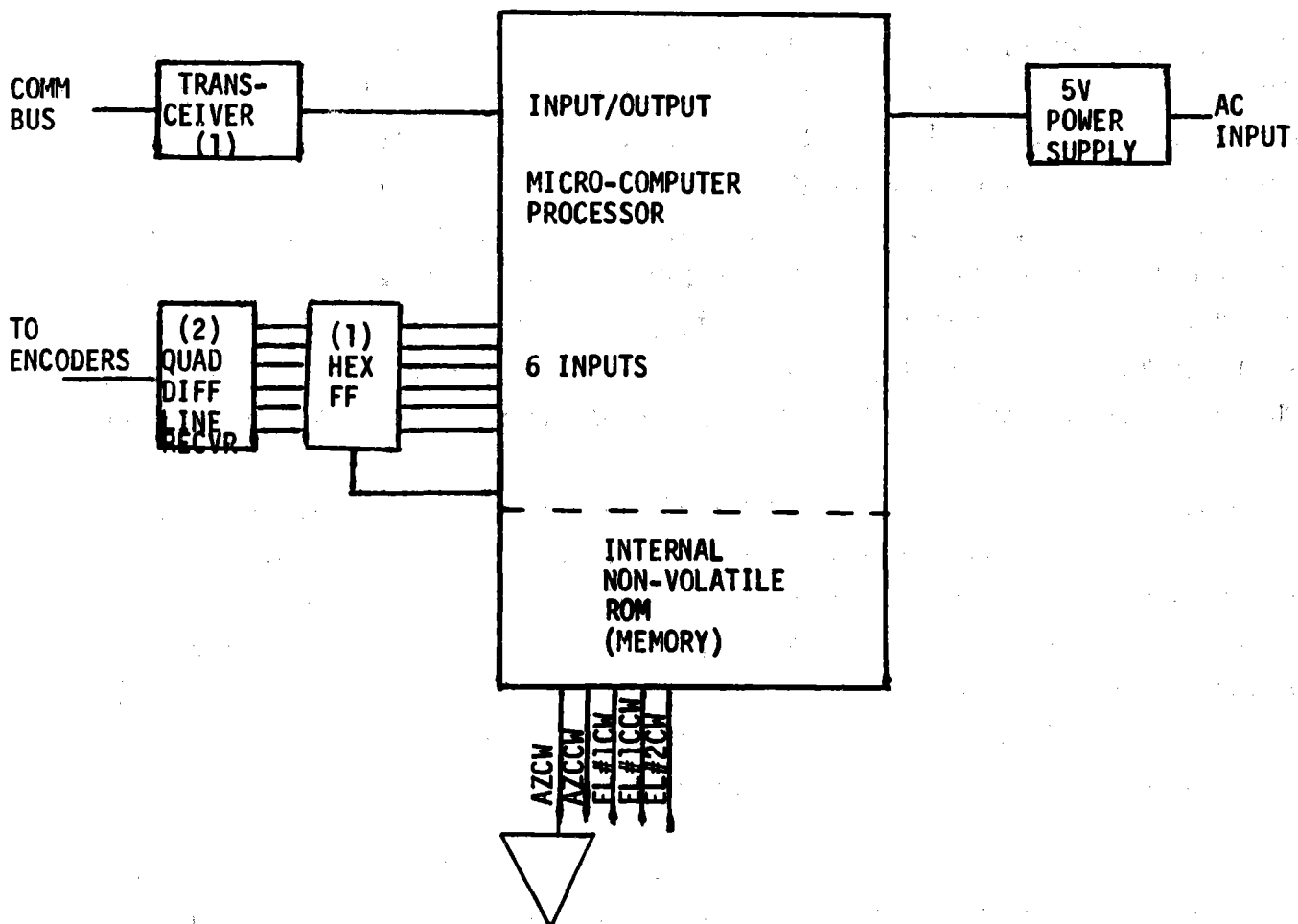


Figure 2-19. Heliostat Controller Microprocessor

If the operating mode should be changed from tracking on the receiver to emergency slew off the receiver, a single command is transmitted to each data distribution interface which transmits the message to each heliostat assigned to it. The heliostat controller then commands the reflected beam to move from the receiver to an aim point near the receiver. The heliostat controller maintains the beam at this aim point until the operating mode is changed by the heliostat array controller. The heliostat controller periodically checks the communications link with the heliostat array controller. If it finds that the communications link is bad, the heliostat controller will continue tracking.

2.3.4.4 Motors/Sensors

Besides the armature and field, the motor housing contains the motor control switching network and an incremental encoder. The control (direction and on/off) of the three-phase motors is accomplished by applying a positive logic signal to the appropriate input network shown in Figure 2-20. This signal is gated with a clock pulse to drive the optically isolated signal triac, which in turn drives the motor. The motor will remain "on" until the command is removed by the processor.

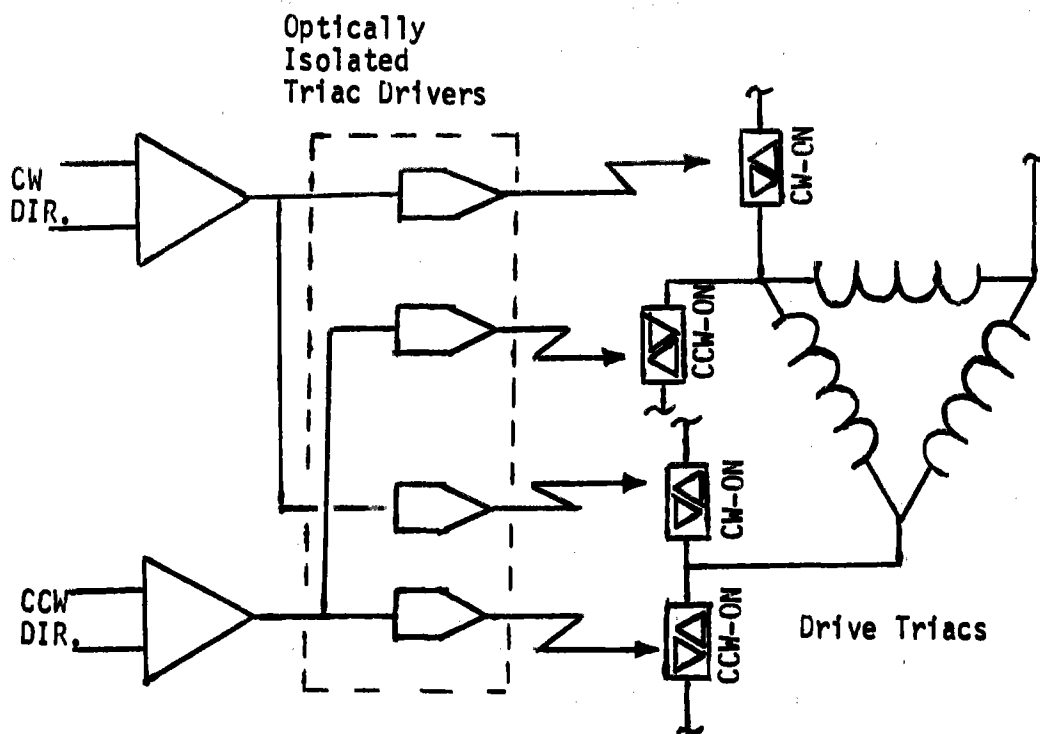


Figure 2-20. Motor Controller

The incremental encoder is a two-channel device which exhibits a logic level shift on each of the channels, but shifted in phase once for each motor revolution. One channel leads the other (in phase), depending upon the direction of the motor shaft movement (CW versus CCW). The data from the two channels are used to latch either of two flip-flops (the one latched is a function of the motor movement). The logic level shift of the encoder is generated by a Hall-effect transducer (integrated circuit package) which senses change in the magnetic field as the magnetic interrupter passes by the sensor. The latched signals are input to the processor and simultaneously an interrupt signal is provided to inform the processor that one revolution of motor movement has occurred.

2.3.4.5 HelioStat Electronic Assembly

The electronic components are at five different locations on the heliostat. The heliostat controller is in an electrical J-box on the drive unit. This was selected over a ground location to give added protection from the environment and ground activity and to minimize the heliostat wire required. A junction box is located on the pedestal which contains a circuit breaker, plug connectors, and terminators for the incoming power and communication fibers. Power to a heliostat can be controlled by activating the switch on the circuit breaker. A manual control box can be plugged into this box for local control of the heliostat. Local manual control isolates this heliostat without affecting the control of any other heliostat in the field. There is a motor mounted on each drive jack and one on the azimuth drive. An incremental encoder is mounted on the motors.

2.3.5 Field Electronics

The field electronics for the collector delivers power and control data to the heliostats and returns information on the heliostat status to the master control.

The data links interface with the collector controller on the elements of the master control which pertain to the controller. A high-data-rate fiber optic cable links the collector controller to data distribution interfaces in the field. Each data distribution interface is connected to 12 to 16 separate strings of heliostats by secondary feeders, again using fiber optics. Data from the collector controller are relayed to the correct heliostat and data from the heliostats are relayed to the collector controller.

The power links interface with the electric power generation subsystem. 4160 VAC three-phase power is transmitted to field transformers by the primary power feeders. The transformers are collocated with the data distribution interfaces. The voltage is stepped down to 480 volts and distributed to the secondary feeders.

Both power and data are carried in the same secondary feeder cable. The secondary feeders are terminated at both ends at data distribution interfaces

and field transformers. Hence, the loss of a transformer does not result in the loss of power to any heliostat. All cables are designed for direct burial to provide adequate protection at minimum cost.

The wiring configuration proposed for the 100 MW Prototype System is designed to enhance efficiency and lower costs. The system incorporates the lower cost of the radial configuration and the reliability of a network system. The field (Figure 2-21) consists of a primary distribution system originating from a central distribution point at which each feeder provides power for two or three transformers. Branch circuits between transformers provide power for the heliostats. This hybrid radial system is not totally redundant, but will provide redundancy in the form of emergency operation to approximately 90 percent of the transformers in the field. With the hybrid system, the heliostats normally supplied by a transformer which has failed are not supplied sufficiently for normal operation, as in the network distribution system, but are able to drive into a stowage position or carry out emergency maneuvers which increase the operating safety of the field.

2.3.5.1 Primary Power

The power distribution network for the 17,700 heliostats, 100 MW solar power plant will consist of 20 primary feeders supplying 4160 volt, three-phase power from the central power distribution point to fifty-seven 225-KVA transformers in the heliostat field, as shown in Figure 2-22. Each three conductors, No. 4 AWG primary, will supply power to two or three transformers. Each transformer will supply 480-volt, three-phase power to 12 to 16 groups of approximately 24 heliostats through three conductors, No. * AWG copper cable. The distribution system will be a hybrid radial network with branch circuit cables running circumferentially along the heliostat arcs.

2.3.5.2 Primary Data Link

The primary data link provides the control interface between the heliostat array controller and the data distribution interface. The communications link consists of an optical transmitter unit compatible in bandwidth to the heliostat array controller, a fiber optic communications line, and a photodetector receiver for converting optical signals to their digital equivalents.

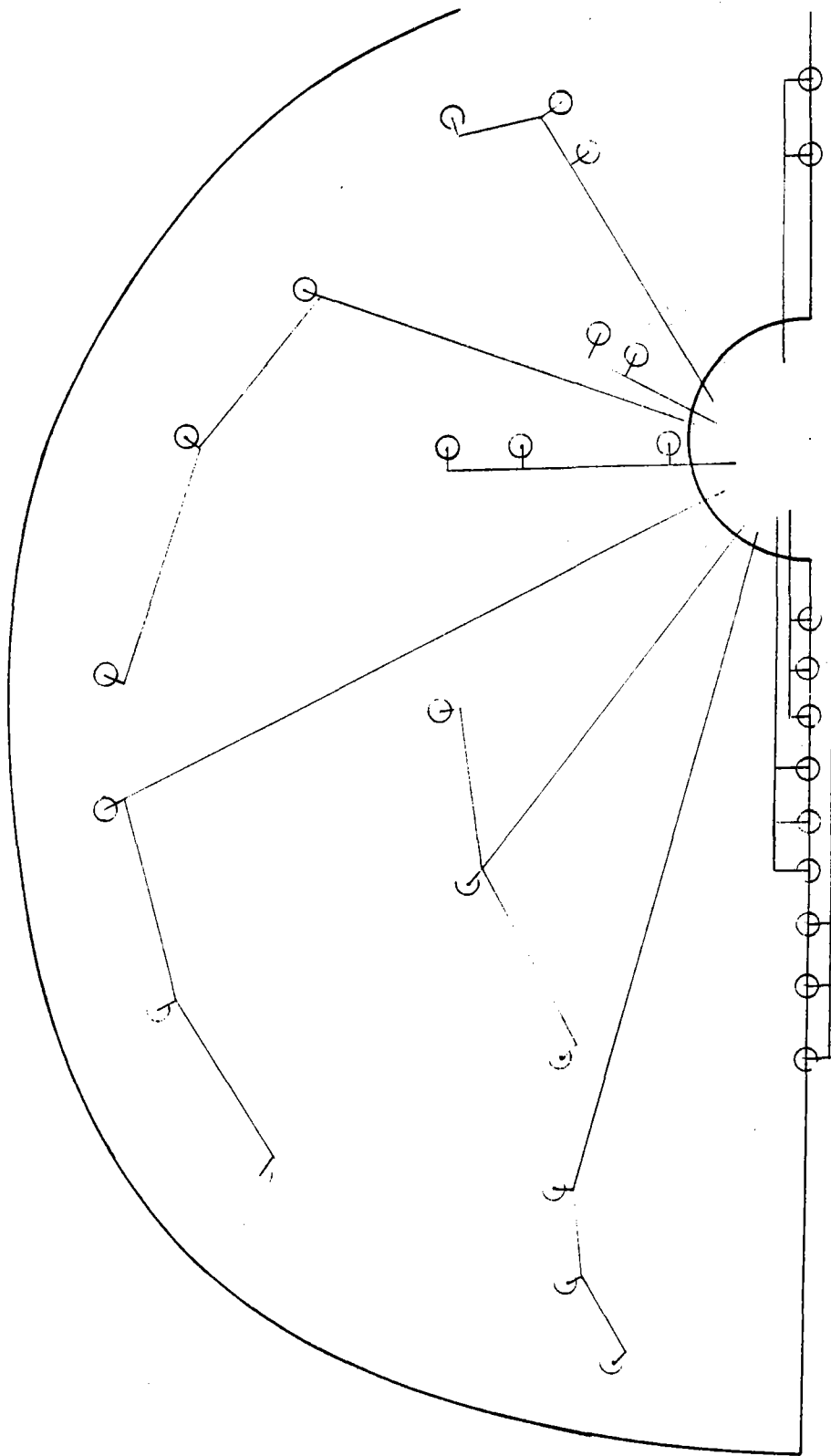


Figure 2-22. Transformer Locations

The field configuration is arranged similar to the primary power feeder. A primary feeder transmits information between the collector controller and 15 to 20 data distribution interfaces. At this point, information is retransmitted along each of the primary feeders to two to three additional data distribution interfaces. Each of the data distribution interfaces communicates along 12 to 16 secondary lines to approximately 24 heliostats (Figure 2-23). This procedure eliminates the need for a lengthy transmission distance between repeaters and conforms to the hybrid power distribution format.

Data Distribution Interface

The data distribution interface will contain two identical printed wiring boards which are similar in construction to the heliostat controller boards. The plastic box will be the same as the box that houses the heliostat controller. The printed wiring boards will be installed with the components facing, thus allowing them to nest and reduce the overall size of the box. The manufacturing flow will be the same as the heliostat controller, but will require a different numerically controlled tape for the automatic component insertion machine. Each data distribution interface will contain the transmitter and receiver components necessary for the interface of primary and secondary communications components. All optical connectors will be mounted on the printed wiring boards to allow for automated inspection techniques.

2.3.5.3 Field Transformers and Interface

The field transformers step the 4160-volt primary power down to 480 volts for distribution through the secondary feeders. Each transformer is rated at 225 KVA with a 4160-volt primary and a 480/270-volt secondary. The secondary of the transformer connects to a main circuit breaker of 100-ampere capacity. A power bus from the main breaker connects to individual 40-ampere circuit breakers for the secondary feeder circuits. The secondary feeder breakers are located in the power distribution panel, as indicated in Figure 2-24. The connectors for the secondary data feeder are also located in this panel for convenience in field hookup.

The requirements for power transmission and cable capacity are determined by the operating voltage and current requirements of the heliostat motors. Each

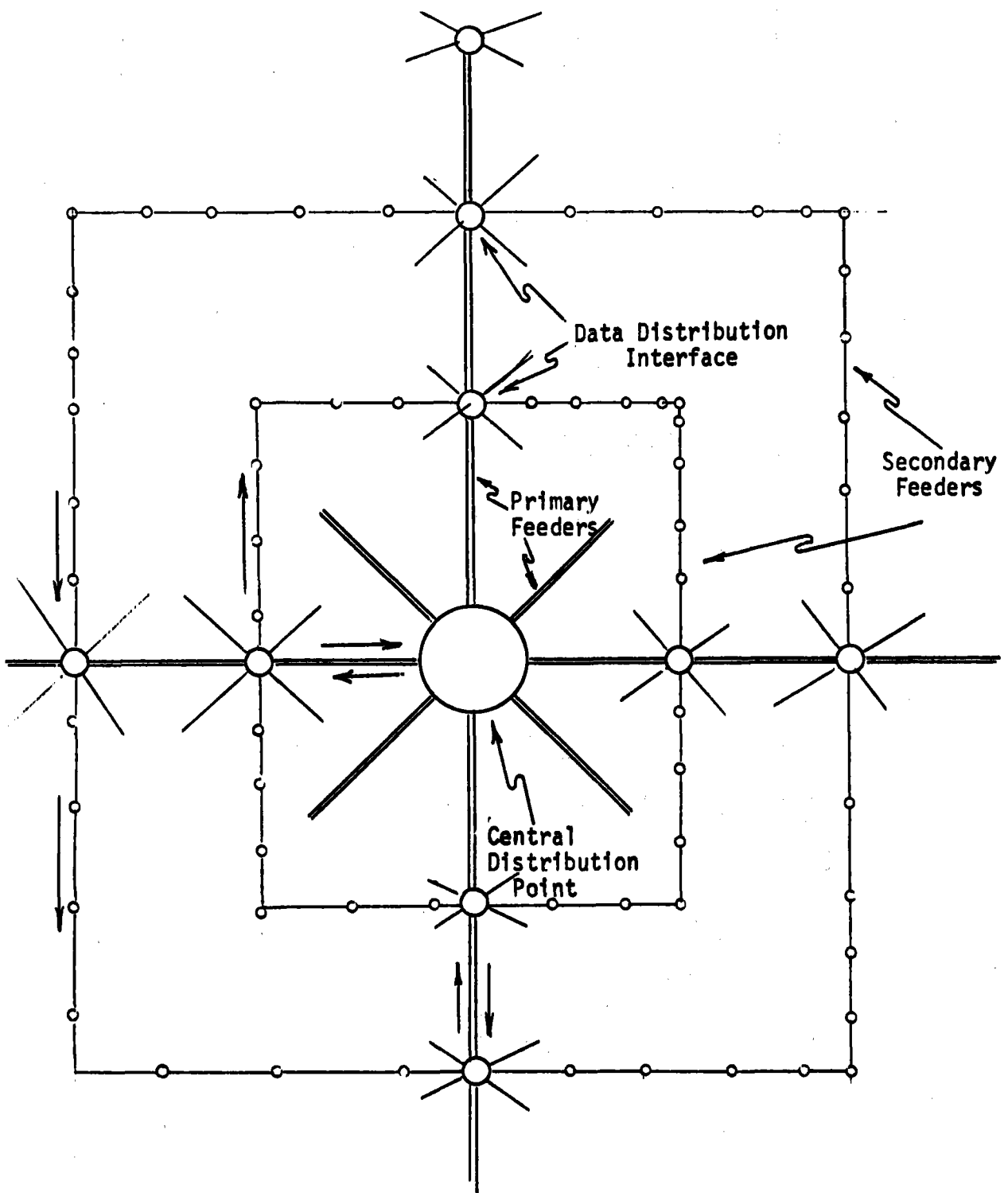


Figure 2-23. Primary Data Link

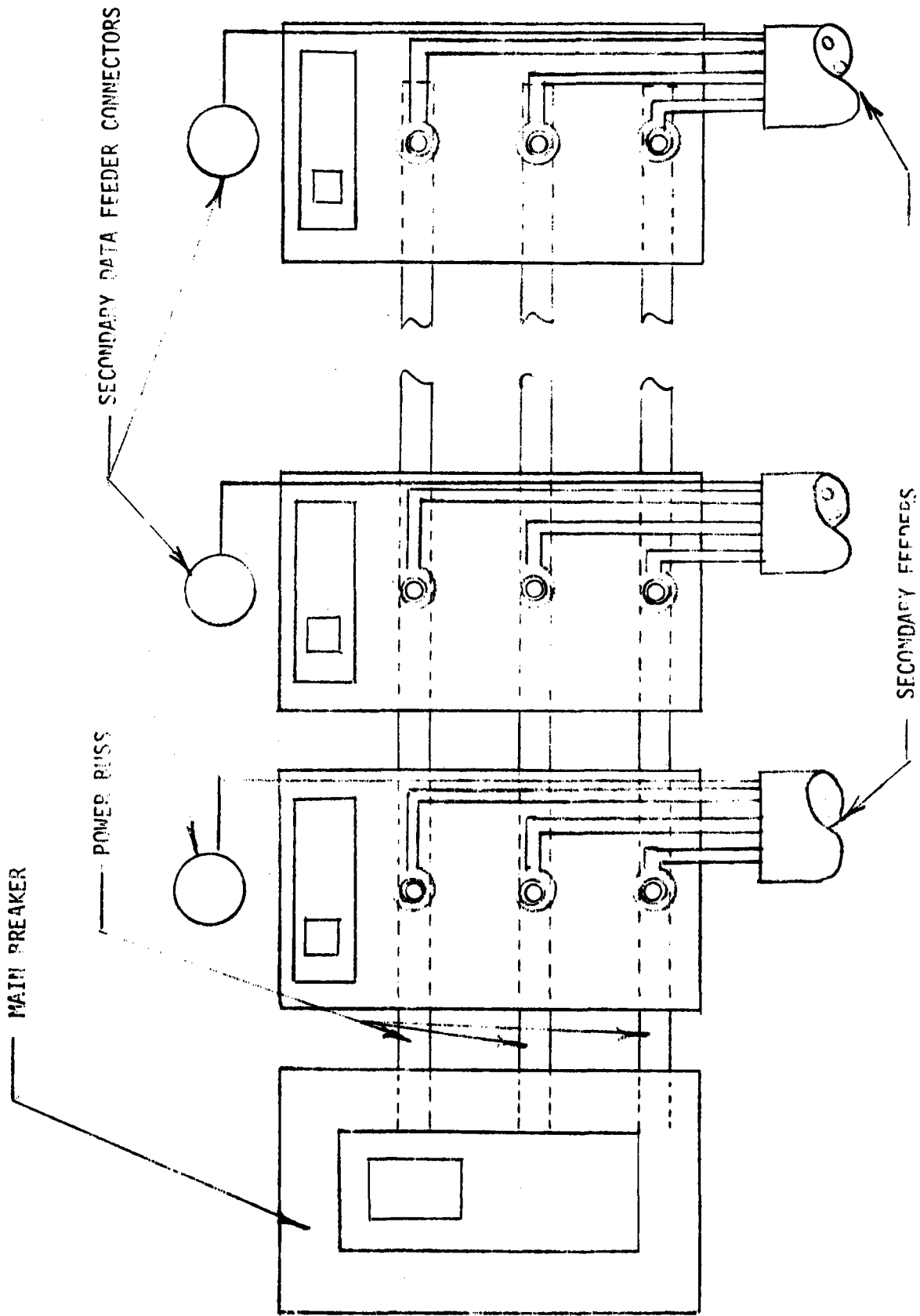


Figure 2-24. Power/Data Distribution Panel

heliostat has three motors with a maximum of two motors operating at one time. For the initial baseline configuration, the motors were to be operated on 240 volts, three-phase power. At this voltage, the current requirements per motor were 3.5 amperes starting current (4 AC cycles) and 1.4 ampere running current. Thus, to start both motors on all 17,700 heliostats in the field simultaneously would require 124,000 amperes at 240 volts, or approximately 51×10^6 volt-amperes of transformer power with very heavy gauge cycle to handle the large currents. It was therefore decided to size the cycle network for a more realistic operating requirement.

The worst-case condition for the operation of the field is the emergency slew, in which all heliostats must be moved off the receiver in 40 seconds or less. To accomplish this, all heliostats must have one motor operating and approximately 16 percent of the heliostats will require both motors in operation. A staggered start of the motors was chosen to reduce the danger of circuit overload; in addition, the secondary voltage was increased to 480 volts to reduce the current in the secondary feeders.

At 480 volts, the current requirements per heliostat (1.5 motors running) would be 0.72 ampere. The transformer requirement for either the 480- or 240-volt system would be 0.60 KVA per heliostat or 10,620 KVA for the entire field.

The number of transformers required to supply low-voltage power to the heliostats and their location in the field is closely related to the cable used in the branch circuits due to voltage regulation and amp capacity requirements. Since the major cost factor in the field network layout is the branch circuit cable and its installation, it is desirable to use the smallest gauge possible to minimize the cost of the cable. The limiting factor on the cable size is the voltage drop from the transformers to the heliostats on the branch circuit due to the distance between heliostats. This limits the number of heliostats supplied by a branch circuit and requires that the transformers be located as close as possible to the heliostats to minimize the voltage drop over the line. Thus, while a lesser number of larger transformers (e.g., 750 KVA) would reduce the cost of transformers alone, a greater number of smaller transformers (e.g., 225 KVA) reduces the overall cost of the field layout because a smaller-gauge cable may be used while maintaining adequate voltage regulation.

The field locations of the 225 KVA transformers for the 17,700 heliostat field is shown in Table 2-13. The locations were developed by determining the number of heliostats in each row (or arc) of the field layout and sectioning the heliostats in each row into groups that can be served by one transformer with adequate voltage regulation. In this manner, the number of transformers required for each group of rows is determined. The location of the transformers is then determined by calculating the number of heliostats a transformer can supply and placing the transformers in such a manner that the rows are fed by an adequate number of transformers and each transformer serves the maximum allowable number of heliostats.

2.3.5.4 Secondary Feeder

The secondary feeder cable is the most costly item in the power distribution network due to the large amount required to connect all the heliostats in the field. The only factor affecting this cost is the size of cable used, since the length is a function of only the field size. The length of the branch circuit cables will be the total arc length of all the heliostat arcs plus a small amount for transformer to arc hookup. For the 17,700 heliostat field, the length required is approximately 290,000 m.

Voltage regulation and amperage requirements determine the conductor size. These requirements are set by the number of heliostat on a line and the line voltage. Due to the distances between heliostats, adequate voltage regulation is the limiting factor in cable gauge selection. Voltage drop calculations, for the desired range of 20 to 25 heliostats on a secondary feeder circuit, indicate that the required wire gauge is No. 8 AWG, 3-conductor copper for the 480 volt, three-phase system. The attendant reduction in wire gauge results in approximately a 50 percent cost savings for the secondary feeder cable with a 480-volt system compared to the 240-volt system of the initial baseline.

The secondary feeder cable also contains the fiber optic secondary data feeder cable. This cable runs from the distribution at the data distribution interface to the heliostat junction boxes. At the data distribution interface, information arriving from the heliostat array controller is channeled to the

Table 2-13

17,700 HELIOSTAT FIELD TRANSFORMER LOCATIONS

| ROW ⁽¹⁾ | TRANSFORMERS IN ROW | TOTAL ARC | LOCATION OF TRANSFORMER ALONG ARC ⁽²⁾ |
|--------------------|------------------------|--------------|--|
| 4/5 | 2 | 360° | $\pm 90^\circ$ |
| 12/13 | 3 | | 0; $\pm 120^\circ$ |
| 20/21 | 3 | | 0; $\pm 120^\circ$ |
| 28/29 | 4 | | 0; $\pm 90^\circ$; 180° |
| 36/37 | 4 | | 0; $\pm 90^\circ$; 180° |
| 44 | 5 | | 0; $\pm 72^\circ$; $\pm 144^\circ$ |
| 51 | 5 | 360° | 0; $\pm 72^\circ$; $\pm 144^\circ$ |
| 58 | 5 | 329° | 0; $\pm 66.0^\circ$; $\pm 132^\circ$ |
| 65 | 5 | 275° | 0; $\pm 55.2^\circ$; $\pm 110.4^\circ$ |
| 72 | 5 | 232° | 0; $\pm 46.40^\circ$; $\pm 92.8^\circ$ |
| 79 | 4 | 192° | $\pm 24^\circ$; $\pm 72^\circ$ |
| 86 | 4 | 159° | $\pm 20^\circ$; $\pm 60^\circ$ |
| 92/93 | 4 | 126° | $\pm 15.8^\circ$; $\pm 48.2^\circ$ |
| 98/98 | 4 | 102° | $\pm 12.8^\circ$; $\pm 33.4^\circ$ |

(1) Rows numbered out from receiver. Row numbers X/X+1 indicates transformers located between Rows "X" and "X+1". Row numbers "X" indicates transformer located in that row of heliostats.

(2) Angles are measured from the central receiver location with North as zero.

appropriate secondary communications line via the data distribution interface processor. The digital information is transformed to an optical signal and routed to the first heliostat in the string. The fiber communications line is housed in the same cable with the 3Ø power lines. At the J-Box in the base of the pedestal, a connector is provided to allow the optical fiber to be routed to the heliostat controller at the top of the pedestal. Optical information is detected by a photo transistor receiver located at the heliostat controller and transformed into a digital signal compatible with the processor requirements. The information address is compared to that of the processor. If the commands are not intended for the heliostat they are retransmitted to the next heliostat in the string.

Return information is handled via the same communications line. The information is transmitted along with the retransmitted signals to a data distribution interface at the end of the secondary data link. (see Figure 2-25). From there, the signals are transmitted to the heliostat array controller. This configuration requires a low-data-rate transmitter and receiver at each heliostat controller.

The repeater configuration eliminates the need for high-quality optical fiber due to the short transmission distance. The loop configuration results in the need for only one-way communication along a single cable.

Due to tolerance requirements, it is necessary to make fiber coupling connections during production. This reduces installation time and labor by requiring only mechanical snap-type connections in the field.

Continuity checks should be made periodically during installation on both the fiber optics and the power cable to ensure proper alignment and reproducibility of signals and phase relationships.

2.3.6 Lightning Protection of the Heliostat Array

A direct attachment of a lightning flash to some component of the collector field and specifically to a heliostat is potentially the most devastating form of discharge. However, a nearby flash that does not actually attach to a part of the heliostat array can also be destructive because of the high intensity electro-

magnetic fields that may be induced into the metal conductors of the system. The peak current in a lightning flash can exceed 200,000 amperes, but 20,000 amperes is a more average value.

The protection objective is to prevent non-recoverable damage when lightning strikes the collector field. Physical damage from a direct strike to the heliostat is permitted, but damage to adjacent heliostats is minimized by a number of protective measures.

System Grounding and Shielding

The ideal approach would be to establish all metal objects at absolute ground potential. If this were possible, no potentially destructive voltages (or currents) would exist to damage electrical or electronic components. Unfortunately, there is no such thing as an equipotential ground; it can only be approximated. However, by making the most of what is economically available, good progress toward achieving the ideal can be reached. To this end, the following grounding and shielding methods will be used.

- a. Electrical power triplets will be shielded with the shields grounded at both ends at the entrance or exit of an electrical termination box or component, such as a drive motor.
- b. Junction boxes, equipment boxes, motors, encoders, etc., will be electrically bonded to the metal structure following good commercial practice.
- c. The heliostat pedestal will be earth-grounded through its mounting on the reinforced concrete pier. The vertical rebar runs in the concrete pier will be welded to the steel conical form which will mate with the steel pedestal. The concrete encased vertical rebar runs penetrate down into the earth approximately 18 feet and will provide an economical and satisfactory ground reference at each heliostat.
- d. The power lines which interconnect one entire system are twisted and encased in a corrugated aluminum sheath. The aluminum sheath is covered with a protective insulation to prevent corrosion and thus no direct connection with earth is achieved. However, considerable capacitance to the

surrounding earth is attained which lowers the impulse impedance of the sheath to ground. The aluminum sheath is peripherally electrically bonded to a grounded J-box at each termination, to provide a closed shield around the power lines, and the J-box is electrically connected to ground through the rebar cage.

Transient Suppression

The wire and equipment shielding and bonding is not expected to exclude all potentially destructive lightning transients. Some transients may exceed the burnout susceptibility threshold of the solid state devices used in the heliostat motor controls and in the signal circuitry.

The use of fiber optics for signal transmission will provide acceptable protection for the input of the microprocessor and the use of optical isolators will protect the output of the microprocessor.

The triac controls for the motors may be protected by placing metal oxide varistors between each line and ground at the input to the triac controls.

Conventional lightning surge arresters are recommended for lightning transient control at the inputs to power distribution transformers located in the field and at the power exit from the power house.

2.4 DESIGN CHANGE SUMMARY

The important design changes are summarized in Table 2-14 with the benefits of each change also indicated. Nearly all of the design changes were initiated to achieve a cost reduction, but the method used varies from weight or part reduction to a change in material, use of emerging technology, or an improvement in the manufacturing, installation, and checkout cost as a result of the design change. In some cases, the design change improves overall performance or allows use of another, more cost-effective component, even though there may be no significant cost reduction in that particular aspect of the design. In the case of the reflector design, significant cost savings have been obtained by using a laminated mirror, which adds weight to the glass while decreasing

TABLE 2-14

DESIGN IMPROVEMENT SUMMARY

Sheet 1 of 4

| Design Element | Initial | Final | Cost Reduction | Weight Reduction | Parts Reduction | Material Change | Manufacturing/Installation/Checkout Benefit | Emerging Technology |
|----------------------|---|---|----------------|---|-----------------|-----------------|---|---------------------|
| Heliostat Size | 37.55 m ² (404 ft ²) increased to 48.33 m ² (520 ft ²) with foam sandwich design | 49.07 m ² (528 ft ²) | X | 153.0 kg (337.4 lb) (Approximate for principal design changes) 579.2 kg (1277 lbs) steel reduction | X | | | |
| Reflector Mirror | Foam sandwich | Laminated | X | | 84 | X | | |
| Glass Weight | 387.3 kg (854 lbs) | 787.2 kg (1734 lbs) | X | -399.7 kg (-880 lbs) | | | | |
| Stiffening Weight | 364.1 kg (803 lbs) | 152.4 kg (336 lbs) | X | 211.7 kg (467 lbs) | | | | |
| Support Structure | Torque tube | Divided main Beam | X | | -2 | X | | |
| Weight/Area | 17.08 kg/m ² (3.50 lbs/ft ²) | 6.45 kg/m ² (1.32 lbs/ft ²) | X | 10.5 kg/m ² (2.16 lbs/ft ²) | | | | |
| Weight | 461.2 kg (1017 lbs) | 316.6 kg (698 lbs) | | 144.7 kg (319 lbs) | | | | |
| Pedestal Type | Bolted base | Tapered base | X | | 2 | | X | |

TABLE 2-14

DESIGN IMPROVEMENT SUMMARY

Sheet 2 of 4

| Design Element | Initial | Final | Cost Reduction | Weight Reduction | Parts Reduction | Material Change | Manufacturing/Installation/Checkout Benefit | Emerging Technology |
|-------------------|--|--|----------------|------------------------|-----------------------------|-----------------|---|---------------------|
| Pedestal (Cont'd) | | | | | | | | |
| Weight | 391.8 kg (864 lbs) | 169.2 kg (373 lbs) | X | 222.6 (491 lbs) | | | | |
| Drive Unit | | | | | | | | |
| Azimuth | | | | | | | | |
| | Gear motor 6.36 kg (14 lbs) | Motor 8.6 kg (19.16 lbs) | X | -2.44 kg (-5 lbs) | X | | | |
| | Worm gear reducer | Helicon gear reducer | X | | | | | |
| | Harmonic drive w/Oldham coupling | Harmonic drive w/o Oldham coupling | X | | 2 (major) | | | |
| | Turret bearing w/precision retainers | Wire race bearing | X | 12.23 kg (26.9 lbs) | 1 (Bearing retainer) | | | |
| | Pinion on separate shaft | Pinion on motor shaft | X | | X | | | |
| | Separate motor mount | Integral motor mount | X | | X (5 miscellan- eous) | | | |
| | Cable stored by external mech. | Cable routed thru center | X | X | X | | | |
| | Cast housing | Welded housing | X | -21.77 kg (-48 lbs) | | | | |

TABLE 2-14
DESIGN IMPROVEMENT SUMMARY

| Design Element | Initial | Final | Cost Reduction | Weight Reduction | Parts Reduction | Material Change | Manufacturing/Installation/Checkout Benefit | Emerging Technology |
|----------------------------|--|--|----------------|-----------------------------|------------------------|-----------------|---|---------------------|
| Drive Unit | | | | | | | | |
| Azimuth (Cont'd) | Circular spline and base | Circular spline and base | X | 5.45 kg (12 lbs) | | | | |
| Elevation Linear Actuators | Translating screw 44.72 kg (98.4 lbs) | Translating nut 31.54 kg (69.4 lbs) | | 26.36 kg (+ 58 lbs) (total) | | | | X |
| | Machine screw | Ball screw | | X | | | | |
| | Gear motor 6.36 kg (14 lbs) | Motor 4.77 kg (10.5 lbs) | X | 3.2 kg (3.5 lbs) | X | | | |
| | Proximity limit switch | No proximity limit switch | X | X | X | | | |
| | Worm gear reducer | Helicon gear reducer | | | | | | |
| | Pinion on separate shaft | Pinion on motor shaft | X | | X | | | |
| | Separate motor mount | Integral motor mount | X | | X (5 miscellaneous) | | | |
| | Backlash adjustment | No backlash adjustment | X | X | X | | | |
| Electronics | Communication on wires | Communication using fiber optics | X | | | | X | X |

2-79

TABLE 2-14

DESIGN IMPROVEMENT SUMMARY

| Design Element | Initial | Final | Cost Reduction | Weight Reduction | Parts Reduction | Material Change | Manufacturing/Installation/Checkout Benefit | Emerging Technology |
|----------------------|---|---|----------------|------------------|-----------------|-----------------|---|---------------------|
| Electronics (Cont'd) | Incremental and 4 bit absolute encoders | Incremental encoder/non-volatile memory | X | | X | | X | X |
| | 240 VAC field wiring | 480 VAC field wiring | X | | | | | |
| | Field controller | Data distribution interface | X | | X | | | |
| | Multipart processor | Single chip processor | X | | X | | X | X |

the structural support weight and improving the reflectivity. A significant reduction in pedestal steel weight is achieved with the new design. In the drive unit, a welded housing is substantially heavier, yet cheaper, than the cast housing, and overall cost reductions are achieved by a reduction in parts. Cost and weight improvements are achieved by use of a new type of linear actuator. In the electronics area, most of the cost savings are obtained by a series of direct, incremental improvements in the design, although manufacturing labor and installation costs are also reduced.

Section 3

MANUFACTURING PROCESS CONCEPTUAL DESIGN

This section contains a description of the manufacturing trade study results, the manufacturing plans, the production plant description, the transportation concept, and the effects of production rates of 2500 to 1 million heliostats per year.

MDAC received support from Arthur D. Little, Inc. in the development of manufacturing approaches and production plant concepts. Pittsburgh Plate Glass provided support in the development of the float glass integration trade study, and furnished insight into issues such as glass handling and transportation. Other companies that assisted MDAC in areas of specialized equipment and processes are listed in Section 1. The manufacturing and engineering personnel also worked closely together to develop a design that represents a low-cost approach suitable for volume production.

3.1 INITIAL BASELINE MANUFACTURING PROCESS

The manufacturing concept for the initial design baseline is described in this section. This concept was established in the Company-sponsored heliostat design, manufacturing, and cost effort conducted in the Spring of 1977 with the support of Arthur D. Little, Inc. The concept calls for a centrally located manufacturing plant which produces components and subassemblies that are shipped to multiple, movable site assembly plants for final assembly.

The central manufacturing plant, Figure 3-1, consists of the following four fabrication and assembly areas: (1) reflector surface assembly area, (2) support components fabrication and finish area, (3) machine shop and drive assembly area, and (4) electrical and electronics assembly area.

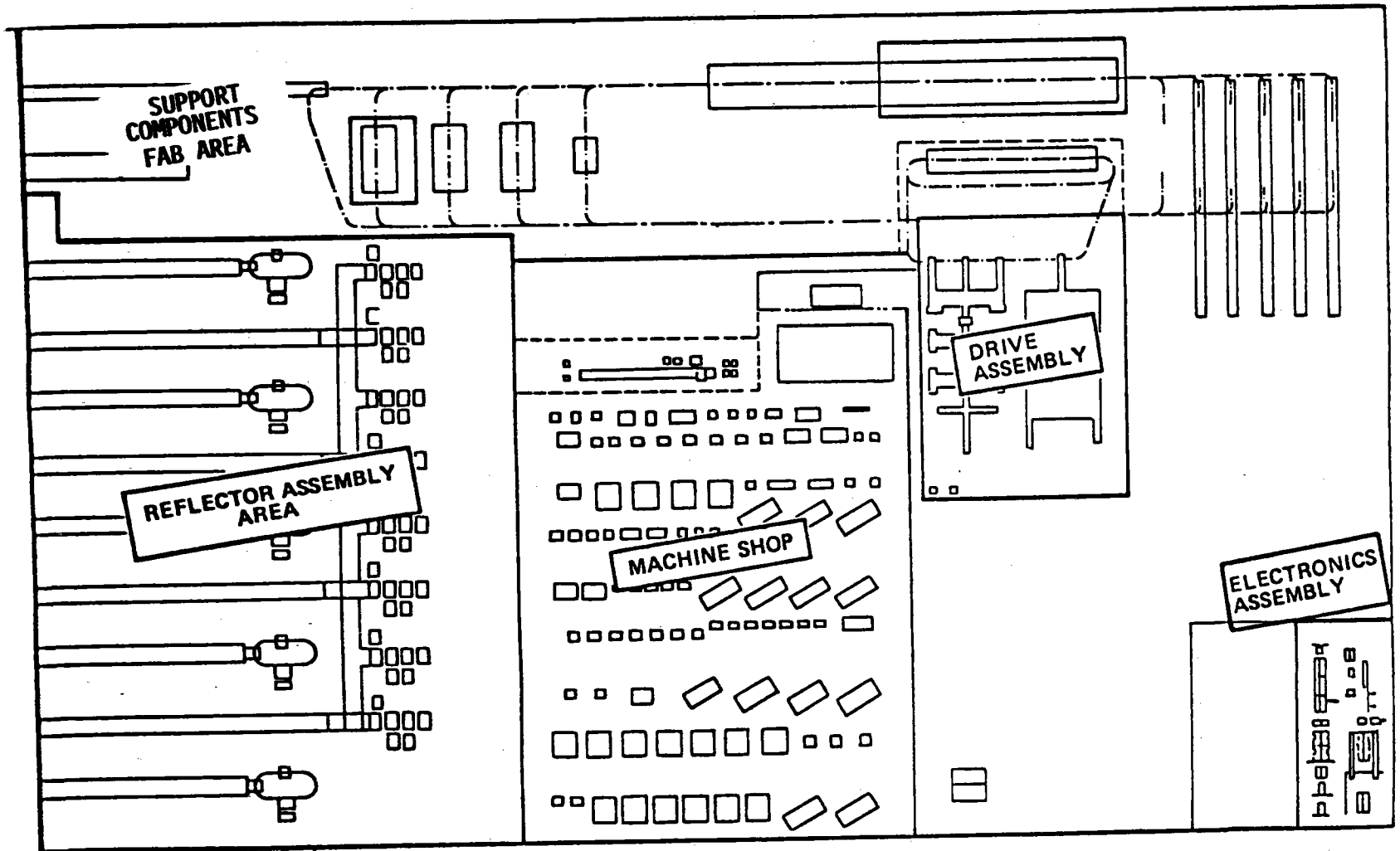


Figure 3-1. Central Manufacturing Plant

The site plants, illustrated in Figure 3-2, are located adjacent to the installation sites and are moved after power plant installations are completed. Four basic assembly operations are conducted in the site plants: (1) assembly of the cross beams to the torque tube, (2) assembly of the cross beams and torque tube to the reflective panels, (3) assembly of the drive units and wiring harnesses to the pedestal, and (4) assembly of the reflective array and supports to the drive and pedestal.

The fully assembled heliostat is then transported to the field and bolted to the foundation.

3.2 MANUFACTURING TRADE STUDIES

This section reports the results of the manufacturing studies.

3.2.1 Trade Study Methods

A trade study begins with the identification and definition of technically feasible options. A print or sketch of alternative designs may be used, or a gross manufacturing approach for each concept may be developed.

An initial estimate is made. Alternatives which are obviously not cost-effective are deleted. Detailed manufacturing plans are prepared to describe the remaining alternatives. The plans include material definition, manufacturing processes, tooling, equipment concepts, and facility requirements to meet the specified production rates. Common requirements and ground rules of the options are listed, as well as characteristic differences between alternatives. The manufacturing approaches are equally optimized for the alternatives to maintain a balance to the study; however, common materials and processes are usually deleted.

The analyses compare the estimated cost to produce each of the alternatives. The analyses include:

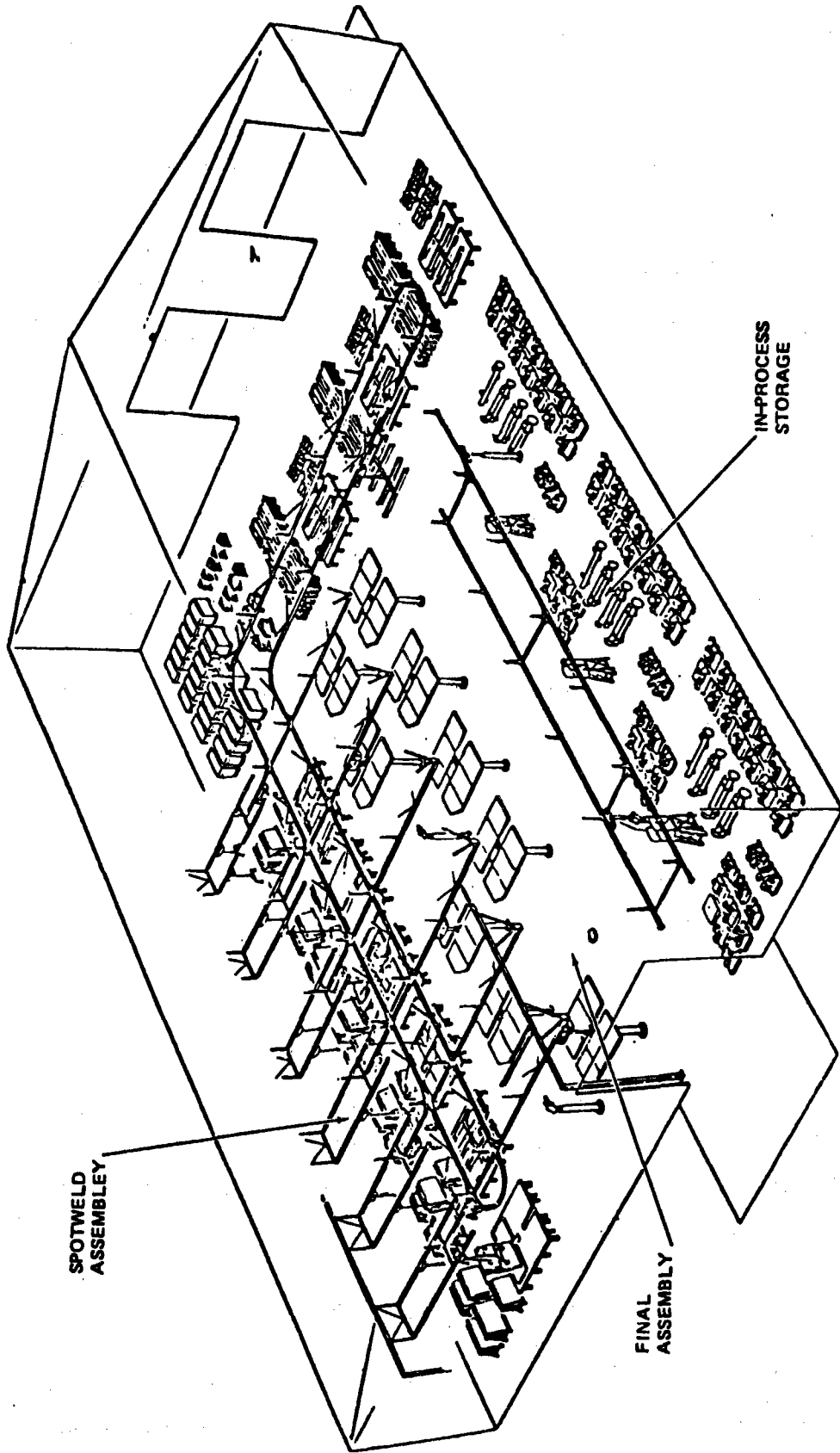


Figure 3-2. Site Manufacturing Plant

- Recurring and nonrecurring costs (or explanation of omissions with an estimate of the effect of such omissions).
- Traceable derivation of cost estimates in the form of references and work sheets.
- A summary of costs reflecting acceptable levels of quality.
- A consistent format to facilitate understanding, and
- An explanation or interpretation of the reasons for unexpected differences or observed trends.

Manufacturing labor rates are developed, based on current national averages for each job skill involved in the study. The facilities and equipment costs for each alternative are reduced to a cost per hour which is then added to the basic hourly job rate. The developed rate represents the hourly cost independent of company or location, and provides a basis for representative costing of the alternatives. The detailed plans for the alternative chosen become the baseline manufacturing concept.

3.2.2 Trade Study Results

The manufacturing trade studies are listed in Table 3-1 together with paragraph and proposal references.

3.2.2.1 M-1 Integral Pedestal/Foundation

This trade study was conducted to define cost reductions which might result from integrating the pedestal and foundation and improving the interface between pedestal and the azimuth drive. Stearns-Roger supported the pedestal/foundation portion of the study.

Four pedestal/foundation interfaces were considered:

- 1) Weld the pedestal to a plate and bolt to the foundation.
- 2) Extend a reinforced concrete piling foundation to the drive unit interface and bolt the drive unit to the foundation.

Table 3-1
MANUFACTURING TRADE STUDIES

| TRADE STUDY | OBJECTIVE | SECTION |
|---|--|----------|
| M-1 Integral Pedestal/Foundation | Minimize joint costs between pedestal and foundation and pedestal and drive unit | 3.2.2.1 |
| M-2 Drive Housing and Drag Link Materials | Reduce material and change to lower-cost material | 3.2.2.2 |
| M-3 Mirror Line Integration | Define production rate for mirror line integration | 3.2.2.3 |
| M-4 Float Glass Line Integration | Define production rate for float glass line integration | 3.2.2.4 |
| * Fusion Glass Line Integration | Define production rate for fusion glass line integration | 3.2.2.5 |
| M-7 Adhesive Application | Minimum cost means for adhesive application | 3.2.2.6 |
| M-8 Site Factory Requirements | Define net cost advantage of a site assembly facility | 3.2.2.7 |
| * Flexspline Optimization | Define low-cost means for flexspline production | 3.2.2.8 |
| * Wave Generator Configuration | Define alternative means of producing low-cost wave generator plug | 3.2.2.9 |
| * Gear Forming Processes | Define minimum-cost means for forming flux and circular spline tooth formation | 3.2.2.10 |
| * Turret Bearing Selection | Examine low-cost alternatives for the turret bearing | 3.2.2.11 |

*Initiated during current study phase.

- 3) Extend the pedestal below grade and cast into the foundation, and
- 4) Extend a reinforced concrete piling foundation about 1.22 m (4 ft) above grade, using a tapered steel tube as a permanent form, flare a matching taper on the bottom of the pedestal, and make a friction joint in the field.

A cost evaluation by Stearns-Roger showed the last method to be the lowest cost. In addition, this approach provides for complete prewiring of the drive unit and pedestal in the factory, automated installation of the drive unit in the field, and adequate leveling of the drive unit prior to alignment. The confidence level for this method is high because of its similarity to commercial practice in tall light standards and similar applications.

Based on the above, the tapered slip fit joint between the pedestal and foundation described in Sections 2.4.2.7 and 2.4.3 was selected.

A second investigation was conducted to reduce the cost of the joint between the pedestal and the azimuth drive unit. A formed plate, welded to the pedestal and bolted to the circular spline, was selected on the basis of minimum material costs.

3.2.2.2 M-2 Drive Housing and Drag Link Materials Reduction

HOUSING - Castings provide blanks for both azimuth drive housing (Figure 3-3) and the drag link (Figure 3-4). Cast blanks for these parts are about four times as expensive as an equivalent amount of plate stock. Trades were conducted to determine whether costs could be reduced by using built-up (welded) parts. Machining the housing is not a factor in this trade since the cost is approximately the same for either approach.

Baseline - Cast Housing - The casting would approximate the final housing configuration except for the possible addition of two torque tube support flanges and support gusset. For purposes of this trade study, it was assumed that the housing can be cast complete without extra cost.

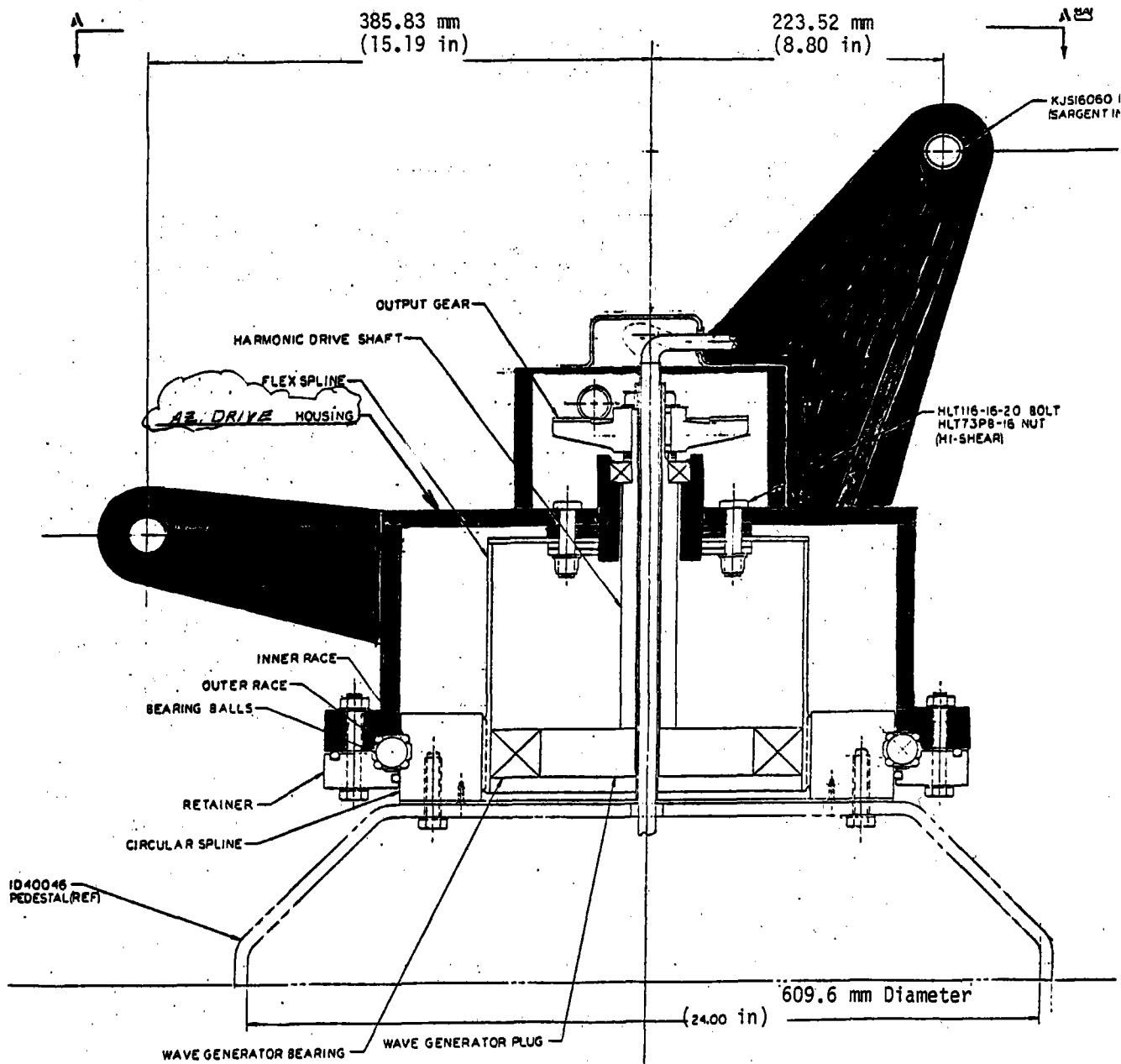
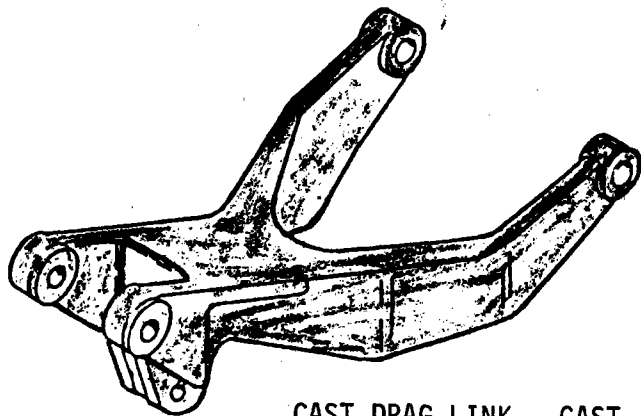
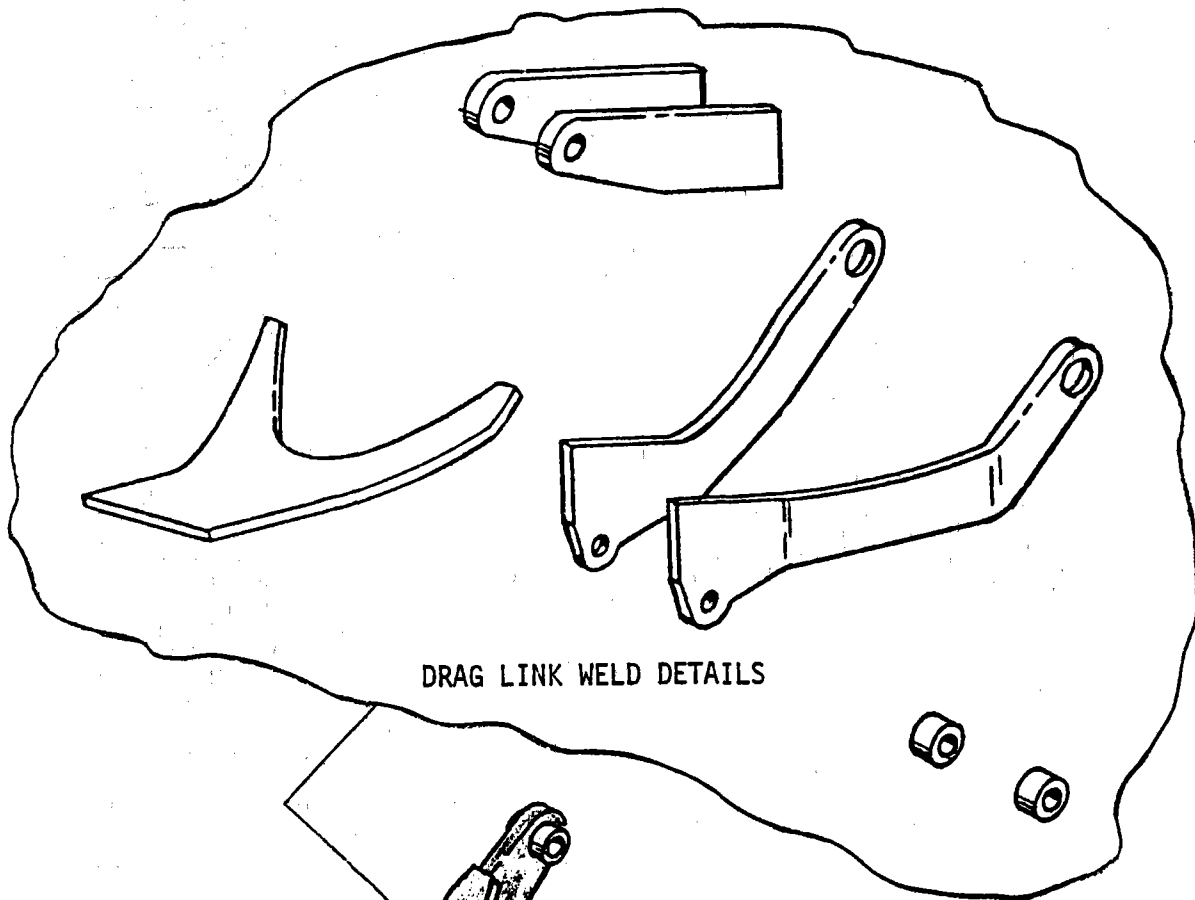


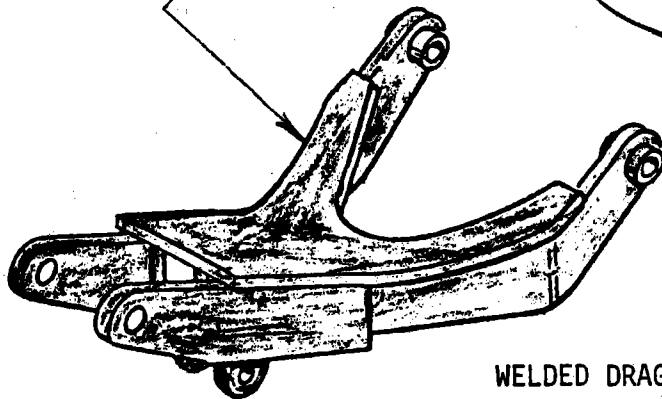
Figure 3-3. Azimuth Drive Housing Assembly



CAST DRAG LINK - CAST



DRAG LINK WELD DETAILS



WELDED DRAG LINK

Figure 3-4. Drag Link Alternatives

Alternative - Welded Housing - The welded housing is an assembly of eight different parts. Estimates of assembly costs were based on current-technology automation. Hence, it is probable that further reduction in assembly costs will result from automation developments in areas of robotic assembly, parts positioning, and simultaneous welding. These factors are considered for the higher production rates.

Current assembly techniques indicate the welded housing cost to be less than 60 percent of the cast housing cost. Further cost reductions can be anticipated from optimizing the structure and utilizing emerging production technology. Hence, the welded structure was selected.

DRAG LINK - Final machining and cleaning operations are the same for cast and built-up parts. Manufacturing costs for these operations are therefore not included in trade summaries and ratios.

Baseline - Drag Link - It is assumed that this part would be cast in the final configuration, leaving only finish machining operations to be performed. Costs reflect the purchase price of the casting, including material, labor, and die costs.

Alternative - Welded Drag Link - The weldment approach involves fabrication and assembly of two arms, four pads, one yoke, and two ears. The arms will be formed at the same time in one die on a mechanical press. The metal pads will be blanked out in a punch press. Parts will then be assembled. Conveyorization and weld automation were based on current technology and are reflected in the cost estimates. Cost reductions for the drag link are approximately the same percentage as for the azimuth drive housing. Other comments also apply, and the welded structure was selected.

3.2.2.3 M-3 Mirror Line Integration

Integration of the mirror line into the factory eliminates double handling of the glass, eliminates a cleaning step, eliminates the need for mirror backing paint, and allows the use of special handling equipment to minimize breakage.

The results of this trade study are illustrated in Figure 3-5. Mirror line integration leads to cost reductions which project a break-even point against capital costs in about 1.5 years at 25,000 units per year. Hence, mirrors will be made on the production line for all production volumes of 25,000 units per year and above.

3.2.2.4 M-4 Float Glass Line Integration

Float glass plants are characterized by very large production rates, much higher than 25,000 units per year, and probably higher than 250,000 units per year. However, at production rates of 500,000 units per year, vertical integration might make sense. This trade study was conducted to determine whether vertical integration at very large production rates is beneficial.

Results of this trade study are illustrated in Figure 3-6. While the figure shows cost reductions which indicate a break-even point in about 3.2 years at a production rate of 250,000 units per year, a typical float glass plant would be operating at only 25 to 50 percent of its capacity. Other markets for the excess capacity would be required to prevent excess costs of intermittent operation.

It should be noted that a float glass manufacturer may be willing to invest in a new facility at less than optimum heliostat production levels. This decision would consider other market uses for glass in the Southwest area, in addition to the heliostat program requirements.

Moreover, the problem of transporting the glass remains essentially unaltered. Hence, the benefit from integrating a float glass plant is marginal, at best for even the highest production rates.

3.2.2.5 Fusion Glass Line Integration

The fusion glass recommended for the mirror is made in a plant with much lower capacity than a float glass plant. Current fusion glass plants would have a characteristic capacity of about 50,000 units per year. A trade study was conducted to determine whether it is profitable to integrate a fusion glass plant into the factory.

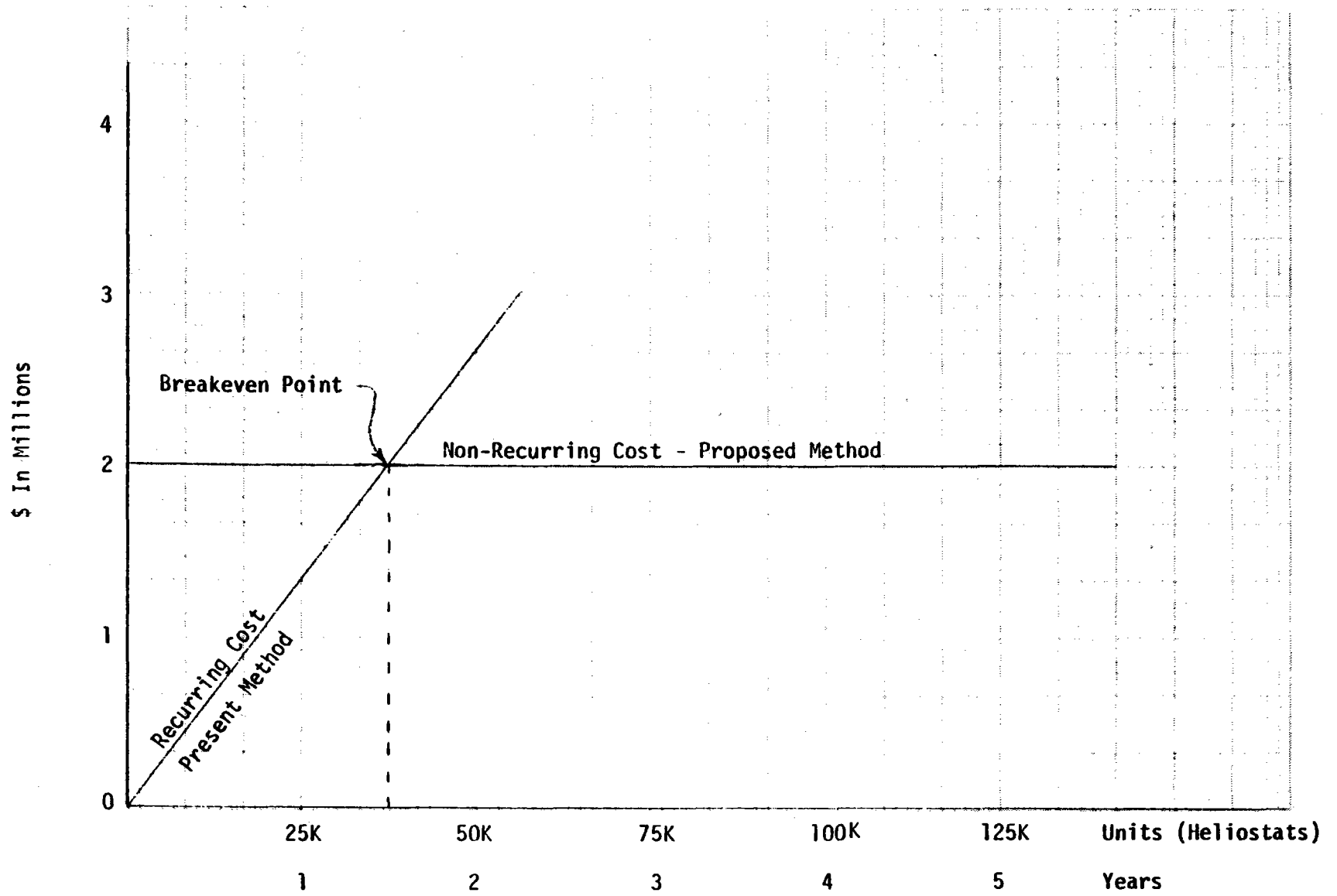


Figure 3-5. Break-Even Chart — Mirror Line Integration

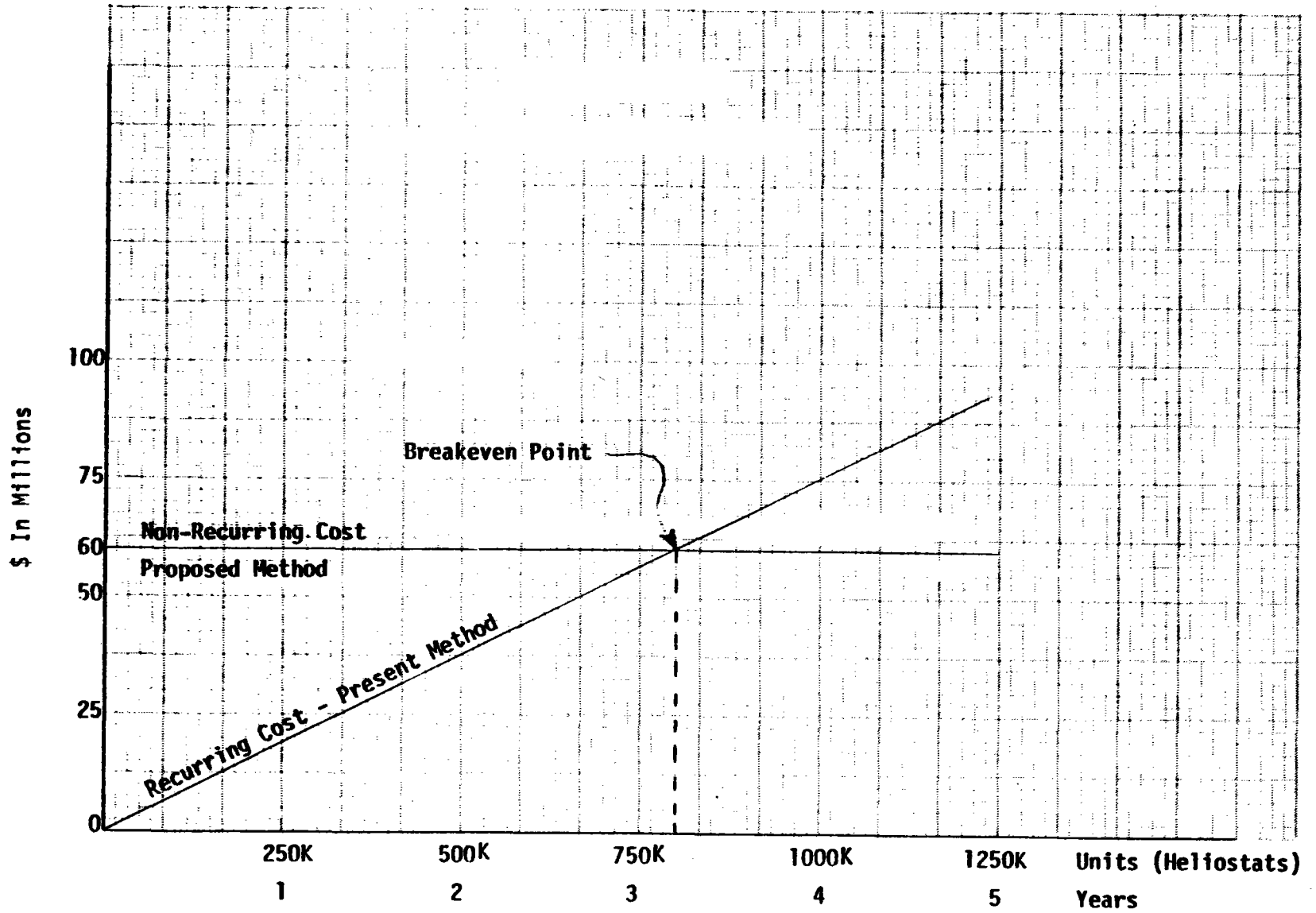


Figure 3-6. Breakeven Chart - Float Glass Plant Integration

Results are illustrated in Figure 3-7. In-line fusion glass production at a 50,000 unit per year rate shows a break-even point at about four years.

While a four-year break-even point would normally be considered marginal, several other factors are important. First, the fusion glass process is versatile. Specially formulated glasses for heliostat mirrors may be produced if appropriate raw materials are available. The present U.S. capacity for fusion glass production would be taxed when heliostats come into major production. Integrating the fusion glass plant has additional advantages of eliminating handling and possibly cleaning steps. Moreover, it is possible that automated handling can allow the use of thinner, higher-reflectivity mirrors.

Hence, fusion glass production is recommended for the higher production rates.

3.2.2.6 M-7 Adhesive Application

A trade study was proposed to determine whether costs could be reduced by alternative adhesive application methods. The design changes resulting from the preliminary design activities have led to a requirement for adhesive spray for the low-cost laminated mirror module and extrusion for bonding the mirror modules to the support structure. Hence, both methods are utilized in the production line.

3.2.2.7 M-8 Site Factory Requirements

On-site factories were required for the initial design because the one-piece reflective unit could not be economically transported off-site. Hence, this trade study focused on the relative merit of final assembly in the on-site factories compared to assembly of transportable units on the foundation.

The study showed that costs may be significantly reduced without operational penalty provided economic installation approaches can be devised. The installation approach described in Section 4.4 is extremely economical. Moreover, several operational advantages accrue to the approach deleting the site factory such as availability of a local labor force and utilities, and the absence of environmental impact.

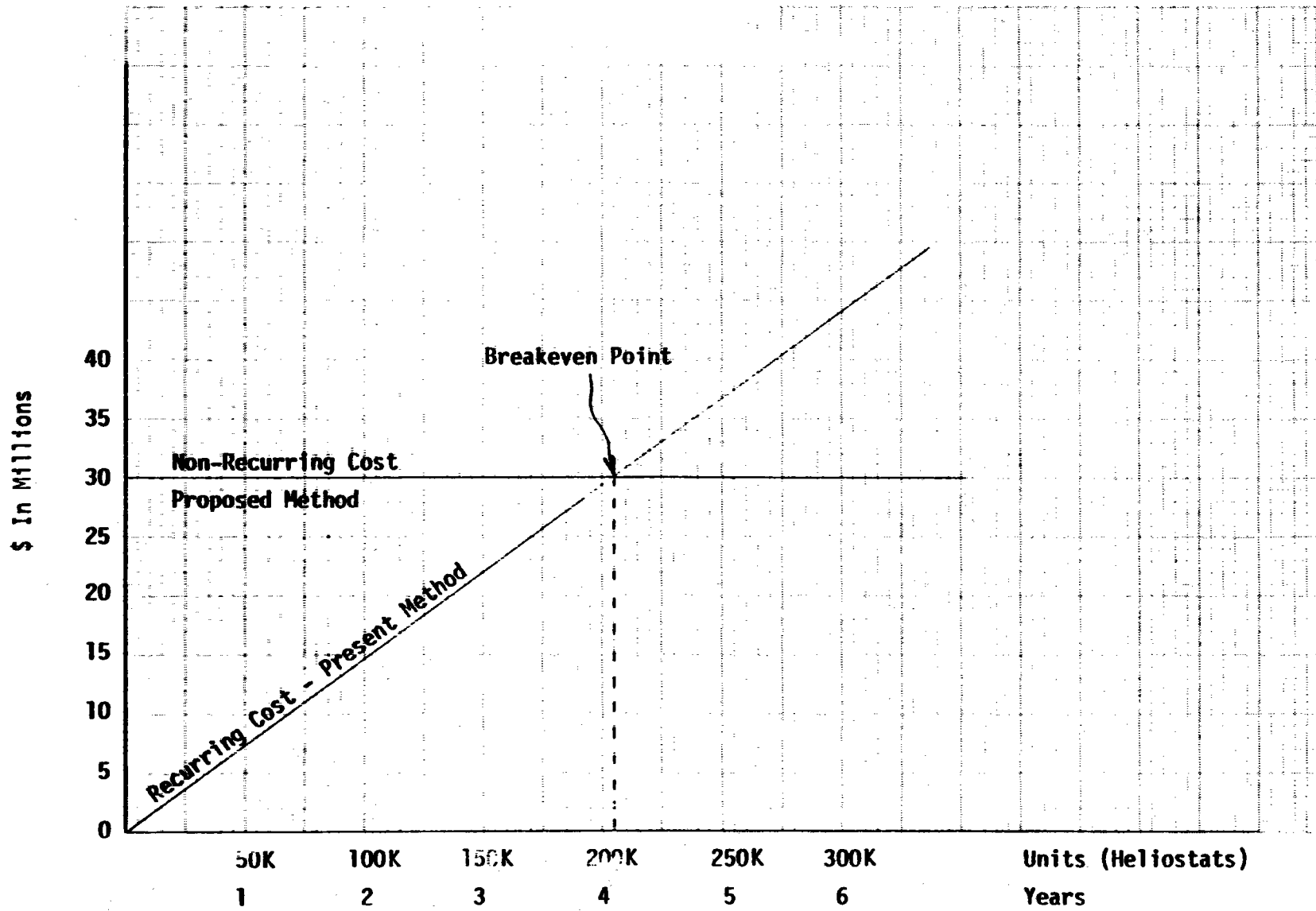


Figure 3-7. Breakeven Chart — Fusion Glass Plant Integration

3.2.2.8 Flexspline Optimization

Alternative methods of forming the flexspline (Figure 3-8) for the Harmonic drive were considered to reduce costs. Costs for the alternatives considered include only the labor, material, equipment, and facility costs that are not common to the two approaches. Gear-forming for the alternatives is assumed to be the same.

Baseline - Machine and Fusion Welded Assembly - Steel tubing with a 9.525 mm (0.375 in) thick wall is machined to 7.925 mm (0.312 in) thickness in the gear area and 3.810 mm (0.150 in) thickness in the remaining area of the flexspline. The top membrane is stamped from a 3.810 mm (0.150 in) steel sheet stock and fusion-welded to the flexspline body. The gear portion of the assembly is broached.

Alternative No. 1 - Deep Draw Can and Weld Gear End - A 3.962 mm (0.156 in) steel blank is deep-draw-pressed to form the membrane and thin-wall portion of the flexspline, including bolt holes. Steel tubing of 9.525 mm (0.375 in) wall thickness is used for the gear portion of the flexspline and inertia-welded to the thin wall of the can. The flexspline is then finish-machined and the gear broached. This approach requires approximately the same fabrication labor but results in lower material costs.

Alternative No. 2 - Weld From Tubing and Sheet - A thin-wall tube 3.810 mm (0.150 in) is fusion-welded to a stamped membrane as in the baseline. The gear portion of the flexspline is formed from 9.525 mm (0.375 in) thick tube as in Alternative No. 1 and inertia-welded to the thin tubes. The flexspline is then finish-machined and the gear broached. Material costs are further reduced while labor costs remain the same.

Both alternatives project cost reductions of at least 50 percent. Alternative No. 2 is tentatively selected on the basis of lower material costs and similarity to the flexspline design previously tested by MDAC.

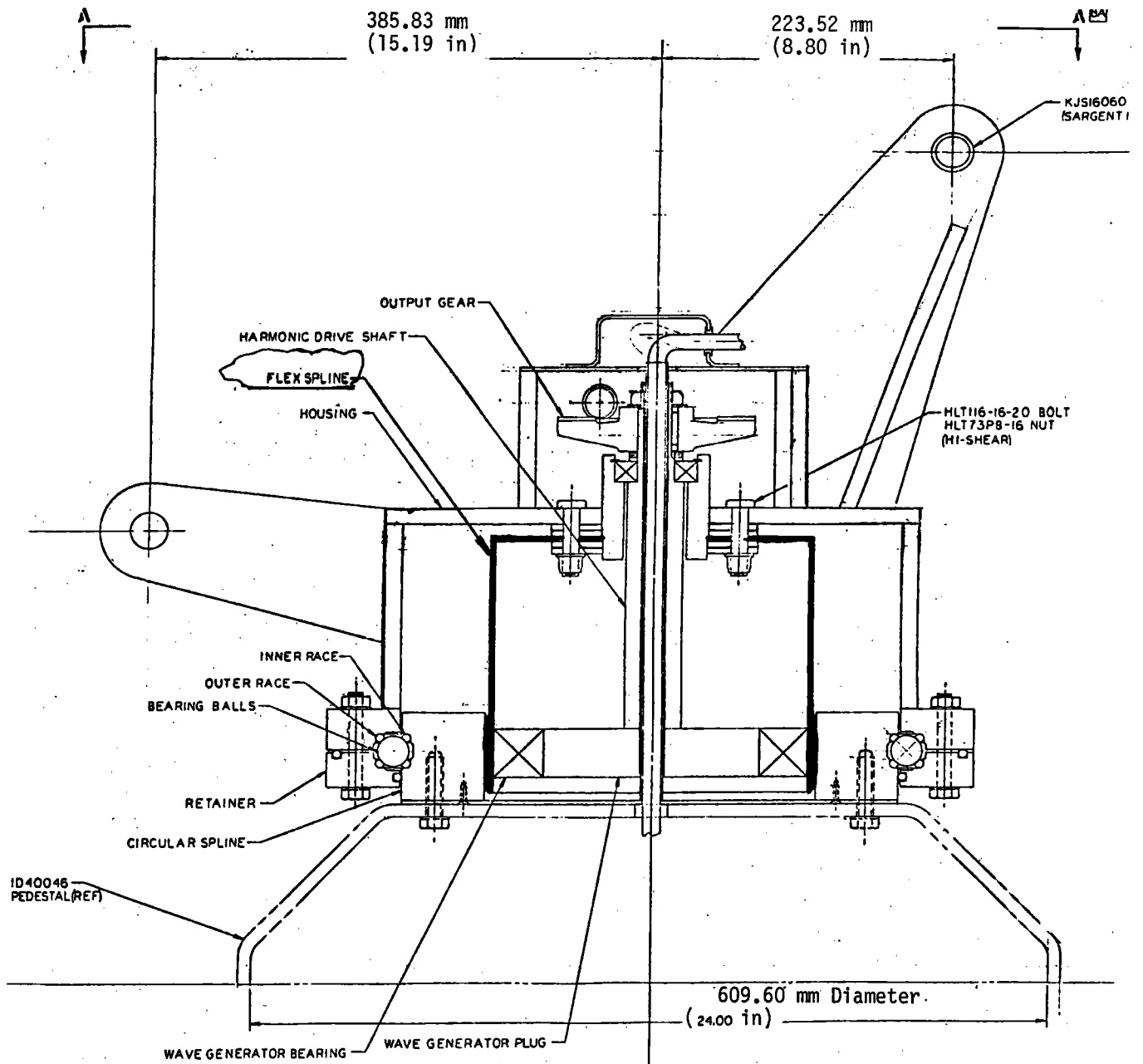


Figure 3-8. Flexspline Assembly

3.2.2.9 Wave Generator Assembly

The wave generator plug of the Harmonic drive (Figure 3-9) was examined to determine whether costs could be reduced by using different methods.

Baseline - Weld and Machine Assembly - A steel disc is sawed from a round bar to form a blank for the wave generator plug. The center hole of the blank is drilled and the blank welded to a steel tubing shaft. The oval shape of the wave generator plug is machined on the blank. Labor and materials cost of this approach are greater than for the alternative. Equipment cost is lower. Manufacturing methods lend themselves to automation.

Alternative - Powdered Metal Form and Inertia-Weld - The wave generator plug is press-formed of powdered metal and then inertia-welded to a steel tubing shaft. While material costs less than the baseline, equipment costs of the powdered metal approach are appreciably higher.

The powdered metal wave generator plug requires a larger press than is currently available. Industry sources indicate that adequate equipment should be feasible by 1985. It is expected that the alternative will be more cost-effective when adequate fabrication equipment becomes available.

3.2.2.10 Gear-Forming Processes

The gear teeth in both the flexspline and the circular spline (Figure 3-10) were examined to determine whether alternative production methods could significantly reduce costs.

Baseline - Hobbing Flexspline Gears - Cost studies indicated seven hobbing machines would be needed for a 25,000-per-year production level. It was estimated that one operator per shift could man these machines.

Alternative No. 1 - Broaching Flexspline Gears - At the same production level, one broaching machine and one operator per shift are required. As a result, the equipment cost is much lower than in the hobbing approach.

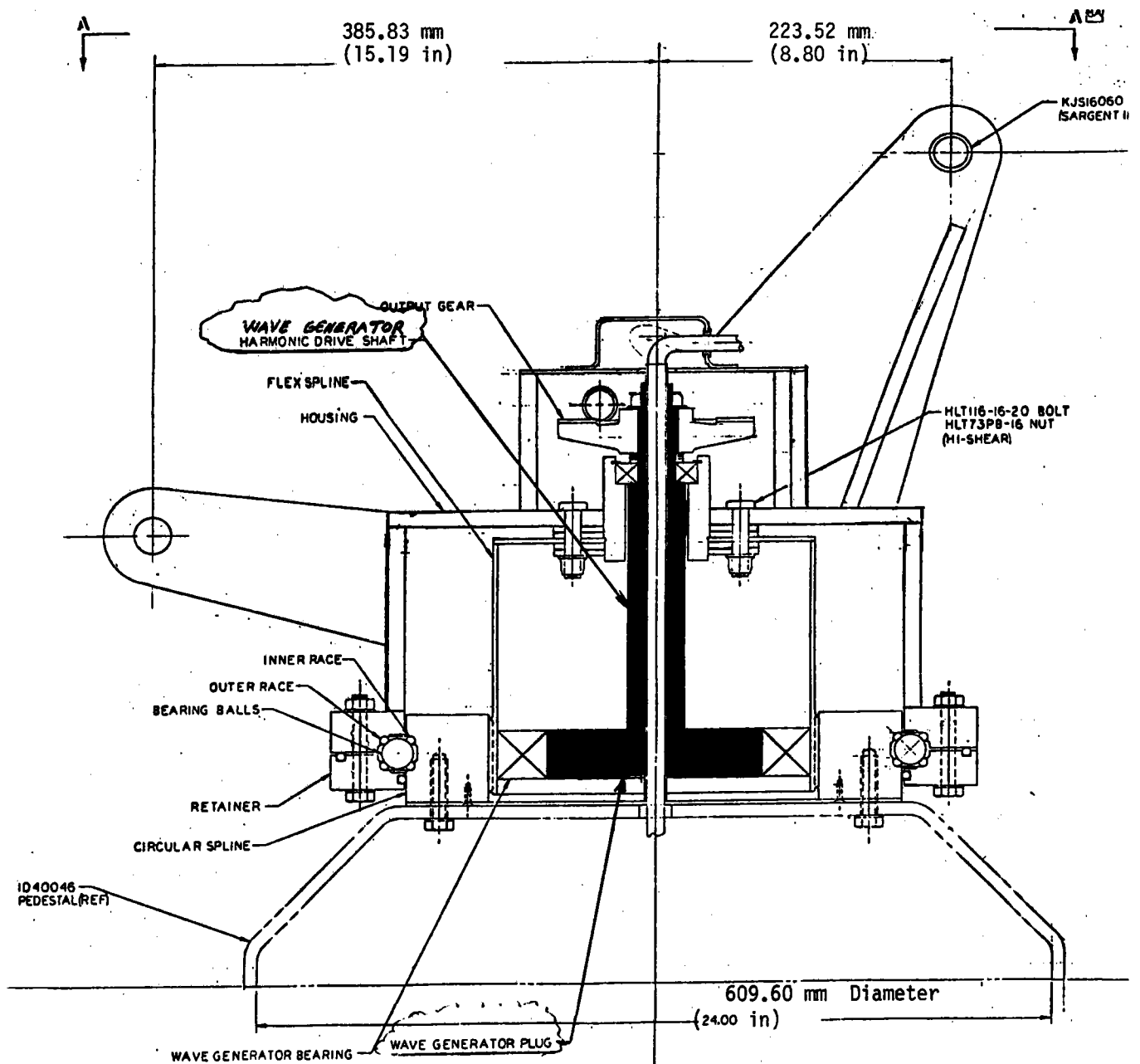


Figure 3-9. Wave Generator Assembly

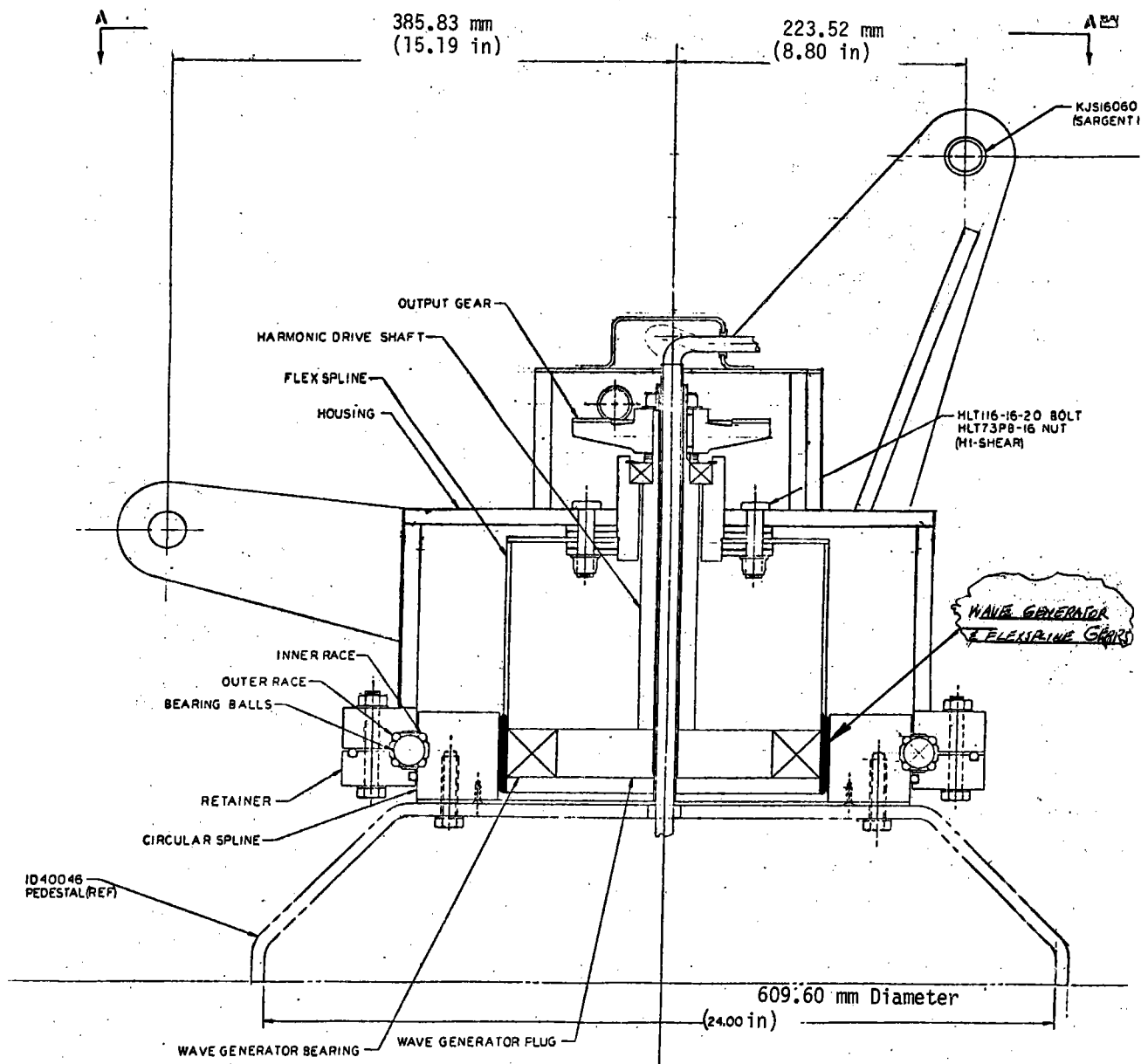


Figure 3-10. Gear-Forming Process Wave Generator and Flexspline Gears

Alternative No. 2 - Shaping Flexspline Gears - To do an equivalent amount of work as in the baseline or first alternative, three shapers and one operator per shift are required. The equipment cost is less than in the baseline method and more than in the broaching method.

Summary - Broaching was found to cost only about 40 percent as much as hobbing. Hence, broaching was selected as the method of gear-forming for the flexspline cost trade studies (Section 3.2.2.8). This method is also used for the circular spline.

3.2.2.11 Turret Bearing Selection

The turret bearing (Figure 3-11) which supports the azimuth drive was also examined to determine whether alternative approaches might reduce cost and production complexity.

Baseline - Precision Ball Bearing - A 355.6 mm (14 in) diameter preloaded and sealed ball bearing with precision inner and outer races and 127.0 mm (1/2 in) steel balls is adequate for this application. Such bearings are available from several companies. For costing purposes, a Kaydon KG series was chosen. The bearing would be installed in precision ($\sqrt{125}$) machined bearing housing areas of the circular spline and the azimuth drive housing. In addition to the bearing cost (approximately \$150 each), precision machining and assembly labor is required.

Alternative - Wire Race Ball Bearing - This design consists of four hardened steel, formed wires or rods assembled into machined grooves of the bearing cavity. These wires form a four-point contact for low-carbon steel balls. After the balls are assembled in the cavity, a retainer with its wire race in position is placed over the ball assembly and tightened by locking bolts until metal-to-metal contact is reached. A preset bolt torque is then applied to each locking bolt to preload the bearing and prevent axial and radial play. For purposes of this estimate, McGill Manufacturing Company, Bearing No. BB-2149 was selected as an appropriate design. However, procurement would involve only bulk components (23.8 mm or 0.987 inch steel balls and two sizes of wire races) with assembly at the heliostat production facility.

CR26A

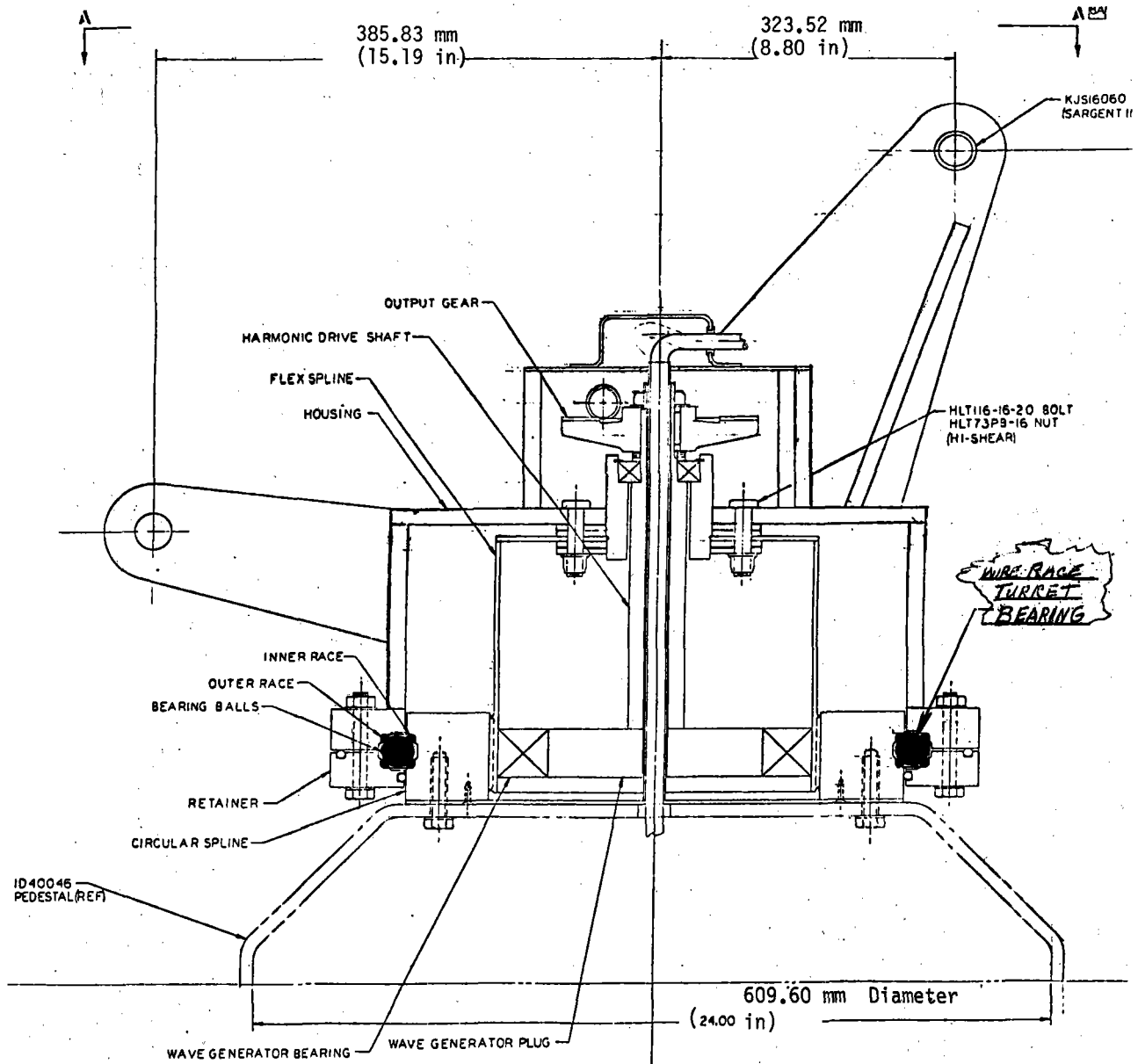


Figure 3-11. Turret Bearing Assembly

In addition to cost savings, there are several sources of supply. An additional benefit of the alternative wire race bearing is the elimination of precision machining steps on the housing and circular spline. The wire race bearing was selected on the basis of a projected 80 percent cost reduction.

3.3 MANUFACTURING PLANS

The design and manufacturing trades resulted in the development of basic engineering design and commercial production concepts. The development of the trade study alternatives required the preparation of manufacturing approaches. The manufacturing approaches for the alternatives selected then became baseline plans.

Manufacturing plans are documented in process flow charts as well as in the analyses supporting the trade studies. Plans reported in this section are based on the appropriate level of automation and materials handling for a 25,000 per year production rate. Arthur D. Little, Inc. assisted MDAC manufacturing and industrial engineers in developing these plans. The plans address such key issues as: (1) glass handling, (2) utilization of industry sources, (3) reduction of touch labor cost, and (4) design simplification for low-cost manufacturing.

(1) Glass Handling - It is recognized that handling concepts for both 1.52 mm (0.060 in) fusion glass and 4.763 mm (0.1875 inch) float glass will require some development for volume production. In particular, the transportation, packaging, and handling of fusion glass to minimize breakage will continue to receive the attention of manufacturing and packaging specialists. Both Pittsburgh Plate Glass Company and Dow Corning Glass have provided assistance in this area. In addition, glass handling equipment suppliers provided data that helped us to select the best method of handling glass with minimum damage.

(2) Utilization of Industry Sources - Both the design and manufacturing concepts provide for utilization of industry sources. With the exception of fusion glass, multiple sources of supply are available for virtually all

components of the design. For example, roll-formed parts are available from numerous sources. Additional design changes were introduced which reduced supplier dependence; e.g., the redesign of the drag link from a casting to a weldment.

(3) Reduction of Touch Labor Cost - A basic concept in these plans is to minimize labor where tooling and equipment could be economically utilized. MDAC experience indicates that when tooling and equipment are used, savings occur not only in labor cost but in related areas such as reduced scrap and rework, less handling damage, and better product consistency. Manufacturing has worked closely with special equipment and process manufacturers to evaluate equipment and tooling concepts that could be included in the plans. Accordingly, our manufacturing plans utilize methods that are well known and proven in industry application, including such processes as fusion welding, machining, broaching, and adhesive bonding. It should be noted that the increasing application of robotics will further reduce labor costs.

(4) Design Simplification for Low-Cost Manufacturing - The engineering and manufacturing approach has emphasized design simplification and elimination of parts to reduce manufacturing costs. Examples include Oldham coupling in the azimuth drive, the pedestal dome mount redesign, and the redesign of the azimuth drive housing and drag link castings to weldments. Similarly, the electronics design has been simplified so that standard processes and equipment permit good commercial manufacturing practice to be utilized. The two-sided, through-hole-plated printed wiring board design is standard in industry. The design accommodates automatic component insertion and flow soldering. These techniques are also standard.

3.3.1 Make-or-Buy

Make-or-buy, in the context of this report, refers to whether finished parts and materials are delivered to the heliostat production facility or whether they are made in the facility. Where proprietary or patented processes are utilized in the facility, a licensing or joint venture arrangement is assumed.

The make-or-buy plan that has been developed for a production rate of 25,000 units per year is given in Table 3-2. The impact on higher production quantities is also indicated.

Make decisions were based on the following factors: (1) to ensure schedule compliance, (2) cost, and (3) to ensure process control. Buy decisions were based on the following factors: (1) the item is commercially available throughout industry, and (2) the production facility would have to acquire a specialized manufacturing capability that could not be fully utilized. For example, at the 25,000 per year level, a fusion glass facility could not be effectively operated or utilized.

The make-or-buy decisions reached represent a balance between those activities that should be concentrated in the heliostat production facility and those items that can be acquired from numerous commercial industry sources. It permits effective use of capital investment in areas of production of heliostats and prevents unnecessary duplication of industrial capability.

3.3.2 Reflector Panel Production and Assembly

The reflector panel manufacturing flow is illustrated in Figure 3-12. The flow has been annotated to indicate areas for application of robotics. The figure also reflects changes that would occur if the fusion glass supplier performed the mirroring and laminating. The assembly facility would then receive a completed laminate. This alternative would reduce the potential for shipping damage and breakage of the fusion glass.

The fusion glass is received from the supplier, stacked vertically on a reusable A frame. The glass is mechanically removed from the frame using an automatic unstacking machine. This machine is hydraulically powered and uses vacuum cups for holding the glass sheet during transfer. The equipment eliminates operators from the glass handling operation, thus providing an increased safety factor.

Two unstacking machines will be used for the fusion glass loading to the conveyor in order to maintain a minimum distance between the pieces of glass and maximum mirror line utilization.

Table 3-2

PROTOTYPE HELIOSTAT HARDWARE TREE

| SUBSYSTEM | ASSEMBLY | SUBASSEMBLY | COMPONENT | SUBCOMPONENT | PART | GUIDELINE MAKE/BUY |
|-------------------------------------|-------------------------------------|---|--------------------|----------------------|-----------------------|-----------------------|
| ● Collector - (Field of Heliostats) | | | | | | M |
| | ● Heliostat - (Includes Controller) | | | | | M |
| | | ● Reflector Panel - (Two Panels make Reflective Unit) | | | | M |
| | | | ● Mirror Module | | | M |
| | | | | | ● Back Lite | B |
| | | | | | ● Adhesive | B |
| | | | | ● Reflective Surface | | M |
| | | | | | ● Front Lite | B |
| | | | | | ● Silver | B |
| | | | | | ● Copper | B |
| | | | ● Support Struture | | | M |
| | | | | | ● Inboard Cross Beam | B |
| | | | | | ● Outboard Cross Beam | B |
| | | | | | ● Diagonal Beams | B |
| | | | | | ● Outboard Angle | B |
| | | | | | ● Joint Fitting | B |
| | | | | | ● Stringer | B |
| | | | | | ● Adhesive | B |
| | | ● Drive Unit | | | | M |

3-28

Table 3-2

PROTOTYPE HELIOSTAT HARDWARE TREE

Page 2 of 7

| SUBSYSTEM | ASSEMBLY | SUBASSEMBLY | COMPONENT | SUBCOMPONENT | PART | GUIDELINE MAKE/BUY |
|-----------|----------|-------------|-----------------|-------------------|----------------|-----------------------|
| | | | ● Azimuth Drive | | | M |
| | | | | ● Housing | | M |
| | | | | | ● Shell | M |
| | | | | | ● Retainer | M |
| | | | | | ● Cover | M |
| | | | | | ● Bolt | B |
| | | | | | ● Oil | B |
| | | | | | ● Seal | B |
| | | | | | ● Bushing | B |
| | | | | | ● Ball | B |
| | | | | | ● Base Plate | B |
| | | | | | ● Stand Pipe | B |
| | | | | | ● Bearing | B |
| | | | | | ● Bearing Race | B |
| | | | | ● Circular Spline | | M |
| | | | | ● Flexspline | | M |
| | | | | | ● Membrane | B |
| | | | | | ● Tube | B |
| | | | | | ● Spline | B |
| | | | | | ● Doubler | B |

Table 3-2

PROTOTYPE HELIOSTAT HARDWARE TREE

Page 3 of 7

| SUBSYSTEM | ASSEMBLY | SUBASSEMBLY | COMPONENT | SUBCOMPONENT | PART | GUIDELINE MAKE/BUY |
|-----------|----------|-------------|-------------------|-------------------|-----------------------|-----------------------|
| | | | | ● Wave Generation | | M |
| | | | | | ● Plug | M |
| | | | | | ● Bearing | B |
| | | | | | ● Drive Shaft | M |
| | | | | ● Motor (Typical) | | B |
| | | | | | ● Motor | B |
| | | | | | ● Helicon Pinion | B |
| | | | | | ● Motor Controller | B |
| | | | | | ● Incremental Encoder | B |
| | | | | ● Input Reducer | | B |
| | | | ● Pedestal | | | M |
| | | | | ● Dome | | M |
| | | | | ● Tube | | B* |
| | | | | ● Access Cover | | B |
| | | | | ● J-Box Cover | | B |
| | | | ● Elevation Drive | | | M |
| | | | | ● Main Beam | | M |
| | | | | | ● Tube | B* |
| | | | | | ● End Plate | B |
| | | | | | ● Fitting | M |
| | | | | | ● Bushing | B |

*Items become "Make" at production rates of 250,000 heliostats per year and higher.

Table 3-2

PROTOTYPE HELIOSTAT HARDWARE TREE

Page 4 of 7

| SUBSYSTEM | ASSEMBLY | SUBASSEMBLY | COMPONENT | SUBCOMPONENT | PART | GUIDELINE MAKE/BUY |
|-----------|----------|-------------------------|------------------------|---------------------|------------------------|-----------------------|
| | | | | ● Drag Link | | M |
| | | | | | ● Bushings, Pins, Etc. | B |
| | | | | ● Stowage Actuation | | M |
| | | | | | ● Stowage Jack | B |
| | | | | | ● Motor | B |
| | | | | ● Tracking Actuator | | M |
| | | | | | ● Tracking Jack | B |
| | | | | | ● Motor | B |
| | | ● Foundation | | | | M |
| | | | | ● Collar | | M |
| | | | | ● Rebar Cage | | M |
| | | | | ● Concrete | | B |
| | | ● Heliostat Electronics | | | | M |
| | | | ● Heliostat Controller | | | B |
| | | | | | ● Power Supply | B |
| | | | | | ● Processor | B |
| | | | | | ● Housing | B |
| | | | | | ● Line Driver | B |
| | | | | | ● Line Receiver | B |
| | | | | | ● Circuit Board | B |
| | | | | ● Data Receiver | | B |
| | | | | ● Data Transmitter | | B |

PROTOTYPE HELIOSTAT HARDWARE TREE

| SUBSYSTEM | ASSEMBLY | SUBASSEMBLY | COMPONENT | SUBCOMPONENT | PART | GUIDELINE MAKE/BUY |
|-----------|----------|--------------------------------------|-------------------------|--------------|-------------------|-----------------------|
| | | | ● Motor Controller | | | B |
| | | | | | ● Triac | B |
| | | | | | ● Resistor | B |
| | | | | | ● Capacitor | B |
| | | | | | ● Board | B |
| | | | | | ● Line Receiver | B |
| | | | ● Control Sensor | | | M |
| | | | | | ● Hall Sensor | B |
| | | | | | ● Disc | B |
| | | | | | ● Line Driver | B |
| | | | ● Pedestal Junction Box | | | M |
| | | | | | ● Box | B |
| | | | | | ● Circuit Breaker | B |
| | | | | | ● Cable Clamp | B |
| | | ● Collector Controller | | | | B |
| | | ● Console | | | | B |
| | | | ● Keyboard | | | B |
| | | | ● Cathode Ray Tube | | | B |
| | | | ● Control Panel | | | B |
| | | ● Central Processing Unit | | | | B |
| | | ● Storage | | | | B |
| | | ● Field Interface | | | | B |
| | | ● Master Control Subsystem Interface | | | | B |

Table 3-2

PROTOTYPE HELIOSTAT HARDWARE TREE

Page 6 of 7

| SUBSYSTEM | ASSEMBLY | SUBASSEMBLY | COMPONENT | SUBCOMPONENT | PART | GUIDELINE MAKE/BUY |
|-----------|---------------------|----------------------|-----------------------------|----------------------|-------------------|-----------------------|
| | | | ● Mode | | | B |
| | | ● Time Pickup | | | | B |
| | ● Field Electronics | | | | | M |
| | | ● Power Distribution | | | | M |
| | | | | ● Primary Feeder | | M |
| | | | | | ● Cable | B |
| | | | | | ● Terminator | B |
| | | | | ● Secondary Feeder | | M |
| | | | | | ● Cable | B |
| | | | | | ● Terminator | B |
| | | | ● Power Distribution Module | | | M |
| | | | | ● Transformer | | B |
| | | | | ● Foundation | | M |
| | | | | ● Distribution Panel | | M |
| | | | | | ● Circuit Breaker | B |
| | | | | | ● Bus Bar | B |
| | | | | | ● Enclosure | B |
| | | ● Data Distribution | | | | M |
| | | | | ● Primary Data Cable | | M |
| | | | | | ● Cable | B |
| | | | | | ● Terminator | B |

PROTOTYPE HELIOSTAT HARDWARE TREE

| SUBSYSTEM | ASSEMBLY | SUBASSEMBLY | COMPONENT | SUBCOMPONENT | PART | GUIDELINE MAKE/BUY |
|-----------|----------|-------------|-------------------------------|--------------|--|-----------------------|
| | | | ● Data Distribution Interface | | | B |
| | | | ● Logic Network | | | B |
| | | | | | ● Data Receiver | B |
| | | | | | ● Data Transmitter | B |
| | | | | | ● Terminator | B |
| | | | | | ● Demultiplexer | B |
| | | | | | ● Multiplexer | B |
| | | | | | ● Processor | B |
| | | | | | ● Universal Asynchronous Receiver/Transmitter | B |
| | | | | ● Panel | | B |
| | | | | ● Housing | | B |

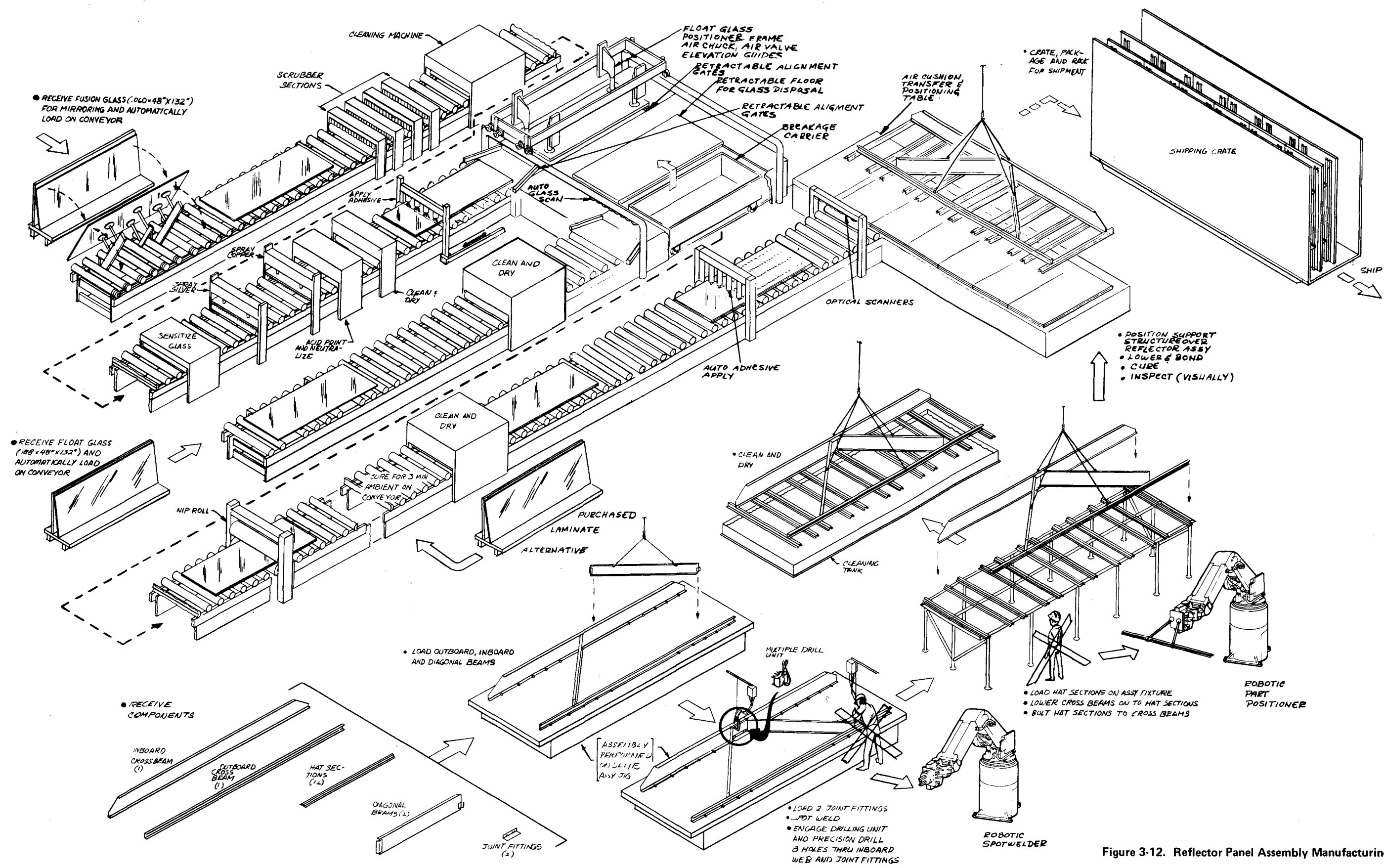


Figure 3-12. Reflector Panel Assembly Manufacturing

The glass is moved on a motorized roller-bed conveyor at approximately 14 feet per minute through all mirroring processes. First, the top surface of the glass is cleaned by a series of cup brushes using cerium oxide in slurry form. Three double-row oscillating scrubbing units, each with twenty-eight 152.4 mm (6 inch) diameter nylon rotary brushes in two staggered rows, are oscillated across the conveyor by a gear motor drive. A slurry tank is located on the right side of the machine. Pull-out scrubbers will be used to ease servicing and changing of brushes. Three 203.2 mm (8 inch) cylinder brushes (2 top; 1 bottom) will clean the glass after it has been scrubbed.

After cleaning, a demineralized water rinse and a silver sensitizer (stannous chloride) are applied by spray pipes across the conveyor line.

The silvering section is equipped with a variable traverse mechanism to move the spray manifold across the conveyor. Solutions will be applied by a low-pressure, airless spray dispensed by a proportionating console. An air blast separator will be used to contain the solutions. Silver is deposited in chemical form as silver nitrate, with chemical reaction caused by use of an alkali and reducer. A second traverse mechanism will lay down a film of pure copper by airless galvanic copper sprays. Demineralized water sprays will thoroughly rinse the copper backing.

The mirror proceeds into a face-down cleaning machine. Eight solid printing rollers with a special neoprene covering revolve in a stripping solution contained in a stainless tank. The acid solution is rinsed from the mirrors by spray nozzles. The mirror is then washed and blast-dried with dry, filtered air.

The mirror is then ready for adhesive application and laminating to the float glass. The adhesive is applied by an airless spray manifold on a variable traverse mechanism. An air blast separator is used to contain the adhesive spray. Exhaust equipment will remove any overspray. The conveyor will be shielded to prevent adhesive accumulation.

The float glass goes through the same cleaning and drying operations as the fusion glass. The float glass backlite is lifted by the automatic unstacking machine and positioned on the mirror glass. The assembly is run through a nip roller, ambient-cured on the conveyor, and fed to three bonding fixtures. The mirror modules are then positioned in groups of six on the fixture for bonding to the structure.

The reflector support structure is composed of an inboard cross beam, two diagonal beams, and an outboard cross beam, all formed from galvanized steel. Two steel joint fittings are used to reinforce the attachment of the diagonal beams to the inboard beam. Twelve galvanized steel hat-section stringers are bolted to the inboard and outboard cross beams.

The details are purchased formed and palletized, and are delivered to the fabrication area after receiving inspection. The inboard, outboard, and diagonal beams are loaded into separate punch presses that automatically punch the bolt holes.

The parts proceed on an overhead monorail to a weld and drill station. The parts are lowered into a floor-mounted fixture and secured. Spot welding of the inboard and outboard areas is accomplished simultaneously. After welding, the bolt holes for attachment to the drive unit are jig-bored.

The welded structure is removed from the weld fixture and proceeds on the monorail to two stringer attach stations.

The 12 stringers are loaded and clamped in position in the assembly fixture. The welded structure is lowered onto the stringers, clamped in place, and bolted.

The structure is removed from the tool and is moved by monorail to a dip clean, rinse and air-dry station prior to bonding the structure to the mirror modules.

A mechanically dispensed adhesive is applied to the mirror. The support structure is lifted from an adjacent conveyor line and positioned on the

mirror modules. The structure is supported on the bonding table. A fixture is used to ensure correct alignment of the mirrors with the interface to the drive unit. The reflector panel is ambient-cured and vacuum-lifted from the assembly line and placed on shipping rack for transfer to the site.

Special exhaust systems will remove vapors emitted by the acids, solvents, and adhesives. The exhaust systems may require scrubbers before the exhaust is released to the outside environment.

Special attention will be given to glass handling and transfer through the production lines. Glass handling equipment will be completely automatic and will include unstacking machines for removing large sheets of glass from vertical storage and placing them on a horizontal conveyor for processing through the production line. Air float tables are used for transfer. Additional handling equipment includes a 90-degree conveyORIZED transfer unit.

3.3.3 Drive Unit Fabrication and Assembly

Table 3-3 identifies the major processes used to fabricate and assemble the drive unit. This section highlights the key fabrication methods, types of equipment involved in each process, and significant features associated with the equipment. The detailed flow of the drive component is shown in Figure 3-13. The flow has been annotated to indicate areas for application of robotics.

3.3.3.1 Parts Fabrication

There are several tubular sections in the drive unit. The largest tubes, the torque tube of the main beam and the pedestal tube, are purchased to the correct length and are sawed only as needed to square the ends for subsequent welding operations. The other tubular sections are contained in the azimuth drive assembly and are also welded before final machining. The sawing setup and cutting operations are done so quickly that they can readily meet all tubular shape production requirements on a daily basis without the need for large in-process storage quantities. The equipment used to saw all large tube stock will be similar to a Marvel Series 25 band saw with automatic

Table 3-3
MAJOR PROCESS SUMMARY

| PROCESS | DRIVE UNIT ASSEMBLY | | | | | |
|----------------|------------------------------|------------------------------|--------------------------|-----------------|--------------|--------------|
| | PEDESTAL DOME ASSEMBLY | AZIMUTH DRIVE ASSEMBLY | ELEVATION DRIVE ASSEMBLY | | | |
| | | | ELEVATION JACK | STOWAGE JACK | DRAG LINK | MAIN BEAM |
| Tube Sawing | X | X | | | | X |
| Tube Sizing | X | | | | | |
| Flame Cutting | X | X | | | X | X |
| Press Blanking | | X | | | | |
| Press Forming | | X | | | X | |
| Welding | X | X | | | X | X |
| Turning | | X | | | | |
| Milling | | X | | | X | X |
| Drilling | X | X | | | X | X |
| Broach | | X | | | | |
| Assembly | X | X | X | X | X | X |

work-handling tables. Smaller, thick-walled stock as well as bar stock will be cut using a power hacksaw similar to a Marvel Series 6/64A with automatic in-feed and clear features.

The tube sizing area will contain a tube expander station (similar to a 350-ton Arrowsmith hydrosizer station). The station will form the truncated conical sections for the pedestal/foundation joint. The hydrosizer uses wedges which force the tubes radially outward to permanent set diameters. The wedges are fitted with shoes to shape the conical sections of the tubes

to fit the outside and inside. The tubes will be staged from the saw area in gravity feed racks and will be automatically fed to and from the expander station in a horizontal mode. The expander station will be constantly monitored by digital readout to provide for fast change-over between the two diameters and assure process control.

The flame cutting area will have two four-head, oxy-acetylene flame-cutting units similar to the LINDE CM56 mechanized cutting systems. The units will operate by template tracer control. The flame-cutting area will contain venting to ensure exhaust of all gases. All plate stock will be stored outside in open racks adjacent to the cutting area. Heavy plate stock will be hoisted by magnetic chucks to roller conveyors for preparation for cutting.

To minimize material waste, different parts will be cut out of the plate stock. For example, the 406.4 mm (16 inch) diameter cap section for the azimuth drive housing will be made from the cull obtained in cutting out the flange sections of the center beam that fit around the 406.4 mm (16 inch) diameter center beam tube.

To reduce handling, cutout sections drop into a cross conveyor container for placement into transport bins for in-process storage. A portable flame-cutting unit supports this area for breakup of cull from the plate stock after it has passed under the cutting carriage. This unit will also cut the access holes in the pedestal. The cutout sections will be used for the access hole covers.

Press blanking equipment consists of an uncoiler, coil-straightener, stock slitter, and a stamping press. An overhead crane will hoist coil stock to the uncoiling station of the stamping line. Coiled stock minimizes material shipping, storage, and handling costs. Two 300-ton mechanical presses form the ear sections of the azimuth drive housing and the side and midsections of the drag link. Another hydraulic press deep-draws the dome sections of

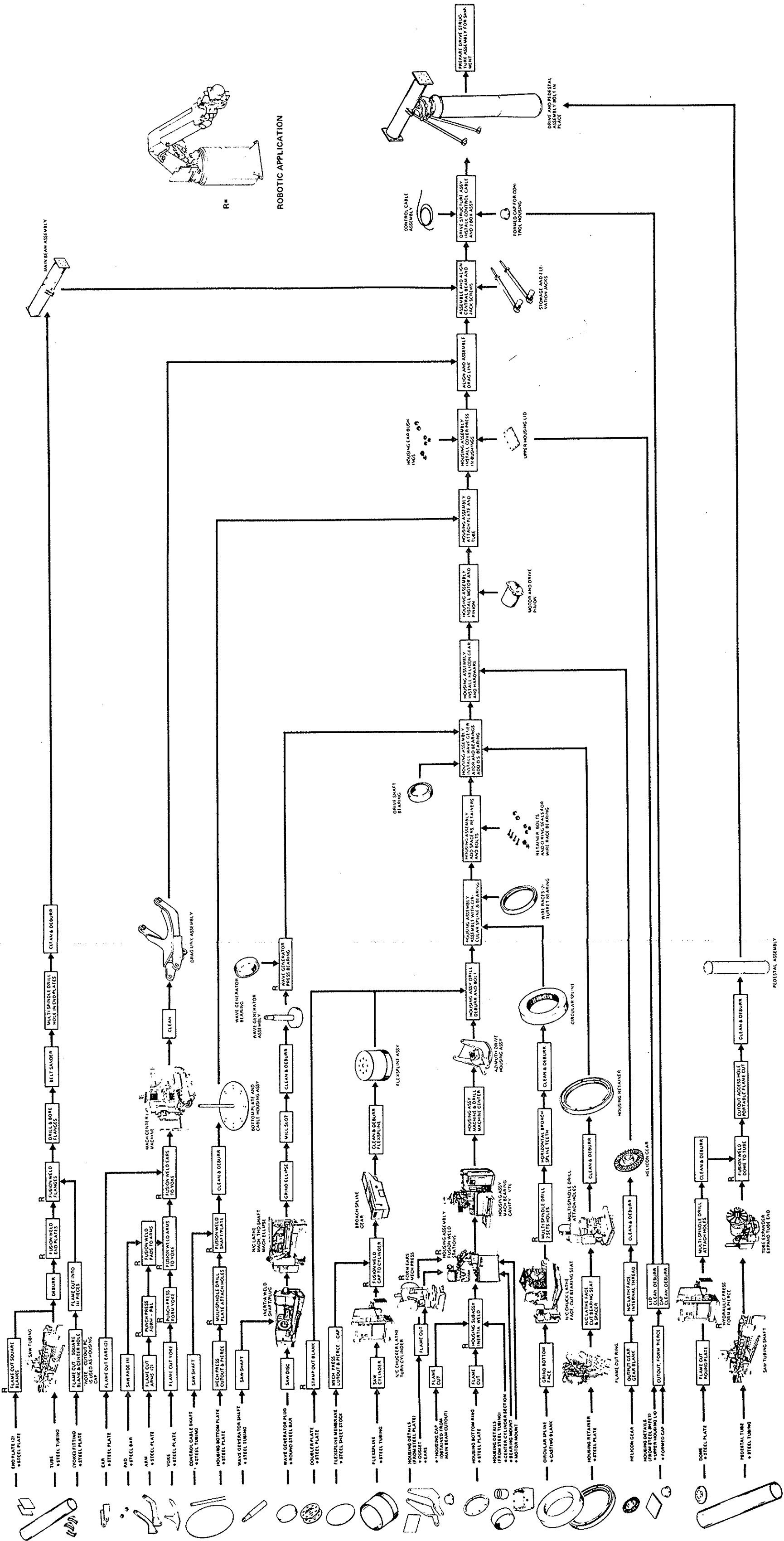


Figure 3-13. Drive Assembly Manufacturing Flow

the pedestal. Ear sections are formed in left and right-hand sets and two midsections of the drag link are formed in one setup to minimize labor and process time.

Both inertia-welding and fusion-welding are utilized. Inertia-welding equipment (similar to Manufacturing Technology Model 180B) is used to join the drive shaft to the wave generator plug. A second inertia-welder (similar to a Manufacturing Technology Model 400B) is used to join the main circular sections of the azimuth drive housing. The drive shaft sections and the sections of the azimuth drive housing are well suited to inertia-welding. No special preparation of the weld surfaces is required. Inertia-welding is a rapid operation and forms repeatably good weld joints. No automated loading or unloading equipment is included at the 25,000-per-year level; however, it can be readily adapted to the equipment.

The main fusion weld stations contain automatic weld positioners and weld heads to facilitate repeatable welds. The area will require venting since the welding is done primarily on galvanized surfaces.

The main beam weld production line contains five stations. The first station welds the side plates onto the sawed tube ends. The second station welds the flanges onto the tube wall. The third station drills and reams the flanges from fixed radial-positioned carriages which slide parallel to the tube center line (Figure 3-14). The fourth station simultaneously belt sands the sides of the plates for parallelism. The fifth station multispindle-drills and taps the reflector panel mounting hole patterns into the side plates. The pattern is located from the drilled flange holes.

The dome is welded to the pedestal directly after the tube expander operation. At a fixed multiple-drill station, the bolt pattern is drilled into the dome end for the bolt to be inserted in the azimuth drive.

These two production lines minimize transport and handling by bringing the processes to assembly. Following these lines, the units are directly hoisted to the assembly area.

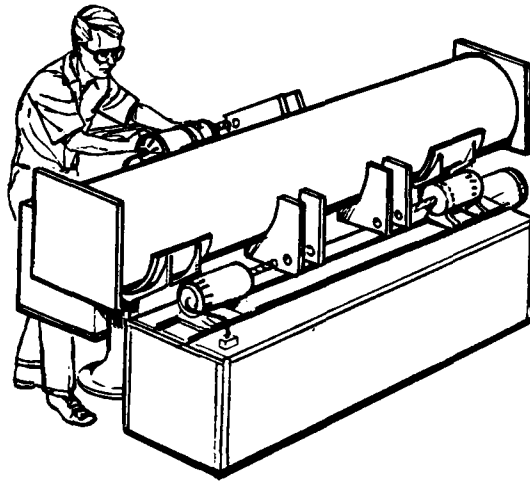


Figure 3-14. Flange Drill Station

Numerically controlled chucker lathes (similar to the Warner Swasey NC-35C) will be used to machine the wire race bearing grooves of the retainer, the housing, and the circular spline. To ensure concentricity between the turret bearing raceways and the gear diameter of the circular spline and maintain their squareness in relation to the pedestal attach plane, these surfaces will be turned, bored, and faced in one setup. The retainer will also be machined in one setup. The flexspline will have its housing mounting diameter and wave generator bearing diameters bored in the same setup to ensure concentricity and establish diameters for the subsequent gear-forming operations. The drive housing will be turned on numerically controlled vertical turret lathes, again machining all critical diameters in the same setup.

The milling operations will utilize equipment similar to the Kearney Trucker four-axis M-200 machining centers. These mills straddle the four-pivot-location ear sections of the azimuth drive housing and drill and ream the attach holes. The motor mounting face will be milled and drilled for the motor seat, shaft, and mounting screws. The top of the drive housing will be face-milled, drilled, and tapped for the cap. The mill fixture will hold the housing and locate it on the turret bearing diameter. The drag link weld assembly will be similarly machined on this equipment.

The broach station forms the gear sections of the flexspline and circular spline. The equipment is of the push type; i.e., broaches are extended through the inside diameter of the circular spline as a male broach set and over the outside diameter of the flexspline as a female set. Each broach set will be constructed of removable sections holding each tooth layer to facilitate replacement for rework. A precision post and plug tool positions the flexspline and guides the broach, keeping the gear wall constant during the broach cycle, and extracts it from the plug during the return stroke.

Multiple drill head equipment is used to drill major bolt hole patterns and tap the circular spline section (equipment similar to the Zagar Open Side Multi-Spindle drill). A special multihead drill station is used to drill the bolt hole location between the flexspline and the azimuth drive housing.

The flexspline and doublers are positioned over the housing register diameter in the inverted position. A clamping ring nests the flexspline and doublers while the drill heads drill past clearance holes in the clamping ring through the doublers, flexspline, and housing. The drilled assembly is then removed for deburring and final preparations for the drive assembly operations.

3.3.3.2 Drive Assembly

The drive housing, doublers, and flexspline are assembled on a mobile assembly fixture. See Figure 3-15.

A wire race is installed in the housing. The circular spline with two pre-assembled wire races is lowered by a handling fixture into position between the flexspline and the housing. The ball bearings are installed between the wire races. The circular spline is further lowered until the ball bearings are in contact with the three wire races. The mobile assembly fixture is transported to the next assembly station for the bearing retainer installation.

The retainer with its wire race and two O-rings is positioned over the circular spline onto the housing. Bolts are then installed through the retainer and housing and torqued to the proper preload setting. The wave generator and drive shaft assembly is lowered into the unit with a portable electromagnetic

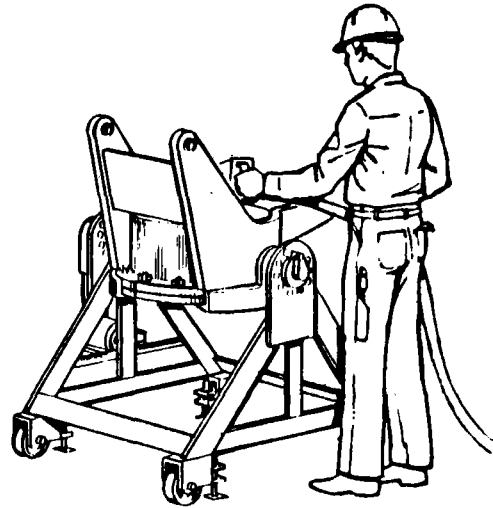


Figure 3-15. Motorized Three Position Carrier Azimuth Drive

chuck. The threaded end of the drive shaft is then captured with a sleeve, allowing the unit to be inverted for the shaft bearing installation. The drive shaft bearing and snap ring are installed. The helicon gear is then assembled into the drive shaft.

The motor and pinion are assembled into the helicon gear and secured to the motor mount. The cover plates are installed, readying the unit for the drive structure and electrical installation.

The elevation components are then assembled onto the azimuth drive assembly. The drag link is positioned so that the pivot points are in line. The drag link is centered and secured in line with the azimuth drive by through-bushings.

After the drag link is lowered to rest on the azimuth housing, the main beam is brought to the station by overhead monorail. The flanges of the beam are then lowered to align with the pivot points of the drag link and housing, centered, and secured by bolts.

The elevation and azimuth drive assembly is then hoisted to the pedestal joining areas where the pedestal has been positioned by monorail and lowered onto the pedestal. As shown in Figure 3-16, a platform allows operators to work at drive height as well as access hold height. Guide pins are used

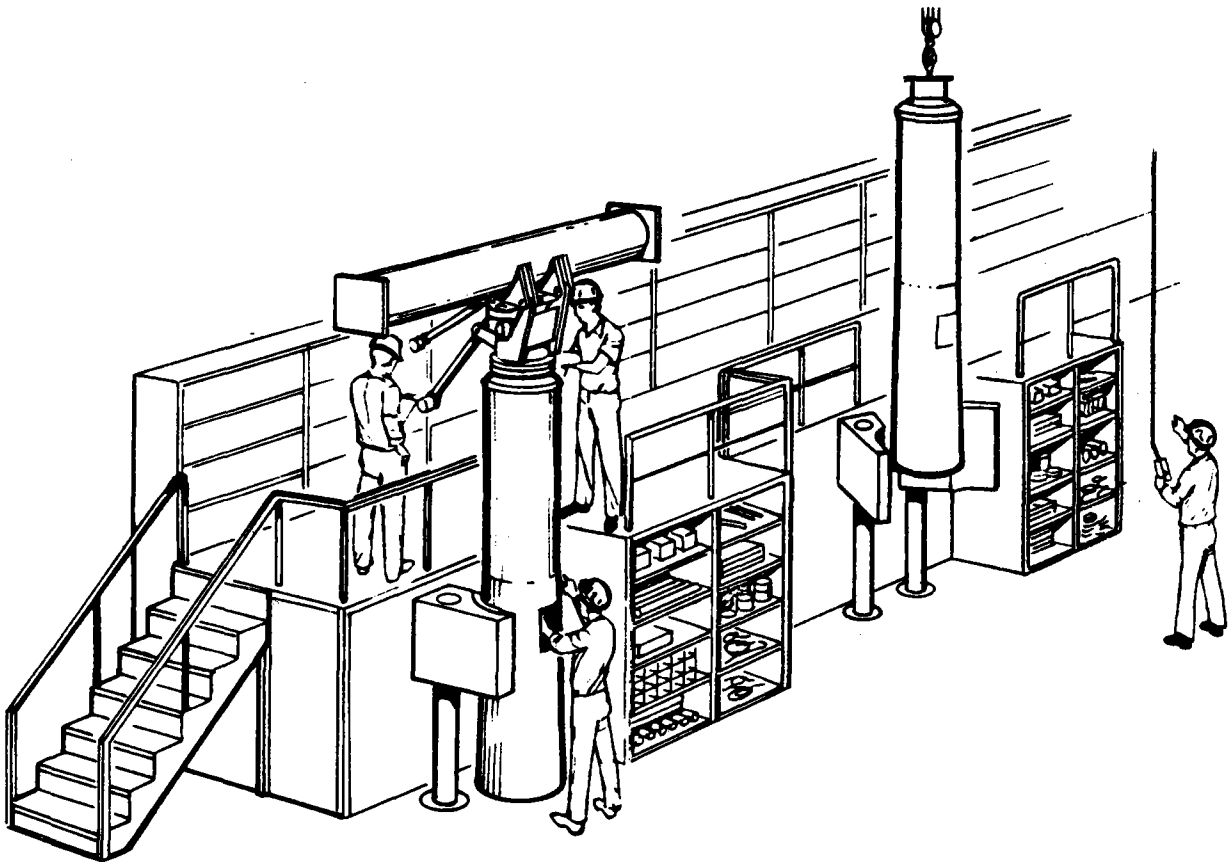


Figure 3-16. Final Assembly Joining Area Drive Unit to Pedestal

to align the hole pattern of the circular spline section on the drive with its corresponding hole pattern in the dome section of the pedestal. After the pins are removed, the joint is secured by driving bolts up through the dome into the circular spline. All tools utilized in this position are portable, hand-operated equipment.

The junction boxes, the heliostat controller, and cables are then installed on the drive structure. The drive unit is then hoisted to the truck loading dock for direct loading into the truck trailer.

3.3.4 Electronic Components

The electronic components (heliostat controller, data distribution interface, and pedestal junction box) have been designated as "buy" items (Section 3.3.1). However, a manufacturing plan was prepared to estimate their cost.

3.3.4.1 Heliostat Controller

The design and manufacturing concept for the heliostat controller utilizes

proven manufacturing processes such as flow soldering and automatic component insertion. The heliostat controller uses a two-sided printed wiring board with plated-through holes. The boards are designed to facilitate automatic insertion of components.

The housing for the heliostat controller is injection-molded with the mounting bracket and printed wire-board guides incorporated in the basic mold. The molded box design will be common to both the heliostat controller and data distribution interface.

The heliostat controller electronic components will by 1985 be in single chip packages or hybrid packages consisting of multiple chips and some discrete components that do not lend themselves to miniaturization. The costs of microcomputers with the capabilities required by the heliostat controller will continue to be reduced as they come into general use.

The heliostat controller components are: a power supply; a single-chip micro-computer; four discrete capacitors; and a hybrid microcircuit package containing three differential line drivers, two quad differential line receivers, three flip-flops, and one fiber optic receiver and transmitter.

As shown in Figure 3-17 and 3-18, the components are automatically inserted into the printed wiring boards, and the component leads are automatically trimmed and clenched. The assembly is placed on a conveyor which travels through fluxing, preheating, flow soldering, and cleaning. The completed board is sample-inspected to ensure compliance with processing specifications. By 1985, automated techniques such as pattern recognition will be utilized for inspection.

After assembly, the boards are mounted on the base of the controller box. The board assemblies will be installed from the bottom and will have one-half of the bottom attached to the card connector, with the connector extending through the half-bottom for connection. The half-bottom and card are then inserted into the cover portion of the box from the bottom. The heliostat controller has only one printed wiring board and associated connector, and

RECEIVE PARTS

3-46

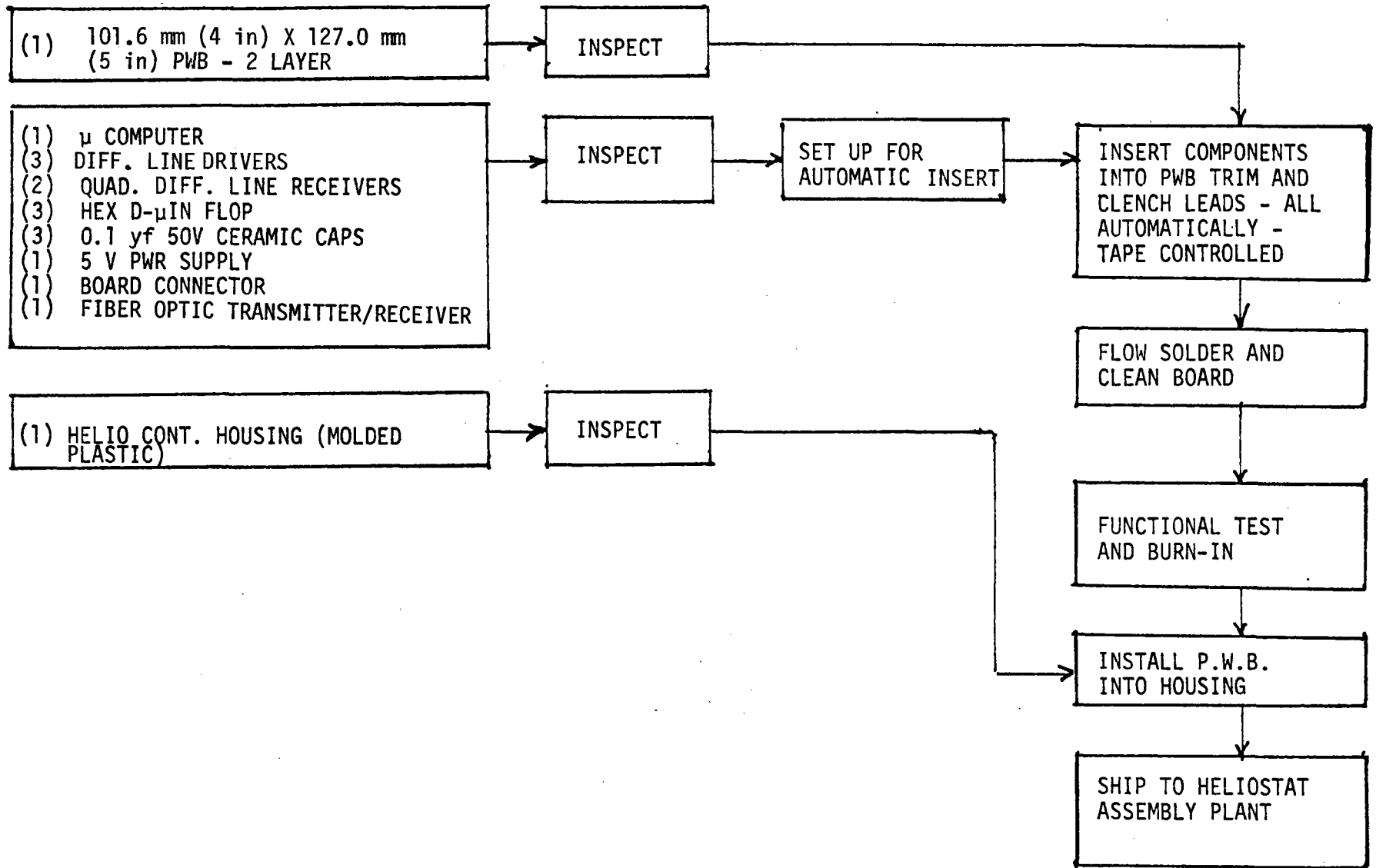


Figure 3-17. Heliostat Controller Manufacturing Flow Chart

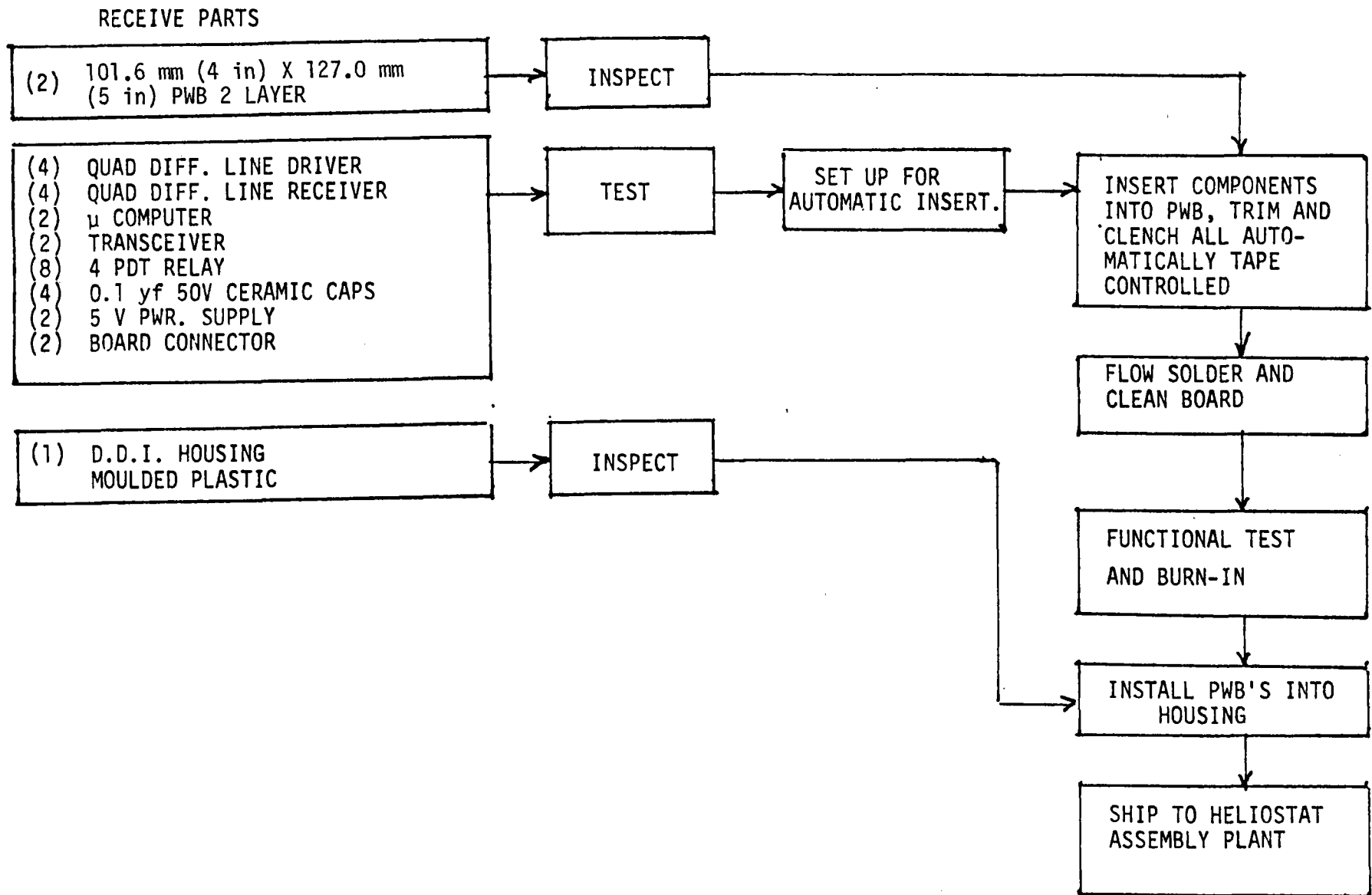


Figure 3-18. Data Distribution Interface (DDI) Manufacturing Flow Chart

therefore has a dummy half-bottom to complete the box closure. The half-bottom has a connector knockout to provide a closure when used as a dummy in the heliostat controller. In addition, it contains a vent hole to prevent condensation on the inside of the box. The half-bottoms are retained by two screws installed into the box rim.

3.3.4.2 Data Distribution Interface

The data distribution interface contains two identical printed wiring boards which are similar in construction to the heliostat controller boards. The boards will be installed with the components facing, thus allowing them to nest and the overall size of the box to be reduced.

The manufacturing operational flow is the same as for the heliostat controller, but requires a separate numerical control program tape for the automatic component insertion machine.

3.3.4.3 Circuit Breaker Junction Box

A cutout is provided on the pedestal to accommodate the field wiring junction, a circuit breaker, and the fiber optic connector. The breaker and fiber optic connectors will be mounted on a bracket in the cutout. An internal protective cover will provide personnel protection from the 480-volt terminations.

The cutout will be covered to protect the box from the weather and animals. The cover will not be water-tight, but it will drain and prevent water inflow.

3.3.4.4 Cable-Harness Assembly

The cable harness preparation area consists of work stations at which complete pedestal wiring harnesses are assembled and tested for continuity. These wiring harnesses consist of the following:

- 1) A 2.743 m (108 in) special cable comprised of three insulated copper power conductors twisted around a central core containing a pair of 1-mm optical fibers. The cable is jacketed for protection and integrity.

- 2) A 2.134 m (84 in) cable assembled at the work station consisting of a three-conductor power cable and motor controller conductors to connect the heliostat controller and stowage motor.
- 3) A 1.524 m (60 in) cable as in Item 2 to connect the elevation motor.
- 4) A 0.305 m (12 in) cable as in Item 2 to connect the azimuth motor.

The harnesses are terminated and attached to the proper connectors, as indicated in Figure 3-19. On completion of a harness, a short electrical and optical test is made for continuity, and the harnesses are sent to the systems functional test bench.

3.3.5 Quality Assurance

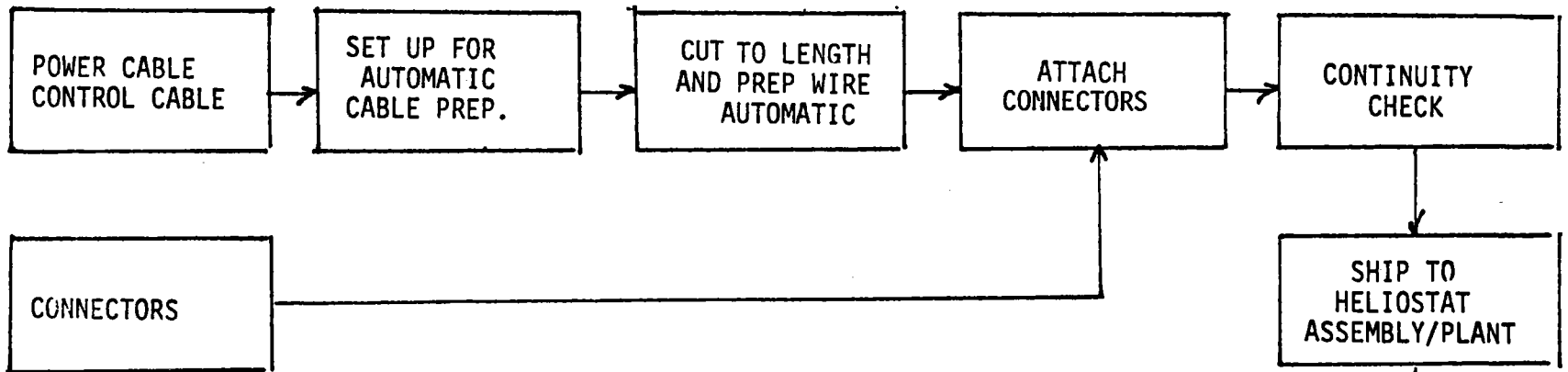
The quality assurance concept for a production rate of 25,000 heliostats per year provides for hardware verification at the highest possible assembly level. Proof of hardware acceptability is thus confirmed by performance rather than by detailed inspection. The quality assurance concept is based on the following preventive controls being imposed:

- Incoming Material - Receiving inspection prevents accepting large quantities of unusable parts or materials.
- Manufacturing - Production inspection guards against producing quantities of unusable parts.
- Test - Finished-article testing minimizes field rework of heliostats.

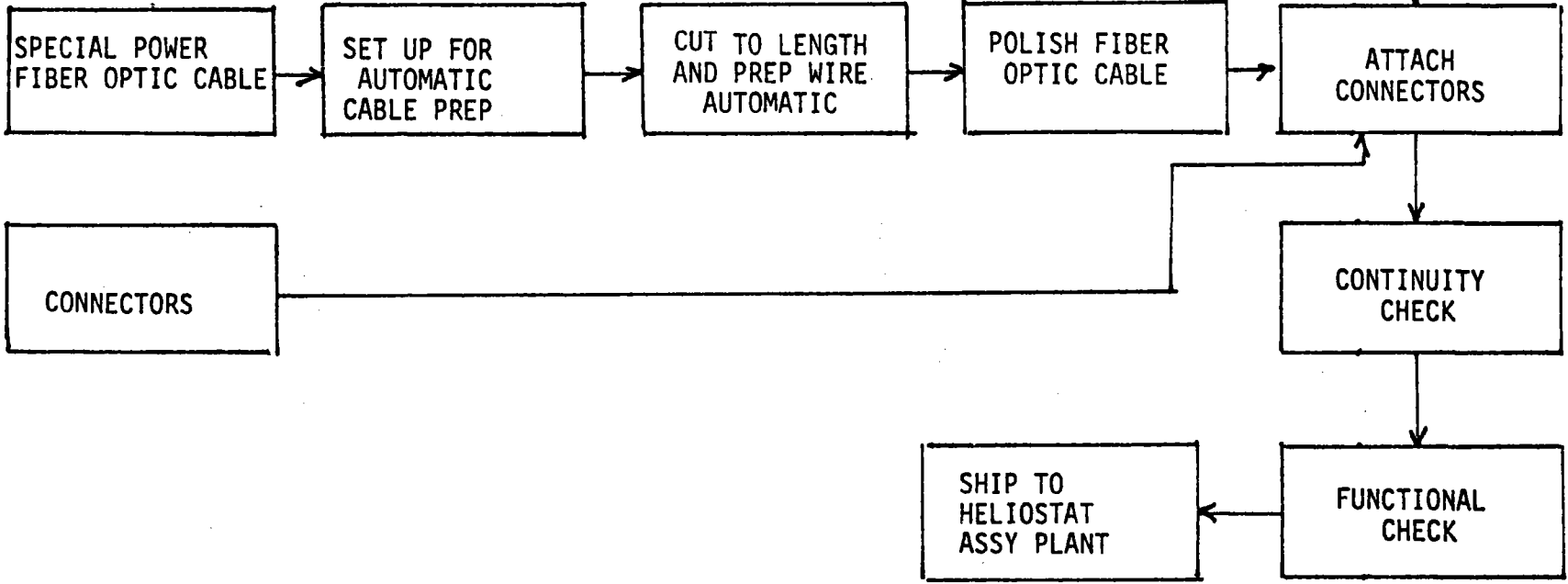
3.3.5.1 Receiving Inspection

A supplier's product is inspected in a production plant primarily to avoid delays. Reputable suppliers will replace unusable materials; however, the replacement material may have a long-lead time and therefore may tend to

RECEIVE PARTS (CONTROL BOX TO MOTORS)



RECEIVE PARTS (PEDESTAL J-BOX TO CONTROL BOX)



3-50

Figure 3-19. Heliostat Control Harness Manufacturing Flow Chart

affect the schedule. The discrepancies one would expect are more in clerical work than from hardware fabrication. Inspection includes checking incoming material for identification, certification, and damage. Sampling techniques based on past supplier performance are used.

Source inspection may be used for material and components with long-lead times, large quantity in the shipment, or a probability of the shipment not meeting specifications. Candidates for inspection at the source include glass, steel, drive motors, encoders, and electronic parts.

3.3.5.2 Manufacturing

Manufacturing must be responsible for product quality. Usually, operators must check their own work. Automated operations such as numerical control machines will have self-checking features. Inspection is done at the fabrication level to ensure that each individual process stays within the tolerance zone. Emphasis is placed on preventive controls rather than corrective actions.

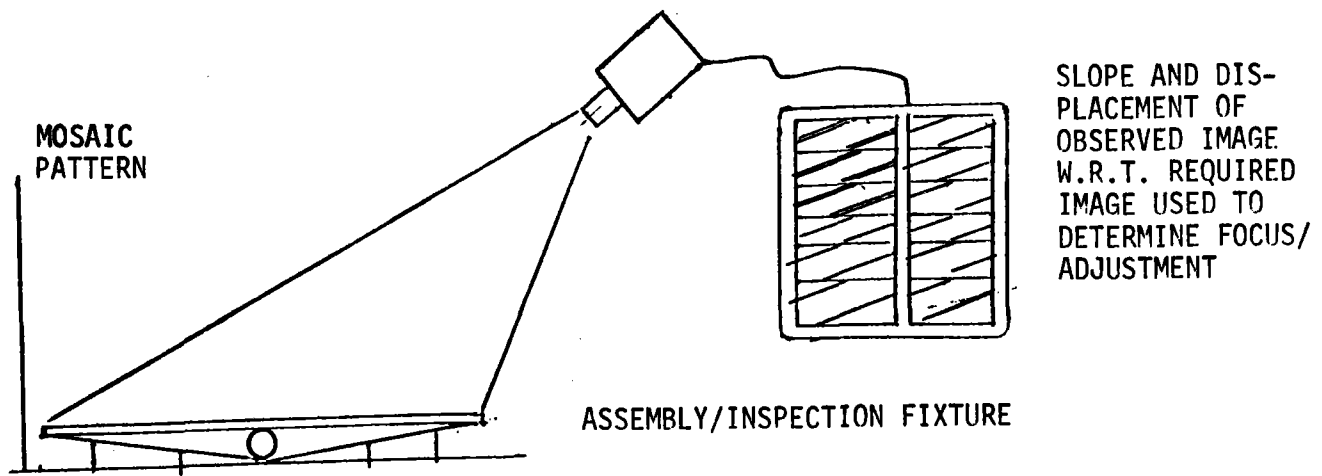
Consistent with the above philosophy, automated, semi-automated, or manually operated systems, processes, or operations should be proved and completed by first-article inspection, followed by periodic inspection of the system, process, or operation.

3.3.5.3 Testing

A quality heliostat drive system with controllers must be used to obtain a failure-free installed heliostat. Functional testing will be performed on all completed drive/control units. The test equipment will operate the drive system through all of its functional parameters and verify that the drive unit and controller were correctly assembled and are functioning correctly. Functional parameters and anomalies will be recorded for evaluation of the production process. The nonorthogonality between the elevation and azimuth drive axes will be determined and recorded in the heliostat controller nonvolatile memory.

The optical quality of the reflector subassembly is equally important to overall heliostat performance. All reflector panels will be measured to ensure they are properly aligned and meet flatness requirements. Adjacent Vidicon imaging (Figure 3-20) is used for this inspection. The reflector panel is viewed by a digital image radiometer which observes a reflected image pattern. The desired image pattern is known and deviations from this pattern, as received by the radiometer, are used by the computer to determine conformance.

CR26A



MIRROR PANEL

Figure 3-20. Digital Image Radiometer

3.4 PRODUCTION PLANT CONCEPT

This section reports on the manufacturing facility, equipment, and manpower requirements developed to support a production rate of 25,000 heliostats per year.

Key assumptions made relative to the plants are:

- The production operations included in the plant are based on make-or-buy decisions (Section 3.3.1).
- The plant concept is based on the manufacturing plan (Section 3.3).
- The plant incorporates required environmental and OSHA controls.
- The production plant is sized to operate on a five-day, two-shift basis.

The production plant layout for manufacture of the major heliostat sub-assemblies--i.e., the drive/control unit and the reflective panel--is presented in Figure 3-21. The plant size required for 25,000 heliostats per year is 62,500 square feet. The physical plant is divided in two major production areas that do not necessarily need to be collocated. For purposes of this report, a collocated layout is presented.

The production plant concepts for the two subassemblies differ considerably. The reflector panel production uses a high degree of automation and mechanized material handling. Mechanized handling and automation are required by the quantities of material being processed. For example, with 12 sheets of 1.524 mm (0.060 in) thick fusion glass and 12 sheets of 4.763 mm (0.1875 in) thick float glass per heliostat (at 25,000 heliostats per year), 300,000 lites of each type of glass are handled or 600,000 lites per year. On the average, a lite of glass must be put into production every 22.5 seconds. The mirroring line must produce mirrored lites every 45 seconds. Lamination of the fusion and float glass must be completed every 45 seconds. Reflector panel subassemblies must be completed every 4.5 minutes to keep pace with the plant output, one heliostat completed every 9 minutes. A drive/control unit must also be produced every 9 minutes.

The skills required to support both types of manufacturing are clearly different. The reflector panel requires material handlers and assemblers, primarily, while the drive unit requires machinist-type skills primarily. For further information see Section 3.4.3.

3.4.1 Plant Layout

As noted in the plant concept (see Figure 3-21), the facility houses both activities. The reflector panel line must be operated under clean room conditions. This requires the panel to be separated from the entire drive unit area and from the weld-up area of the reflector panel framework as well. Since most of the glass will be stored outside, the glass wash areas are located outside of the panel line area to further ensure cleanliness along the mirroring activities. Low-cost air curtain passageways between these areas will maintain the cleanliness requirements with no inconvenience to the operator.

Floor space requirements for under-roof glass storage is based on a one-shift supply for both the fusion and float glass lines. This allows material handlers sufficient time for periodic loading of the A-frames from the field into the glass queues with minimum under-roof storage area.

As shown in the layout (Figure 3-21), the glass line flow is continuous and straight line from raw storage to shipping, which minimizes total square footage as well as material handling. In support of the main conveyor flow, overhead monorails will carry empty A-frames back to the field for return to glass suppliers, deliver the support frames to the glass, and deliver the assembled panels to the shipping area.

The mirroring line is located next to an outside wall to minimize plumbing costs between the outside tank supply and in-house applications.

The drive fabrication and assembly activities are also aligned along straight line flows between raw storage and shipping. The stamping, sawing, and flame-cutting areas are situated next to the outside storage areas to minimize flow distance and under-roof storage requirements. These areas, as well as the welding and machining process areas following, will contain overhead air filtering equipment to continuously clean air.

3.4.2 Major Equipment Requirements

The major equipment requirements are summarized in Tables 3-4 and 3-5 for the drive and reflector panel activities. The equipment is concentrated in the drive unit area where metal forming, joining, removal, and assembly are done. Wherever practical, automatic handling equipment has been included to minimize operator handling effort, especially where operation cycle times involve manual loading or unloading. For example, shuttle-type loaders allow machining at the same time hardware is loaded and unloaded on the numerical control machining centers and vertical turret lathes. This also allows individual operators to service more than one machining activity. Automatic positioners and gravity-fed conveyors allows the large bulky items such as the main beam and pedestal to roll to their next station rather than be handled

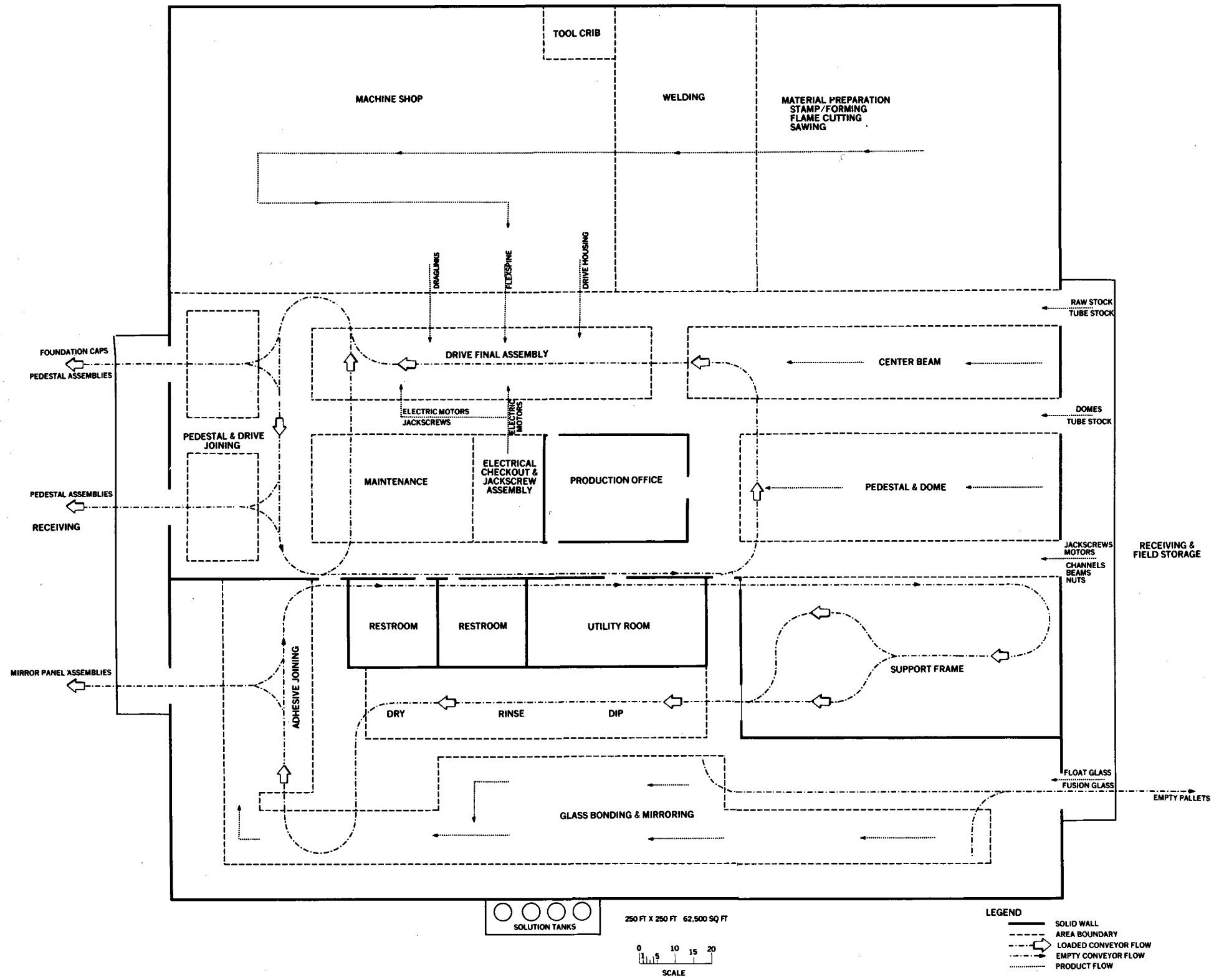


Figure 3-21. Block Flow Plant Layout

Table 3-4
 PROTOTYPE HELIOSTAT DRIVE UNIT
 PRELIMINARY EQUIPMENT CONFIGURATION - 25K/YEAR

| <u>Major Equipment</u> | <u>Number Required</u> |
|--|------------------------|
| Flame cutter | 2 |
| G&L vertical turret lathe | 2 |
| Numerical control lathe | 2 |
| Automatic lathe | 1 |
| Hydrosize machine | 1 |
| Punch press line w/coil straight | 1 |
| Hydraulic press (300 ton) | 2 |
| Deep Draw Press | 1 |
| Small press | 1 |
| Multi-drill station | 5 |
| Numerical control milling machine center K&T | 4 |
| Conventional mill | 1 |
| Fusion welder | 6 |
| Inertia welder | 2 |
| Marvel saw | 2 |
| Broach | 1 |
| Automatic Clean Deburr Station | 1 |
| Cam grinder | <u>1</u> |
| Total | 36 |
| <u>Minor Equipment</u> | |
| Material handling (Conveyors, hoists) | 106.68 m (350 ft) |

between stations. Where items require several positions for assembly, such as on the azimuth drive, specialized equipment allows multiple part orientation by single operators. The type of handling equipment and tooling reduces the cost of major machine tool investment.

Table 3-5
 PROTOTYPE HELIOSTAT REFLECTOR
 PRELIMINARY EQUIPMENT CONFIGURATION - 25K/YEAR

| <u>Major Equipment</u> | <u>Number Required</u> |
|------------------------------------|------------------------|
| Adhesive application-bond station | 3 |
| Mirroring line | 1 |
| Deionized water system & heater | 1 |
| <u>Minor Equipment</u> | |
| Conveyor | 121.92 m (400 ft) |
| Monorail | 182.88 m (600 ft) |
| Assembly jig | 2 |
| Clean & dry station (Beam & glass) | 2 |
| Nip roller Station | 1 |
| Glass handling equipment | 3 |

3.4.3 Direct Labor Manpower

Direct labor manpower by labor classification is summarized in Table 3-6 through 3-8. As noted earlier, the skill level for the drive production is higher than for the reflector panel activities. However, both activities require only four distinct classifications--material handler, welder, equipment monitor, and assembler. Laborers in these classifications should be available and/or readily trainable in the Southwest. The indirect skills have not been included here since the direct skills are significant for labor costing and trade-offs, whereas indirect items tend to be factored percentages of the direct labor base. It should be noted that while some automation has been

Table 3-6

(Page 1 of 2)

PROTOTYPE HELIOSTAT DRIVE UNIT
TOUCH LABOR MANNING - 25K/YEAR

| <u>Item</u> | <u>Touch Manning</u> | <u>Skills/Classification</u> |
|--|----------------------|--|
| Center Beam/Torque Tube Fabrication | 18 | 6 "B" welders 8 General machinists 4 Material handlers |
| Pedestal & Foundation Cap Assembly | 12 | 4 "B" welders 6 General machinists 2 Material handlers |
| Flame Cutting | 8 | 4 Numerical control machinists 4 Material handlers |
| Stampings/Press | 10 | 8 General machinists 2 Material handlers |
| Saw Cutting | 6 | 4 General machinists 2 Material handlers |
| Broaching | 1 | 1 General machinist |
| Inertia Welder | 1 | 1 "B" welder |
| Fusion Welder | 6 | 6 "B" welder |
| Final Assembly (Pedestal, Drives, T Tube) | 6 | 3 "A" assemblers 3 "B" assemblers |
| Drive Assembly (Azimuth) | 10 | 10 "B" assemblers |
| Clean, Deburr and Degrease | 4 | 4 Process machine operators |
| Drilling | 4 | 4 General machinists |

Table 3-6

(Page 2 of 2)

PROTOTYPE HELIOSTAT DRIVE UNIT
TOUCH LABOR MANNING - 25K/YEAR

| <u>Item</u> | <u>Touch Manning</u> | <u>Skills/Classification</u> |
|-------------|----------------------|---|
| Turning | 8 | 2 Numerical control machinists 6 General machinists |
| Milling | 4 | 2 Numerical control machinists 2 Material handlers |
| | <hr/> | |
| | Subtotal Drive 98 | 8 Numerical control machinists 37 General machinists 17 "B" welders 4 Process machine operators 3 "A" assemblers 13 "B" assemblers 16 Material handlers |

presented, industrial robots would further significantly reduce direct labor requirements.

3.5 TRANSPORTATION CONCEPT

This section discusses the approaches to packaging, transportation, and handling of both incoming materials and completed assemblies.

It was assumed that the heliostat factory is within an 80.467 km (50 mile) radius of the installation site. For a general production location, truck transportation is more flexible and economical than rail transportation. Motor freight classifications of items were evaluated to reduce costs from class rates to point-to-point rates, where feasible. In addition, Freight All Kinds rates utilizing piggyback shipments were studied. Table 3-9 shows present National Motor Freight Classification Data for major items.

Table 3-7
 PROTOTYPE HELIOSTAT REFLECTOR
 TOUCH LABOR MANNING - 25K/YEAR

| <u>Item</u> | <u>Touch Manning</u> | <u>Skills/Classification</u> |
|--------------------------------------|----------------------|---|
| Support Structure Fabrication | 6 | 4 "B" press operators 2 Material handlers |
| Support Structure | 12 | 4 "B" welders 3 "B" assemblers 5 Material handlers |
| Reflective Surface/Support Structure | 18 | 6 "B" assemblers 8 Material handlers 4 Packers |
| Reflective Panel Fabrication | 16 | 2 "B" assemblers 2 Chemical operators 8 Line tender-coating operators 4 material handlers |
| Subtotal Reflector | 52 | 4 "B" press operators 4 "B" welders 11 "B" assemblers 19 Material handlers 2 Chemical operators 4 Packers 8 Line tender-coating operators |

Table 3-8
 PROTOTYPE HELIOSTAT ELECTRICAL ASSEMBLY
 TOUCH LABOR MANNING - 25K/YEAR

| <u>Item</u> | <u>Touch Manning</u> | <u>Skills/Classification</u> |
|-------------------------|----------------------|--|
| Electronic/Harness Area | 9 | 4 "B" assemblers 2 "C" assemblers 3 Test technicians |
| Subtotal Electrical | 9 | 4 "B" assemblers 2 "C" assemblers 3 Test technicians |
| TOTAL | 159 | 8 Numerical control machinists 37 General machinists 4 "B" press operators 21 "B" welders 4 Process machine operators 3 "A" assemblers 28 "B" assemblers 2 "C" assemblers 3 Test technicians 35 Material handlers 4 Packers 2 Chemical operators 8 Line tender-coating operators |

NOTE: Manning requirements based on two shifts (8 hrs/shift), five day/week

Table 3-9
 NATIONAL MOTOR FREIGHT
 CLASSIFICATION (NMFC) DATA FOR MAJOR ITEMS

| ASSEMBLY | NMFC ITEM | NMFC ARTICLE NAME | CLASS RATES |
|--------------------------|-----------------|---|-------------|
| Reflector Panel Assembly | 137440 Sub 2 | Mirrors, not bent, exceeding 120 united in. but not exceeding 15-ft length or 7-1/2-ft width. | 70 |
| Drive Assembly | 133300 Sub 1 | Machinery Group, Machinery | 45 |
| Cross Beams | 104420 | Iron or Steel, Beams, | 35 |
| Main Beam | 133390 | Machinery Group, Machine Parts | 45 |
| Pedestals | 133390 Sub 4 | Machinery Group, Machine Parts | 45 |

Packaging is designed for protection of the part and optimum loading of a standard truck trailer. All packaging can be handled with conventional forklift equipment. In all concepts, cushioning material is placed between metal-to-metal interfaces (e.g., between a strap and part) to prevent abrasion. Packaging is designed to minimize material and labor costs, while providing adequate protection of materials.

Incoming Material

Incoming raw material includes glass, steel channels (cross beams), steel hat sections (stringers), and steel tubing (pedestal and main beam). Suppliers' handling and packaging methods were studied to aid in formulating our recommendations.

Glass - Glass is packed on metal A-frame fixtures to take advantage of the material's high compression edge strength. The A-frame can be forklifted. Handling individual lites presents a special problem due to the thin material (1.588 mm or 0.063 inch and 4.763 mm or 0.188 inch). Lites will be handled with vacuum equipment which supports the glass over its entire area. The lite is brought to a horizontal attitude, and placed upon a roller conveyor to move through the various processing operations, such as mirroring and bonding. Use of proper protective clothing and procedures when handling glass will be strictly enforced. Where important to safety, redundant or fail-safe systems will be made mandatory to reduce the occurrence of accidents. Proper lighting conditions and safety measures will be monitored.

Formed Steel - The cross beams are relatively long (approximately 6.1 km or 20 feet), relatively thin 1.984 mm or 0.785 inch steel channels. Each beam weighs approximately 140 pounds. They are placed flat on wooden 2 by 4's, reverse-nested, formed into a bundle of 2268 to 3402 kg (5,000 to 7,500 pounds), and strapped across 1 by 4 hold-downs. The bundles are stacked by a forklift onto a trailer, forming a high-density load.

The stringers are approximately 130-inch long, relatively thin (0.04 inch) steel hat sections. They are handled in the same manner as the cross beams. The stringers are strapped in bundles of 1134 to 2268 kg (2,500 to 5,000 pounds). The bundles are unloaded with a forklift for handling by the factory conveyor system.

The pedestal is made of 60.96 cm (24 inch) diameter steel tubing, weighing approximately 181 kg (400 pounds). The main beam is a 40.64 cm (16 inch) diameter steel tube, weighing approximately 54 kg (120 pounds). Each is stacked across wooden 2 by 4's and strapped over 1 by 4 hold-downs.

Steel plate for the drive assembly will be received on pallets or strapped to wooden 2 by 4's.

Incoming Parts

Incoming parts include electric motors, actuators, and various bearings and bushings. Bearings and other small parts are individually wrapped and bulk-packed in fiberboard cartons. The containers are then palletized. Electric motors are individually packed in fiberboard boxes. Unit containers are then palletized so they can be handled with a forklift. The actuators are approximately 1.5 m (60 inches) long and weigh 22.68 kg (50 pounds). They will be strapped to a pallet having cover blocks which also provide for stacking. The pallets are stacked by forklift, and each stack is strapped together.

Shock Sensitive Equipment - Calibration equipment, controllers, junction boxes, and other electrical equipment will be cushion-packed in fiberboard or wooden containers (depending on weight) for protection from shock and vibration. The containers will be palletized to provide forklift capability.

Factory-to-Site Shipments - The heliostat will be shipped from the factory to the installation site as three subassemblies: two reflector panel assemblies and the drive/control unit assembly.

Reflector Panel - Each panel is handled from its mirror side with the reflector panel installation equipment (Figure 4-4). As shown in Figure 3-22, the panels are supported on edge on a base structure with the larger inboard cross beam down. After the base is loaded, a cushioned hold-down assembly is installed across the top of the panels and strapped to the base. The loaded base assembly (four reflectors) weighing approximately 2720 kg (6,000 pounds) is forklifted onto a lowboy trailer and secured to the bed. The load is covered with a flexible, opaque tarpaulin to prevent glare hazards for other vehicles. A lowboy trailer is used to keep the load under the 4.267 m (14 ft) height restrictions.

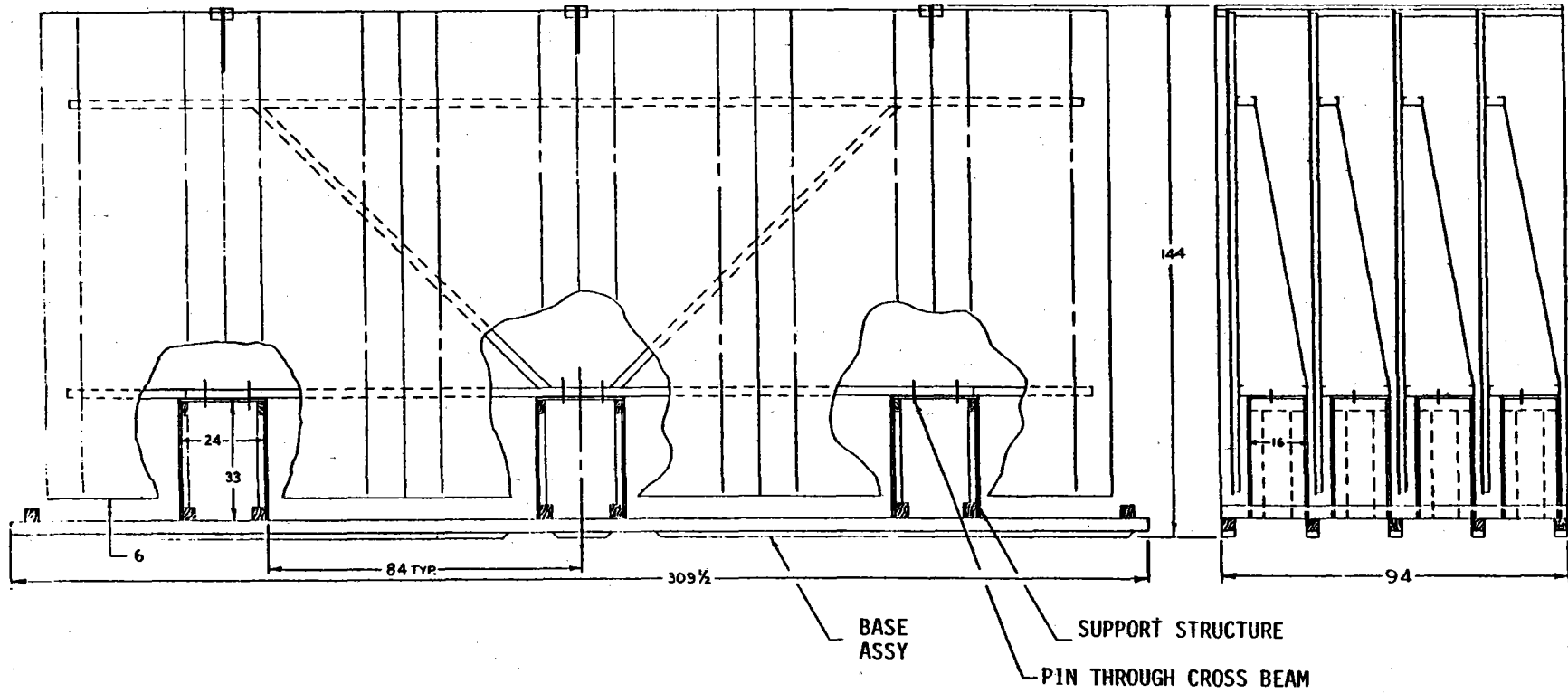


Figure 3-22. Reflector Panel Assembly Shipping and Handling Fixture

Drive/Control Unit - This assembly is approximately 4.1 m (163 inches) long and weighs approximately 1,900 pounds. The assembly is unloaded with the drive/pedestal assembly installation equipment, described in Section 4. It is shipped with the actuators attached and facing up. Specially fitted, 12.192 m (40 ft) flatbed trailers will be utilized for shipment of the drive assembly from the factory to the site. A welded metal rack (approximately 9.1 m or 30 ft long, 0.6 m or 2 ft wide, and 1.5 m or 5 ft high) is secured along one side of the trailer. Wooden blocking is secured to the trailer bed to provide stops for the main beam. The main beam is placed on the bed at a 24-degree angle to the side of the trailer to provide for nesting and high-load density. The pedestal is pointing up to the aft, at a 40-degree angle to the horizontal, to keep the load under height restrictions. The main beam is strapped to the wooden blocking to provide hold-downs, and the pedestal is supported by the metal rack. The trailer is loaded starting at the aft end. Twelve assemblies can be loaded on one trailer.

3.6 PRODUCTION CONCEPTS FOR 250,000 AND 1,000,000 HELIOSTATS PER YEAR

The changes that occur between the 25,000 heliostats per year and higher production quantities are described in this section. Generally, these changes relate to tradeoffs in transportation of raw materials and finished assemblies versus specific plant sites. These considerations will determine the optimum location of manufacturing facilities. Each facility will be sufficiently automated so these production rates can be achieved. The increasing application of techniques such as programmable industrial robots and pattern recognition will reduce "touch" labor to primarily maintenance and machine-tending.

3.6.1 250,000 Heliostats Per Year Production

As noted earlier, the drive unit and reflector panel assemblies do not need to be collocated. Their separation and other significant changes for these production rates are discussed next.

Reflector Panel Assembly

Fusion glass facilities for mirroring and laminating would be located adjacent to float glass plants. This could be in areas such as Fresno, California and Wichita Falls, Texas. The fusion glass plants with in-line mirroring would be dedicated to solar production. Float glass would be moved to the fusion glass facility for laminating. The plant would be highly mechanized, utilizing automated material handling and inspection techniques. Mirror modules would be shipped by rail and truck to the reflector panel assembly factory. This facility would be relatively small, automated, and located within a 50-mile radius of the installation sites. Roll-formed parts would be received from suppliers, staged, and automatically fed onto conveyor production lines. Industrial robots will perform the handling, drilling, fitting, and welding operations. Pattern recognition equipment will monitor glass and mirroring quality.

Drive Unit Assembly

The drive unit production facility will be automated and set up to minimize parts flow and handling. For example, the main beam and pedestal assembly will be automatically rolled and welded from sheet stock. The advantages of receiving sheet stock and forming tubing in-plant is based on the higher packaging densities achieved in transporting flat plate rather than tubing. Other changes would include:

- Automatic Inertia Welding - This would replace fusion welding in areas such as dome-to-pedestal, flexspline cap-to-cylinder, and end plates-to-main beam. Assembly of the flexspline to the azimuth housing with bolts would be replaced by inertia welding.
- Net Shape Parts - During the likely time frame of this production, it is anticipated that powder metallurgy processing for the wave generator will be within the state of the art. The flexspline would be capable of being deep-draw-formed, which would eliminate machining operations.

- Robotic Assembly - The drive unit will be assembled with industrial robots. Detail parts for the assembly will be produced on dedicated automatic equipment with robotic loading and unloading of parts and conveyerization of parts to the assembly area.

3.6.2 1,000,000 Heliostats Per Year Production

The major changes for this production rate will be duplicate automated facilities, located to minimize transportation costs. The activities described for the 250,000 heliostats per year production rate (i.e., robotic assembly and net form shape) should apply for the higher volume. Other significant changes are described in the following text.

Reflector Panel Assembly

- Dedicated Mirror Module Production Facility - The production base would be able to utilize the float glass output of a dedicated facility located in the Southwest. Fusion glass facilities would be an integral part of this complex. The result would be automated handling from glass manufacturing through mirror module completion.
- Reflector Panel Assembly - These facilities would be automated similar to the plant described for a 250,000 per year production rate.
- Roll-Formed Parts - The production volume could warrant roll-forming by the steel producers. This would reduce handling costs.

Drive Unit Assembly

The assembly facility would be similar to the concept described for production of 250,000 heliostats per year. However, multiple facilities would be required to sustain higher production.

Section 4

INSTALLATION AND CHECKOUT CONCEPTUAL DESIGN

The installation and checkout procedures are designed to accomplish, in a timely, well-organized, and cost-effective manner, the emplacement and performance verification of heliostats at relatively high production rates.

4.1 INITIAL BASELINE PROCESS

The initial installation and checkout process is shown in Figure 4-1 for a typical heliostat.

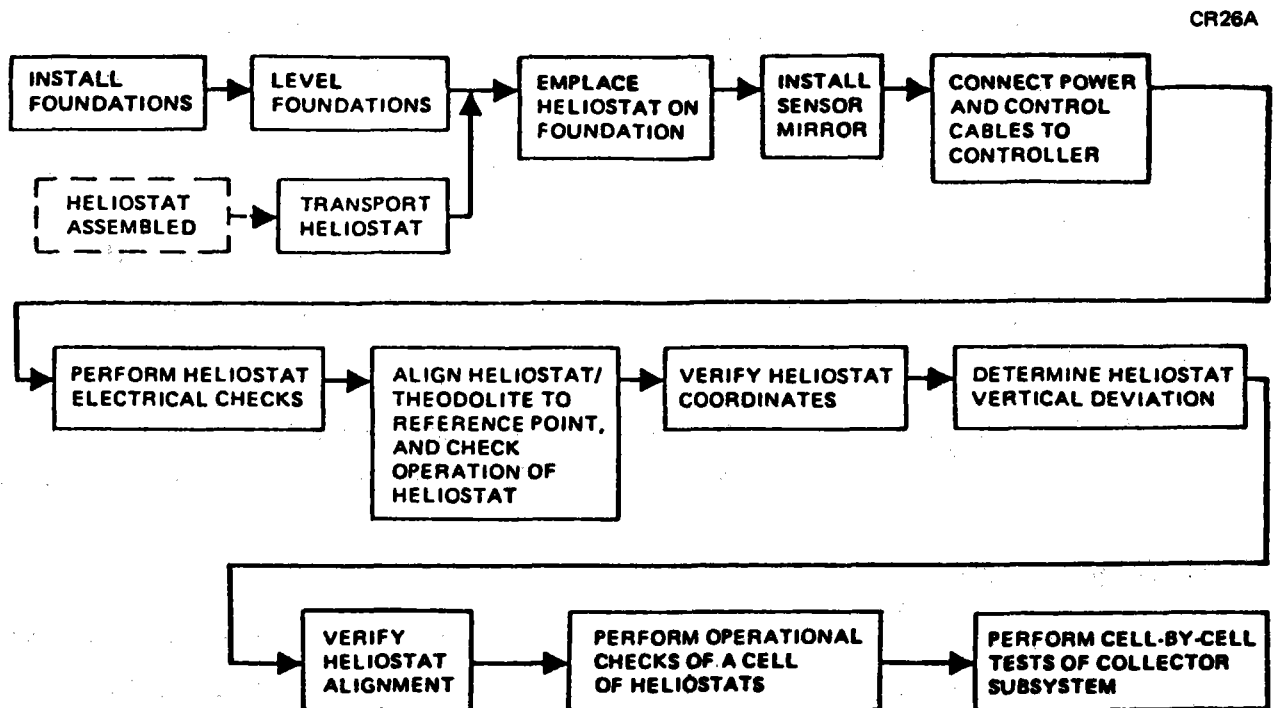


Figure 4-1. Installation and Checkout Flow

In the field, some of these tasks would be performed in parallel. Checkout would be accomplished by using a mobile test set to verify the integrity of the field controller/individual heliostat interface. A subsystem test would verify proper tracking, slew-off, and stowage performance on a cell-by-cell

basis. Final system checkout to verify proper subsystem interfacing and total system performance would then be performed.

4.2 INSTALLATION AND CHECKOUT TRADE STUDY RESULTS

Originally, two trade studies were to be discussed in this section. However, Trade Study I-1, Optimum On-Site Transportation, was deleted because the design change to on-site heliostat assembly obviated the need to transport a completed heliostat.

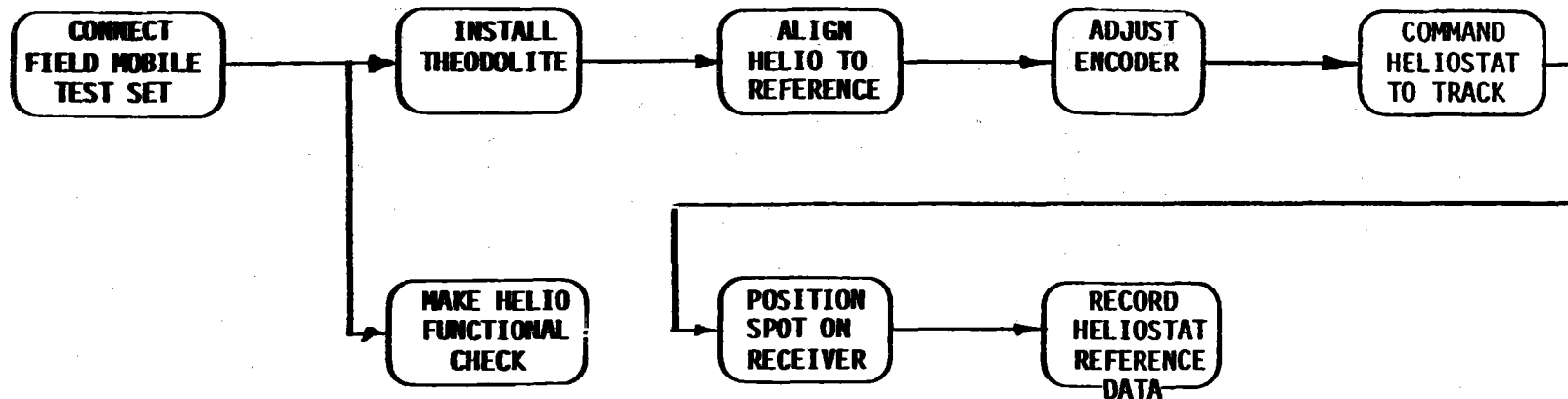
I-2 Collector Checkout

This study was set up to select an optimum checkout procedure, based on the pilot plant techniques, for use on the commercial plant. However, the hardware and software designs have since changed so much that a direct comparison of the checkout procedures cannot be made. Instead, a new checkout procedure has been developed to complement the prototype heliostat design.

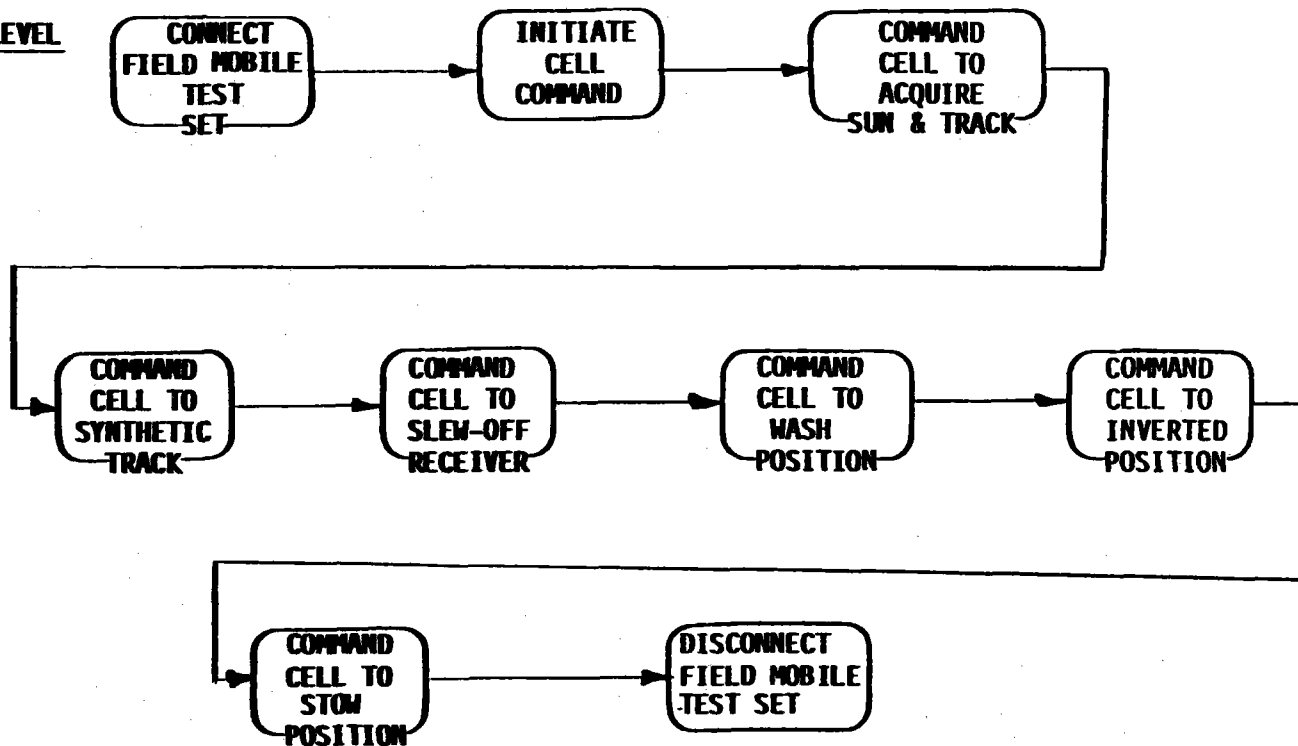
Initial Baseline Approach (Figure 4-2) - To check out the pilot plant heliostat, the heliostat is referenced to a known benchmark; the encoder is physically set to match the heliostat reference, and an operational checkout of a cell of heliostats (24) is made. In this open-loop approach, there is no tracking in the true sense of the word. The mechanical alignment of the hardware is progressively refined to a predetermined set of heliostat movement algorithms.

Prototype Heliostat Approach (Figure 4-3) - In this approach, a similar, progressive alignment to the tracking algorithms occurs. Two alternative methods are used to achieve the correction. For about half of the heliostats (the northern part of the field), the positioning is favorable to an interactive man/machine alignment procedure. For the southern part of the field, an automatic search mode is required. In either case, after initial offset errors are removed, the alignment is done in two steps, followed by short tracking periods (120 seconds and 80 seconds). The image positioning is checked after each tracking period with a digital image radiometer which senses the deviation of the heliostat image centroid from its optimum track.

HELIOSTAT LEVEL



CELL LEVEL



4-3

Figure 4-2. Alignment and Checkout - Pilot Plant

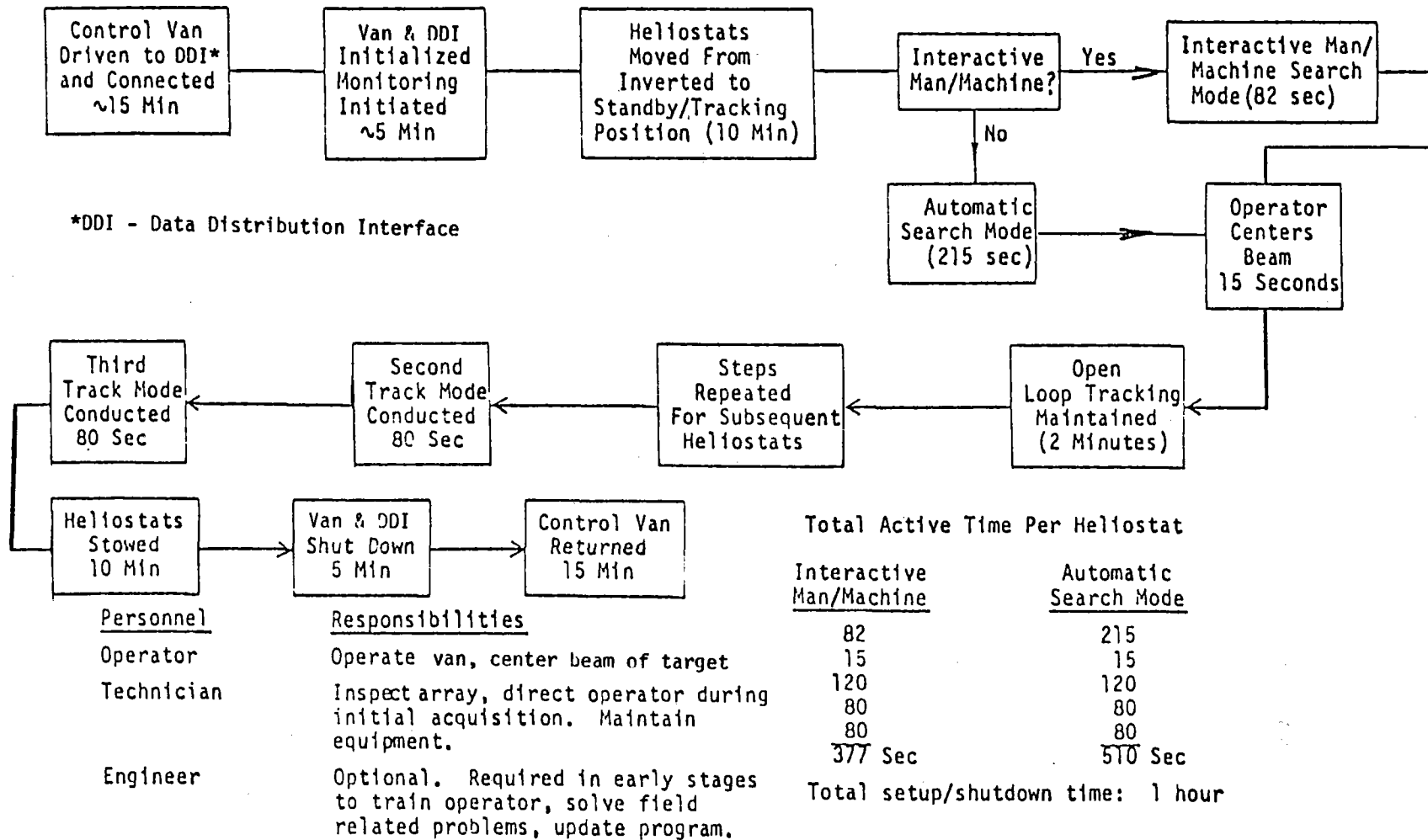


Figure 4-3. Initial Alignment Procedure Block Flow Diagram – Prototype HelioStat

The digital image radiometer then feeds correction data to the heliostat controller for updating the heliostat position and movement algorithm variables. Hence, the prototype heliostat alignment does include tracking. The two alignments are accomplished in an average of 6 minutes, and virtually eliminate any installation tolerances in position and tilt so that the heliostats assume a proper track of the sun.

Summary of Results - The significance of this trade study is the large reduction in time required for heliostat checkout.

In the original approach developed for the Pilot Plant, the alignment was basically a physical and mechanical process that aligned the mirror surface and position encoders to benchmarks. For the prototype heliostat approach, there is no physical or mechanical adjustment. Installation position and angular errors are compensated electronically in software. The digital image radiometer is the main reason that the prototype heliostat checkout approach is feasible. Not only is the positioning of the image of the reflector on the target determined, but the centroid and power distribution of that image are also determined. With the automatic algorithm updating capability, the checkout activity can be considered as a closed loop. The time of the two approaches is compared in Table 4-1.

4.3 INSTALLATION CONCEPT DESCRIPTION

The heliostat installation concept is to build up the heliostat in the field from subassemblies which have been assembled and checked out in the factory. This concept provides the benefits of factory assembly in the form of high accuracy and efficiency and simplifies the field installation by minimizing tasks which must be performed in the field.

4.3.1 Subassembly Description

The four basic units to be installed for the collector are the foundation, drive unit, reflector panels, and cable installation.

Table 4-1

HELIOSTAT ALIGNMENT AND CHECKOUT

| <u>INITIAL BASELINE</u> | <u>TIME PER HELIOSTAT (MIN)</u> | <u>PROTOTYPE</u> | <u>TIME PER HELIOSTAT (MIN)</u> |
|---------------------------------------|---------------------------------|--|---------------------------------|
| Set heliostat ref. determine & verify | 48 | Auto Search (1/2 field) | 7.2 |
| Heliostat Positioning | 10 | Manual Search Alignment (1/2 field) | 4.9 |
| Initial Ops Check | 7.5 | Average Alignment | 6.0 |
| Total C/O Align (open loop) | 65.5 | Apportioned Setup time/ cell | 2.5 |
| | | Total C/O & Align (open loop) | 8.5 |

TIME SAVING PER HELIOSTAT = 65.6 min (initial baseline)

-8.5 min (prototype)

57.1 min (reduction in alignment time)

Foundation - The foundation will be formed in place by drilling holes 0.61 m by 6.71 m (2 ft by 22 ft), installing a prefabricated rebar cage with a tapered form, both of which extend 4 feet above grade, and filling the cage and the form with concrete. The rebar cage and the tapered form will be brought to the site on standard flatbed and utility-type vehicles.

| <u>Subassembly</u> | <u>Dimensions</u> | <u>Weight</u> | <u>Special Operation</u> |
|--------------------|---|----------------------|--------------------------|
| Rebar Cage | 0.61 m (2 ft) dia. x 7.64 m (25 ft) long | 195 kg (428.2 lb) | Vert within 2° |
| Tapered Form | 0.61 m (2 ft) dia. x 1.22 m (4 ft) long | 31.5 kg | Vert within 2° |

Drive Unit - These units will be assembled and checked out at the factory, and delivered to the site on flatbed trailer, with 12 on each trailer. The drive units will be placed over the tapered foundation and loaded with 3000 pounds of force; they will then be vibrated to ensure proper seating.

| <u>Subassembly</u> | <u>Dimensions</u> | <u>Weight</u> | <u>Special Operation</u> |
|--------------------|--------------------|--------------------|---|
| Drive Unit | 0.61 m (2 ft) dia. | 365 kg (803 lb) | Positioned within 0.305 m (1 ft) cube and + 2° to North-South |

Reflector Panel - These units consist of six identical laminated mirrors assembled on a support structure. Two reflector panels will be bolted to the main beam of the drive unit and form the heliostat reflective unit.

| <u>Subassembly</u> | <u>Dimensions</u> | <u>Weight</u> | <u>Special Operation</u> |
|--------------------|------------------------------------|---------------|--|
| Reflector Panel | 290.5 ft L x 132 in W x 20 in D | 1528 lb | Positioning accomplished by jig-drilled mating holes |

Cable (Power/Control) - The power and control cabling will be delivered to the field in precut lengths with factory-installed power wire terminals and optical connectors and the cables rewound on the original spools. The power and fiber optic control cables will be in the same armored sheathing so that only one cable needs to be buried. The cable will run from the power distribution and data distribution interfaces to heliostat groups, and then serially from heliostat to heliostat. Electrical and optical connections will be made at each heliostat.

| <u>Subassembly</u> | <u>Description</u> | <u>Weight</u> | <u>Special Operations</u> |
|--------------------|---|---------------|---|
| Field Cabling | 3 conductor No. 8 AWG copper + 1 fiber optic cable within an armored sheath | 0.386 lb/ft | Connect power and optical leads into and out of heliostat J-Box |

4.3.2 Foundation Installation

The foundation will be a 0.61 m (2 foot) diameter drilled pier embedded 6.71 m (22 ft) below grade. The drilled pier will have a 1.22 m (4 foot) extension above grade formed by a galvanized steel, tapered tube section filled with concrete. The pedestal will be force-mounted on this pier extension.

The procedure for emplacing the drilled pier foundations uses standard construction techniques. The cast in place concrete pier foundations can be used with most soil conditions. The pier hole will be excavated by drilling an open hole; if the sidewalls do not collapse, the reinforcement concrete will be placed as required to fill the hole. If the soil conditions are conducive to sidewall collapse, the pier can be placed by the Intrusion-Prepakt method, regardless of the sidewall stability. In this method, the hole is drilled and concrete grout displaces the soil as it is removed from the hole in a single operation. Then, reinforcement will be forced into the grouted hole before the mortar begins to set. In any case, the pier will be installed with the 4-foot extension above grade.

The equipment required to emplace the heliostat foundations includes hydraulic cranes for lifting and manipulating ironwork and flatbed tractor/trailers for hauling the bracing materials. Hole drilling and concrete hauling equipment will be furnished by a contractor and included in the price of the service.

4.3.3 Drive/Control Unit Installation

The drive/control unit will be fully assembled and checked out at the factory. The drive unit uses grease as a lubricant so that leakage of oil during shipment is not a problem.

The positioning requirements for the pedestal are: the reference mark must be within ± 2 degrees of true North, the pedestal must be within 2 degrees of local vertical, and the joint between the mating parts (foundation and pedestal) must be close to 0.8 mm (1/32 inch) or less. The drive unit installation equipment is illustrated in Figure 4-4. The machine is capable of lifting the drive unit from the flatbed trailer, rotating to vertical, and rotating to a reference North-South alignment. A stereoscopic TV monitor assists the operator in placing the drive unit on the foundation. Loading weights and vibrators are incorporated to seat the drive unit on the foundation. The following procedure is used for installing the drive unit/pedestal assembly:

- 1) Lift the drive unit from the flatbed trailer with the drive unit installation machine and rotate it to the vertical position.
- 2) Position the bottom end of the pedestal over the foundation and lower it over the tapered portion of the foundation.
- 3) Adjust the position of the drive unit to within ± 2 degrees of true North.
- 4) Engage the pedestal setting assembly of the pedestal installation machine, increase pressure and vibrate until the gap between the material surfaces is 1/32 inch or less.
- 5) Fill the drive unit with oil.

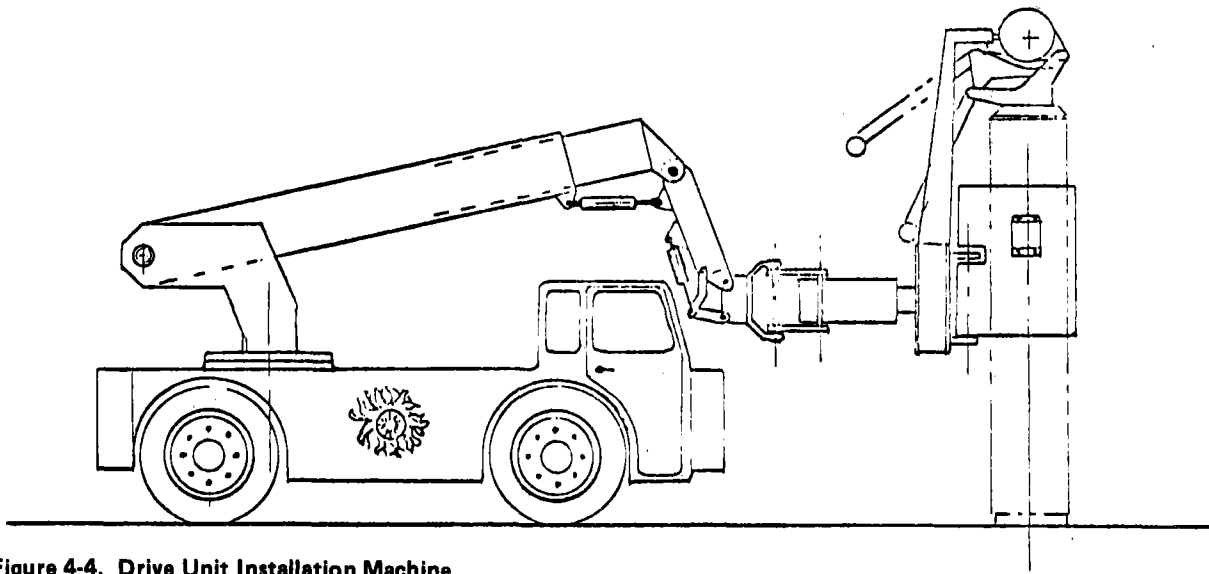


Figure 4-4. Drive Unit Installation Machine

The equipment required to install the drive/control unit consists of a flatbed trailer (modified) and pedestal installation machine. Because of the scheduling constraint and the task time requirements (see Section 4.5), two sets of installation equipment and two crews will be needed to use the 25,000 drive/control units immediately at one site. The crews will be made up of 1 millwright, 1 laborer, and 1 equipment operator.

4.3.4 Reflector Panel Installation

Installation of the reflector panels to the drive unit is straightforward. All the critical positioning and aligning are done at the factory by either precision assembly, machined surface mating or jig-drilled holes. The only field requirement is to install the mirrors at a rate of 104 pairs of panels per day.

The reflector installation equipment (Figure 4-5) is a modified, large straddle crane. This equipment carries reflector panels and provides manipulating devices that pick up and position individual panels during the installation process. Covered work platforms for personnel are provided.

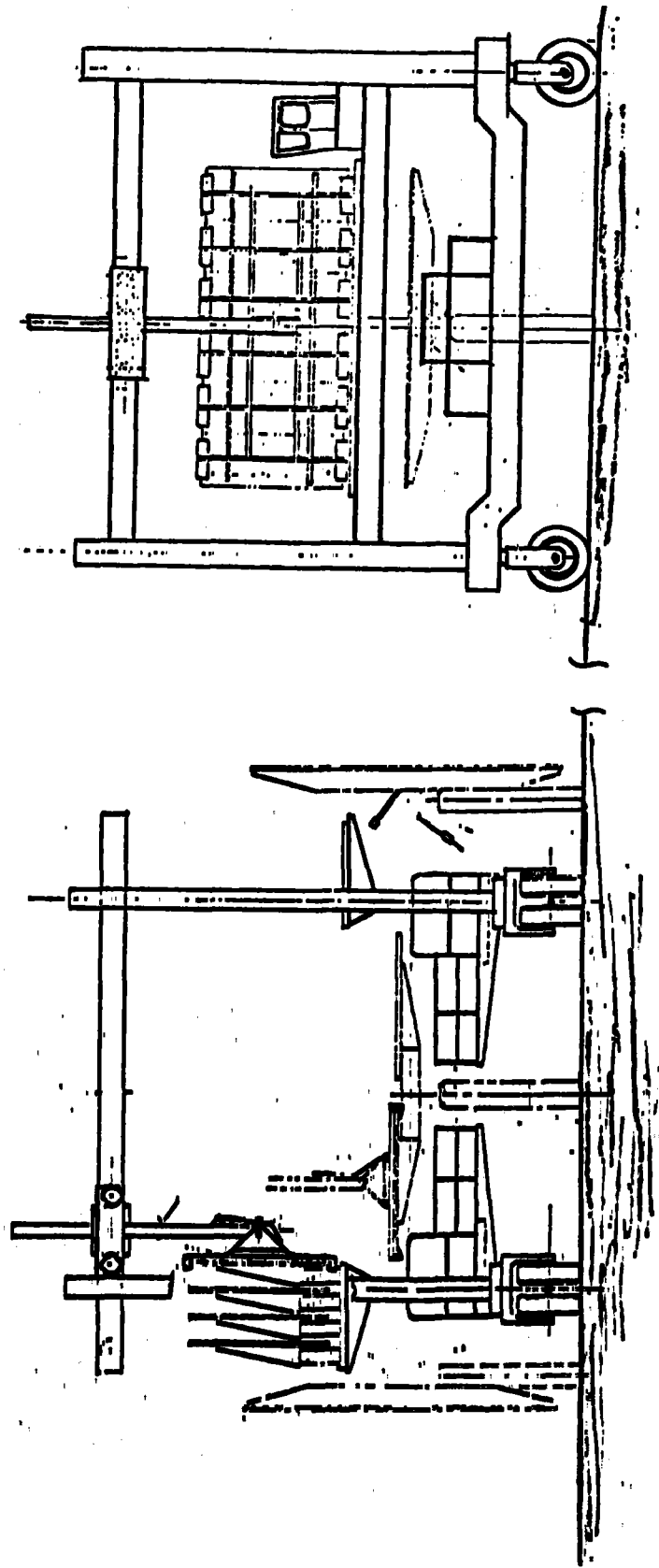


Figure 4-5. Reflector Installation Equipment

The installation sequence is:

- 1) Two pallets of reflector panels are loaded on the sides of the reflector installation equipment.
- 2) The crane is positioned over the installed drive unit/pedestal assembly.
- 3) The manipulator engages the reflector panel, picks it up, and moves the panel to a position that will allow mating to the drive unit flange under the guidance of the operator.

Note: The manipulator allows movement in several directions: panel swiveling and rotation, full lateral positioning, and limited fore and aft (36 inch) positioning.

- 4) When the flanges are within mating distance, eight bolts are installed to secure the reflector panel to the drive unit. Panels on both sides will be installed simultaneously.
- 5) The manipulator is disengaged from the reflector; workstands are retracted and the machine moves on to the next pedestal. Reflector panels are supplied to the machine for every fourth heliostat in the present design.

The reflector installation equipment and high-lift forklift is used to reload the reflector magazines in the installation equipment. Based on the scheduling constraints of 104 heliostats per day, there is a requirement for five sets of installation equipment and five crews.

A crew will consist of 6 men--2 millwrights, 2 laborers, 1 forklift driver, and 1 forklift equipment operator.

4.3.5 Cabling Installation

The interheliostat field cabling is a single armored cable containing three No. 8 electrical conductors and one fiber optic cable.

The requirements for the installation of this cable are based on the amount and type of vehicular traffic, the possibility of damage from rodents, and other damage-causing activities over the 30-year life of the collector field. To conform with these requirements and the National Electrical Code (NEC), the interheliostat wiring must be buried at least 24 inches deep, and the primary power cables must not be installed straight or taut. Slack must be allowed for settlement and earth-moving after installation. Most of these requirements are stated in government safety regulations. While some variances may be acceptable, these codes should be followed to meet the system lifetime requirements at reasonable cost.

Installation procedures for these cables were developed to minimize the time and manpower utilized. The cable is "plowed in" using a machine that slices a V groove in the soil to the desired depth and feeds the cable into the bottom of the groove before the soil is allowed to fall back in place. Cables are emplaced at 21 m/sec (250 ft/hr) with this automated approach. There are 951,000 feet of branch circuit wiring to emplace. Thus, the total field cable installation task requires about 3,804 hours. One installation machine operated on a two-shift basis is adequate for installing a commercial plant in one year.

The crew required to install the cable includes a plow operator/driver and two laborers.

4.4 ALIGNMENT AND CHECKOUT CONCEPT DESCRIPTION

The heliostat alignment task adjusts the tracking software to compensate for tolerances allowed in installations, and verifies the basic operation of the heliostat with respect to its components and other subsystems.

4.4.1 Alignment

The requirements for individual heliostat alignment are that the heliostat track the sun accurately enough so that the solar image is on its nominal aimpoint each day of the year from sunrise to sunset. Since this alignment is done open loop, there is no operational feedback to indicate misalignment. The

accuracy of the initial alignment and subsequent alignments determines the efficiency of the heliostat over its life.

No mechanical adjustments are required for the heliostat after installation. The alignment is done by establishing and adjusting position relationships in the heliostat controller to reflect the differences between the programmed placement of the heliostat and the actual position of the unit. New position information is input on the first alignment, and vertical errors are compensated on a subsequent alignment.

During the alignment task, there can be no severe weather conditions that might affect accuracy. The wind must be below 11.6 m/s (26 mph) so that a steady image will be projected on the target. Extreme temperatures, below 32°F and above 120°F, must be avoided as the image characteristic might change enough to cause the digital image radiometer to misread the centroid signature of the heliostat. As with other heliostat installation and checkout tasks, the alignment must take minimum time and manpower.

The procedure for aligning a heliostat follows the task flow shown in Figure 4-3. The control van is connected into the data distribution interface once for 24 heliostats as the heliostats read positioning information off a common optical data bus. The group of heliostats is then activated, moved to standby positions, and established on track. At this point, the activities of the alignment branch into two categories: interactive man-machine alignment in the northern half of the field, and automatic search in the southern half.

In the interactive alignment, a sighting mirror is placed on edge of the reflector, and the installer views the position of the image with respect to the alignment target. A verbal command is then given to the alignment operator in the control van that brings the spot onto the target. Once the spot is on the target, the digital image radiometer is used to establish the exact position and provide the updated information position on.

The automatic search technique will be used in the southern portion of the field because the heliostats will be in a nearly horizontal position during much of the day. This makes it inconvenient to attach a sighting mirror and observe the solar image. In the automatic search, the heliostat is moved in an expanding spiral search pattern until the target is intercepted. After the target is intercepted, the digital image radiometer is used to set the exact position and update it as in the interactive technique.

The interactive man/machine approach takes an average time of 295 seconds to complete the alignment. The automatic procedure takes an average time of 430 seconds to complete due to the need to search for the target. The interactive man/machine technique will be employed whenever possible.

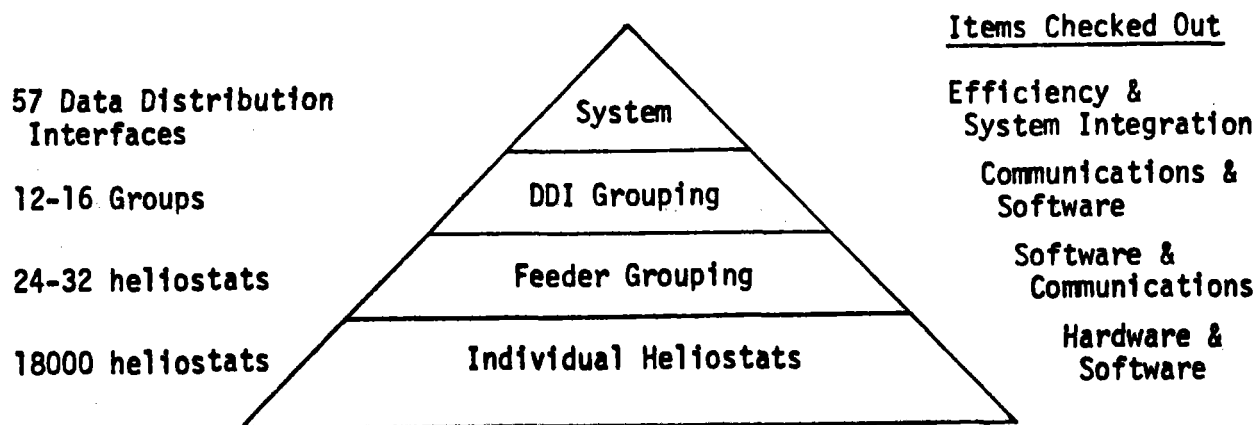
These alignment procedures are expected to be 100 percent reliable with respect to software. The only condition that could cause the alignment to be unsatisfactory is equipment failure. If this occurs during alignment, the problem will be handled as unscheduled maintenance.

The equipment required to perform the alignment includes the van-mounted test set, an alignment target permanently emplaced on the tower, the digital image radiometers (which are permanently located at six strategic sites in the field), and a sighting mirror for the man/machine procedure.

The personnel involved in this task will be two technicians and a field engineer. Based on the scheduling constraints and task time requirements (Section 4.5), three crews, three control vans, and three sighting mirrors will be needed to complete the task.

4.4.2 Checkout

The requirements for checkout transcend several levels of equipment. The basic purpose of checkout is to ensure that each element of the system is functioning according to specifications. To do this properly, the checkout must be done from the bottom up--first at the individual heliostat level, then for the group of heliostats on a single feeder, next at the data distribution interface level, and finally at the system level.



At the single heliostat level, the checkout will verify that the heliostat is tracking (accomplished in parallel with alignment), and the image quality is satisfactory (automatically determined by the digital image radiometer during alignment). A physical inspection will also be made for lubrication leaks and installation damage.

The group of heliostats on a single secondary feeder are checked to see that the data and power transmission from each heliostat to the next is correct, particularly, that the signals transmitted and received at the data distribution interface are correct. This checkout may be done from the master control room in a manual operating mode, or by interaction with the data distribution interface in the field.

The check of the data distribution interface verifies the power and communications loops from the heliostat array controller to the distribution center and the ability of the data distribution interface to correctly address heliostats and generate its interior commands (e.g., stow, unstow).

System-level checkout is accomplished in conjunction with the checkout of the overall plant and includes interface verification.

4.5 INSTALLATION AND CHECKOUT RESOURCE UTILIZATION

A short study was undertaken to determine the best method of allocating personnel and special equipment to sites for installation and checkout activities at production rates of 25,000 heliostats per year for 10 years and 250,000 heliostats per year for 10 years.

Three constraints were imposed on the study:

- Production rate must be exactly satisfied by the installation schedule; e.g., no backlogs or surpluses of heliostat parts at the site. This requires a daily installation average rate of 104 units.
- 18,000 heliostats per field.
- 40-hour weeks; 48 weeks per year.

The following objectives, in descending order of priority, were established:

- 1) Satisfy demands and constraints.
- 2) Minimize number of crews and equipment.
- 3) Minimize intersite movements of equipment and people.
- 4) Finish sites successively to provide visibility and control of problem areas.

To satisfy these objectives, the following approaches were determined to be most attractive:

- 1) For the 25,000 production rate, with five crews installing reflector panel assemblies, activate one site at a time.
- 2) For the 250,000 production rate, with 46 crews installing reflector panel assemblies, activate one site at a time.

4.5.1 Supporting Data and Assumptions

The data used to support this study include results of installation and checkout analyses, collector hardware design, and special support equipment design. The resources needed for foundation preparation and installation and production rates were defined by our subcontractor, Stearns-Roger. The costs associated with heliostat foundations are not considered in this part of the study because they are already charged against CBS 4440.

Certain assumptions were made for the study. The major assumptions are:

- Heliostat assembly and installation will be accomplished by performing the following tasks in the sequence shown in Figure 4-6, and using the resources allocated to each task.
- Field cables will be cut to length and terminated in the factory.
- Alignment of heliostats will be achieved by software changes; i.e., no mechanical adjustment at the heliostat.
- All foundations will be installed and cured before the heliostat inspection and checkout.

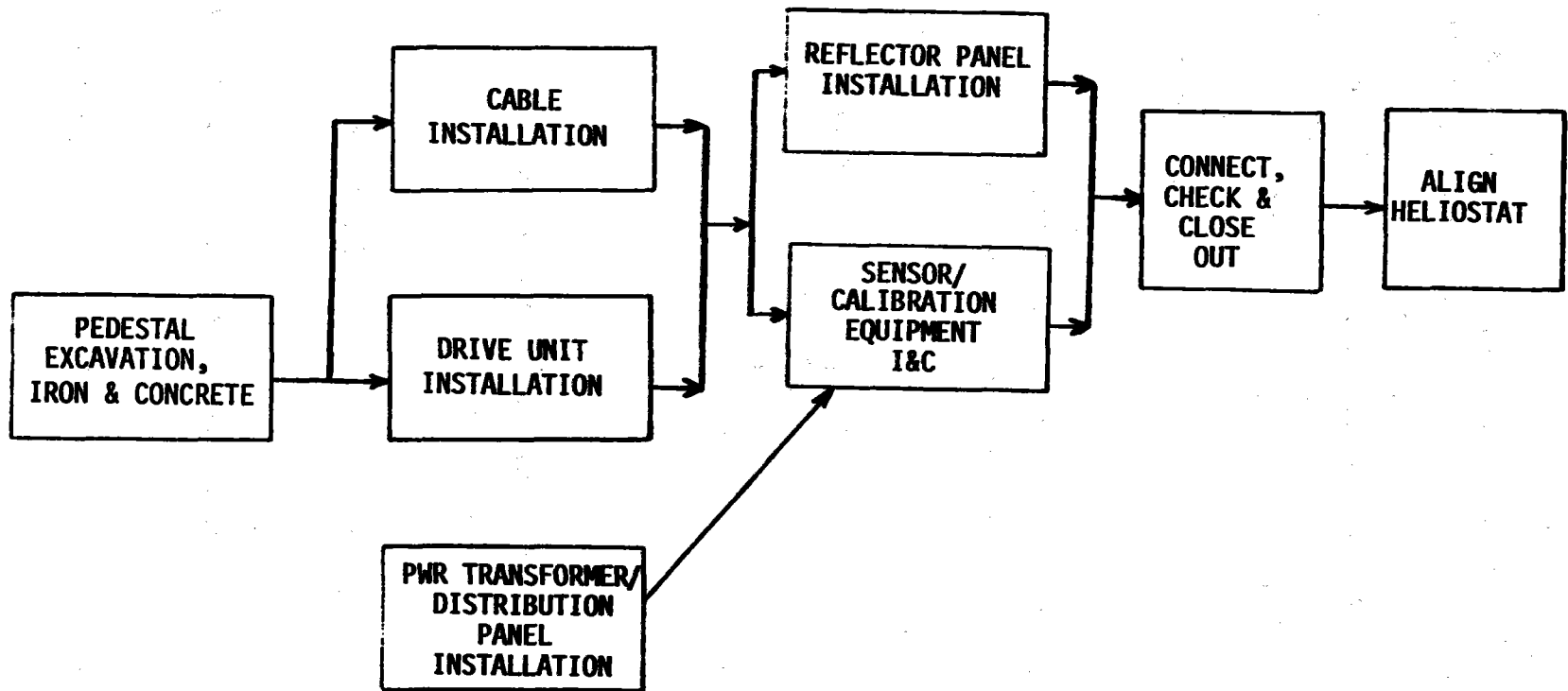
4.5.2 Study Results

At an installation rate of 25,000 heliostats per year, MDAC determined that the only two logical approaches to crewing were:

Alternative A1 - With five crews installing panels, work on sites one at a time.

Alternative A2 - With one crew at each site installing panels, work on five sites at a time.

The required equipment and personnel for each alternative are given in Table 4-3.



NOTE: Task descriptions are given in Table 4-2

Figure 4-6. Installation Task Sequence

Table 4-2
INSTALLATION TASKS

| <u>Task No.</u> | <u>Time/Heliostat</u> | <u>Resource Allocation</u> |
|---|----------------------------|---|
| 1. Pedestal Excavation, Iron and Concrete | 30 min/heliostat | Covered in CBS 4440 |
| 2. Cable Installation | 18 min/heliostat | 1 Cable Plow 1 Cable Plow Operator 2 Laborers |
| 3. Drive Unit Installation | 18 min/heliostat | 1 Pedestal/Drive Assy Installation Equipment 1 Installation Equipment Operator 1 Millwright 1 Laborer |
| 4. Power Transformer/ Distribution Panel Installation | 90 min/312 helio- stats | 1 Millwright 2 Laborers 1 Truck 1 Forklift 1 Truck Driver |
| 5. Reflector Panel Installation | 21 min/heliostat | 1 Reflector Panel Assy Installation Equipment 1 Installation Equipment Operator 1 Hi-Lift Forklift 2 Forklift Operators 2 Millwrights 2 Laborers |
| 6. Sensor/Calibration Equipment I&C | 8 hrs/3000 heliostats | 1 Field Engineer 1 Electrician 1 Volt-Ohm Meter 1 Oscilloscope |
| 7. Connect, Check & Close Out | 15 min/heliostat | 1 Electrician 1 Laborer 1 Test Set |
| 8. Align Heliostat | 10 min/heliostat | 1 Field Engineer 2 Technicians 1 Mobile Field Test Station |

Table 4-3

RESOURCE REQUIREMENTS - ALTERNATIVES A1 AND A2

| <u>Resource</u> | <u>Required Level of Equipment/Personnel</u> | |
|--|--|----------------|
| | <u>A1t. A1</u> | <u>A1t. A2</u> |
| Cable Plows | 4 | 5 |
| Drive/Control Unit Installation Equipment | 2 | 5 |
| Trucks | 1 | 1 |
| Forklifts | 1 | 1 |
| Reflector Panel Installation Equipment | 5 | 5 |
| Hi-Lift Forklifts | 2 | 5 |
| Test Sets | 4 | 5 |
| Mobile Field Test Stations | 3 | 5 |
| Laborers | 26 | 32 |
| Millwrights | 13 | 16 |
| Equipment Operators | 16 | 20 |
| Truck Drivers | 1 | 1 |
| Field Engineers | 4 | 6 |
| Electricians | 4 | 5 |
| Technicians | 6 | 10 |

Better
Choice



At a 250,000 heliostats per year installation rate, MDAC determined that logical approaches were:

Alternative B1 - With 46 crews installing panels, work on one site at a time.

Alternative B2 - With 23 crews installing panels at each site, work on two sites simultaneously.

Alternative B3 - With one crew installing panels at each site, work on 46 sites simultaneously.

The equipment and personnel required for each alternative are given in Table 4-4.

4.6 INSTALLATION AND CHECKOUT SUMMARY

The installation and checkout procedures are summarized in Table 4-5. The procedures take advantage of design changes to facilitate low-cost installation and checkout, and utilize MDAC-developed low-cost alignment procedures.

Table 4-4

RESOURCE REQUIREMENTS - ALTERNATIVES B1, B2, AND B3

Required Levels of Equipment/Personnel

| <u>Resource</u> | <u>Alt. B1</u> | <u>Alt. B2</u> | <u>Alt. B3</u> |
|--|----------------|----------------|----------------|
| Cable Plows | 40 | 40 | 46 |
| Drive/Control Unit Installation Equipment | 18 | 18 | 46 |
| Trucks | 1 | 2 | 2 |
| Forklifts | 1 | 2 | 2 |
| Reflector Panel Installation Equipment | 46 | 46 | 46 |
| Hi-Lift Forklifts | 18 | 18 | 46 |
| Test Sets | 33 | 34 | 46 |
| Mobile Field Test Stations | 22 | 22 | 23 |
| Laborers | 225 | 228 | 280 |
| Millwrights | 111 | 112 | 140 |
| Equipment Operators | 150 | 150 | 184 |
| Truck Drivers | 1 | 2 | 2 |
| Field Engineers | 23 | 23 | 24 |
| Electricians | 33 | 34 | 46 |
| Technicians | 44 | 44 | 46 |

Best
Choice

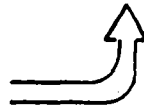


Table 4-5

INSTALLATION AND CHECKOUT CHANGE SUMMARY

| <u>I&C Consideration</u> | <u>Was</u> | <u>Is</u> | <u>Effect</u> |
|------------------------------------|---|--|---|
| Checkout procedure | Gimbal axis encoders, hardware mechanically zeroed at intervals | Software algorithms constants reset at intervals | Alignment done quickly, reliably, and accurately with a semiautomated technique |
| Installation concepts | Pre-assembled heliostats | Pre-assembled, pre-checked reflector panels and pedestals assembled <u>in situ</u> | Simplifies field activities |
| Subassembly concepts: | | | |
| • Foundation | I&C procedures undefined | Formed in place, prefabricated rebar cage, form for top; brought to site on standard-type vehicles | Fast, simplified foundation installation. Standard types of transportation & handling equipment, standard construction techniques |
| • Drive Unit/Pedestal | Bolted to foundation | Factory-assembly & checkout jammed onto foundation stub | Fast, simplified installation |
| • Reflector Panels | Came from factory mated to pedestal | Critical positioning and alignment with drive unit/pedestal done through machined surface mating | Site alignment activities limited to those of beam positioning |
| • Cabling | I&C procedures undefined | Power & fiber optic control cables in same sheathing. Implaced by special hi-speed plow. Length and terminations tailored at site. | Simple, fast installation. |
| Resource Allocation and Scheduling | No previous definition | Crew, equipment, sequences defined and optimized. | Cost and schedule efficiency. |

Section 5

OPERATIONS AND MAINTENANCE CONCEPTUAL DESIGN

Operations and maintenance (O&M) support is directed toward two primary objectives: (1) achieving and maintaining specified system availability, and (2) providing the necessary support with minimum expenditures for labor and materials. Because of the large quantity of heliostats in the collector subsystem and a basic design which does not rely on maintenance to achieve minimum availability, there is little risk that the required availability will not be satisfied. Thus, low-cost O&M support concepts can be considered without concern that they will affect system availability.

5.1 INITIAL BASELINE PROCESS

The initial O&M requirements were determined by a hardware analysis to identify significant components for maintenance and related maintenance tasks. Maintenance-significant items for the initial baseline are listed in Table 5-1, which also presents a brief description of their scheduled and unscheduled maintenance requirements.

Two concepts developed for the 10 MWe plant--the mirror cleaning method and the off-site repair location--were rejected for the larger plant because they were not found to be cost-effective on a commercial scale of operations. For the commercial plant, a rapid, automated mirror cleaning process would be more efficient, and on-site repair would be justified for the larger quantities at each site. Trade studies conducted for the 100 MWe plant are reported in this section.

5.2 OPERATIONS AND MAINTENANCE TRADE STUDY RESULTS

5.2.1 0-1 Optimum Repair Level Analysis

This trade study was conducted to reduce maintenance costs by determining whether line-replaceable units (LRU's) should be repaired or replaced and

Table 5-1
 MAINTENANCE SIGNIFICANT ITEM LIST

| COMPONENT | CORRECTIVE MAINTENANCE | SCHEDULED MAINTENANCE |
|---|---|---|
| Heliostat and Field Controller | Remove and replace on failure. Minor repair on-site. | None |
| Elevation and Azimuth Drive Assemblies | Remove and replace on failure. | None |
| Elevation and Azimuth Drive Motor & Reducer | Remove and replace on failure. | None |
| Elevation and Azimuth Shaft Encoder | Remove and replace on failure. | None |
| Elevation and Azimuth Shaft Turn Pick-off | Remove and replace on failure. | None |
| Pedestal | Structural repair or remove and replace. | None |
| Reflector Panel | Remove and replace. Clean when badly soiled. | Clean |
| Reflector Structure | Structural repair or remove and replace. | None |
| Field Cables | Electrical repair or remove and replace. | None |
| Power Distribution Panel | Remove and replace detail parts. Replace panel for major damage. | None |
| Power Transformer | Remove and replace on failure. | None |
| Test Support Station | Remove and repair components on failure. | Calibrate, inspect, clean, adjust, and lubricate. |

the most cost-effective means of repair, where applicable.*

The collector subsystem LRU's were subjected to the Optimum Repair Level Analysis (ORLA) computer model, as shown in Figure 5-1. In the initial screening, four LRU's were dispositioned: a mirror module should be discarded if broken; the power transformer, digital camera, and camera heater/cooler, all having an expected failure rate of less than one per year per site, should be surveyed on failure to determine the extent of damage and, if salvageable, they should be repaired locally or at the manufacturer's facility. The remaining LRU's were analyzed by the ORLA model, with the results shown in Table 5-2. Sample computer runs, including sensitivity analyses, are presented in Appendix F.

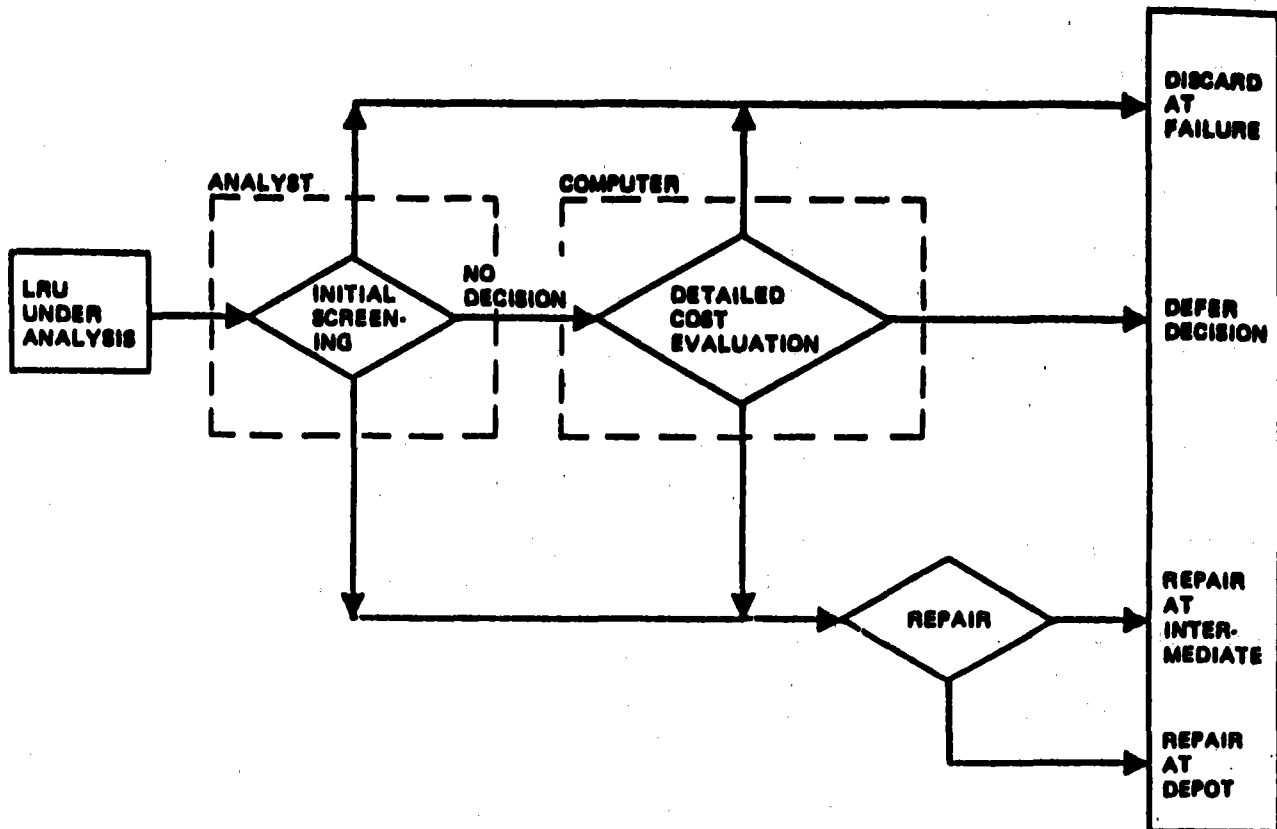


Figure 5-1. Optimum Repair Level Analysis (ORLA) Methodology

* An LRU is an assemblage of parts which is to be replaced as a unit in the event of a failure of any part in the unit.

Table 5-2

OPTIMUM REPAIR LEVEL ANALYSIS RESULTS

| LINE-REPLACEABLE UNIT | RELATIVE REPAIR COST | | | SELECTION |
|-----------------------------|----------------------|----------------|---------|-----------|
| | OFF-SITE REPAIR | ON-SITE REPAIR | DISCARD | |
| Azimuth Drive Unit | 3.5 | 1.0 | 4.3 | On-Site |
| Linear Actuator | 1.5 | 1.0 | 2.2 | On-Site |
| Azimuth Drive Motor | 1.4 | 1.0 | 1.6 | On-Site |
| Elevation Drive Motor | 1.4 | 1.0 | 1.7 | On-Site |
| Heliostat Controller | 0.9 | 1.0 | 1.3 | Off-Site* |
| Data Distribution Interface | 0.3 | 1.0 | 0.2 | Discard* |

* Decision could vary with number of sites and production rates.

On-site repair was indicated as the most cost-effective for all items except the printed circuit boards. Factors contributing to the on-site repair decision appear to be the relatively high packaging and shipping costs for off-site repair, and the relatively low cost of support equipment and facilities for establishing a repair capability at each site. The computer model runs were based on six sites within an 800-km (500-mile) radius of the assumed off-site repair facility. Other runs were made based on 50 sites within an 800-km (500-mile) radius without any change in designated repair location.

The heliostat control printed circuit boards appear to be best handled by off-site repair. With additional sites, this would be a firmer decision. However, sensitivity tests indicate an increase in repair man-hours or a decrease in unit cost would make the discard option more attractive. Therefore, this decision should be reexamined in the future. The data distribution interface circuit boards appear to be discard items, primarily due to the low number of failures per year. A greater number of deployed sites would tend to make off-site repair feasible. Also, an increase in failure rate or unit cost and/or a decrease in repair man-hours would support an off-site repair decision.

There are no apparent "break points" at which a change in designated repair locations would occur; i.e., higher production rates (with some probable reduction in unit costs) and an increased number of sites do not tend to change the repair locations. There does appear to be merit in having a single company that operates two or more sites in immediately adjoining areas pool its on-site, off-line repair tasks at one site, providing a low-cost packaging, handling, storage, and intersite transportation scheme can be devised.

Repair locations as determined by this trade study are given in Appendix G.

5.2.2 0-2 Reflector Cleaning

This trade study was conducted to determine the least costly method of cleaning the heliostats so as to maintain field efficiency. Two methods of cleaning the reflector mirrors were selected for study--the spray-soak

method and the mechanical scrub method. The spray-soak method uses a specially formulated cleaning solution. The solution is sprayed on the mirror, allowed to soak for a predetermined length of time, and spray-rinsed with deionized water. The mechanical scrub method uses only deionized water. Soft bristle brushes scrub the mirror, and it is then rinsed in deionized water.

The analysis showed that the cost of cleaning was not directly related to the method, but rather to the task time. Procedures could be developed for both methods to reduce the task times to an acceptable level.

Studies of the two optimized cleaning methods showed that costs had little sensitivity to equipment types. This relationship held until each field had only a two-man crew. At this level, the only changes were the equipment costs (acquisition, O&M). The choice of a cleaning method became subjective rather than economic.

The two MDAC equipment concepts for spray-soak and mechanical scrub are illustrated in Figure 5-2 and 5-3. The spray-soak uses two trucks at one-minute intervals. The first truck applies the wash solution, and the second applies a high pressure deionized water rinse. The mechanical scrubber uses a water flush, a soft bristle brush scrub, and a deionized water flush.

The significant costs of the cleaning methods are summarized in Figure 5-4. It should be noted that labor cost is directly proportional to task time, fuel cost is related to the task time and the number of machines, and operating time and cleaning agent cost is a function of the percentage of active cleaning agents used in the wash solutions.

The approaches considered have minimal technical risk. MDAC has tested the spray-soak method and found it to be effective. The mechanical scrubbing method has not been tested by MDAC, but other studies indicate it to be effective. Since men drive the spray-soak trucks around the field, there is a threat of damage to the heliostats, especially as the task is repetitive to the point of boredom. The mechanical-scrub method requires the machine to

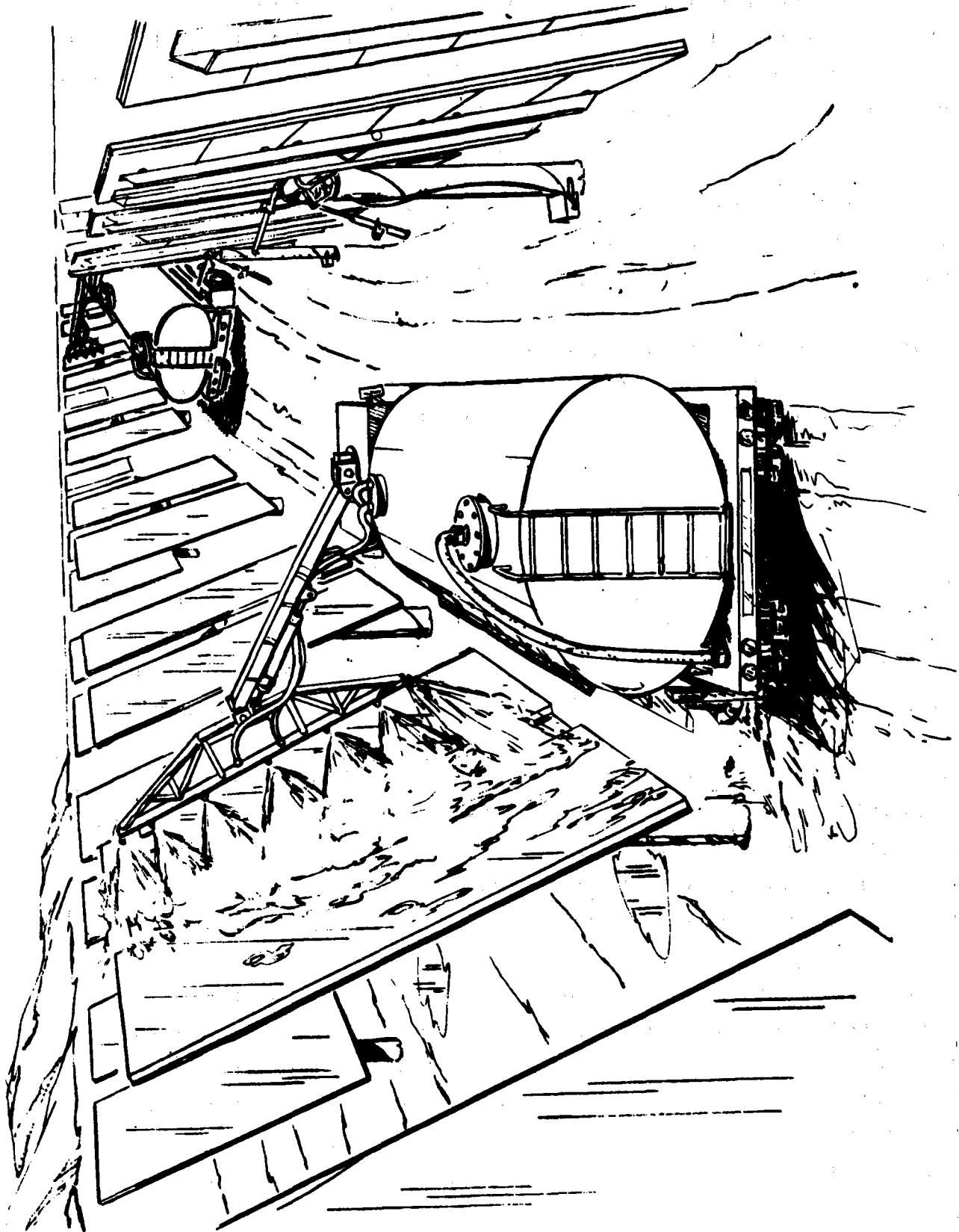


Figure 5-2. Spray-Soak Reflector Washing Equipment

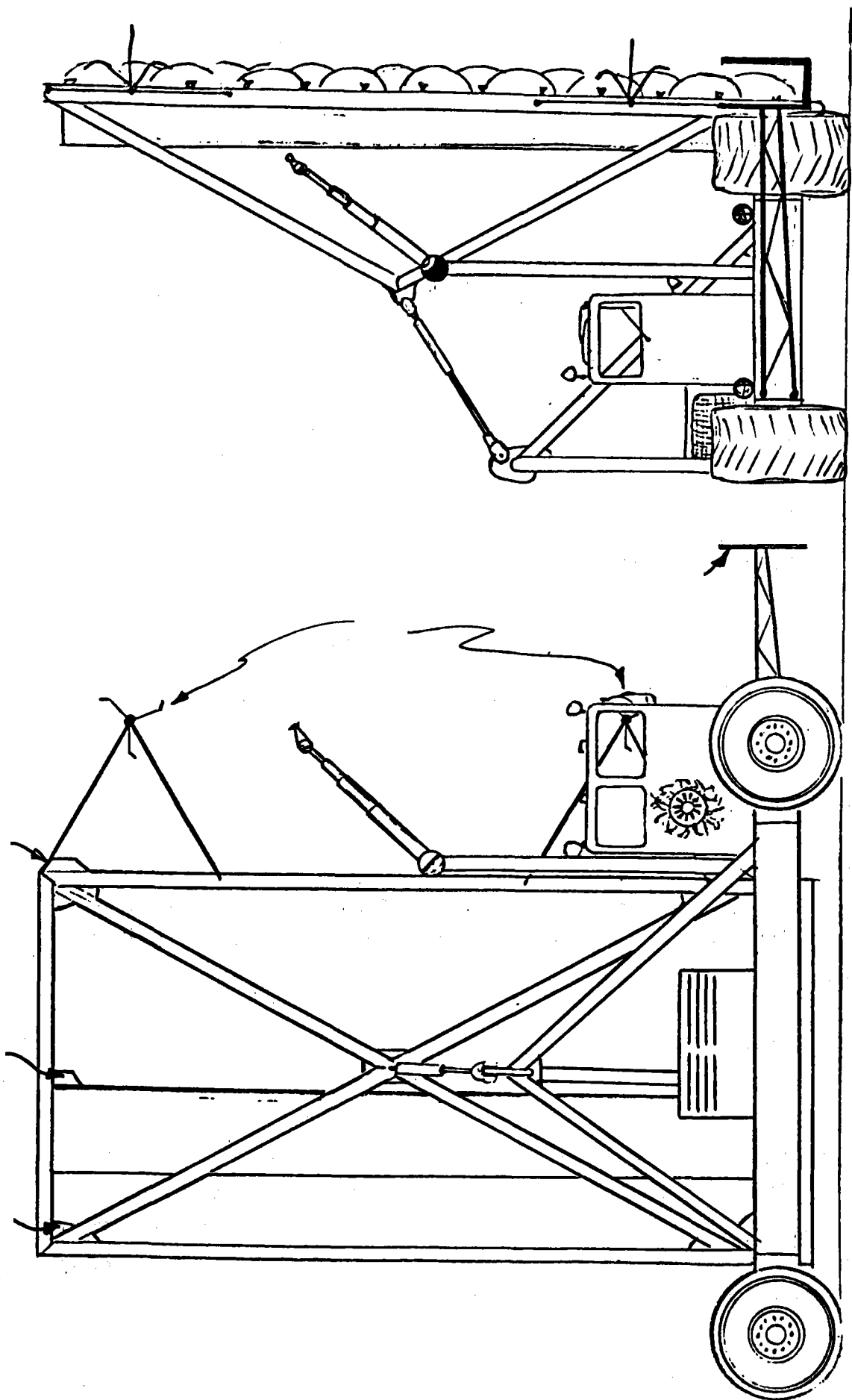
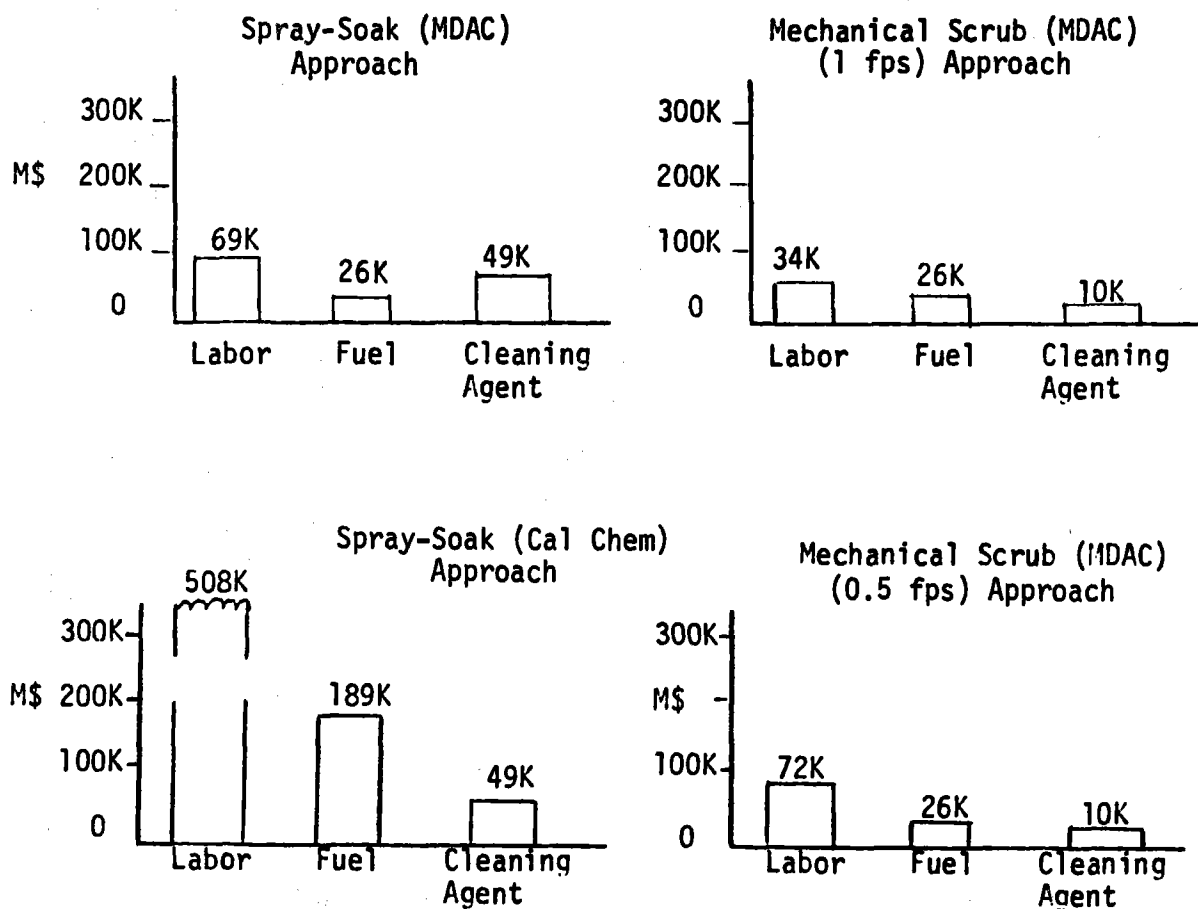


Figure 5-3. Mechanical Scrub Reflector Washing Equipment



NOTE: 1 fps = 0.305 m/sec

Figure 5-4. Annual Recurring Cleaning Costs

be near the heliostats. The steering and head positioning must be done by an automated system to ensure consistent cleaning. A secondary benefit of the automated system is to reduce operator fatigue by changing his role and making him a monitor.

The environmental impact of each cleaning method is important. In the Cal-Chem approach, all cleaning agents are collected so there is no environmental deterioration. This collection, however, increases the time and cost for the cleaning task. In the MDAC spray-soak method, the cleaning agents are not collected and fall to the ground at a rate of 160 grams/m²/month. Of this amount, the cleaning concentrate content is only 1.4 grams/m²/month. These agents are biodegradable in the long run, but their short-term environmental impact has not been determined.

The mechanical scrub method uses only deionized water. This water also falls to the ground. Water is used at a rate of 37.8 liters per heliostat for wash and rinse and results in 183 grams/m²/month being dumped on the ground. Again, short- and long-term effects of this moisture must be determined on local flora and fauna.

Projections of 30-year life-cycle costs of the four methods analyzed are summarized in Table 5-3. The slight acquisition cost penalty for the mechanical scrub approach is offset by the lower cost of the cleaning solution. Therefore, direct costs are even. There are other factors like environmental impact, heliostat damage incidence, and maintenance frequency that could force the selection one way or the other.

5.3 OPERATIONS AND MAINTENANCE ANALYSES

Operations and maintenance analyses include both scheduled and unscheduled maintenance. Reliability analyses are conducted on the collector design to determine mean time between failure. The reliability analyses are based on extensive, cataloged data of experience with similar components. Wherever possible, test data are used on the actual part in a comparable application.

The field maintenance concept is to remove and replace failed LRU's. For each LRU, analysis is developed which defines the actions required to remove and replace, the support equipment, the crew size, the time required to remove and replace, and any support facilities needed. These analyses are based heavily on MDAC experience with similar activities during the Collector SRE in the Pilot Plant Phase I Program.

Data derived from the reliability and maintenance analyses are recorded on logistics support analysis work sheets. The work sheets for significant items in maintenance of the collector subsystem are provided in Appendix G. Reference is made to these data to determine requirements for scheduled and unscheduled maintenance, spares and repair parts, maintenance man-hours, support equipment, and facilities.

Table 5-3

LIFE CYCLE COST COMPARISON OF HELIOSTAT CLEANING METHODS
 MECHANICAL SCRUB VS SPRAY SOAK
 (30-YEAR LIFE CYCLE)

| | <u>MECHANICAL SCRUB</u> | | <u>SPRAY-SOAK</u> | |
|---|-------------------------|---------------------|----------------------------------|-------------------------|
| | <u>1/2 fps SPEED</u> | <u>1 fps SPEED</u> | <u>CAL CHEM (>.1 fps)</u> | <u>MDAC (1 fps)</u> |
| Vehicle Investment (Replace Every 10 Years) | \$1,440,000 | \$ 720,000 | \$ 1,440,000 | \$ 600,000 |
| Diesel Fuel | \$ 790,920 | \$ 790,920 | \$ 5,686,200 | \$ 789,840 |
| Cleaning Solution | | | | |
| • Deionized water | \$ 275,400 | \$ 275,400 | \$ 240,570 | \$ 240,570 |
| • Active cleaner | \$ — | \$ — | \$ 1,239,300 | \$1,239,300 |
| Operator Labor | \$2,160,000 | \$ 1,036,800 | \$15,265,800 | \$2,073,600 |
| Maintenance Labor | \$ 182,520 | \$ 182,520 | \$ 1,312,200 | \$ 182,520 |
| TOTAL | \$4,848,840 | \$ 3,005,640 | \$25,184,070 | \$5,125,830 |

NOTE: 1 fps = 0.305 m/sec

The following support equipment is required for corrective and scheduled maintenance tasks:

- | | |
|-------------------------------------|--|
| • Mobile Crane | Heliostat hoisting |
| • Forklift | Miscellaneous heavy equipment handling |
| • Hoisting Slings - General Purpose | Heliostats and miscellaneous equipment hoisting |
| • Pickup Truck | General purpose |
| • Reflector Washing Equipment | Heliostat reflector cleaning |
| • Collector Field Test Station | Subsystem and component level fault isolation and test |

5.3.1 Scheduled Maintenance

Scheduled maintenance requirements are summarized in Table 5-4. Particular attention has been given to reducing scheduled maintenance wherever possible. For example, when lubricating the Harmonic drive, the traditional method would be to check the oil level periodically, which requires approximately two minutes including access time. The physical check of the oil level has been eliminated in favor of visual inspection for oil leaks, which is included in the general area inspection. Assuming a conservative one minute differential, this approach saves 300 man-hours per year for an 18,000 heliostat field.

The general area inspection includes visual checks for corrosion, weathering, structural integrity, glass breakage and cracks, condition of seals and bonding, oil leaks, animal and bird intrusion or damage, and vegetation growth. Although indicated as annual, the general area inspection is not intended to be a once-a-year inspection of the total field. The idea is to sample the field on a regular basis to discover incident conditions which, if not corrected, can become major problems. Monthly inspection of approximately one-twelfth of the field is recommended--preferably in circumferential sections.

Table 5-4
SCHEDULED MAINTENANCE

| REQUIREMENT | TASK | FREQUENCY | MANHOURS PER TASK | MANHOURS PER YEAR |
|---|-----------------------------------|--------------------|----------------------|----------------------|
| <u>SUBSYSTEM EQUIPMENT</u> | | | | |
| Heliostat Field | Area/Corrosion Control Inspection | Annual | 1200 | 1200 |
| Heliostat Reflectors | Clean | 30 Days | 338 | 4056 |
| Heliostat Array Controller | Inspect & Service | (SERVICE CONTRACT) | | |
| <u>SPECIAL SUPPORT EQUIPMENT</u> | | | | |
| Handling Sling | Load Certification | Annual | 2 | 2 |
| Mobile Test Van Printer, Tape Reader, CRT/ Keyboard, Recorder, etc. | Inspect & Service | Weekly | 2 | 104 |
| Measurement Equipment | Calibrate | 6 Months | 6 | 12 |
| | | | | 5,374 |

In the cleaning procedure, two trucks with spray heads move continuously across the field at approximately 1 foot per second. The lead truck sprays the acidic washing solution on the heliostat as it passes. The second truck lags about one minute (two heliostats) behind the lead truck to allow for soak time. The lag truck sprays the heliostat with deionized water to rinse off the cleaning solution to complete the task. Runoff is not collected and falls on the ground.

The frequency of reflector cleaning is very site-dependent, seasonal, and weather-dependent. MDAC has chosen a one-month interval for cleaning as perhaps representative of long-term average cleaning rates. The MDAC 1 fps spray-soak method (Section 5.2.2) has been selected for man-hour and cost projections.

5.3.2 Unscheduled Maintenance

The on-line unscheduled maintenance tasks and maintenance man-hours per task for the collector subsystem are summarized in Table 5-5. The estimated elapsed maintenance time and skill requirements are also indicated. Task elements considered include fault isolation, access time, component removal and replacement, and test and checkout time after fault correction.

Table 5-6 summarizes the on-line maintenance man-hour requirements per year based on the predicted maintenance actions per year and the task man-hours shown in Table 5-5. The equipment quantity per site and the mean time between maintenance actions as derived from the reliability analyses are provided for reference.

The individual component failure rates or mean time between failure estimates were obtained largely from historical data on other but similar systems. For example, the drive and storage motor estimates were obtained from Reference 1, which was a study to determine the accident probabilities in nuclear power plants. These data were obtained from commercial power plant experience (fossil and nuclear) and therefore give the failure characteristics under the same environment as in this program. The drive assembly estimates were obtained by using operational data from McDonnell Douglas aircraft experience

Table 5-5

ON-LINE CORRECTIVE MAINTENANCE MANHOURS PER TASK

| <u>Maintenance Significant Item</u> | <u>Task</u> | <u>EMT</u> * | <u>Manhours</u> | | | | <u>Total</u> |
|-------------------------------------|-------------|--------------|-----------------------|----------------------|-----------------------|---------------|--------------|
| | | | <u>Elect Tech</u> | <u>Mech Tech</u> | <u>Equip Oper</u> | <u>Rigger</u> | |
| 1. Drive Assembly, Azimuth | R&R | 4.0 | 4.0 | 8.0 | 4.4 | 2.8 | 19.2 |
| 2. Jack Assembly, Tracking | R&R | 2.2 | 2.2 | 2.2 | | | 4.4 |
| 3. Jack Assembly, Storage | R&R | 2.2 | 2.2 | 2.2 | | | 4.4 |
| 4. Drive Motor, Azimuth | R&R | 1.7 | 1.7 | 1.7 | | | 3.4 |
| 5. Drive Motor, Elevation | R&R | 1.9 | 1.9 | 1.9 | | | 3.8 |
| 6. Drive Motor, Storage | R&R | 1.9 | 1.9 | 1.9 | | | 3.8 |
| 7. Heliostat J-Box | Repair | 1.6 | 3.2 | | | | 3.2 |
| 8. Heliostat Control Electronics | R&R | 1.3 | 2.6 | | | | 2.6 |
| 9. Heliostat Power/Data Cables | Repair | 1.8 | 3.6 | | | | 3.6 |
| 10. Field Power/Data Cables | Repair | 3.5 | 7.0 | | | | 7.0 |
| 11. Data Distribution Interface | R&R | 1.6 | 3.2 | | | | 3.2 |
| 12. Power Transformer | R&R | 2.4 | 4.8 | 2.4 | 1.1 | | 8.3 |
| 13. Power Distribution Panel | Repair | 1.6 | 3.2 | | | | 3.2 |
| 14. Heliostat Array Controller | Repair | 1.0 | (Service Contract) | | | | |
| 15. Pedestal | Repair | 1.0 | | 2.0 | | | 2.0 |
| 16. Reflector Structure | Repair | 1.5 | | 3.0 | | | 3.0 |
| 17. Reflector Panel | R&R | 2.0 | | 4.0 | 1.0 | | 5.0 |
| 18. Digital Camera | R&R | 1.5 | 3.0 | | | | 3.0 |
| 19. Camera Cooler/Heater | R&R | 1.5 | 3.0 | | | | 3.0 |

*Estimated Elapsed Maintenance Time

Table 5-6

ON-LINE CORRECTIVE MAINTENANCE MANHOURS PER YEAR

| <u>Maintenance Significant Item</u> | <u>Qty</u> | <u>MTBMA *</u> | <u>Ma/Yr **</u> | <u>Elect Tech</u> | <u>Mech Tech</u> | <u>Equip Oper</u> | <u>Rigger</u> | <u>Total</u> |
|-------------------------------------|------------|----------------|-----------------|--------------------|------------------|-------------------|---------------|--------------|
| 1. Drive Assembly, Azimuth | 18,000 | 18.9 | 175 | 700 | 1,400 | 770 | 490 | 3,360 |
| 2. Jack Assembly, Tracking | 18,000 | 20.4 | 162 | 356 | 356 | | | 712 |
| 3. Jack Assembly, Storage | 18,000 | 20.4 | 8 | 18 | 18 | | | 36 |
| 4. Drive Motor, Azimuth | 18,000 | 16.4 | 201 | 342 | 342 | | | 684 |
| 5. Drive Motor, Elevation | 18,000 | 16.4 | 201 | 382 | 382 | | | 764 |
| 6. Drive Motor, Storage | 18,000 | 16.4 | 10 | 19 | 19 | | | 38 |
| 7. Heliostat J-Box | 18,000 | 47.9 | 69 | 221 | | | | 221 |
| 8. Heliostat Control Electronics | 18,000 | 33.7 | 98 | 255 | | | | 255 |
| 9. Heliostat Power/Data Cables | 90,000 | 101 | 33 | 119 | | | | 119 |
| 10. Field Power/Data Cables | 18,057 | 244.8 | 13 | 91 | | | | 91 |
| 11. Data Distribution Interface | 57 | 3,617.9 | 1 | 3 | | | | 3 |
| 12. Power Transformer | 57 | 8,771.9 | 0.4 | 2 | 1 | 1 | 1 | 4 |
| 13. Power Distribution Panel | 57 | 1,169.6 | 3 | 6 | | | | 6 |
| 14. Heliostat Array Controller | 1 | 1,000 | 4 | (Service Contract) | | | | |
| 15. Pedestal | 18,000 | 505.1 | 7 | | 14 | | | 14 |
| 16. Reflector Structure | 18,000 | 462.9 | 7 | | 21 | | | 21 |
| 17. Reflector Panel | 216,000 | 46.3 | 71 | | 284 | 71 | | 355 |
| 18. Digital Camera | 6 | 16,162 | 0.2 | 1 | | | | < 1 |
| 19. Camera Cooler/Heater | 6 | 6,460 | 0.02 | .1 | | | | < 1 |
| | | | <u>1,060</u> | <u>2,515</u> | <u>2,837</u> | <u>842</u> | <u>490</u> | <u>6,684</u> |

*Mean Time Between Maintenance Actions

**Maintenance Actions Per Year

and applying factors for the difference in environment and duty cycle. This estimate was then compared with and confirmed by data from References 2 and 3. The estimates for the electrical and electronic assemblies were obtained by actual part counts and part failure rates from References 2, 4, and 5. Cable failure rates were obtained from Reference 2.

The off-line unscheduled maintenance requirements are summarized in Table 5-7. The indicated on-site and off-site repair locations are justified, as noted in the earlier discussion of optimum repair level analyses. Maintenance man-hours per task and total man-hours per year per repair location are provided.

5.3.3 Spares and Repair Parts

A preliminary spares analysis was conducted based on the hardware configuration and the mean time to repair. Results of this analysis to identify spare LRU quantities are presented in Table 5-8. Repairable LRU's, upon failure, are removed from the system, placed in the repair cycle, and subsequently returned to spare stock inventory. Initial spares quantity for these items is the sum of the pipeline quantity and a 30-day contingency supply. The quantity is equal to the maximum number of items in the repair pipeline at any given time and is based on the failure rate and the repair cycle time. A repair cycle time of five days is projected for on-site repair and 30 days for off-site repair. The 30-day contingency quantity is equal to the number of predicted failures in a 30-day period, and provides a cushion in the event of delays in repair; it also accounts for a nonlinear failure rate. The initial spares quantity for nonreparable LRU's (i.e., those discarded at failure) is set at the predicted number of failures per year plus the 30-day contingency quantity. The initial spares quantity will be procured and stocked at the repair location when the first year of operation begins.

The discard factor represents the number of failures which result in the LRU being discarded instead of repaired, primarily due to the extensive damage. The product of the total number of failures per year and the discard factor equals the number of replacement LRU's to be procured at the beginning of the second and subsequent years.

Table 5-7
OFF-LINE REPAIR
MAINTENANCE MANHOURS

| <u>Maintenance Significant Item</u> | <u>Repair Location</u> | <u>Ma/Yr*</u> | <u>Mnhr Per Repair</u> | <u>On-Site Mnhrs</u> | <u>Off-site Mnhrs</u> |
|-------------------------------------|------------------------|--------------------|------------------------|----------------------|-----------------------|
| 1. Drive Assembly, Azimuth | On-site | 175 | 5.5 | 963 | |
| 2. Jack Assembly, Tracking | On-site | 162 | 3.0 | 486 | |
| 3. Jack Assembly, Storage | On-site | 8 | 3.0 | 24 | |
| 4. Drive Motor, Azimuth | On-site | 201 | 2.5 | 503 | |
| 5. Drive Motor, Elevation | On-site | 201 | 2.5 | 503 | |
| 6. Drive Motor, Storage | On-site | 10 | 2.5 | 25 | |
| 7. Heliostat Control Electronics | Off-site | 98 | 3.5 | | 343 |
| 8. Heliostat Array Controller | On-site | (Service Contract) | | | |
| 9. Power Transformer | Off-site | 0.4 | 10.0 | | 4 |
| 10. Digital Camera | Off-site | 0.2 | 3.0 | | 1 |
| | | | | 2,504 | 348 |

*Maintenance Actions Per Year

Table 5-8
SPARES REQUIREMENTS - LINE REPLACEABLE UNITS

| <u>Maintenance Significant Item</u> | <u>Sys. Qty</u> | <u>Ma/Yr*</u> | <u>Repair Loc</u> | <u>Pipe-line Qty</u> | <u>30-Day Cont.</u> | <u>Initial Spares</u> | <u>Discard Factor</u> | <u>Replacement Spares/Y</u> |
|-------------------------------------|-----------------|---------------|--------------------|----------------------|---------------------|-----------------------|-----------------------|-----------------------------|
| 1. Drive Assembly, Azimuth | 18,000 | 175 | On-site | 3 | 15 | 18 | .05 | 9 |
| 2. Jack Assembly, Tracking | 18,000 | 162 | On-site | 3 | 14 | 17 | .05 | 8 |
| 3. Jack Assembly, Storage | 18,000 | 8 | On-site | 1 | 1 | 2 | .05 | 1 |
| 4. Drive Motor, Azimuth | 18,000 | 201 | On-site | 3 | 17 | 20 | .05 | 10 |
| 5. Drive Motor, Elevation | 18,000 | 201 | On-site | 3 | 17 | 20 | .05 | 10 |
| 6. Drive Motor, Storage | 18,000 | 10 | On-site | 1 | 1 | 2 | .05 | 1 |
| 7. Heliostat J-Box | 18,000 | 69 | In-place | 0 | 0 | 0 | 0 | 0 |
| 8. Heliostat Control Electronics X | 18,000 | 98 | Off-site | 8 | 8 | 16 | .05 | 5 |
| 9. Heliostat Power/Data Cables | 90,000 | 33 | In-place | 0 | 0 | 0 | 0 | 0 |
| 10. Field Power/Data Cables | 18,057 | 13 | In-place | 0 | 0 | 0 | 0 | 0 |
| 11. Data Distribution Interface | 57 | 1 | Discard | 0 | 1 | 2 | 1.0 | 1 |
| 12. Power Transformer | 57 | 0.4 | Off-site | 1 | 1 | 2 | .25 | 0.1 |
| 13. Power Distribution Panel | 57 | 3 | In-place | 0 | 0 | 0 | 0 | 0 |
| 14. Heliostat Array Controller | 1 | 4 | (Service Contract) | | | | | |
| 15. Pedestal | 18,000 | 7 | In-place | 0 | 0 | 0 | 0 | 0 |
| 16. Reflector Structure | 18,000 | 7 | In-place | 0 | 0 | 0 | 0 | 0 |
| 17. Reflector Panel | 216,000 | 71 | Discard | 0 | 6 | 77 | 1.0 | 71 |
| 18. Digital Camera | 6 | 0.2 | Off-site | 1 | - | 1 | .05 | - |
| 19. Camera Cooler/Heater | 6 | 0.02 | Discard | 1 | - | 1 | 1.0 | .02 |

*Maintenance Actions Per Year

Line-item repair parts and quantities cannot be predicted at this time. Repair parts costs are projected as 10 percent of the cost to repair each part.

Spare LRU's to support on-line maintenance and repair parts for on-site, off-line maintenance must be stored indoors. Temperature or environmental conditioning is not a critical factor. Approximately 74.3 m² (800 ft²) of floor space should be adequate. Inventory control, warehousing, and receipt and issuing of spares should be integrated with similar on-site functions and is the equivalent of approximately a one-man level of effort.

5.4 OPERATIONS AND MAINTENANCE CHANGE SUMMARY

During the course of the study, design changes in both hardware and maintenance processes contributed to cost reductions for collector subsystem maintenance. The significant changes are summarized in Table 5-9 and discussed in this section.

The results of the computerized analyses show that most components can be most economically repaired at on-site facilities. Two factors were crucial in these repair policy decisions: (1) transportation costs, and (2) minimum requirements for special support equipment at the repair location. The economic benefits of this change in maintenance will be evident when a life-cycle cost analysis is completed.

While no verified reflector cleaning process has yet been developed, several methods have been identified, each using different equipment. The baseline method, developed by a supplier, could use any process eventually developed. However, the method of stopping at each heliostat for from seven to eight minutes is far too costly. Consequently, the method selected is one using two spray trucks working in tandem. The first truck applies a cleaning solution on the surface of the reflector; the second truck follows at a distance commensurate with the soak time required of the cleaning solution, rinses the solution, and loosens soil from the reflector surface using deionized water. This method shows a cost reduction over the baseline method of approximately five to one.

Table 5-9

OPERATIONS AND MAINTENANCE CHANGE SUMMARY

| REQUIREMENT | WAS | IS | EFFECT |
|-------------------------|--|---|--|
| Off-Line Repair | Optimized for Pilot Plant and Applied to Commercial Plant - (All Off-Site) | Optimized for Commercial Plant | Majority of Items Repaired On-Site - Reduced Maintenance Support Costs |
| Reflector Cleaning | Single Tanker Truck Carrying Both Wash & Rinse Solutions. Stop at Each Heliostat to Wash, Then Rinse | Separate Trucks for Wash & Rinse Solutions. "Drive Through Technique" One Minute Spacing Between Wash. & Rinse Trucks | Reduce Cleaning Time by a Factor of 7. Reduce Overall Cleaning Cost by Approximately 5 |
| Unscheduled Maintenance | Initial Baseline Hardware - Remove & Replace or Repair In-Place, Whichever Most Cost Effective | Low Cost Configuration - Remove & Replace or Repair In-Place Whichever Most Cost Effective | Lower Parts Count & Reduced Complexity Equals Higher Reliability & Fewer Maintenance Actions & Less Time per Task |
| Scheduled Maintenance | Initial Baseline Hardware Periodic lubrication of heliostat drive units | Low Cost Configuration - <ul style="list-style-type: none"> • Eliminate Scheduled Lubrication in Favor of Inspect for Oil Leaks • Alignment Recalibration Check Performed by Software | <ul style="list-style-type: none"> • Reduce Lubrication Manhours by Approximately 50 Percent • Fast, Accurate. Less Costly |

Hardware design changes resulting in reduced complexity and fewer parts have increased predicted reliability. Of course, the higher reliability figures have reduced the number of annual maintenance actions projected. Also, the lowered complexity of the design contributed to shorten the time needed for repair.

Scheduling maintenance tasks severely affects costs since any scheduled task must be performed 18,000 times. Two design improvements during the study have lowered periodic maintenance requirements.

The lubricant seals in the drive mechanisms now have a predicted life of at least 30 years. Use of these seals coupled with the low working stress imposed on the drives, permits deletion of all periodic lubrication tasks. The possible need to lubricate drive units remains. This would follow a seal failure, and the fault would be indicated by the presence of oil or grease stains external to the drive units.

The second cost reduction is in the periodic alignment of the heliostats. This requirement cannot be eliminated, but improvements in the method of realignment reduces the task time and the man-hours required. This cost reduction comes from the application of automated checks, use of the digital imaging radiometer to verify alignment of the heliostats, and performing recalibration through software changes rather than mechanical adjustments.

5.5 REFERENCES FOR SECTION 5

- 1) WASH-1400, Reactor Safety Study, An Assessment of Accident Risks in U.S. Commercial Nuclear Power Plants, US AEC. October 1975.
- 2) Failure Rate Data Handbook (FARADA), Naval Weapons Station, Corona, CA. (Undated)
- 3) Non-Electronic Reliability Notebook, RADC-TR-75-22, Hughes Aircraft Company, January 1975. AD/A-005.657.
- 4) MIL-HDBK-217B, Reliability Stress and Failure Rate Data for Electronic Equipment, September 1974.
- 5) Handbook of Piece Part Failure Rates, T-70-48891-007, June 1970, Martin Marietta.

Section 6

SPECIFICATION VERIFICATION AND OPTIMIZATION

This section presents an analysis of our design to verify, in part, that it meets requirements of DOE Specification 001 and other requirements believed important by MDAC. The evidence of compliance of the preliminary design with the specification is given, along with the source of data. Areas requiring additional test verification are indicated, together with the development/implementation phase or stage at which MDAC would recommend such verifications.

6.1 OPTIMIZATION OF REQUIREMENTS

Several heliostat configuration parameters can affect the field layout. Among these are the clearout circle (the zone swept out by the heliostat as it rotates about its azimuth axis), the mirror reflectivity, the mirror area, and the ratio of mirror area to clearout circle area.

MDAC developed a simplified computer program to estimate the aggregate effect of these parameters on the field layout. Results from this computer program were used to help select the heliostat configuration. The program and results are described in Section 6.1.1.

The total effect of tracking and beam quality errors leads to an interception factor at the receiver which depends on these errors, the heliostat location, and the time and day. The errors are functions of wind speed and direction, heliostat orientation, and ambient temperature.

MDAC has also performed some additional requirements optimization of effects of the above variables on beam errors and received power. Results are described in Section 6.1.2.

6.1.1 Configuration Analyses

The collector field is laid out in a series of concentric circles, as indicated in Figure 6-1. The heliostats are positioned along rays emanating from the tower. Heliostats in each row are aligned along the gap between the heliostats in the next row inward. The field configuration is called a radial stagger.

Since the number of heliostats per circle is a constant, the azimuthal spacing between heliostats increases with increasing radius from the tower. In order to retain reasonable packing densities of heliostats, it is necessary to reset the azimuth spacing periodically as illustrated in Figure 6-2. The zone in which the azimuth spacing is reset is called a slip plane. The prototype heliostat field layout is assumed to have a circumferential road in the slip plane.

Changing the heliostat configuration has an effect on the field layout in some portions of the field. The circle centered on the azimuth axis and containing the superimposed plan views of the heliostat when face up and face down (Figure 6-2) is called the clearout circle. The clearout circles of adjacent heliostats should retain an average 0.3 m (1 ft) clearance to ensure that heliostats do not physically contact each other. The clearout circle and the mirror area contained in a clearout circle are both dependent on heliostat configuration.

The computer program STATFLD was written in order to provide heliostat field layouts and allow comparison of the effect on field sizing of various input parameters. The field layouts are based on a radial stagger array with circumferential roads placed where the number of rays is to be expanded. The circumferential roads eliminate the need for deleting and shifting heliostats, as was required previously. A main access road to the south is also used.

The tower height may be fixed or may be determined by the program to give an elevation angle at the outermost row of 11 degrees, resulting in a heliostat

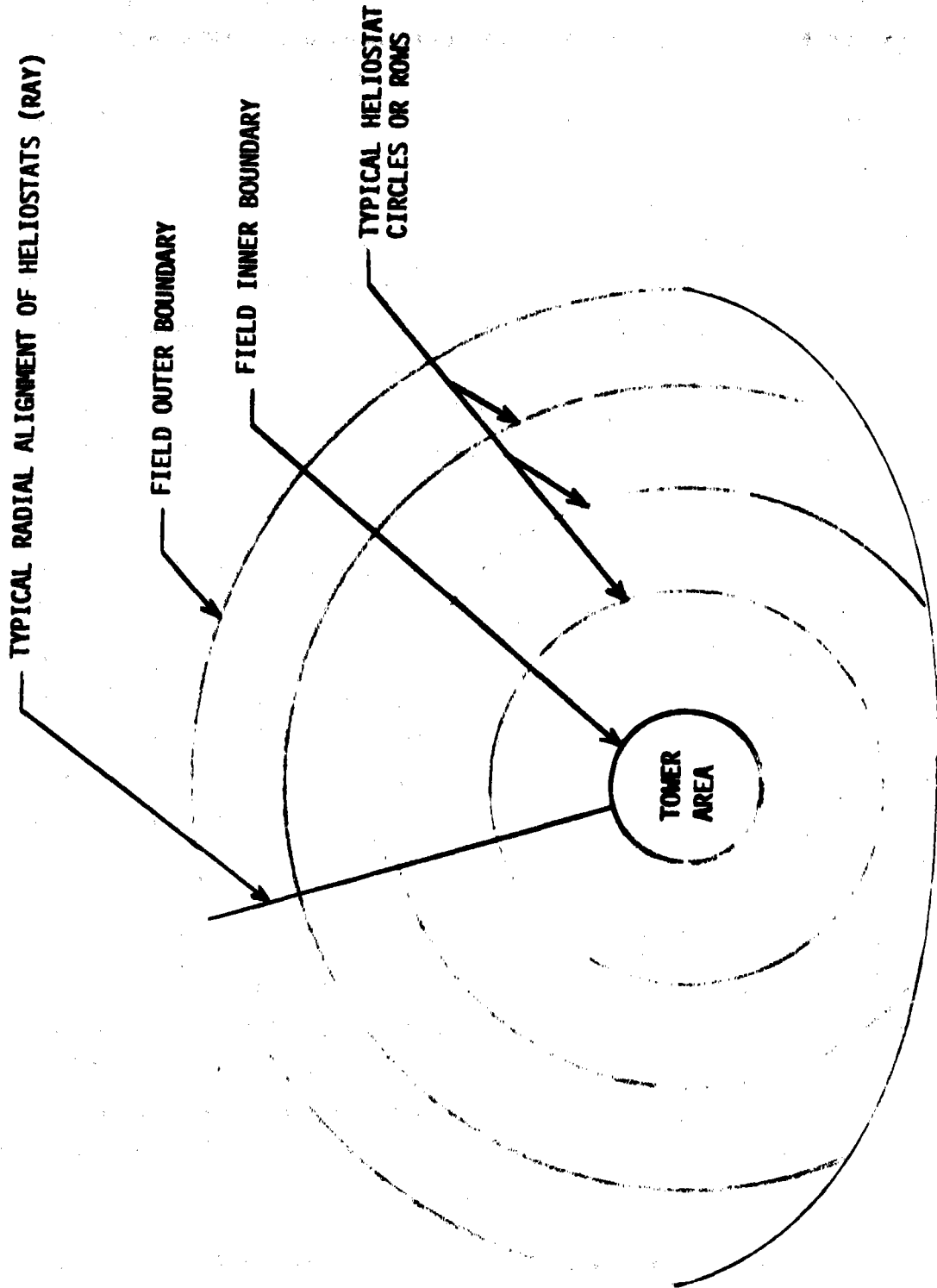


Figure 6-1. Commercial Collector Field Layout

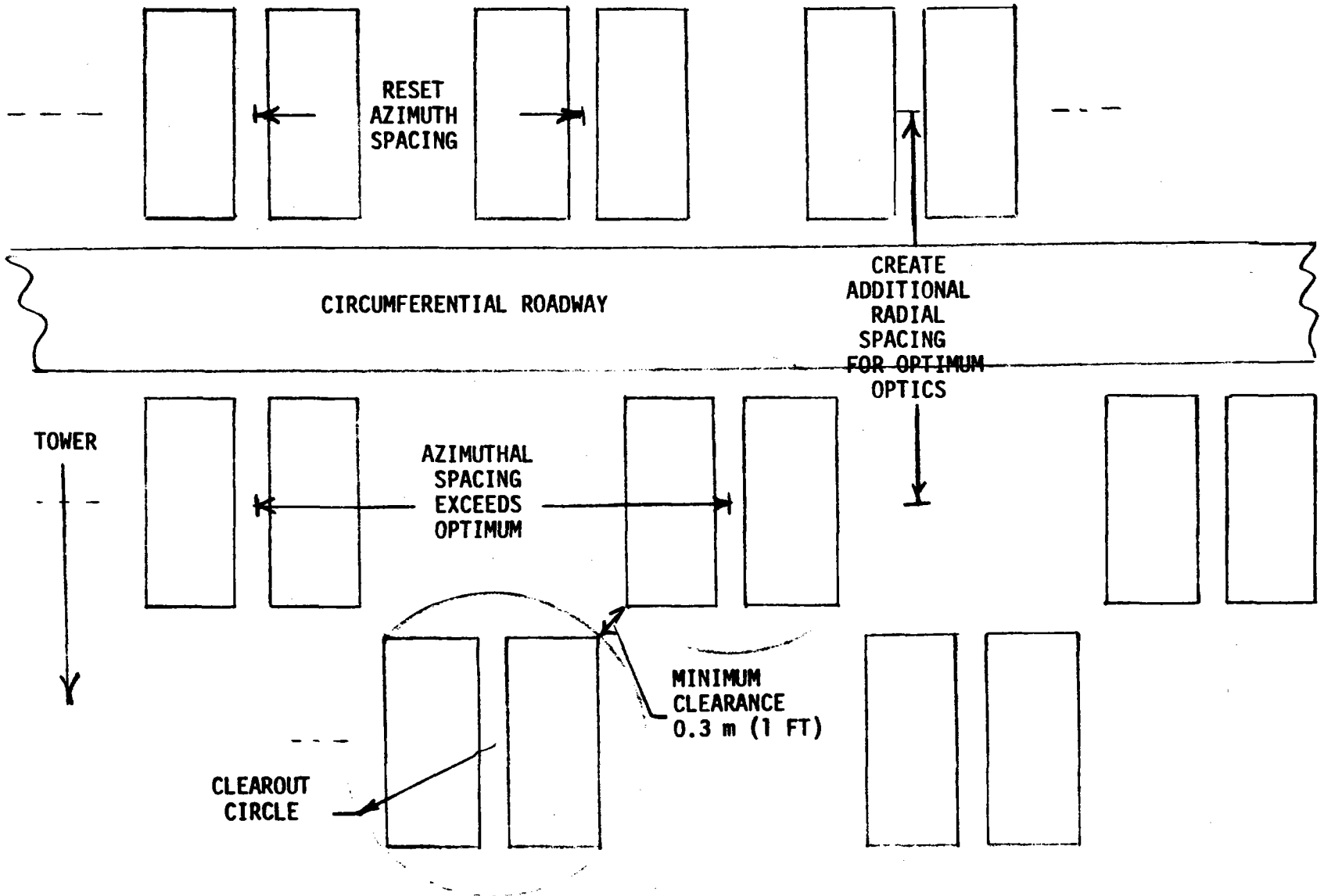


Figure 6-2. Resetting Azimuth Spacing

field envelope geometrically similar to the 100 MW field designed by the University of Houston. Average atmospheric attenuation and shadowing and blocking can also be considered.

Input parameters are:

- Mirror area per heliostat
- Total effective mirror area
- Mirror width
- Clearout circle
- Circumferential road width
- South road width
- Maximum elevation angle
- Tower height (optional)
- Maximum and minimum azimuth spacing

The output values consist of:

- Total mirror area
- Total number of heliostats
- Tower height,

and for each row:

- Radius
- Elevation angle
- Spacing to first and second row inward
- Azimuthal spacing
- Number of heliostats
- Diagonal distance to nearest heliostat
- Total arc (degrees).

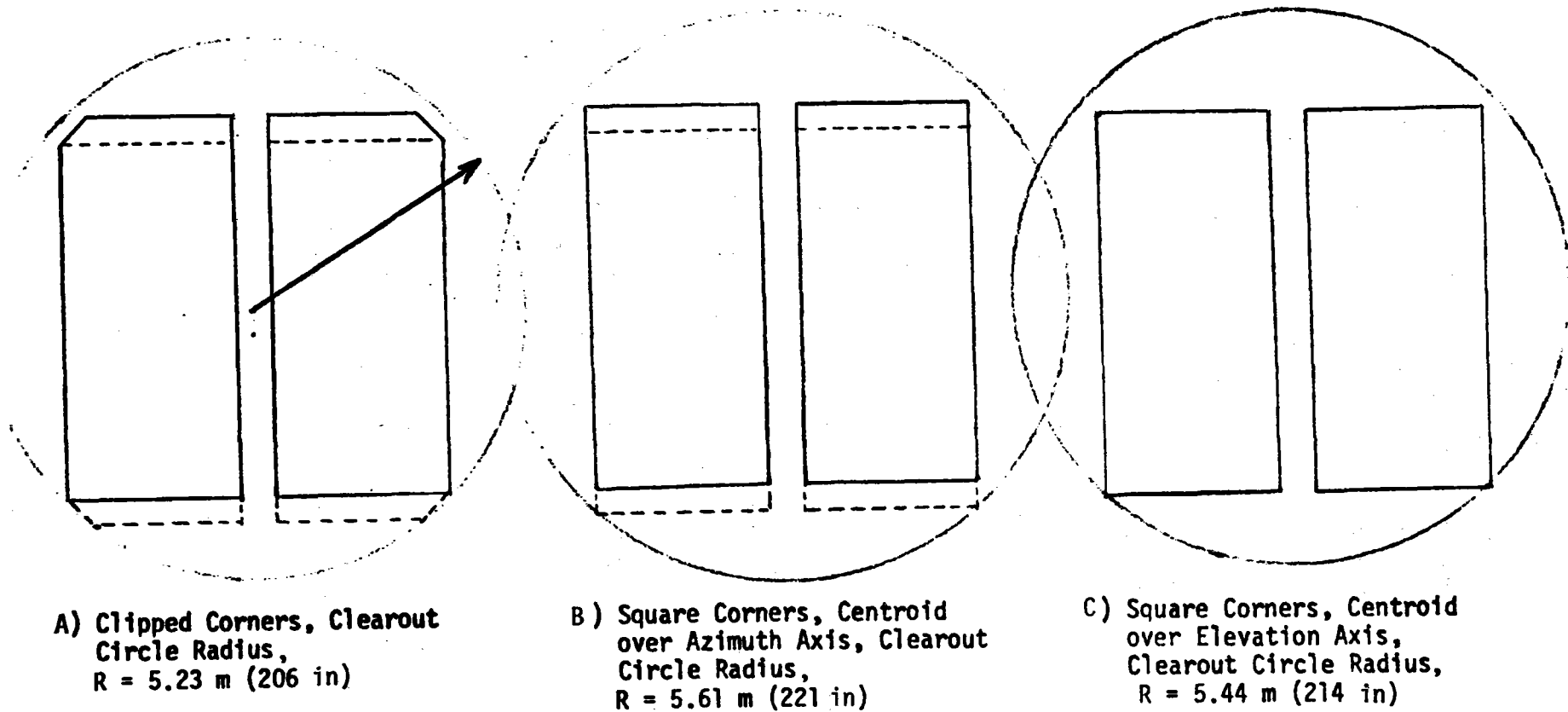
The operation of STATFLD is described below.

- 1) The radius of the first circle is found based on tower height and required elevation angle.
- 2) The azimuthal spacing is set to the minimum.

- 3) The radius of subsequent rows is determined by using an algorithm for optimal spacing, based on University of Houston optimization results, and determining the radius necessary for physical clearance of heliostats. The larger of the two radii is selected.
- 4) The azimuthal spacing of each subsequent row is fixed since the angular spacing of rays does not change until a slip plane or circumferential road is inserted. When the azimuthal spacing exceeds the maximum value specified, that row is replaced with a circumferential road.
- 5) The next row radius is computed and azimuthal spacing is set to the minimum.
- 6) Steps 3, 4, and 5 are repeated until the required mirror area is matched to the input value.
- 7) If requested, the tower height is modified based on the elevation angle of the last row of heliostats and the entire field is once again computed. This process is repeated until the elevation angle of the last row is approximately 11 degrees.

STATFLD was used to determine the impact of using square corners for the mirror modules on the field layout. Figure 6-3 illustrates the three cases considered. Because the reflective unit centroid cannot be located directly above the azimuth axis in both the face-up and face-down positions, the circle swept out by the heliostats is affected by clipping two of the corners or by shifting the mirror centroid to be over the elevation axis.

Table 6-1 shows results from STATFLD for these three cases. While the clipped corner configuration does have the minimum clearout circle, this is at a loss of 0.3 m^2 reflector area. With the reflector centroid over the elevation axis, the increased reflector area (hence, fewer heliostats) almost exactly compensates the field impact of the greater clearout circle. The clipping is an extra cost operation which wastes material and reduces the reflector area. Hence, the analysis leads to the conclusion that the corners should not be clipped.



NOTE: Dashed line indicates inverted position

Figure 6-3. Impact of Configuration on Clearout Circle

Table 6-1

EFFECT OF CONFIGURATION ON FIELD LAYOUT

| Configuration | Area (m ²) | No. of Heliostats | Field Radius (m) |
|------------------------------------|---------------------------|----------------------|---------------------|
| A) Clipped Corners | 48 | 17,763 | 1,035 |
| B) Centroid Over Elevation Axis | 48.31 | 17,649 | 1,032 |
| C) Centroid Over Azimuth Axis | 48.31 | 17,649 | 1,059 |

With the reflector centroid over the azimuth axis, the field size must grow by about 25 m. This small difference should be considered only if there is no net benefit in loads or structural design which results from the location of mirror centroid. Since there are loads and structures benefits of placing the centroid over the azimuth axis, Configuration C was chosen.

STATFLD also has the capability of weighting the mirror area by the beam attenuation factor which is appropriate to the slant range. This factor becomes potentially important in considering the effects of filling or partially filling in the slot and effects of changes in mirror reflectivity.

STATFLD was run for configurations with a full slot, a half slot, and no slot (non-inverting). Table 6-2 shows the results. The tower height was allowed to vary, maintaining an elevation angle of 11 degrees from the outermost heliostat. In addition, the effect of a 1 percent improvement in reflectivity is estimated based on the above data. The "tower cost effect" column is the reduction in tower cost allocated to the heliostats and normalized to a cost of \$65/m².

The amplification factor defined in Table 6-2 is a factor which relates the direct improvement of a 1 percent increase in reflectivity (or equivalent area gain within the clearout circle) to the total improvement including reduction of beam attenuation and reduction of tower cost. The amplification factor is calculated to be about 1.23. Hence, a 1 percent improvement in reflectivity of a heliostat at \$65/m² has a direct equivalent cost reduction of \$0.65/m² and a total effect of 0.65 x 1.23 = \$0.80/m².

Table 6-2
AMPLIFICATION FACTOR

| Configuration | Area (m ²) | No. of Heliostats | Field Area Ratio | Tower Height (m) | Tower Cost Effect (Fraction of Heliostat Cost) |
|--|---------------------------|----------------------|---------------------|------------------------|---|
| Full Slot | 48.31 | 17,725 | 1.0 | 259 | 1.0 |
| Half Slot | 50.91 | 16,775 | 0.9973 | 253 | 0.9911 |
| No Slot | 53.51 | 15,950 | 0.9967 | 247 | 0.9821 |
| Equivalent Effect of 1% Reflectivity Change | 48.79 | 17,545 | 0.9997 | ~ 258 | 0.9983 |

Amplification Factor = $\frac{\text{Effective Cost Reduction}}{\text{Direct Cost Reduction}}$

= $\frac{\text{Area Ratio}}{(\text{Field Area Ratio} \times \text{Tower Cost Effect}) - 1}$

= 1.23

Additional calculations were made to determine the effect of different maximum azimuthal spacings (Step 4 of STATFLD operation). The differences noted which result from maximum spacing ratios (spacing to heliostat width) from 2.2 to 2.58 appeared to be well under computational uncertainty.

6.1.2 Requirements Optimization Studies

Requirements optimization was undertaken in two areas: the allowable backlash in the linear actuators, and the degree of curvature to be used in mirror modules.

The effect of actuator backlash was determined using a Monte Carlo simulation of single heliostat dynamics, including drive backlash, hysteresis, and stiffness.

The time of day, wind direction, and gust velocity are three examples of the variables that were randomly selected. The sensitivity of beam error to actuator for a backlash single heliostat is shown in Figure 6-4. The CONCEN program was used to determine the amount of spillage that would occur with this beam error. The resulting spillage is shown in Figure 6-4. Increasing the backlash to that of a ball screw would increase the power spillage 0.3 percent, which is equivalent to approximately \$23 per heliostat.

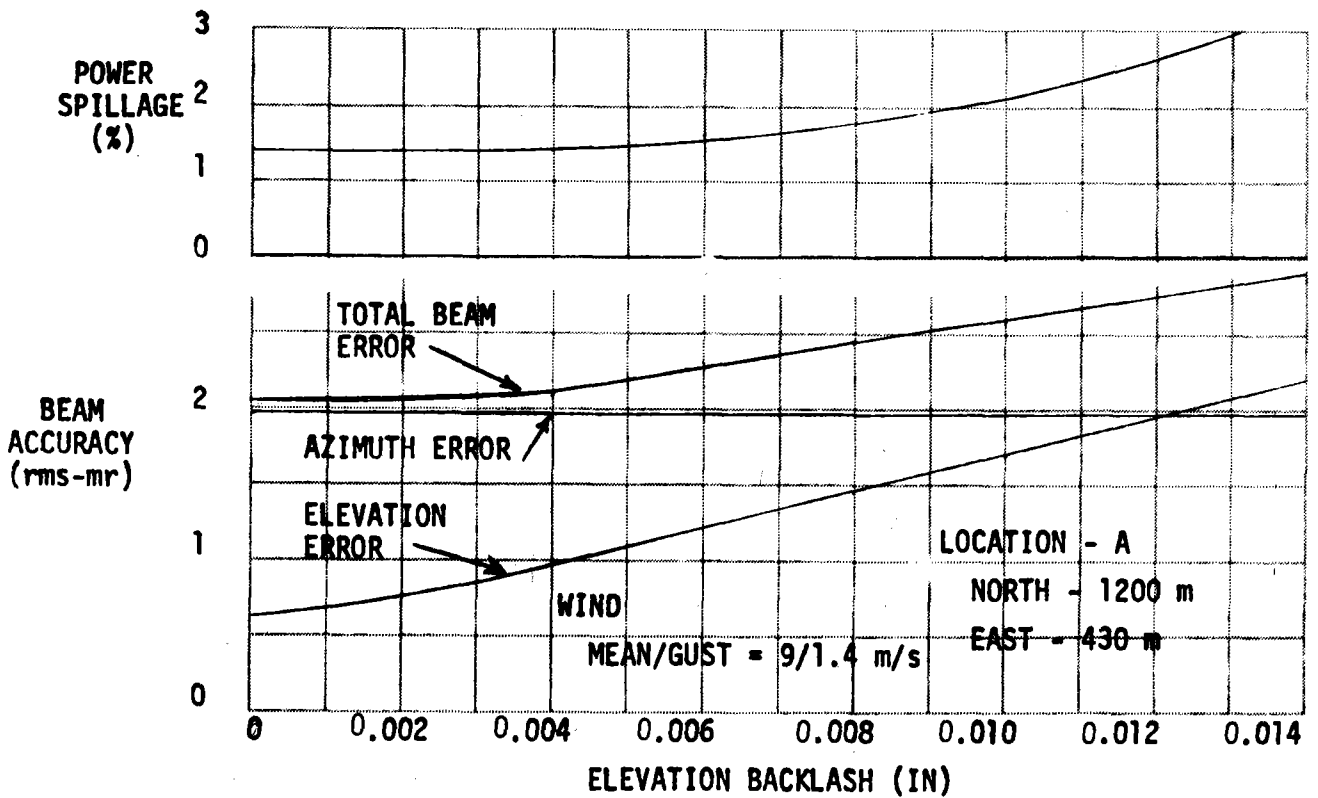


Figure 6-4. Effect of Backlash on Beam Error and Power Loss

Curvature in the mirror modules was used to minimize the beam spread at the receiver due to thermal expansion effects. The objective of this study was to define the panel curvature at the bonding temperature of 21°C (70°F) which keeps the image at the receiver bounded to its smallest size over the total operating temperature range (0° to 40°C or 32° to 104°F). Figure 6-5 illustrates the approach.

If a small curvature is established in the mirror at the bonding temperature, the mirror will become more concave as the temperature rises. Perfect focus will be achieved at a temperature of 25° to 30°C or 77° to 86°F. Above this

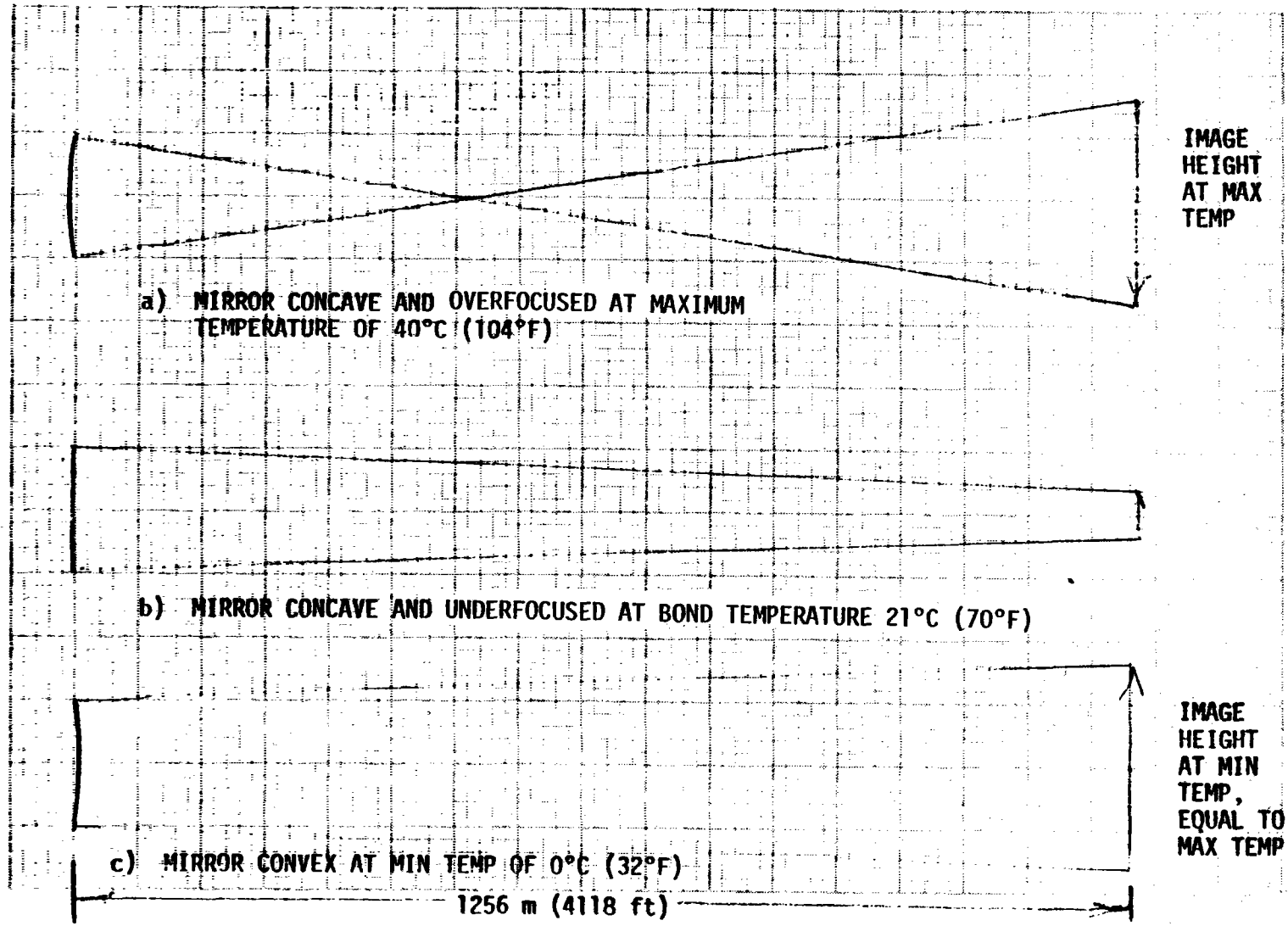


Figure 6-5. Mirror Curvature Requirement

temperature range, the mirror will be overfocused. The image height, assuming perfect optics, at 40°C (104°F), is set equal to the underfocused image height at 0°C (32°F), and the problem solved to provide the minimum image height and the curvature at the bonding temperature.

The required curvature was found to be about 2,000 m (6,800 ft). The maximum image height at the target was 13 m (40 ft). The height at the minimum temperature would be about 18 m (59 ft) if the panel were bonded flat at 21°C (70°F). Hence, even the very small curvature recommended is beneficial.

The above analysis also indicates a potential benefit to be derived from using a structural support which matches the thermal expansion coefficient of the float glass more closely than the steel stringers presently used. Advanced composites were investigated and a hat stiffener was designed with thermal expansion properties equivalent to glass and bending stiffness equivalent to the steel hat stiffeners. The cost of a composite stiffener appears high at this time, but further development and higher production rates should make this more attractive.

6.1.3 Availability

The availability of a single heliostat was calculated by utilizing the MTBF and MTTR results from Table 6-3. The failures per day rate was calculated for each heliostat component by dividing the operational hours per day by the MTBF. A value of 10 hours per day was used for the dynamic components (pedestal, reflector), and 0.5 hour per day for stowage elements. The failures per day were then multiplied by the MTTR to obtain the average downtime hours per day. This value was then used to calculate the individual component availability and the heliostat availability.

The downtime of the heliostat due to field component failures is calculated in a similar manner. The results show that the heliostat will be "down" about 0.000368 hour per day on the average due to heliostat component failures, and 0.000325 hour per day on the average due to field component failures, or a total of 0.000693 hour per day on the average. This converts to an availability of 0.999931 for a 10-hour day.

Table 6-3
COLLECTOR AVAILABILITY

| | <u>MTBF</u> <u>(HRS)</u> | <u>F/DAY</u> <u>(10⁻⁶)</u> | <u>MTRR</u> <u>(HRS)</u> | <u>H/DAY</u> <u>(10⁻⁶)</u> |
|-------------------------------|--|--|-----------------------------|--|
| Drive Assembly, Az | 340,136 | 29.4 | 4.0 | 117.6 |
| Jack Assembly, Track | 366,300 | 27.3 | 2.2 | 60.6 |
| Jack Assembly, Stowage | 366,300 | 1.37 | 2.2 | 3.0 |
| Drive Motor (2) | 295,858 | 67.6 | 1.8 | 121.7 |
| Stowage Motor | 295,858 | 1.69 | 1.9 | 3.2 |
| Heliostat Junction Box | 862,069 | 11.6 | 1.6 | 18.6 |
| Heliostat Control Electronics | 606,060 | 16.5 | 1.3 | 21.5 |
| Heliostat Cable (5) | 9,090,909 | 5.5 | 1.8 | 9.9 |
| Pedestal | 9,090,909 | 2.64 | 1.0 | 2.6 |
| Reflector Structure | 8,333,333 | 2.88 | 1.5 | 4.3 |
| Reflector Panel | 10,000,000 | 2.4 | 2.0 | 4.8 |
| Data Distribution Box | 206,186 | 48.5 | 1.6 | 77.6 |
| Power Transformer | (Redundant transformers - failure does not cause outage) | | | |
| Power Distribution Box | 66,667 | 150 | 1.6 | 240 |
| Field Cables | 4,545,454 | 2.2 | 3.5 | 7.7 |

10-Hour Operating Day; 24-Hour Actual Day; 0.5-Hour Stowage Day

6.2 SYSTEM PERFORMANCE

The system performance is a measure of the amount of redirected energy from the heliostats that is incident on the receiver. The subsystem requirements are specified by categorizing the performance errors into two groups. Those that cause an error in the direction of the reflected beam are called beam pointing errors, and those that cause a spreading of the beam are called beam quality errors. These performance errors are discussed below.

Beam Pointing - Beam pointing error includes such things as atmospheric refraction, control dynamics (including effect of wind on drives), and heliostat alignment. Heliostat alignment includes azimuth axis tilt after installation, latitude and longitude errors, and time error. A heliostat alignment scheme is used to reduce these errors. The error source, subsystem requirement, and analysis method are described in Table 6-4. Structural support errors include bending of the pedestal, drive systems, mirror module support structure, and foundation as a consequence of gravity and winds acting upon the heliostat. The center-of-gravity offset and the wind blowing across the reflective surface result in a moment which deflects the support structure. Bending of the support structure produces a beam pointing error.

Beam Quality - The theoretical beam shape from a single heliostat is determined by the slant range, the angle of reflection, the number, size, shape, cant angle, and curvature of the mirror segments, and the angular location of the sun. Any deviation of the mirror surface from the nominal flat or cylindrical curvature will cause a difference in beam size from the theoretical size. Surface slope errors arise from glass surface waviness or deformation due to mounting errors, temperature effects, wind loading, or gravity loading. The error sources, description, estimation method, and subsystem requirements are shown in Table 6-5.

Heliostat Performance - Because of geometrical conditions, the performance of a heliostat is dependent upon the location of the heliostat relative to the receiver, environmental conditions, and time of day. MDAC has investigated the performance for the different reference locations shown in

Table 6-4

BEAM POINTING ERRORS - CHARACTERISTICS

(Page 1 of 2)

| Error Source | Description | Estimation Method | Subsystem Requirements |
|---|---|--|---|
| Tower/Receiver | Movement of tower caused by temperature and winds, foundation settling. | Analysis by Stearns-Roger. | Horizontal movement of receiver will be less than 3 inches (σ). |
| Control Dynamics A. Motor Granularity B. Sensor Granularity C. Drive System With & Without Winds | A. Varying loads will cause different number of motor turns per motor pulse. B. Only single motor resolution. C. Drive backlash, stiffness, and hysteresis add variation in movement. Winds add to drive variation. | A. SRE and open loop test data incorporated in simulation. B. Model sensor in simulation. C. SRE and open loop test data incorporated in simulation. | A. Motor turn control will be less than 2 turns. B. Sensor will count each complete motor turn. C. Harmonic drive initial backlash will be less than 0.5 mrad peak-to-peak. Stiffness will be greater than 10×10^6 in-lb/rad and less than 12.5×10^6 in-lb/rad. Single input turn will produce less than 0.2 mrad of azimuth gimbal movement. Jack drive initial backlash from all sources will be less than 0.002 in. (1σ). Total stiffness will be greater than 180,000 lb/in and less than 260,000 lb/in. Single input turn will produce less than 0.3 mrad elevation gimbal movement. Temperature difference on drive loop will not produce more than 0.2 mrad max angle change. |
| Heliostat Alignment | Errors in time, latitude, longitude, azimuth and elevation reference, position pedestal tilt and non-orthogonality produce a beam error. | Previous alignment tests. | Alignment scheme will reduce all these errors to less than 0.8 mrad (σ). |

Table 6-4

BEAM POINTING ERRORS - CHARACTERISTICS

(Page 2 of 2)

| Error Source | Description | Estimation Method | Subsystem Requirements |
|--------------------------------------|---|---|---|
| Refraction | Atmospheric refraction of beam from sun to heliostat and heliostat to receiver. | LOWTRAN atmospheric refraction computer code. | A software model will correct sun to heliostat refraction to less than 0.4 mrad (1σ). |
| Foundation | Wind and gravity loads produce an elastic/plastic deformation of the foundation. Plastic deformation is also a function of soil settlement characteristics. | Structural analysis | A maximum allowable foundation settlement or plastic displacement of 0.05 mrad (1σ) and an elastic displacement of 0.5 mrad (1σ) must be included in allowable structural deflection limit. |
| 6-16 Support Structure/ Main Beam | Wind and gravity loads produce elastic deformation. | NASTRAN analysis and wind tunnel data. | An equivalent EI of 5.0×10^9 and 1.8×10^9 lb-in ² for the main beam and cross beams, respectively. |
| Pedestal | Wind and gravity loads produce elastic deformation. | NASTRAN analysis and wind tunnel data. | An equivalent EI of 9.3×10^9 lb-in ² . |

Table 6-5
BEAM QUALITY - CHARACTERISTICS

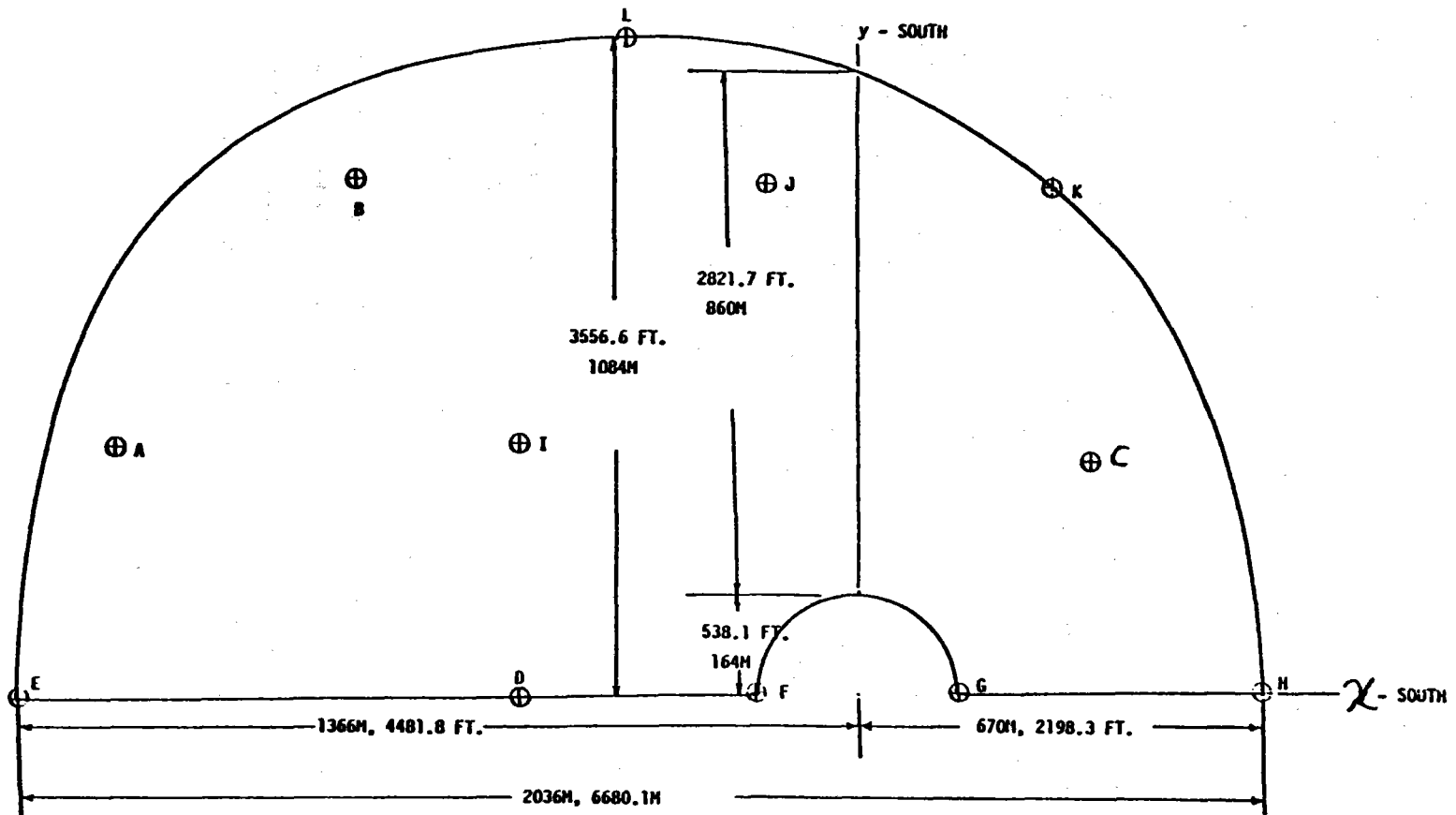
| Error Source | Description | Estimation Method | Subsystem Requirements |
|---|--|-------------------------------------|---|
| Mirror Module Deformation From Temperature | Materials have different thermal coefficients of expansion. | NASTRAN analysis | A change from reference temperature of ΔT shall not produce an error slope greater than $1.1 \times 10^{-6} \Delta T \chi$, where χ is the distance from center of panel. |
| Mirror Module Deformation From Gravity | Mirror module and support structure deflect under gravity. | NASTRAN analysis | Slope from gravity on surface shall not produce errors more than $A \sin \psi$ where A is TBD and ψ is elevation angle. |
| 617 Mirror Module Deformation From Wind Loads | Mirror module and support structure deflect under wind loads. | NASTRAN analysis | Winds on surface shall not produce error slopes greater than TBD envelope for winds below 12 m/s (27 mph) and any angle of attack. |
| Surface Waviness | Mirror surface has characteristic waviness. | Previous analysis and SRE test data | After mounting glass, error slope at evenly measured points less than 1 inch apart over surface of panel shall be less than 0.65 mrad (1σ). |
| Specular Dispersion | Mirror surface has some specular dispersion. | SRE measurements | Before glass is mounted, 95% of reflected beam shall be within 4 mrad of centerline. |
| Panel Alignment | Mirror normal of panel is not parallel to heliostat normal because of manufacturing tolerance. | Analysis of construction tolerance | Panel normal shall not deviate more than 0.5 mrad (1σ) from heliostat normal as a result of panel construction and mounting. |

Figure 6-6 and different environmental conditions. The beam pointing accuracy for a representative set of these locations is shown in Table 6-6. A Monte Carlo simulation of a single heliostat dynamics, including drive backlash, hysteresis, and stiffness, was used to transform the error sources into reflected beam errors. The time of day, wind direction, and gust velocity are examples of variables that were randomly selected. Beam error is expressed in a coordinate system centered at the heliostat, with one axis horizontal and one axis through the receiver.

A representative beam shape at the receiver is shown in Figure 6-7 for a heliostat at location D. The density pattern was calculated using the MDAC simulation called CONCEN. The mirror segments are canted and curved along the long axis for focusing at the maximum range of the array. The numbers on the figures represent the relative beam intensity, with 1 being 10 percent of the maximum. Since no beam errors were included in the calculation, the image shape shown in Figure 6-7 represents the theoretical beam shape. The effects of the beam quality errors listed in Table 6-5 upon the image size are illustrated in Figure 6-8. The amount of power outside the theoretical beam size plus 1.4 mrad is less than 2.5 percent.

6.3 SPECIFICATION VERIFICATION SUMMARY

The use of a perturbation technique on a mature initial design concept has ensured that the final baseline design meets the performance, design, and environmental specifications in Specification 001. The design treated in Section 2 satisfies these specifications. Table 6-7 summarizes the performance and design requirements and cross references the sections which treat each item specified or its verification. The requirements in this Phase I study were verified by analysis, similarity, or limited laboratory test data. The verifications will be completed in tests to be conducted in Phase II.



| LOCATION | METERS | | FEET | | LOCATION | METERS | | FEET | |
|----------|--------|-----|---------|--------|----------|--------|------|---------|--------|
| | x | y | x | y | | x | y | x | y |
| A | -1200 | 430 | -3937.2 | 1410.8 | H | 670 | 0 | 2198.3 | 0 |
| B | -800 | 860 | -2624.8 | 2624.8 | I | -550 | 430 | -1804.6 | 1410.8 |
| C | 400 | 430 | 1312.4 | 1410.8 | J | -164 | 800 | -538.1 | 2624.8 |
| D | -550 | 0 | -1804.6 | 0 | K | 300 | 800 | 984.3 | 2624.8 |
| E | -1366 | 0 | -4481.8 | 0 | L | -400 | 1084 | -1312.4 | 3556.6 |
| F | -164 | 0 | -538.1 | 0 | | | | | |
| G | 164 | 0 | 538.1 | 0 | | | | | |

Figure 6-6. Heliostat Reference Locations

Table 6-6

ESTIMATE OF BEAM POINT ACCURACY

| Error Source | Beam Pointing Accuracy (mrad-rms) | | | | | Comment |
|---|-----------------------------------|---------------------|---------------------|---------------------|---------------------|---|
| | Location A Az/E1 | Location B Az/E1 | Location C Az/E1 | Location F Az/E1 | Location H Az/E1 | |
| 1. Tower/Receiver | 0.90/0.20 | 0.90/0.20 | 0.90/0.20 | 0.90/0.20 | 0.90/0.20 | Tower movement from wind. |
| 2. Motor Turn Granularity | 0.15/0.12 | 0.18/0.17 | 0.21/0.28 | 0.26/0.26 | 0.28/0.28 | Command ± 1 turn (σ). |
| 3. Sensor Granularity | 0.12/0.12 | 0.04/0.05 | 0.06/0.08 | 0.07/0.07 | 0.08/0.08 | Count each motor turn. |
| 4. Drive System A. No Winds | 0.45/0.21 | 0.43/0.21 | 0.15/0.24 | 0.39/0.13 | 0.11/0.15 | Drive Characteristics: Azimuth backlash = 1.1×10^7 N-m/rad Elevation backlash = 0.5 mrad Elevation Stiffness = 24,000 N-m |
| B. Mean (Gust) = 9 m/s (1.4 m/s) | 1.89/0.73 | 2.26/0.60 | 0.62/0.10 | 1.28/0.45 | 1.06/1.12 | |
| 5. Alignment | 0.40/0.55 | 0.50/0.35 | 0.75/0.40 | 0.75/0.45 | 0.80/0.45 | Error after alignment correction, initial errors of tilt = 2 degrees (σ), non-orthogonality = 3 mrad, time = 2 sec (σ), latitude = 0.05 degree (σ), position = 3 inches (σ) |
| 6. Refraction | 0.00/0.34 | 0.00/0.34 | 0.00/0.34 | 0.00/0.34 | 0.00/0.34 | Refraction error left after algorithm correction, caused by temperature, pressure, and atmospheric content variation. |
| 7. Foundation | 0.31/0.32 | 0.35/0.36 | 0.57/0.70 | 0.64/0.62 | 0.69/0.68 | Foundation settlement = 0.05 mrad (σ) Elastic displacement = 0.5 mrad (σ). |
| 8. Gravitational | 0.30/0.40 | 0.15/0.52 | 0.10/0.90 | 0.25/0.87 | 0.05/0.97 | Residual algorithm correction of deadweight bending of drive and pedestal. |
| 9. Pedestal/Support Structure Max Wind = 12 m/s (27 mph) | 0.06/1.09 | 0.01/0.18 | 0.02/0.07 | 0.09/0.79 | 0.08/0.11 | Moment created by wind causes pedestal/foundation bending. |
| TOTAL RSS VALUE | 2.22/1.58 | 2.55/1.06 | 1.46/1.33 | 1.91/1.55 | 1.77/1.75 | |

PEAK VALUE OF FLUX DENSITY = .148R7E+04 W/SQM, CONTOURS IN TENTHS, P = PEAK

Mirror Size: 7.3 m x 7.3 m

Date: Dec 21 Hour: 1200

Location: 550 mN, 0 mE (Location D)

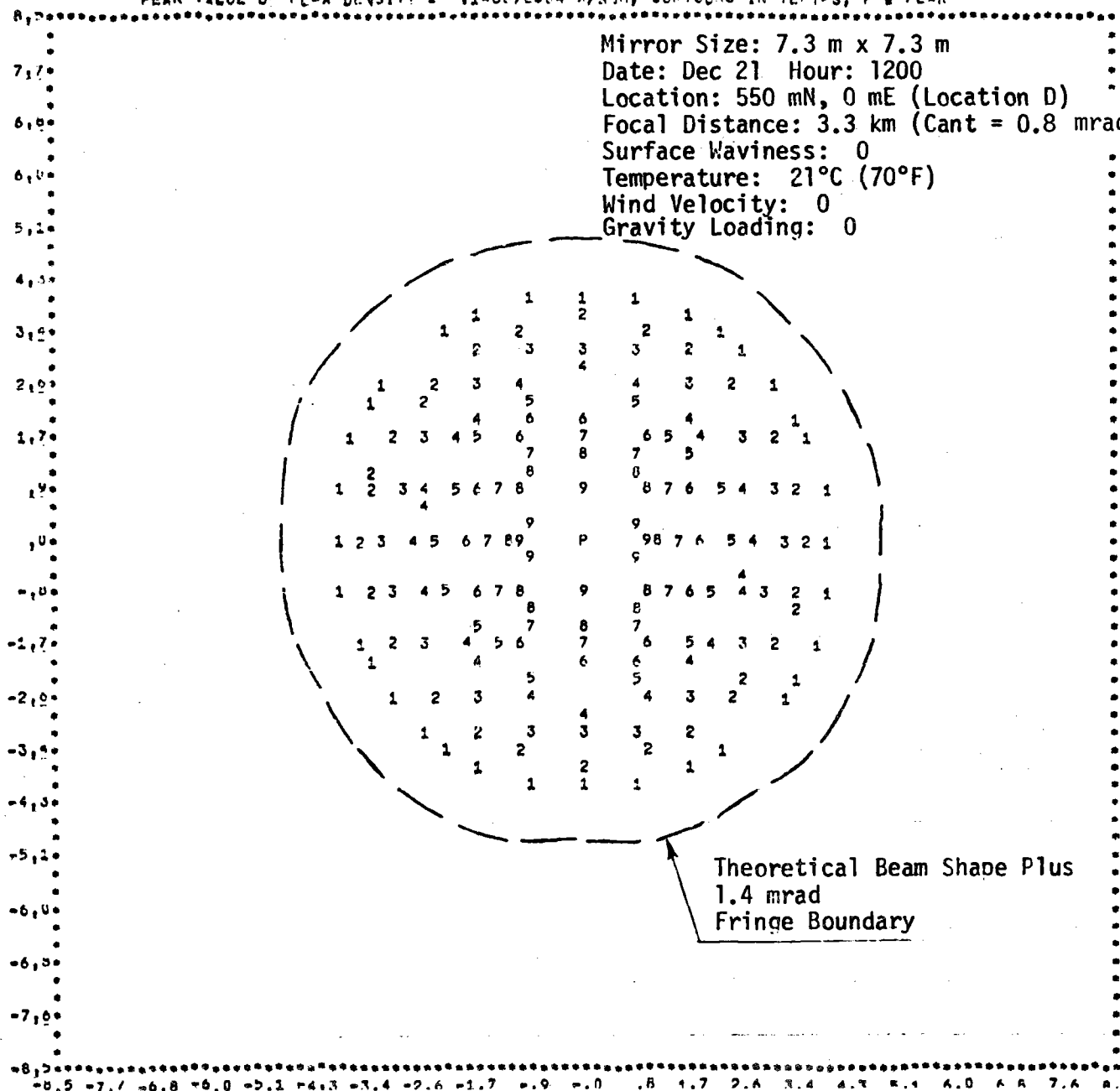
Focal Distance: 3.3 km (Cant = 0.8 mrad, Curv = 0.0005 m⁻¹)

Surface Waviness: 0

Temperature: 21°C (70°F)

Wind Velocity: 0

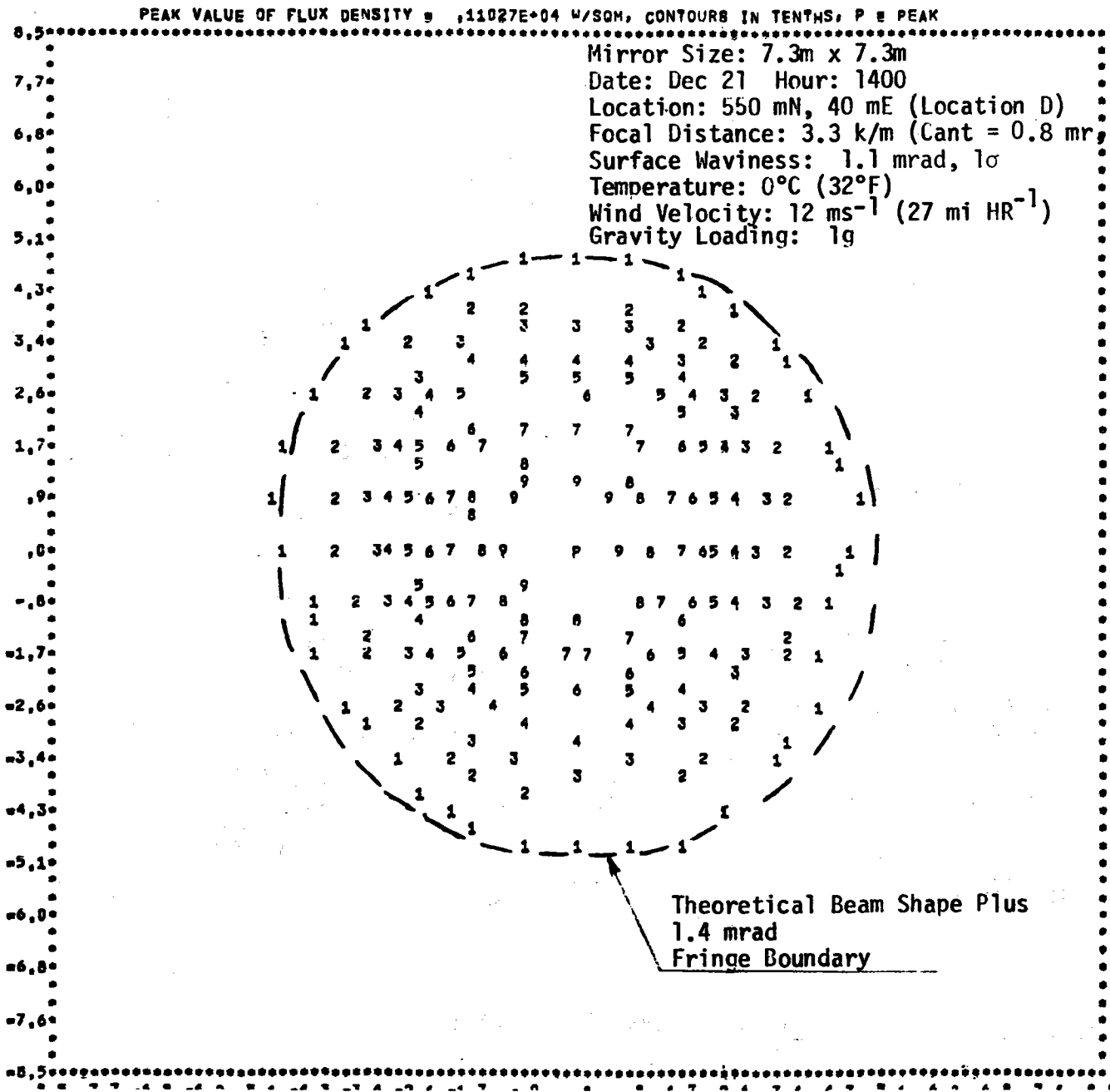
Gravity Loading: 0



Theoretical Beam Shape Plus
1.4 mrad
Fringe Boundary

6-21

Figure 6-7. Theoretical Beam Shape — No Errors



6-22

Figure 6-8. Beam Shape With Errors

Table 6-7

VERIFICATION OF SPECIFICATION 001

(Page 1 of 5)

| PARAGRAPH NUMBER | REQUIREMENT | VERIFICATION |
|------------------|---|--|
| | <u>PERFORMANCE</u> | |
| 3.1.1.1 | Heliostat Availability Greater than 0.97 | Analysis, Greater than 0.099. See Section 6.1.3. |
| 3.1.1.2 | Interchangeability | Design for All Locations is the Same, No Field Adjustment Required |
| 3.1.1.3 | Protect Against Electrical Transients | Transient Suppressors Used, Optical Data Transmission and Switching Used |
| | <u>ENVIRONMENTAL</u> | |
| 3.1.2.1 | Wind <ul style="list-style-type: none"> • Operational Limit TBD • Survival Wind, 40 m/s (90 mph), Angle of Attach = $\pm 10^\circ$ • Dust Devils, 17 m/s (40 mph) | Initiate Stowage at 16.1 m/s (36 mph) (No Change from Reference 1) Analysis, Section 2.4 Analysis, Section 2.4 |
| 3.1.2.2 | Temperature <ul style="list-style-type: none"> • Survive -30°C (-22°F) to $+50^\circ\text{C}$ ($+120^\circ\text{F}$) • Performance Optimized from 0°C (32°F) to 40°C ($+104^\circ\text{F}$) | Analysis, Section 2.4 Analysis, Section 6.1.2 |
| 3.1.2.3 | Earthquake, Seismic Zone #3 (UBC) | Analysis, Section 2.4 |

Table 6-7

VERIFICATION OF SPECIFICATION 001

(Page 2 of 5)

| PARAGRAPH NUMBER | REQUIREMENT | VERIFICATION |
|------------------------------|--|---|
| 3.1.2.4 | Snow, 250 Pa (5 lbs/ft ²) | Much Less than Survival Wind |
| 3.1.2.5 | Rain | Test, Reference 1 |
| 3.1.2.6 | Ice, 50 mm (2 inches) | Test, Reference 1 |
| 3.1.2.7 | Hail, 20 mm (3/4 inch) at 20 m/s (65 fps), 25 mm (1 inch) at 23 m/s (75 fps) | Test, Section 2.3.3 |
| 3.1.2.8 | Sand Storm per MIL-STD-810B | Test, Reference 1 |
| 3.1.2.9 | Lightning | Transient Suppressors Incorporated, HelioStat Grounded through Foundation |
| <u>HELIOSTAT PERFORMANCE</u> | | |
| 3.2.1 | Operating Periods | Control and Drive Allow Operating from Sunrise to Sunset |
| 3.2.2 | Target | HelioStat Evaluated Against All Three Targets - Section 7 |
| 3.2.3 | Field Positions | HelioStat Evaluated at Required Positions - Section 7 |
| 3.2.4 | Reflectivity | Clean Reflectivity Projected to be 0.92 to 0.95 - Section 2.2.2 |
| 3.2.5 | Reflective Area | Area Selected at 49 m ² (528 ft ²) |

6-24

VERIFICATION OF SPECIFICATION 001

| PARAGRAPH NUMBER | REQUIREMENT | VERIFICATION |
|---------------------|--|--|
| | <u>DRIVE AND CONTROL</u> | |
| 3.3.1.1 | Fail-Safe Operation | Loss of Data Link Does Not Result in Loss of Tracking - Stowage by Manual Command Loss of Power is Unlikely. Each Heliostat is fed from Two Transformers. If Power is Lost, a Portable Power Supply will Effect Safe Stowage. |
| 3.3.1.3 | Limit Controls as Required | Electronic Limit Controls Provided via the Control System |
| 3.3.2.1 | Tracking Accuracy Controlled | Analysis and Test Data, Section 6.2 |
| 3.3.2.2 | Acquisition Within 180 sec. | Slew Rates of 0.2 deg/sec Insure Rapid Acquisition in Less than 60 sec. |
| 3.3.2.3 | Continuous Tracking During Intermittent Clouds | Automatically Provided by Open Loop Control |
| 3.3.2.4 | Provide for Aiming Strategy | Automatically Provided by Software |
| 3.3.2.5, 3.3.2.6 | Shutdown Safely | Follow Prescribed Control Algorithm Shutdown within 15 Minutes |
| 3.3.3.1 | Manual Control | Available from Master Control, Data Distribution Interface and Heliostat |
| 3.3.3.2 | Alignment Control | Accomplish as in Initial Alignment, Section 4.5 |

VERIFICATION OF SPECIFICATION 001

| PARAGRAPH NUMBER | REQUIREMENT | VERIFICATION |
|------------------|------------------------------------|--|
| 3.3.4.1 | Failure Indication | Loss of Reference, Data or Power Detected by Heliostat or Data Distribution Interface and Reported. Inability to Track Also Reported. |
| 3.3.4.2 | Emergency Shutdown | All Heliostats off Target Within 30 Seconds |
| 3.5 | <u>PHYSICAL CHARACTERISTICS</u> | |
| | Access Space | Spacings are Adequate for Access by Maintenance Personnel and Vehicles |
| | Safe Stowed Positions | Normal Stowage Vertical, Face Down Stowage Available for Extended Shutdown and High Winds |
| | Easy Removal for Maintenance | Maintenance Analyses, Section 5.4 |
| | 30-Year Design Life | Test, Reference 1 |
| 3.6 | Design for Reliability | Analysis, Test - Section 5.4 |
| 3.7 | <u>MAINTENANCE</u> | |
| | Reflector Design for Easy Cleaning | Laminated Glass Mirror is Readily Cleaned, Chemically Inert |
| | Easy Service and Repair | Maintenance Analysis, Section 5.4 |
| | Normal Skills | Maintenance Analysis, Section 5.4 |

Table 6-7

VERIFICATION OF SPECIFICATION 001

| PARAGRAPH NUMBER | REQUIREMENT | VERIFICATION |
|------------------|----------------------------------|--|
| 3.8 | Standard Materials and Processes | Commercially Available Materials and Processes Used in All Parts |
| 3.9 | Electrical Transient Protection | Provided by Transient Suppressors, Optical Data Transmission, and Optical Switching |
| 3.11 | Interchangeability | All Parts Interchangeable with No Field Adjustments |
| 3.12 | <u>SAFETY</u> | |
| | •Minimize Hazards | Conformance with Safety Codes (OSHA, NEMA, etc) |
| | •Fail-Safe | Provisions Include: <ul style="list-style-type: none"> • Redundant Power Source • Heliostats Continue to Track if Data Lost • Redundant Data Paths to Secondary Feeder • Manual Stowage Capability |
| | •Safe Stow Capability | Face Down or Vertical Stowage Available |
| | •Local Heliostat Lockout | Switch Provided on Heliostat and at Data Distribution Interface |
| | •Hazard and Fault Indication | Automatically Available from Return Data Stream |
| | •Safety Regulations | Analysis for Compliance |

6-27

APPENDIX A

HELIOSTAT BASELINE DESIGN DESCRIPTION

Appendix A

HELIOSTAT BASELINE DESIGN DESCRIPTION

The design selected as the baseline for the prototype heliostat is illustrated in Figure A-1. This appendix provides a descriptive summary of the heliostat for reference purposes.

Mirror Module - The mirror module is a bonded sandwich consisting of a second-surface silvered mirror of iron float glass, a foam core, and a thin, galvanized steel back sheet. Total reflective surface area is 38m^2 (408.3ft^2).

Support Structure - The support structure consists of a tubular main beam and four channel cross beams. Twelve mirror modules are back bolted to the cross beams with shallow cups to spread the load.

Drive Unit - Azimuth rotation is obtained by three reduction stages. The first stage is integral with a 240-VAC, three-phase induction motor, the second stage is a worm/gear pair, and the third is a Harmonic drive unit. The elevation drive employs two machine screw jack actuators coupled with a drag link to provide for the required 180-degree rotation. Each jack is driven by a similar gear motor. The azimuth housing and drag link are castings.

Pedestal/Foundation - A tubular steel pedestal is attached to the drive unit on the upper end and to the foundation on the lower end by bolted flanges. The foundation may be either a precast spread footing or a drilled pier. The anchor bolts are wired to the reinforcement in either case.

Controls - The heliostat employs open-loop control (i.e., no beam sensor) with motor revolution counters for tracking and four-bit absolute encoders on both gimbal axes for periodic update restart capability.

A heliostat controller located on each heliostat retains the motor revolution counts and generates error signals from data transmitted by field controllers.

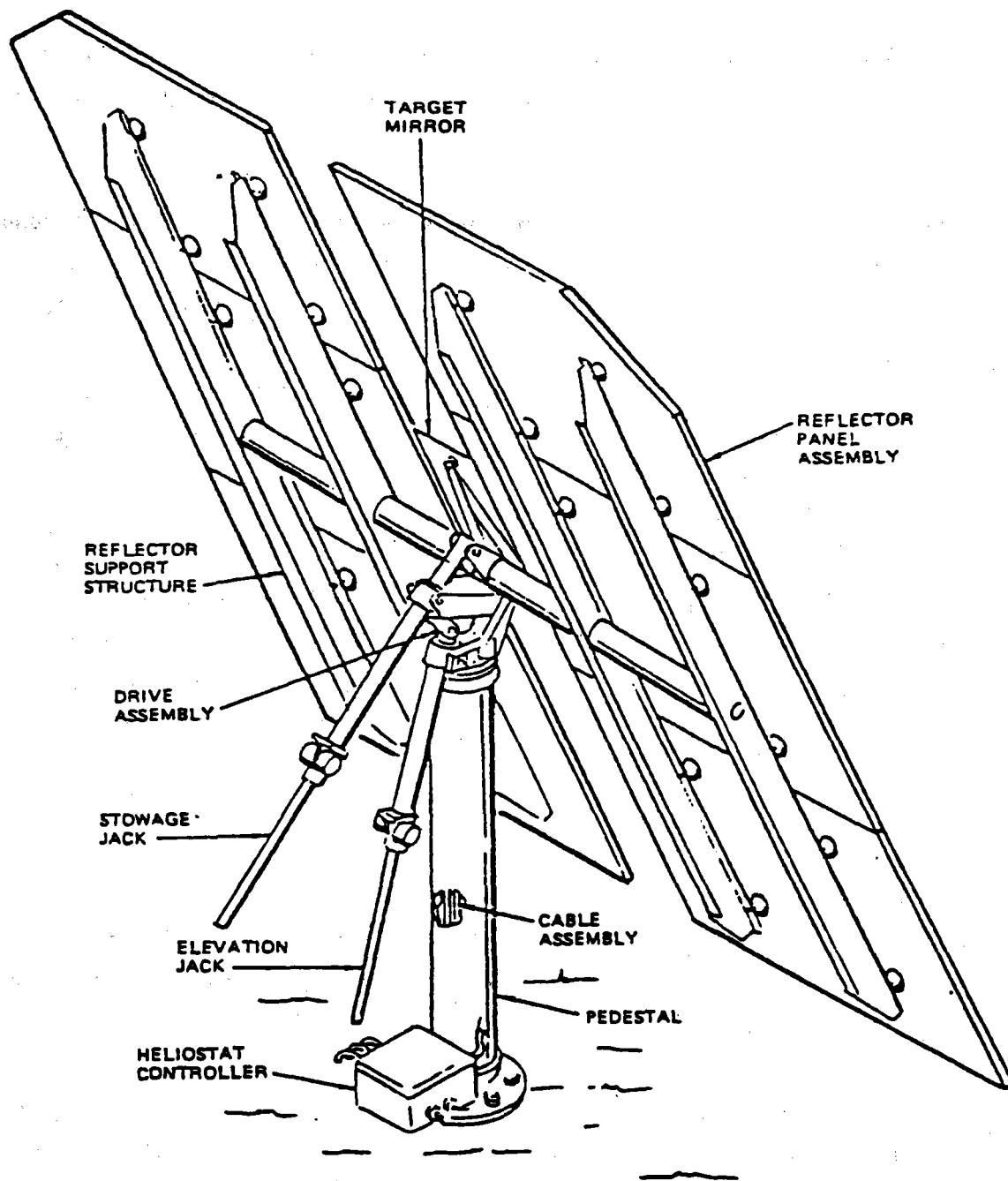


Figure A-1 Heliostat Assembly - Initial Baseline Design

The motor controller section of the heliostat controller then executes the required motor revolutions indicated by the error signal.

Field controllers are located to service approximately 24 heliostats. The field controllers serve as a data interface with the master controller and calculate time, ephemeris, and gimbal axis position data to transmit to the heliostat controller.

The field electronics (Figure A-2) include primary feeders of high voltage power and high data rate communication to the field transformers and field controllers, respectively. Both hookups are serial. Branching networks from the transformers connect approximately 24 heliostats in a serial or daisy chain arrangement. Similarly, a serial connection is used between the field controllers and the heliostat controllers.

A-5

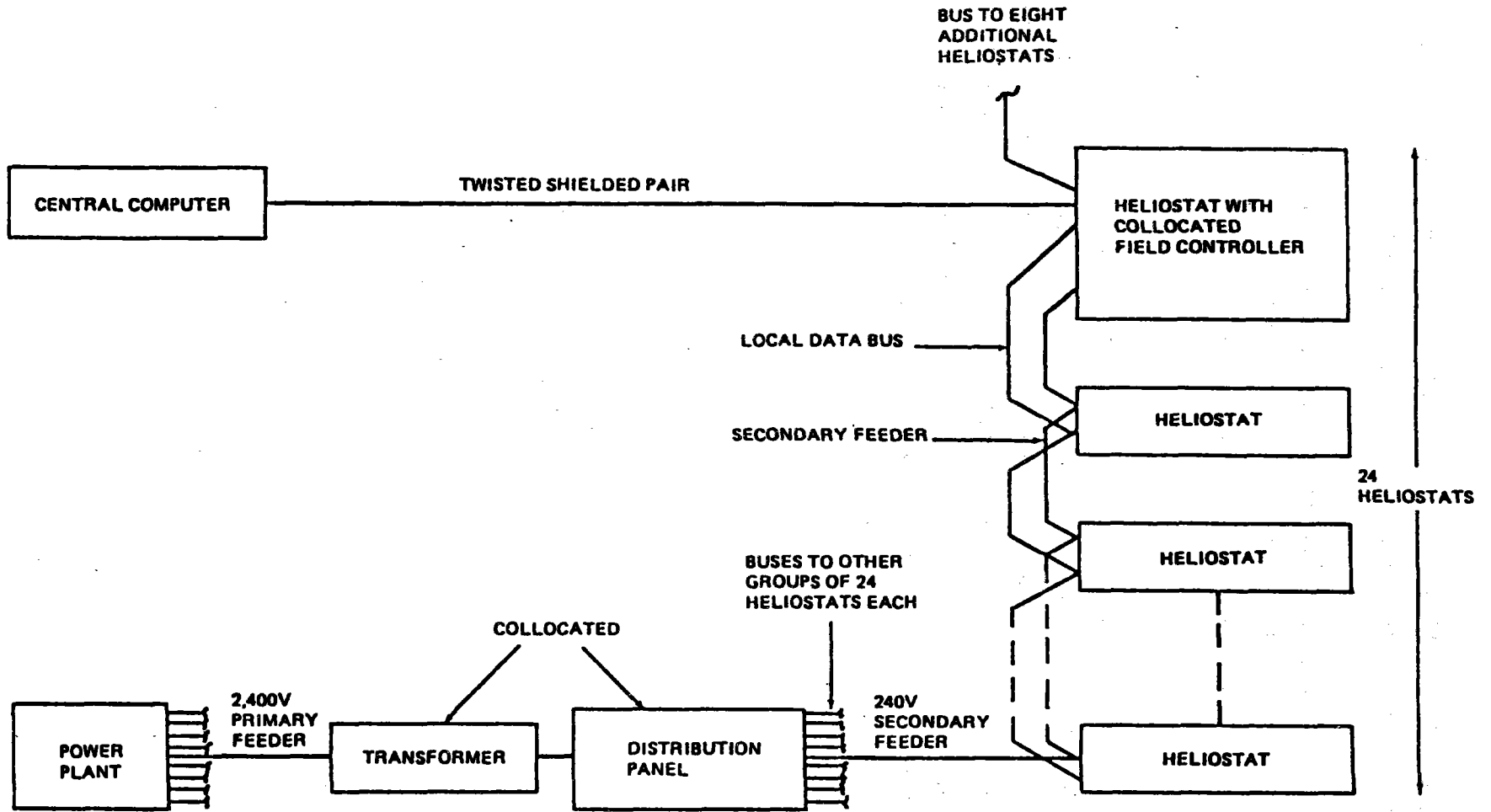


Figure A-2 Branch-Collector Field Network

APPENDIX B

PERFORMANCE AND DESIGN

REQUIREMENTS SUMMARY

APPENDIX B
PERFORMANCE AND DESIGN
REQUIREMENTS SUMMARY

The heliostat design is based on the performance and design requirements of RFP EG-77-R-03-1468, Specification 001. In general, these requirements are similar to those used in the Central Receiver Solar Thermal Power System, Phase 1 effort. The environmental exceptions are minor and include a lower maximum temperature, higher average rainfall, and additional specifications such as maximum 24-hour rainfall rate and hailstone specific gravity. The environmental conditions are summarized in Tables B-1 and B-2.

Environmental, design, and performance requirements of the specification have been used throughout the design effort, and in general, the initial and final baseline designs meet all of the requirements of Specification 001. It should be noted that the collector is able to continue to operate throughout the survival temperature range and up to the stowage initiation wind speed. The operational range is the range of conditions throughout which all performance specifications are to be met.

Table B-1
OPERATIONAL ENVIRONMENTAL CONDITIONS

| Environment | Requirement | | | | | | | | | | | | | | | | | | |
|----------------------------------|--|--------------------|----------------------|-----|----|-----|----|-----|----|-----|----|------|---|-------|---|-------|---|------|-----|
| Gravity | 1 g | | | | | | | | | | | | | | | | | | |
| Ambient Air Temperature | 0 to 50°C (32 to 120°F) | | | | | | | | | | | | | | | | | | |
| Winds: | | | | | | | | | | | | | | | | | | | |
| 1. Wind Speed | 0 to 11.6 m/s (26 mph) includes 1.3 gust factor. | | | | | | | | | | | | | | | | | | |
| 2. Wind Speed Frequency | <table style="margin-left: auto; margin-right: auto;"> <thead> <tr> <th style="text-align: center;"><u>Speed (m/s)</u></th> <th style="text-align: center;"><u>Frequency (%)</u></th> </tr> </thead> <tbody> <tr><td style="text-align: center;">0-2</td><td style="text-align: center;">29</td></tr> <tr><td style="text-align: center;">2-4</td><td style="text-align: center;">21</td></tr> <tr><td style="text-align: center;">4-6</td><td style="text-align: center;">19</td></tr> <tr><td style="text-align: center;">6-8</td><td style="text-align: center;">14</td></tr> <tr><td style="text-align: center;">8-10</td><td style="text-align: center;">8</td></tr> <tr><td style="text-align: center;">10-12</td><td style="text-align: center;">5</td></tr> <tr><td style="text-align: center;">12-14</td><td style="text-align: center;">3</td></tr> <tr><td style="text-align: center;">> 14</td><td style="text-align: center;">< 1</td></tr> </tbody> </table> | <u>Speed (m/s)</u> | <u>Frequency (%)</u> | 0-2 | 29 | 2-4 | 21 | 4-6 | 19 | 6-8 | 14 | 8-10 | 8 | 10-12 | 5 | 12-14 | 3 | > 14 | < 1 |
| <u>Speed (m/s)</u> | <u>Frequency (%)</u> | | | | | | | | | | | | | | | | | | |
| 0-2 | 29 | | | | | | | | | | | | | | | | | | |
| 2-4 | 21 | | | | | | | | | | | | | | | | | | |
| 4-6 | 19 | | | | | | | | | | | | | | | | | | |
| 6-8 | 14 | | | | | | | | | | | | | | | | | | |
| 8-10 | 8 | | | | | | | | | | | | | | | | | | |
| 10-12 | 5 | | | | | | | | | | | | | | | | | | |
| 12-14 | 3 | | | | | | | | | | | | | | | | | | |
| > 14 | < 1 | | | | | | | | | | | | | | | | | | |
| 3. Stowage Initiation Speed | 16.1 m/s (36 mph) | | | | | | | | | | | | | | | | | | |
| 4. Wind Rise Rate During Stowage | 0.01 m/s ² (1.3 mph/min). Heliostat shall withstand, without catastrophic failure, a maximum wind of 22.4 m/s (50 mph) from any direction. | | | | | | | | | | | | | | | | | | |
| 5. Wind Profile | <p>Use Power Law Velocity Profile:</p> $V_Z = V_{10m} \left(\frac{Z}{10m} \right)^{0.15}$ <p>where:</p> <p>V_Z = mean wind velocity at height Z</p> <p>V_{10m} = reference wind velocity at height of 10 m</p> <p>0.15 = power law exponent for flat open country</p> | | | | | | | | | | | | | | | | | | |

Table B-2
SURVIVAL ENVIRONMENTAL CONDITIONS

| Environment | Requirement |
|---|---|
| Gravity | 1 g |
| Ambient Air Temperature | -30 to 50°C (-22 to 120°F) |
| Winds: | |
| 1. Maximum Wind Speed Stowed | 40.2 m/s (90 mph) with ± 10 deg angle of attack |
| 2. Align Elevation Axis with Mean Wind Vector | For γ = angle from elevation axis: $\gamma = \pm 26$ deg No Damage Any γ No Catastrophic Failures |
| 3. Wind Profile | Use Power Law Velocity Profile: $V_Z = V_{10m} \left(\frac{Z}{10m}\right)^{0.15}$ |
| Earthquake | Seismic zone 3 (Uniform Building Code) |
| Snow/Ice | 250 Pa (5 psf) snow load 50 mm (2 in.) ice load |
| Hail | Specific Gravity ≤ 0.9 Survive at any orientation: 20 mm (3/4 in.) at 20 m/s (65 ft/s) Survive at stowed position: 25 mm (1 in.) at 23 m/s (75 ft/s) |
| Rain | Average annual rainfall - 750 mm (30 in.). Maximum 24 hour rate 75 mm (3 in.) |
| Dust Devils | With wind speeds up to 17 m/s (40 mph) |
| Sand Storm | Survive tests per MIL-STD-810B, Method 510. |
| Lightning | Protection provided on an optimized cost/risk basis |

APPENDIX C

HELIOSTAT SIZING ANALYSES:

FOCUSED VERSUS UNFOCUSED

The effects of reflector size and focusing versus nonfocusing were determined using the MDAC CONCEN computer program. Results are given below.

The effect of mirror panel size on performance was determined using CONCEN, with and without certain key errors included, for both a pilot plant and a commercial array. The results indicate that the difference in plant performance due to increased mirror size is negligible.

Table C-1 compares the fractional spillage between the initial and final baseline heliostats, and shows that for a typical condition (December 21), the total power at the receiver is the same to within less than one percent for either errors included or neglected.

In order to indicate the magnitude of the effect of focusing prototype heliostats in a commercial-size array, two extreme cases were run using the CONCEN programs for spring equinox, summer solstice, and winter solstice. For one case, all heliostats were flat, representing the nonfocused condition. In the other case, each heliostat is focused by panel canting and single curvature for its particular slant range to the receiver. Spherical focusing was used throughout. In order to isolate the effect of focusing, no errors were assumed. The pertinent system parameters assumed were:

Tower height = 250 m
Receiver diameter = 17 m
Receiver height = 25 m
Array width = 2300 m
Total number of heliostats = 27012*
Type of array = cornfield (N-S, E-W)
Heliostat size = 7.4 m x 7.3 m

The total incident energy in the vicinity of the receiver, the total received energy (that which is intercepted by the receiver), and the percentage spillage are given in Table C-2.

*The number of heliostats used for this comparison is not representative of 100 MW commercial system, but the impact of focusing on spillage is valid.

Table C-1

BASELINE SYSTEM (408 FT² HELIOSTAT)

| | <u>Total Incident Power</u> | <u>Total Received Power</u> | <u>Fractional Spillage</u> |
|-----------------|---------------------------------|---------------------------------|--------------------------------|
| No errors | 37.178 MW | 37.133 MW | .0012 |
| Errors included | 36.979 MW | 36.225 MW | .0204 |

FINAL BASELINE HELIOSTAT SYSTEM (528 FT² HELIOSTAT)

| | | | |
|-----------------|-----------|-----------|-------|
| No errors | 36.653 MW | 36.645 MW | .0002 |
| Errors included | 36.528 MW | 35.797 MW | .0200 |

System parameter values:

Receiver diameter = 6.92 m ($\leq 60^\circ$ incidence on 8 m dia.)

Receiver height = 14 m

Tower height = 88 m (center of heliostat to center of receiver)

Date = December 21; hour = 1400

Atmosphere = 23 km visibility

No errors: Temp. = 70°F; Wind = 0; no gravity loading; waviness = 0

With errors: Temp. = 32°F; Wind = \approx 26 mph; Gravity = 1 g.; waviness =
1.1 mr, 1σ

Pointing error: Horizontal = 3.4 mr; vertical = 1.7 mr, 1σ

Each heliostat focused by canting and cylindrical curvature for its
location

Table C-2

ENERGY SPILLAGE ASSESSMENT

| | <u>Total Incident Energy (MWhr)</u> | <u>Total Received Energy (MWhr)</u> | <u>% Spillage</u> |
|--------------------|---|---|-----------------------|
| <u>March 21</u> | | | |
| Focused | 6298.5 | 6298.3 | .003 |
| Unfocused | 6298.5 | 6282.1 | .26 |
| <u>June 21 -</u> | | | |
| Focused | 7561.8 | 7561.3 | .007 |
| Unfocused | 7561.8 | 7546.2 | .21 |
| <u>December 21</u> | | | |
| Focused | 4996.8 | 4996.7 | .002 |
| Unfocused | 4996.8 | 4981.5 | .31 |

*The number of heliostats used for this comparison is not representative of 100 MW commercial system, but the impact of focusing on spillage is valid.

For the unfocused cases the spillage is primarily contributed by the outer region ($\sim 1.5\%$) and by the inner heliostats ($\sim 1.1\%$), with those inbetween contributing a negligible amount. An intermediate focus condition, such as two or three fixed focus settings, is expected to show spillage performance essentially equal to that with individual focusing. These results indicate that canting and/or focusing for the commercial array is hardly justified.

APPENDIX D
SUMMARY OF SUPPORTING LABORATORY
AND MANUFACTURING PROCESS TESTS

A series of tests was conducted to obtain data for support of design trade studies to select the mirror module. Tests included salt spray, hail, flatness, and thermal cycling. Tests were also conducted to evaluate methods for producing low cost laminated mirrors.

Environmental tests were conducted on 27 small coupons 12.7 cm square (5-inch) and six specimens 0.76 by 1.22 m (30 by 38 inches). Salt spray tests were performed to determine the relative durability of various mirror backings and low-cost glass laminates. Coupons tested incorporated numerous types of mirror backings and edge treatments. Hail tests were performed on three panel designs to establish their ability to survive when exposed to a severe hail storm.

Thermal cycling tests were performed to evaluate the cumulative effects of high and low temperatures on the panels. Temperature and strain measurements were recorded and the resulting stresses were evaluated. Pre- and post-test flatness measurements were made to determine any permanent deformation/warping induced by the thermal cycling.

Production development tests were conducted on glass laminates using various methods of adhesive application and pressure devices, including pressure rollers, presses, and vacuum pressure.

D.1 SALT SPRAY TESTS

Coupons were arranged in slotted plastic trays and positioned in the chamber at a 60-degree angle from the horizontal with the coated side of the mirrors facing upwards. A 5-percent salt solution was used. Table D-1 describes the coupons tested, specifies hours tested, and rates the degradation. Detailed descriptions of the small coupons and discussions of the results of the salt spray tests are expanded below.

A1a through A1d -- Four 12.7-cm (5-inch) square mirrors were cut from "as delivered" 3.2-mm (1/8-inch) float glass mirrors with chemically deposited silver, flash-copper-coating and Glidden gray mirror backing paint. The mirrors did not show any visible degradation after 262 hours of exposure. Coupons A1c and A1d were returned to the chamber and then removed after an additional 72 hours (334 hours total) of exposure. Some minimal edge penetration was evident for specimen A1c as shown in Figure D-1.

Table D-1
SALT SPRAY COUPON TEST RESULTS

| Number | Type | Hours | Degradation |
|--------|--|-------|----------------------|
| A1a | Glidden Gray Mirror Backing Paint | 262 | None |
| A1b | " " " " " | 262 | None |
| A1c | " " " " " | 334 | Minimal |
| A1d | " " " " " | 334 | Minimal |
| A2a | Glidden White Acrylic Mirror Backing Paint | 209 | Slight |
| A2b | " " " " " " | 209 | " |
| A2c | " " " " " " | 209 | " |
| A2d | " " " " " " | 209 | " |
| A3a | Glidden Gray Plus High Reflectance White Paint | 257 | None |
| A3b | " " " " " " " | 257 | " |
| A3c | " " " " " " " | 257 | " |
| A3d | " " " " " " " | 257 | " |
| A4a | Same as A3a Plus Adhesive Bonded Steel Tab | 257 | None |
| A4b | " " " " " " " | 257 | " |
| A4c | " " " " " " " | 257 | " |
| A4d | " " " " " " " | 257 | " |
| C1a | Laminated Mirror With Backing Paint and Interior Transparent Adhesive | 219 | None |
| C1b | " " " " " " " | 219 | " |
| C1c | " " " " " " " | 219 | " |
| C1d | " " " " " " " | 219 | " |
| C2a | Laminated Mirror Backing Paint Removed With Interior Transparent Adhesive | 219 | Slight (Sealed Edge) |
| C2b | " " " " " " " | 219 | Severe (Cut Edge) |
| C2c | " " " " " " " | 219 | Slight (Sealed Edge) |
| C2d | " " " " " " " | 219 | Severe (Cut Edge) |
| - | Non-Laminated Mirrors With Backing Paint Removed With Interior Reflective Adhesive | 257 | Severe |

D-3

D-4

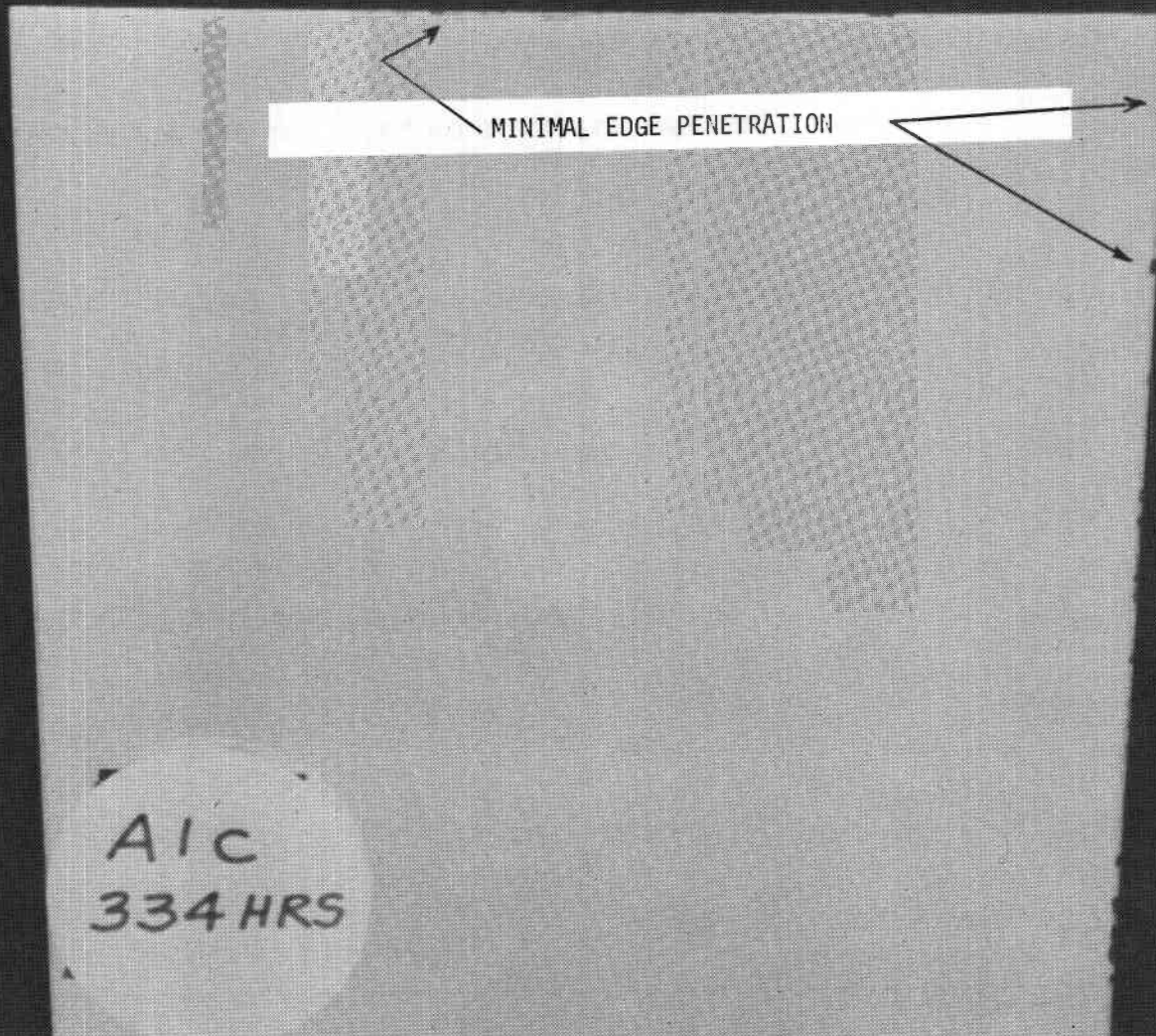


Figure D-1

Salt Spray Coupon Alc with Glidden Gray Backing Paint

D-5

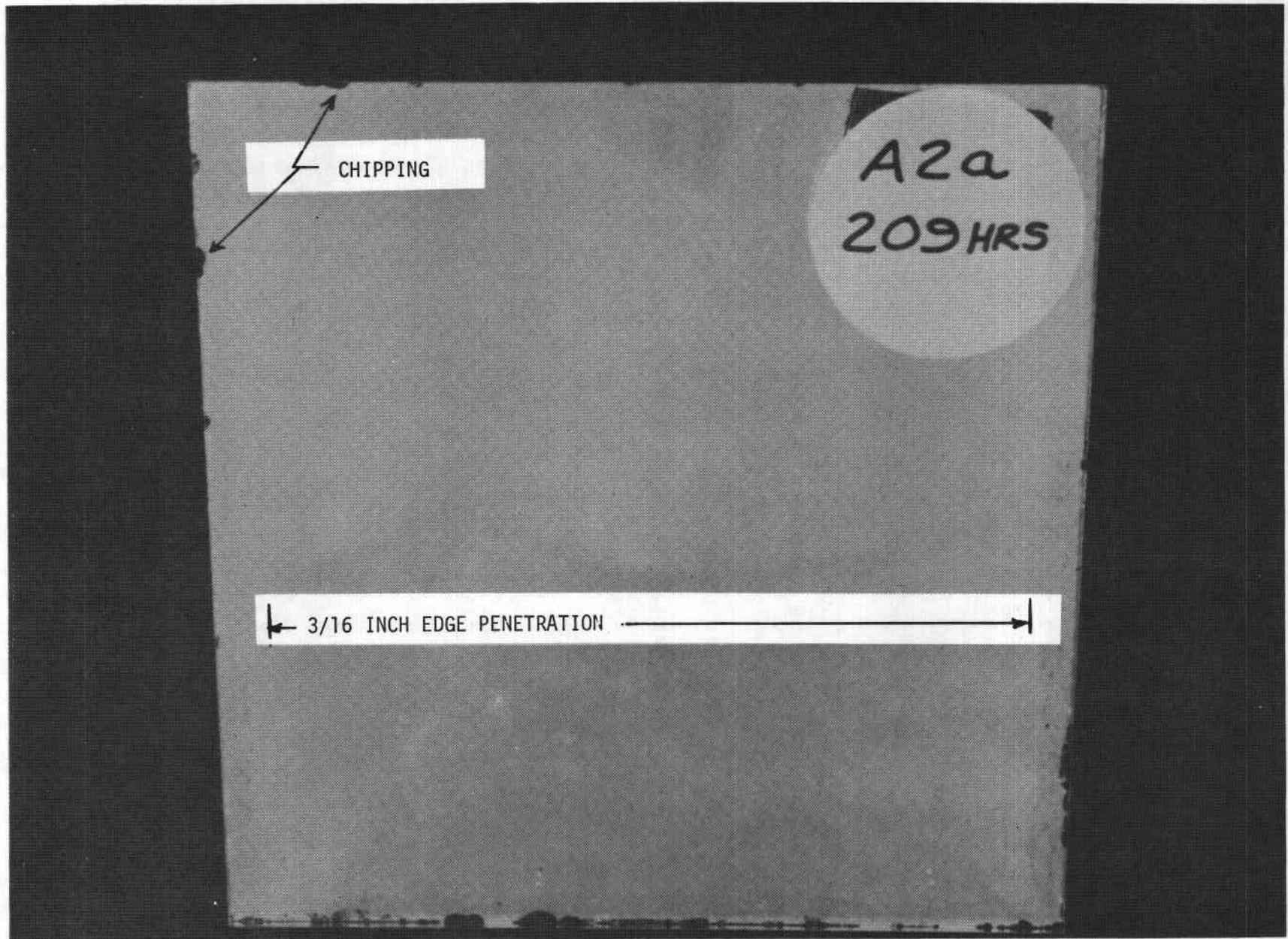


Figure D-2

Salt Spray Coupon A2a with Glidden White Acrylic Backing Paint

was evident, as shown in Figure D-1 for specimen Alc.

A2a through A2d -- Four 12.7-cm (5-inch) square mirrors were cut from "as delivered" 3.2-mm (1/8-inch) ASG Sheet glass mirror with Glidden white acrylic backing paint. An exposure of 209 hours caused edge penetration of 5 mm (3/16 inch) and chipping as shown in Figure D-2.

A3a through A3d -- These mirrors were identical to the mirrors A1a through A1d except they were sprayed with No. 6 high-reflectance white paint manufactured by Triangle Paint Company. There was no degradation noted after 257 hours of exposure. These laminates would not reach as high a temperature as those with the gray paint under backlighting conditions.

A4a through A4d -- This configuration utilized the same mirror specified for A3a with a galvanized steel tab bonded to it with 3M 3535 adhesive. The tab is shown in Figure D-3 after 257 hours exposure. The mirror showed no deleterious effects.

C1a through C1d -- All four mirrors were the type described for A1a with Glidden gray backing paint. An adhesive (3M 3535) was applied by spatula to the mirrors and a 3.2-mm (1/8-inch) thick piece of float glass was attached to it. Coupons C1a and C1b were made with Ford glass and C1c and C1d were made with Pittsburgh Plate glass. The edges of C1b and C1c were sealed. After 219 hours of exposure, no degradation was noted.

C2a through C2d -- These mirrors were the same as C1a except the Glidden gray backing paint was removed and the adhesive was applied directly to the bare copper. Coupons C2a and C2b were made with Ford glass and C2c and C2d from Pittsburgh Plate glass. C2a and C2c were made with sealed edges while the edges of C2b and C2d were cut. Edge sealing made considerable difference in edge degradation as shown in the photographs for coupons C2a and C2d (Figures D-4 and D-5). Severe degradation occurred when edges were not sealed while only slight penetration occurred with sealed edges. Close examination disclosed that minute pin holes in the sealed edge allowed seepage through the adhesive. If the adhesive were applied evenly, rather than with ridges as shown in C2d, and the edges were well sealed, this configuration could be expected to survive the salt spray environment.

D-7

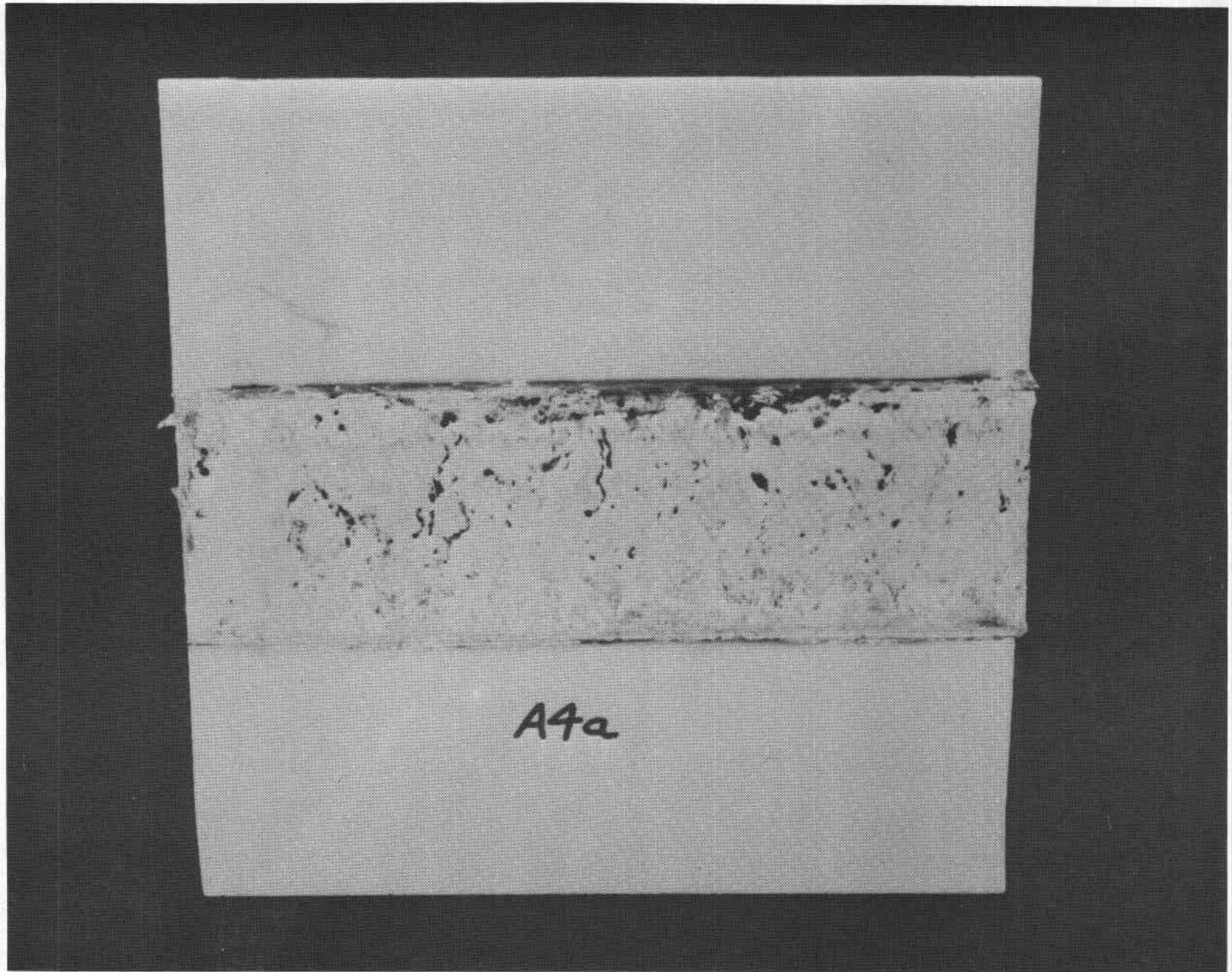


Figure D-3 Salt Spray Coupon A4a with Galvanized Steel Tab

D-8

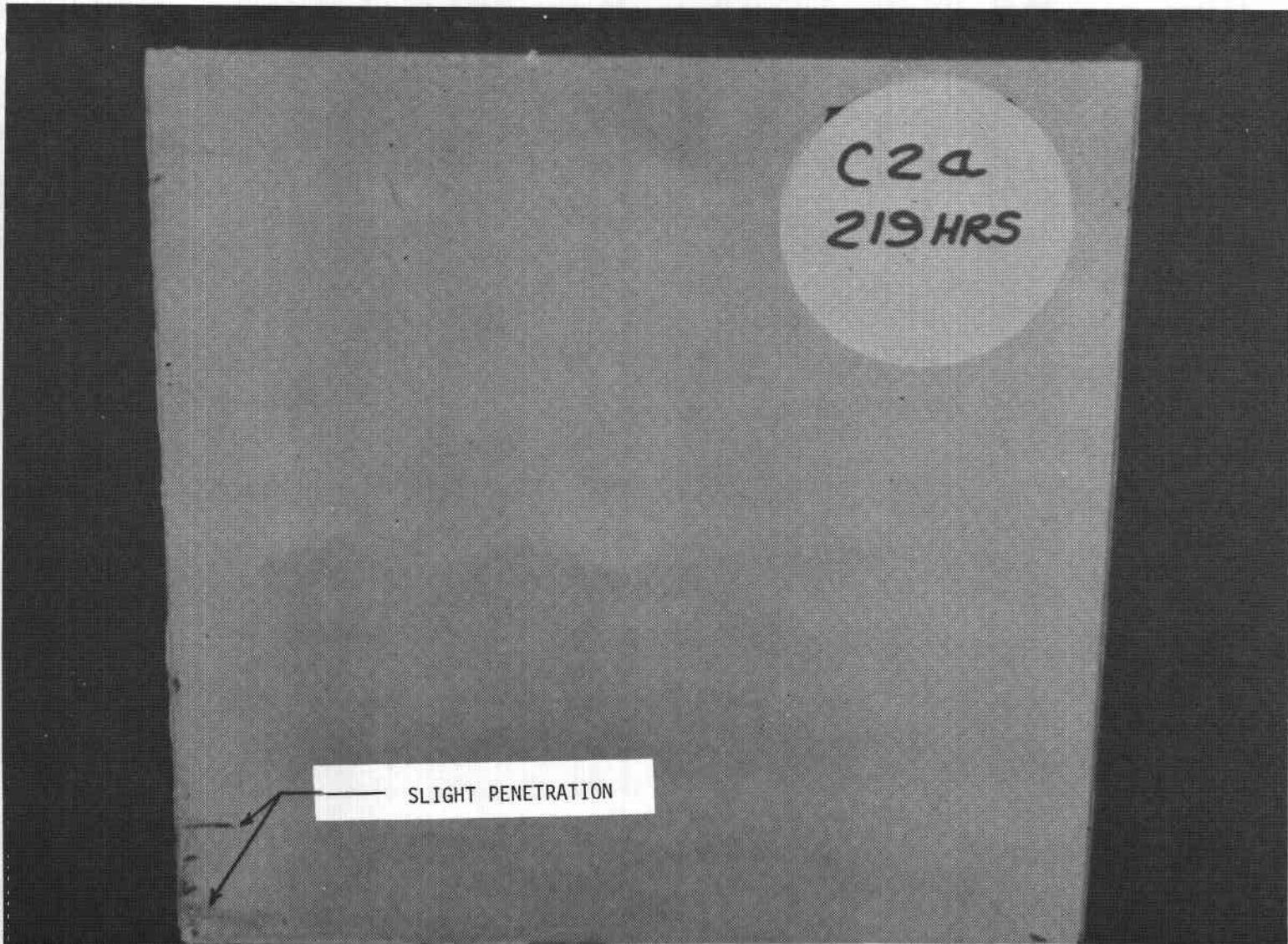


Figure D-4 Salt Spray Coupon C2a Laminated with Sealed Edge

D-9



Figure D-5 Salt Spray Coupon C2d Laminated with Cut Edge

D-10

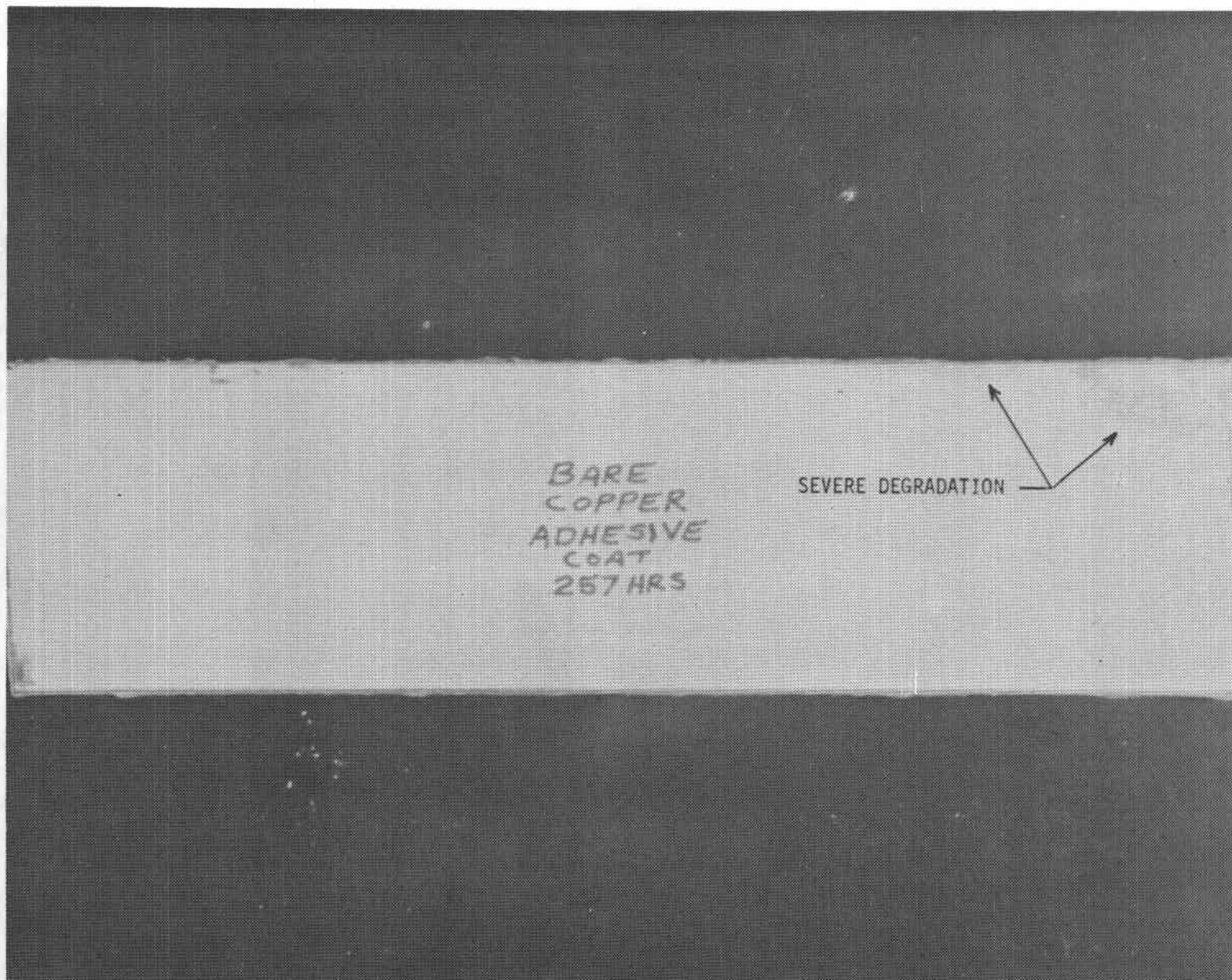


Figure D-6 Salt Spray Coupon with Interior Reflective Adhesive

Several additional mirrors were prepared by removing the backing paint and applying the adhesive directly to the bare copper, but glass was not laminated to it. Figure D-6 shows regions of severe degradation after 257 hours of exposure, even though the edges were sealed.

In conclusion, the mirrors covered with Glidden gray and those with Glidden gray plus high-reflectance white survived the salt spray test far better than the other candidates. However, mirrors covered with adhesive applied directly over bare copper should not be ruled out. The adhesive seems to provide adequate protection where properly applied. Tests evaluating various application techniques of adhesive and edge sealing techniques should be performed before final conclusions are drawn.

D.2 HAIL IMPACT TESTS

Three candidate designs were tested for hail survivability. The mirrors were impacted six times with hail stones having 19-mm (0.75-inch) and 25-mm (1-inch) diameters at velocities of 20 m/s (65 ft/sec) and 23 m/s (75 ft/sec), respectively.

The simulated hail impact tests were conducted in the MDAC Experimental Stress Analysis Laboratory. A schematic diagram of the test setup is shown in Figure D-7. A hail stone was made by freezing water to the proper diameter using a special aluminum mold. The hail stone was then loaded into the launch tube. The manual valve was opened and the reservoir was pressurized to a predetermined value. The spring-driven valve was opened and the pressure was released, driving the hail stone down the launch tube to strike the target. The launch tube had two electric eyes located a known distance apart at the target end. The electric eyes were connected to a timing device. The time for the hail stone to travel this known distance was measured and the velocity was determined.

Test results are given in Table D-2.

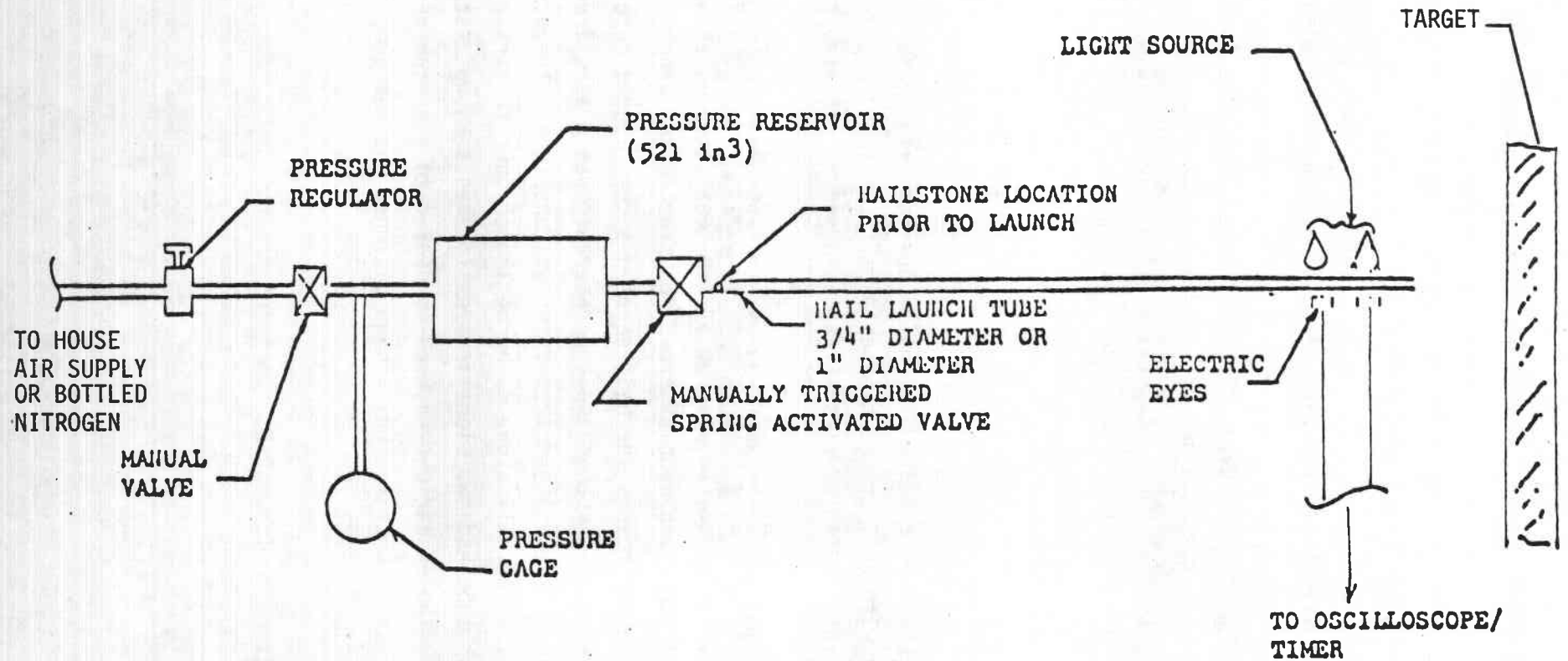


Figure D-7 Schematic of Hail Test Setup

TABLE D-2
HAIL IMPACT TEST RESULTS

| Panel | 19-mm (3/4-inch) diameter at 20 m/s (65 ft/sec) | 25-mm (1-inch) diameter at 23 m/s (75 ft/sec) |
|--|---|---|
| D1b 1/8-inch thick mirror supported with corrugated sections | No damage | Failed at corner |
| D2b 1/8-inch thick mirror supported with hat sections | Failed on edge | Failed on edge and corner |
| E1b 1/8-inch thick mirror laminated to 1/8-inch thick glass | No damage | No damage |

The panels tested and their failure points are discussed in the following paragraphs.

D1b: 3.2-mm (1/8-inch) Mirror Supported with Corrugated Sections -- This panel consisted of a 0.76 by 1.22-m (30 by 48-inch) float glass mirror 3.2-mm (1/8-inch) thick coated with Glidden gray backing paint with a 28-gauge corrugated stiffener bonded to the back side with 3M 3535 adhesive.

The panel was impacted a total of six times with 19-mm (3/4-inch) diameter hail stones at a velocity of 20 m/s (65 ft/sec) at four locations, as shown in Figure D-8.

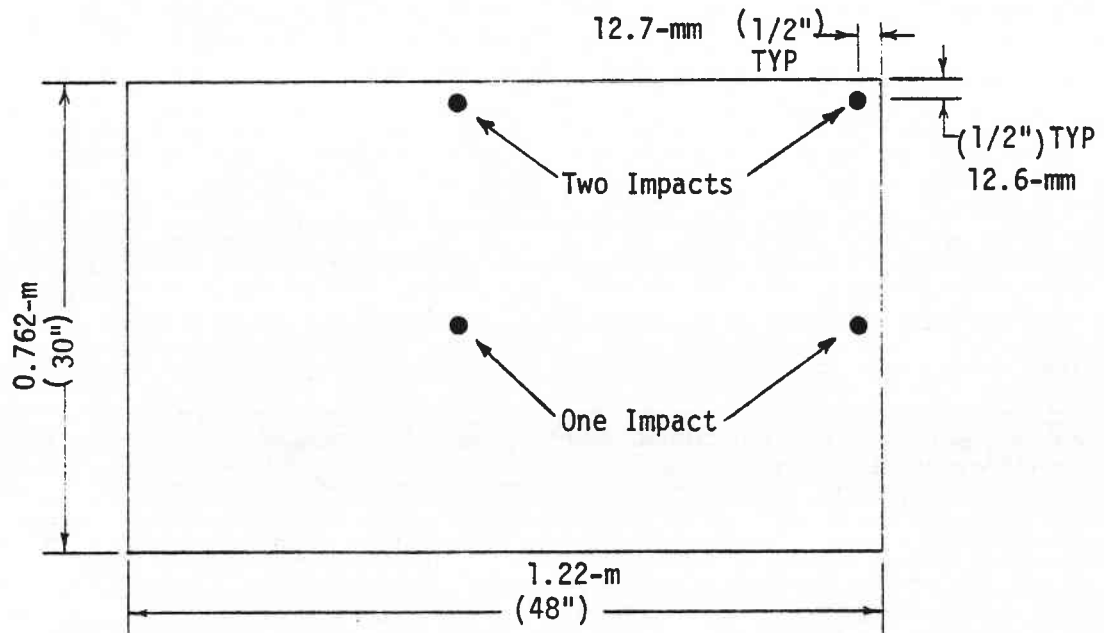


Figure D-8 Typical Hail Impact Locations

No fractures occurred. The test was repeated with 25-mm (1-inch) diameter hail stones at a velocity of 23 m/s (75 ft/sec) and a fracture occurred in the corner after the second impact (See Figure D-9).

D2b: 3.2-mm (1/8-inch) Mirror Supported with Four Hat Sections -- This panel incorporated the same size and type of mirror as D1b. Four 20-gauge hat stiffeners were bonded to the back side with 3M 3535 adhesive.

A failure in the edge of this panel resulted from the first impact with a 19-mm (3/4-inch) diameter hail stone traveling at 20 m/s (65 ft/sec); see Figure D-10. It survived four other shots. The opposite side of the panel and a corner of it fractured when hit with a 25-mm (1-inch) diameter hail stone at 23 m/s (75 ft/sec).

E1b: 3.2-mm (1/8-inch) Mirror Laminated to 3.2-mm (1/8-inch Thick Float Glass --

This panel was made from the same size and type of mirror as D1b. Stiffening was accomplished by laminating a piece of 3.2-mm (1/8-inch) float glass to

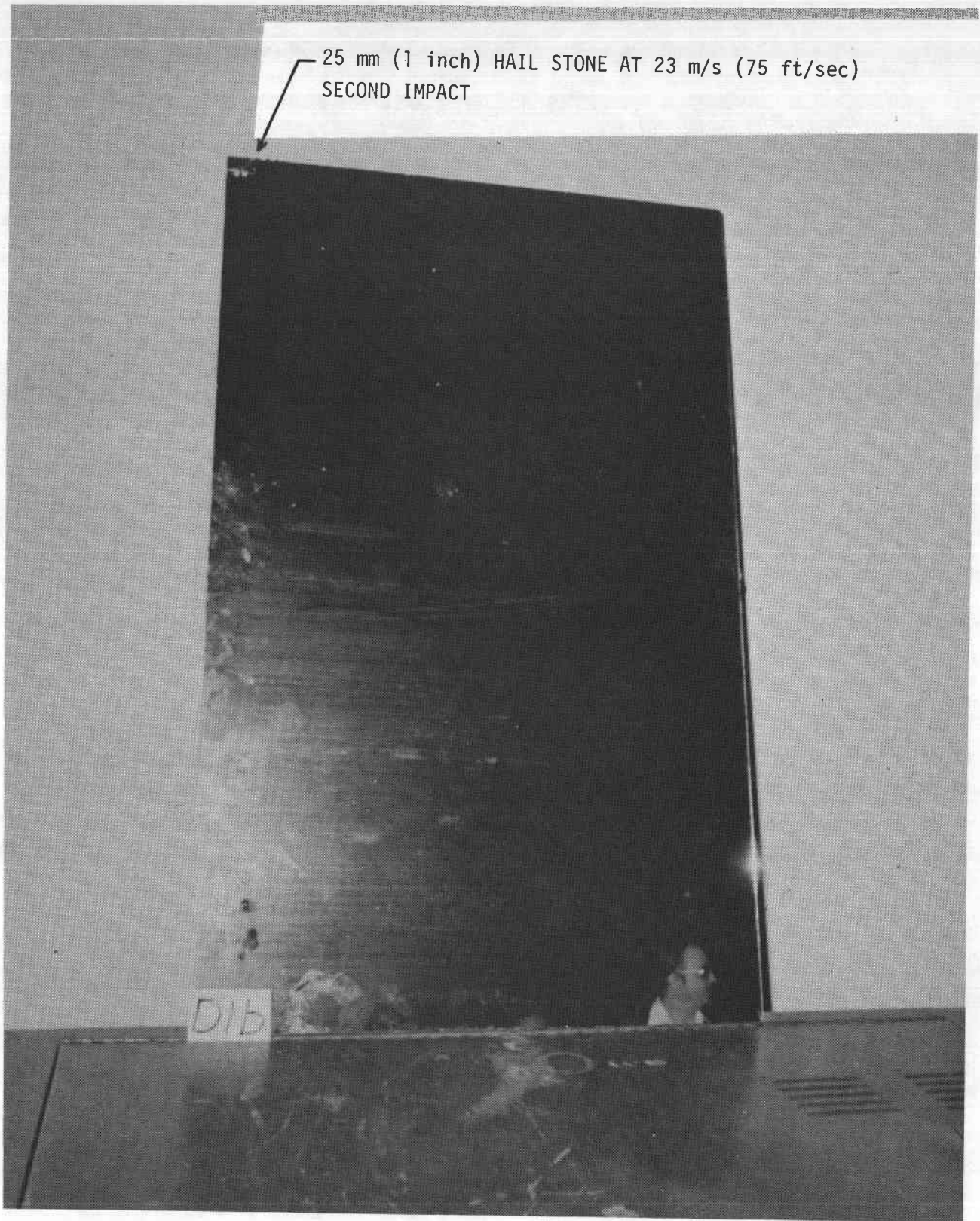


Figure D-8 Hail Impact Test Panel D1b

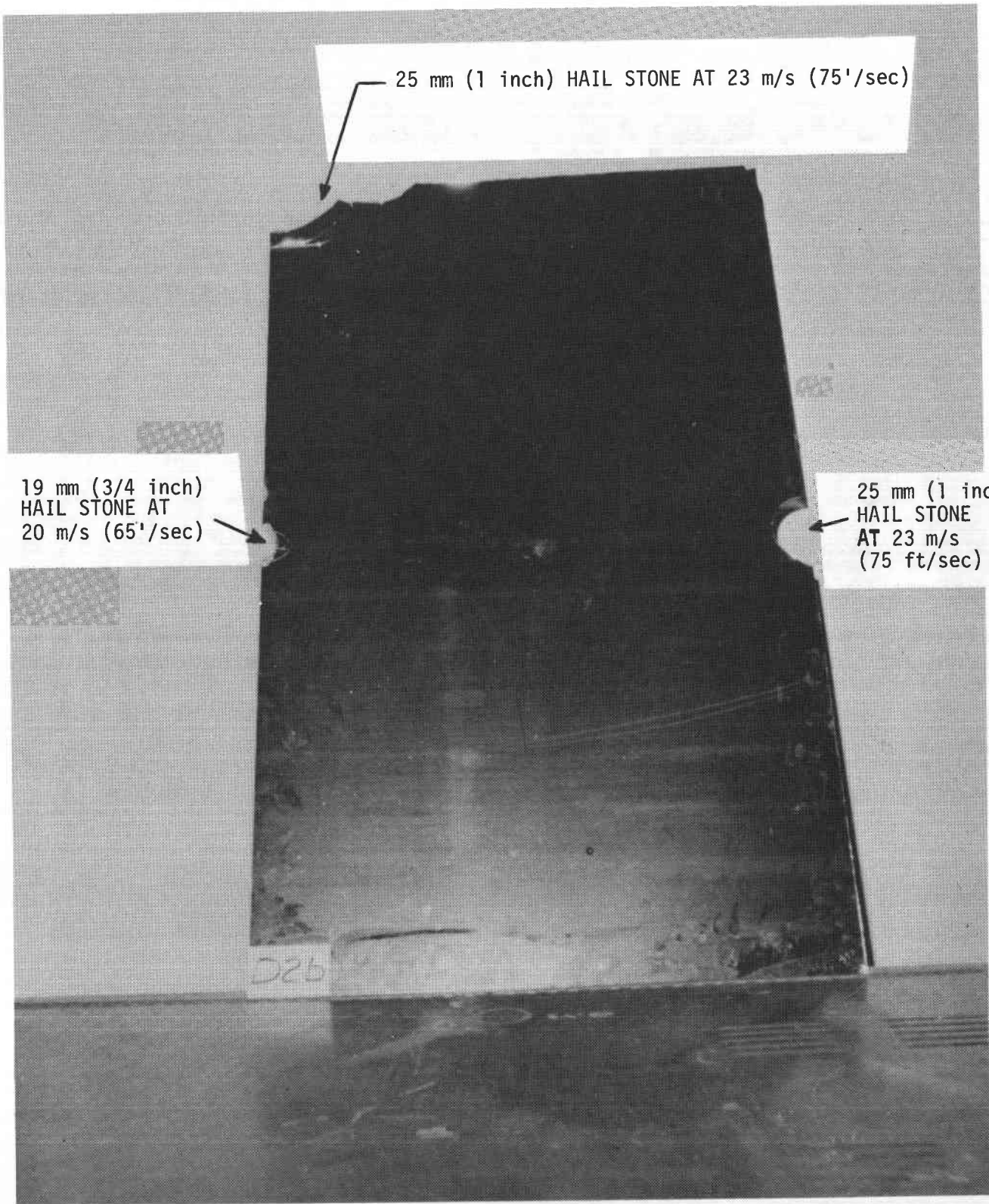


Figure D-9

Hail Impact Test Panel D2b

the back of the mirror using 3M 3535 polyurethane adhesive. Two 18-gauge hat stiffeners were then bonded to this low cost laminated mirror. No damage was noted on this panel from any of the hail impacts.

It may be concluded that the laminated panel is adequate for use in hail environments since this configuration survived all impacts. However, it should be noted that the impact with the 25-mm (1-inch) diameter hail stone at 23 m/s (75 ft/sec) is a requirement for the inverted position only. All panels were tested on the front side. It has not been demonstrated that the corrugated panel would fail if struck on the back side.

D.3 THERMAL CYCLING TESTS

Three panels identical to configurations D1b, D2b, and E1b were instrumented with strain gauges and thermocouples. The panels were all placed in a 1.83 by 1.83 by 1.22-m (6 by 6 by 4-foot) temperature/altitude chamber located in Structures Laboratory. They were subjected to 72 temperature cycles at a rate of approximately 4 hours per cycle reaching temperature extremes of -30°C (-22°F) and $+50^{\circ}\text{C}$ (120°F).

The chamber was set to cycle automatically by using an autocontroller which followed a cam profile. Typical chamber temperature profiles are shown in Figure D-10. A Brush recorder was used to record the individual panel temperatures versus the control thermocouple temperature. These data are shown in Figure D-11. Figure D-12 shows the relative position of the panels in the chamber and Figure D-13 shows the chamber controller and data acquisition system.

Four strain gauges and four thermocouples were placed on the laminated panel E1a. Three strain gauges and three thermocouples were placed on each of the other two panels. Strain gauge and thermocouple location and number designation are presented in Figure D-14.

Printouts show no strain in excess of $70 \mu \text{ in/in}$ (system accuracy within $\pm 5 \mu \text{ in/in}$). Typical stress levels for the three panels are presented below.

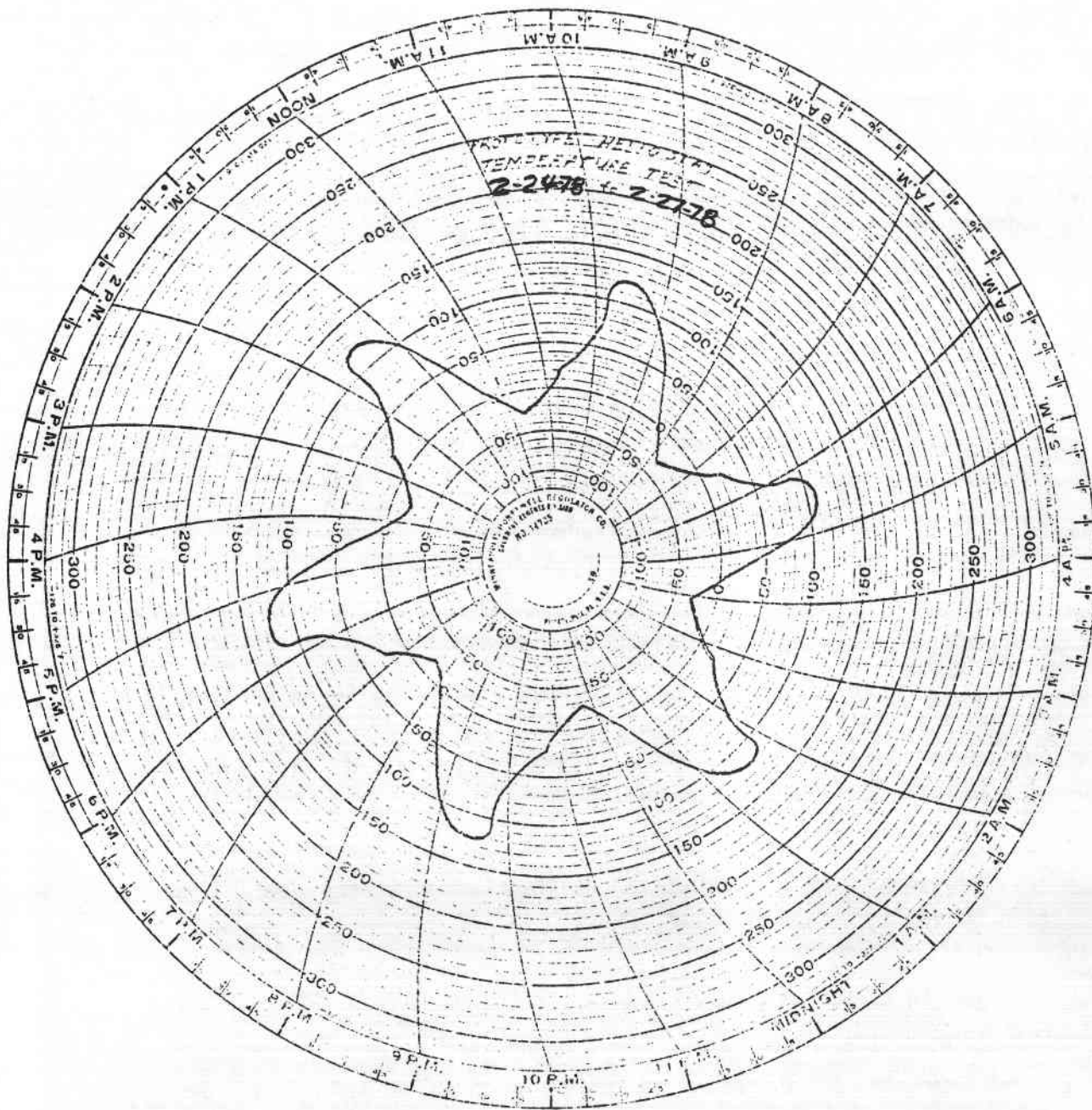


Figure D-10 Typical Chamber Temperature Profiles

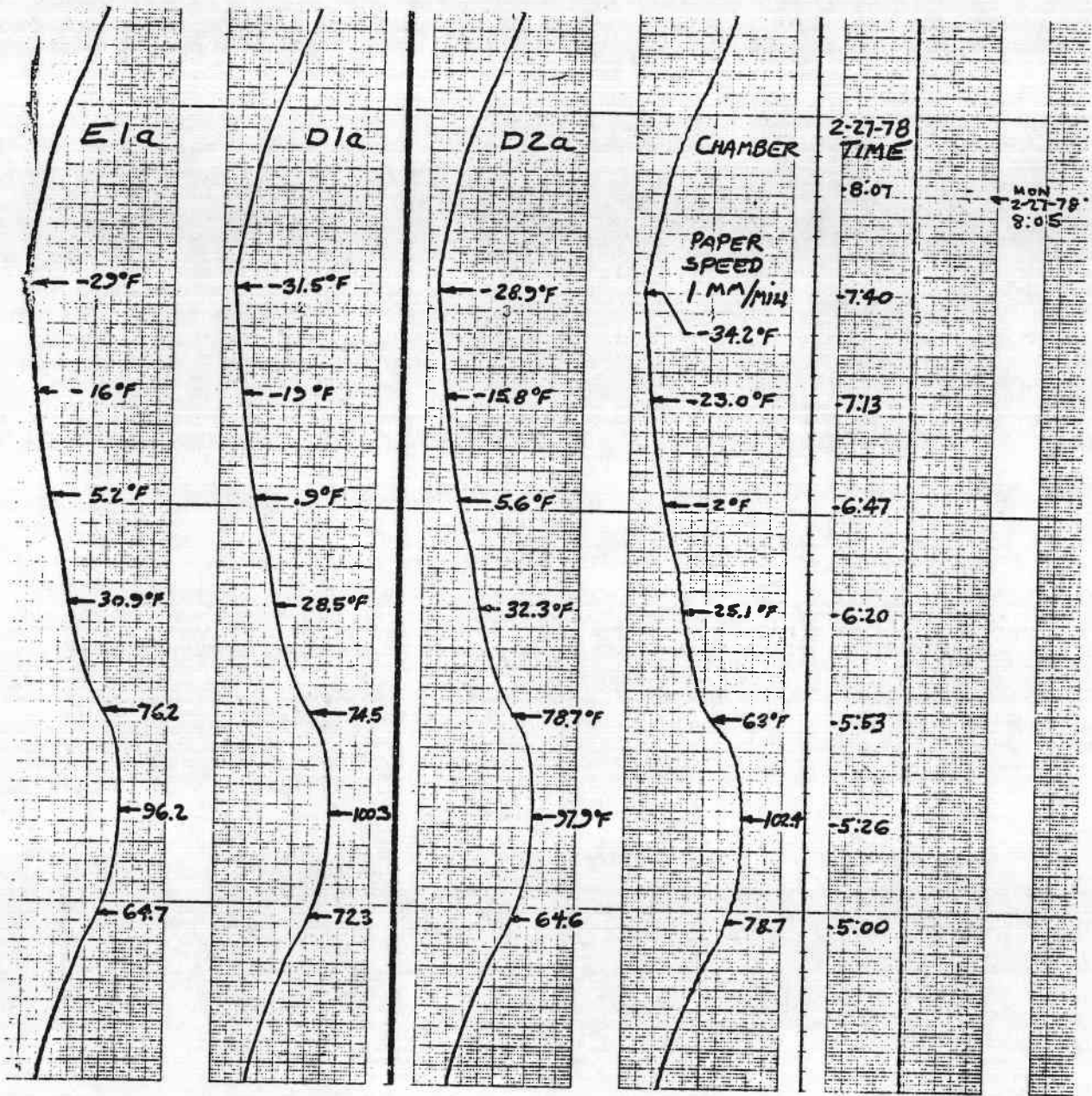


Figure D-11 Brush Recorder Printout

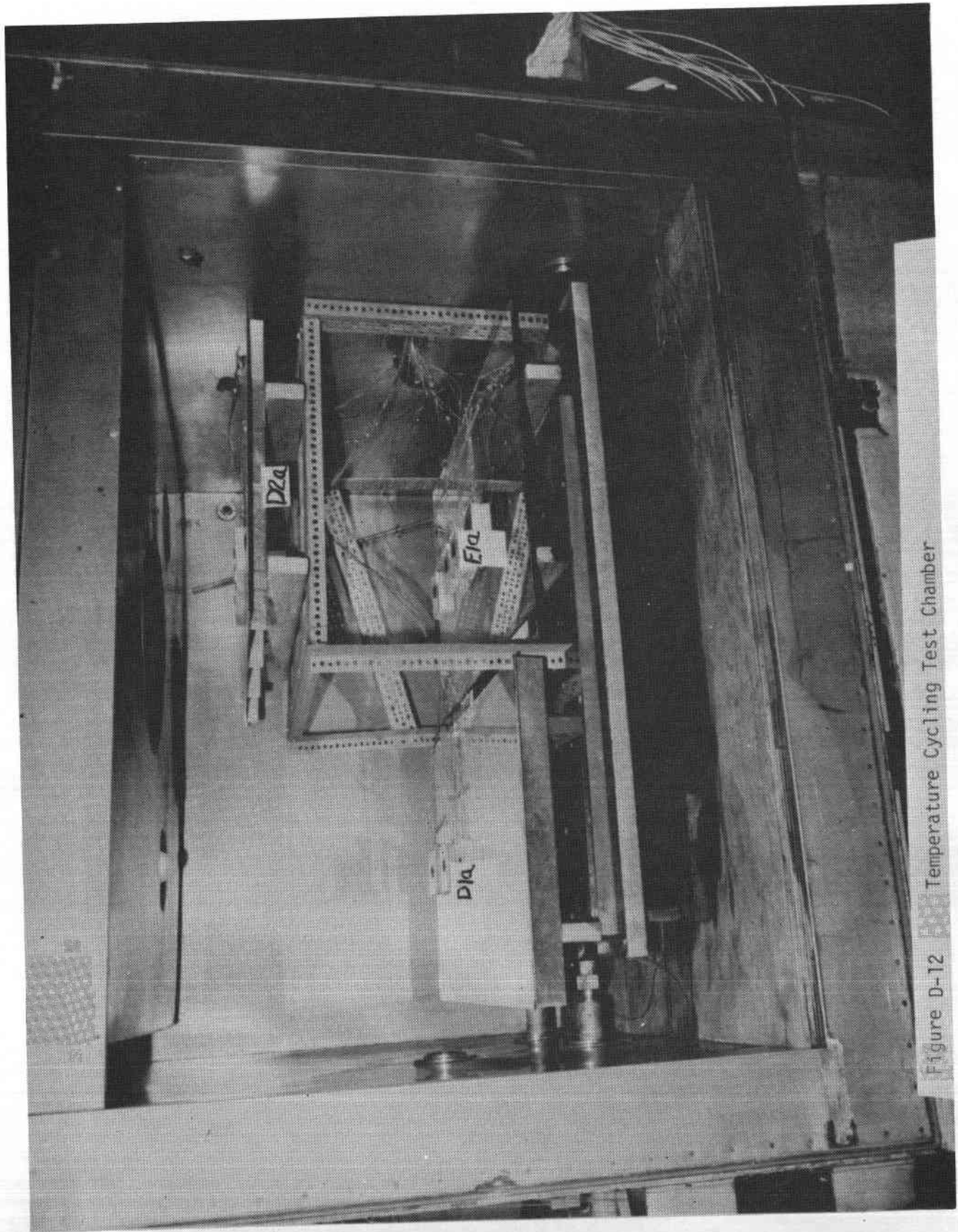
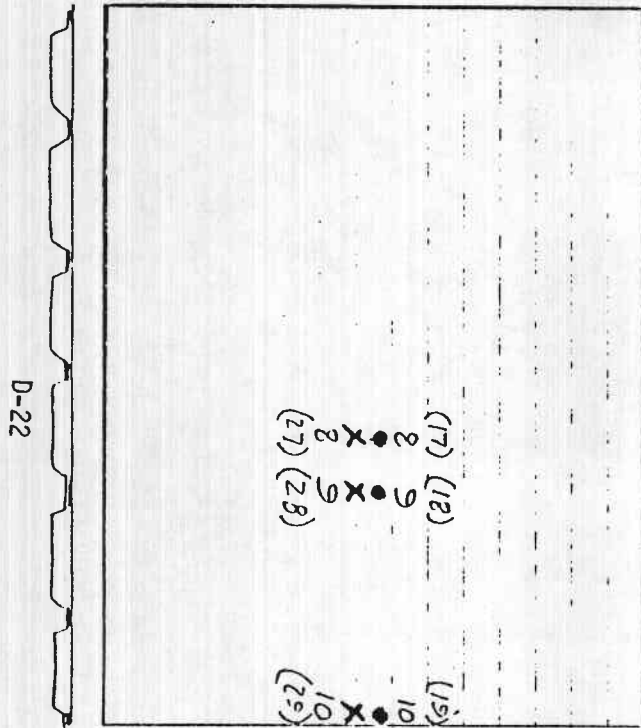


Figure D-12 Temperature Cycling Test Chamber

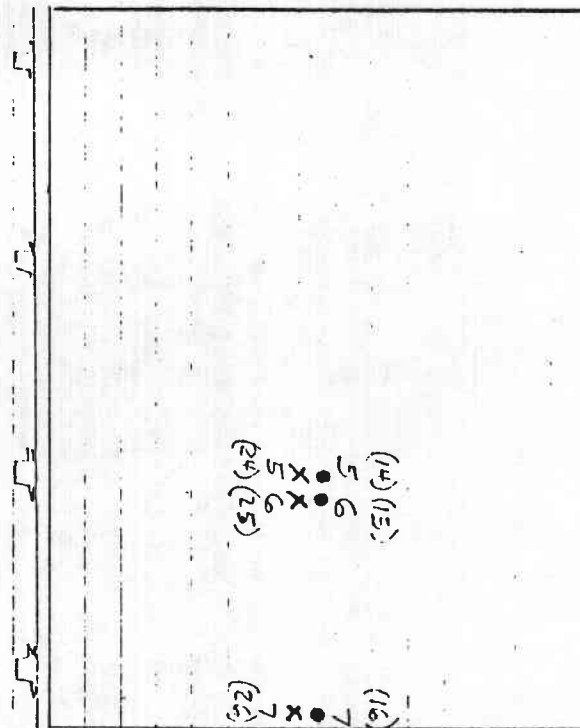


Figure D-13 Data Acquisition System

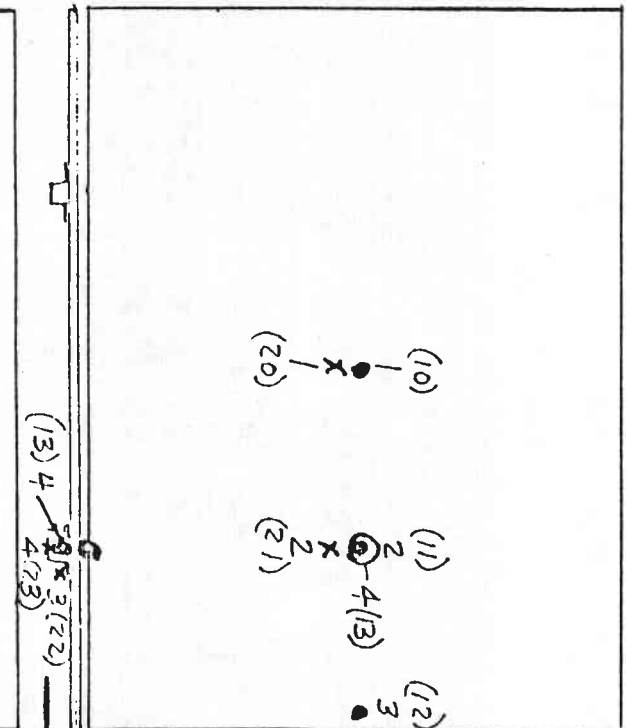
D1a
1T50945-1
CORRUGATED STIFFENER



D2a
1T50945-501
HAT STIFFENER

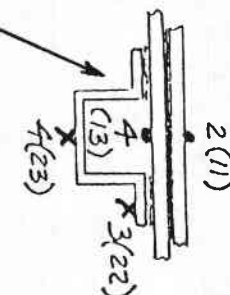


E1a
1T50946
LAMINATED



- STRAIN GAGE - UNIAXIAL
- x THERMOCOUPLE TYPE "T", CU/C
- () DORIC CHANNEL NO.

Figure D-14 Thermal Cycling -22°F to 120°F, 4 Hr/Cycle, 72 Cycles



D-23

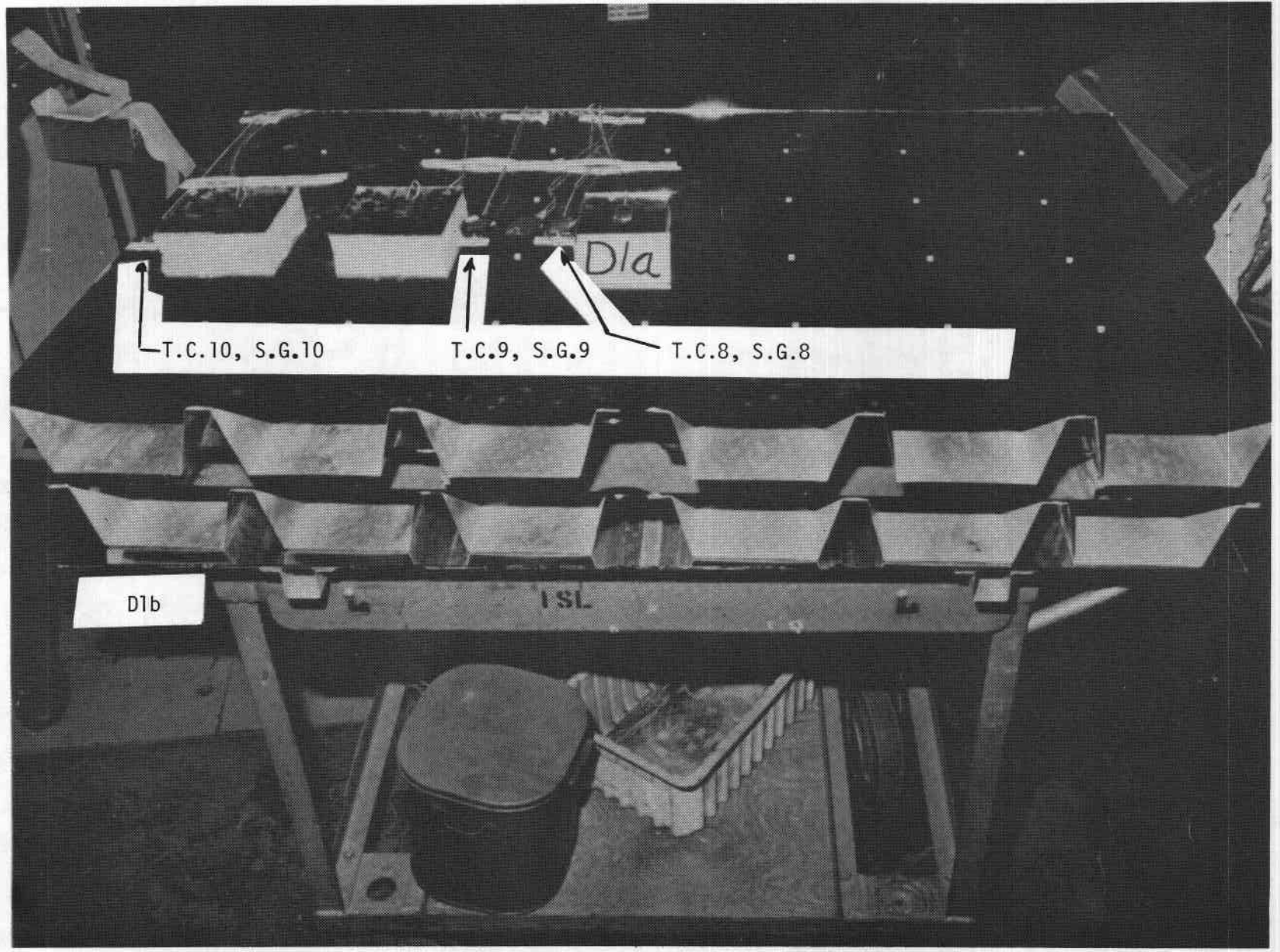


Figure D-15 Corrugated Stiffened Panels

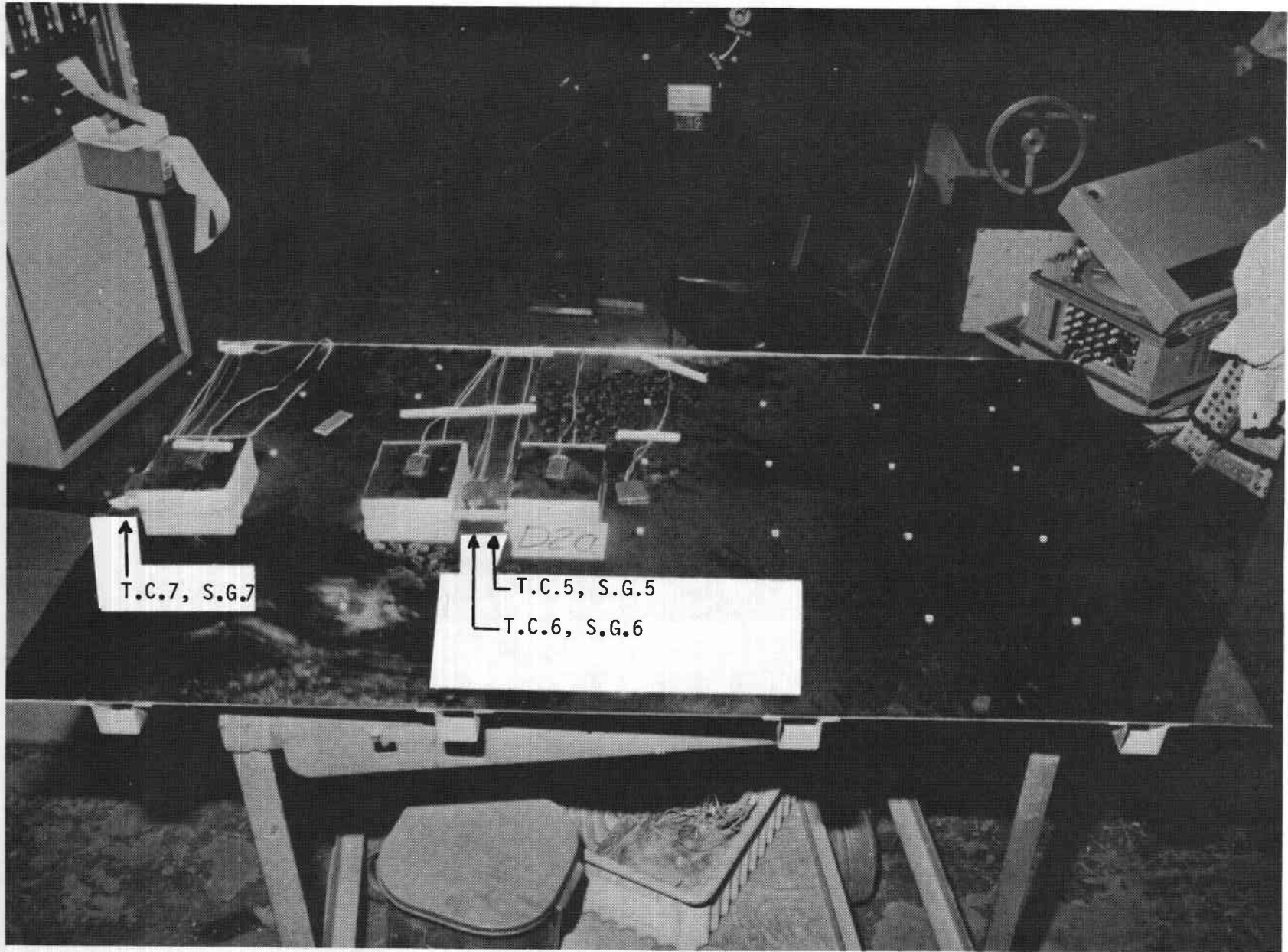


Figure D-16 Hat Stiffened Panel

D-25

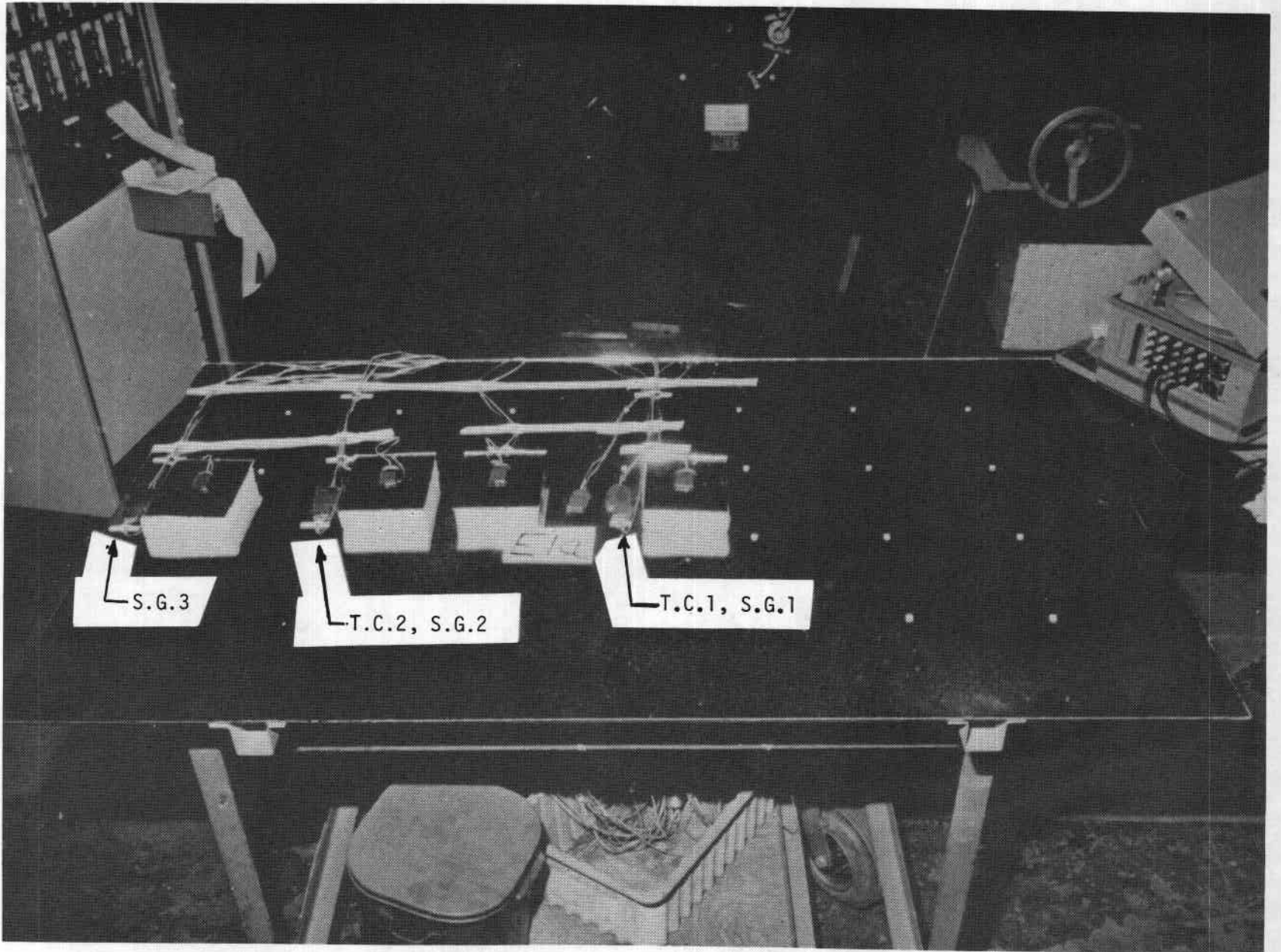


Figure D-17 Laminated Panel

At the conclusion of the thermal cycling tests, during which each of the three test panels was subjected to 72 cycles of temperature change, the panels were placed on a surface table and measured for flatness. Measurements were made at 28 points on a 0.15-m (6-inch) grid on the glass surface so each point was 15.24 cm (6 inches) from adjacent points. The measurements were then compared with those made at the same points before the thermal cycling began.

The maximum change in Panel D2a -- the specimen of 3.2-mm (1/8-inch) glass sheet reinforced with four hat section stiffeners of 20-gauge steel -- was 0.32 mm (0.0125 inch). Panel D1a, of 3.2-mm (1/8-inch) thick glass sheet reinforced with 28-gauge corrugated steel, showed a maximum change of 0.69-mm (0.027 inch). The laminated panel had a maximum change of 1.96-mm (0.077 inch).

These results indicated that the laminated panel showed the largest difference. However, these tests were somewhat inconclusive because the panels were not leveled at three points before and after the thermal cycling. It is recommended that additional permanent-deformation tests be performed.

| <u>Panel</u> | <u>Maximum Stresses</u> | | <u>Location</u> | <u>Temp</u> | |
|----------------|-------------------------|------------------|-----------------|-------------|-------------|
| | <u>Measured</u> | <u>Predicted</u> | | <u>°C</u> | <u>(°F)</u> |
| E1a laminated | -420 psi | -45 | S.G.3 | +45 | +113 |
| E1a laminated | +360 psi | +105 | S.G.3 | -34 | -30 |
| E1a laminated | -390 psi | -45 | S.G.2 | +45 | +113 |
| D1a corrugated | -680 psi | -444 | S.G.10 | -34 | -30 |
| D1a corrugated | +190 psi | +193 | S.G.10 | +45 | +113 |
| D2a hat | -460 psi | -77 | S.G.5 | -34 | -29 |
| D2a hat | +160 psi | +34 | S.G.5 | +44 | +112 |

Photographs of each of the panels with instrumentation locations are shown in Figures D-15 through D-17.

Because of the low strain levels and system noise, resolution is somewhat uncertain. However, it can be concluded that the magnitude of stresses are generally correct and acceptable. The stresses are somewhat higher than predicted. However, these differences are not considered to be significant because of the uncertainty in the readings.

D.4 BACKLIGHTING TESTS

Backlighting tests have not been conducted in this phase because of the unavailability of reflector components required to simulate the preferred-candidate low-cost fusion glass laminated reflector. The test specimens fabricated for the thermal cycling tests are sufficiently different from the fusion-glass laminate to make backlighting test results from these specimens invalid for the laminate. Key differences are the mirror backing paint and glass thickness. The candidate laminate configuration consists of 1.52-mm (0.060-inch) fusion glass bonded to 4.76-mm (3/16-inch) float glass. The chemically deposited silver on the fusion glass would be flash-coated with copper. The adhesive bonding is transparent, but would decrease the specular reflectivity of the copper for backlighting to decrease light reflected from the array during inverted stowage with daylight conditions. The reflectivity of the copper would decrease the maximum temperature and, hence, induced stresses.

Backlighting tests are recommended for near full-scale reflector panels under long-term exposure, since crack propagation in the glass is a function of time-at-stress.

D.5 PRODUCTION DEVELOPMENT TESTS OF LOW COST LAMINATED MIRRORS

Method/Facility -- The MDAC Adhesives Laboratory has laminated various thicknesses of glass using 1XA3404-2 polyurethane adhesive using different methods of pressurization. Pressure rollers, vacuum pressure, and presses were used in the laminating process along with different methods of adhesive application.

Specimen Descriptions -- 9 by 48-inch glass panels 1/16-inch thick and 9 by 48-inch panels 3/16 inch thick representing the mirror module configuration

were laminated using a manual pinch roller to apply pressure to the bondline. Lap shear strength data were developed to determine rate of cure of the 1XA3504-2 adhesive.

Results and Conclusions -- The 1XA3504-2 adhesive has 40 psi shear strength within 5 minutes, which fits into a rapid-production assembly line schedule. The pressure rollers have shown that this method is a good concept and will result in acceptable bonded-laminated mirror modules.

Bonding stringer supports with the 1XA3504-2 using a cartridge gun that dispenses and mixes at the same time allows the adhesive application to be completed within the 2-1/2 minute potlife of this material. Within 10 minutes the adhesive has attained a shear strength of 80 psi.

D.6 LARGE-PANEL TESTS

Large mirrors have not yet been fabricated because of the lack of pressure rollers 48 inches in width.

APPENDIX E

A LINEAR-ELASTIC METHOD TO CALCULATE THE THERMAL
STRESSES AND DEFLECTIONS OF A THIN GLASS PLATE
STIFFENED BY STEEL STRINGERS

APPENDIX E

A LINEAR-ELASTIC METHOD TO CALCULATE THE THERMAL STRESSES AND DEFLECTIONS OF A THIN GLASS PLATE STIFFENED BY STEEL STRINGERS

The thermal stresses and deflections due to the difference in thermal coefficients of expansion of glass and steel have been calculated using a technique developed at MDAC and correlated with test results. This linear elastic analysis method is based on geometric compatibility: the deflections of the glass plate and the steel stiffener at the bondline must be identical, and both constituents have the same radius of curvature. Using the cross-sectional and material properties of each constituent--area, moment of inertia, modulus of elasticity, coefficient of thermal expansion, and distance between neutral axes--the radius of curvature, changes in slope, and stresses due to a temperature change can be calculated. Each material is assumed isotropic, and the adhesive bond thickness and properties are not included in the calculations. As with beam theory, a plane section is assumed to remain plane before and after deformation. The dominant effect is bending; shear deformation of the panel is neglected. Measured deflections of the composite panel in recent MDAC tests correlated well with the predicted deflections using this method. This good correlation adds confidence to use of this quick hand method to predict thermal stresses and deflections for this type of composite structure.

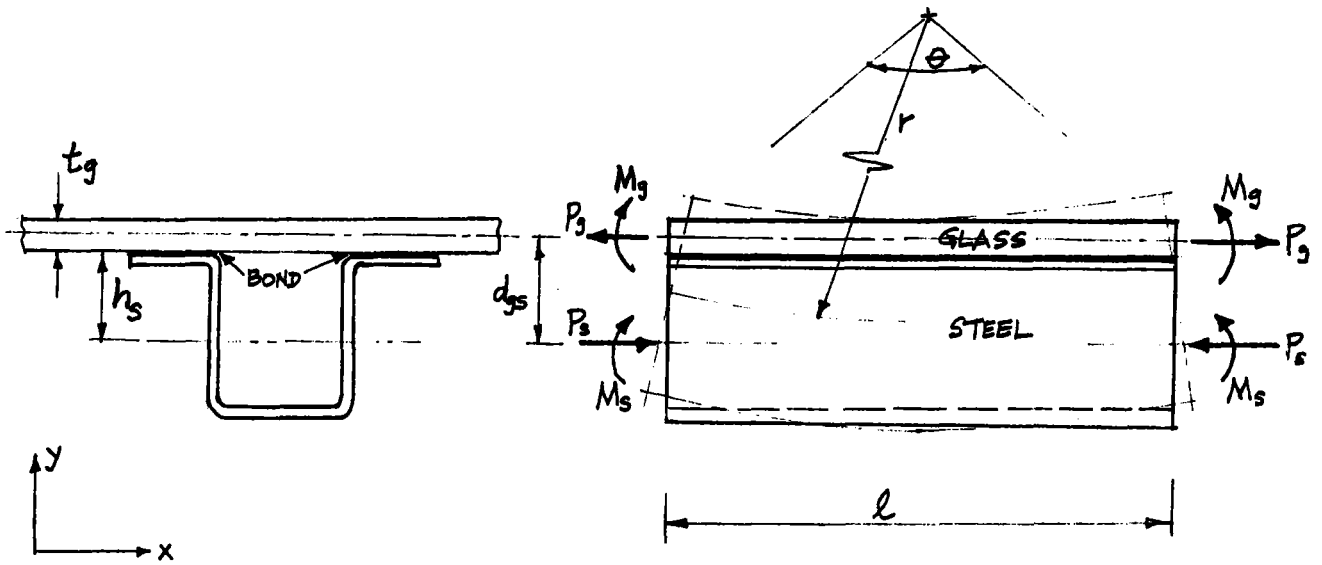


Figure E-1 Glass/Steel Stiffener Composite Panel

Given: A steel stringer bonded to a glass plate and subjected to a temperature change ΔT . Find: stresses in the glass, and the deflection of the composite panel for a temperature change of the entire composite. Since the steel has a higher coefficient of thermal expansion than the glass, the steel increases in length more than the glass, resulting in curvature of the composite. If the temperature change is positive (warmup), the steel elongates the glass with force P_g , the glass shortens the steel with force P_s , and the glass is on the concave side of the steel, with a radius of curvature r .

- Let: E_g = modulus of elasticity of the glass, psi
 I_g = moment of inertia of the glass per unit width about its own neutral axis, in^4/in
 E_s = modulus of elasticity of the steel, psi
 I_s = moment of inertia of the steel stringer about its own neutral axis per unit width, in^4/in
 d_{gs} = distance between neutral axes of glass and steel, in.
 α_g = coefficient of thermal expansion for glass, $\text{in}/\text{in}/^\circ\text{F}$
 α_s = coefficient of thermal expansion for steel, $\text{in}/\text{in}/^\circ\text{F}$
 ΔT = temperature change, $^\circ\text{F}$

- M_g = bending moment required to produce curvature r in the glass, in-lb/in
 M_s = bending moment required to produce curvature r in the steel, in-lb/in
 A_g = cross-section area per unit width of the glass, in²/in
 A_s = cross-section area per unit width of the steel, in²/in
 t_g = thickness of the glass, in.
 h_s = distance from the bond line to the neutral axis of the stiffener, in.
 ℓ = panel length, in.
 σ_g = stress in the glass, psi

From equilibrium of forces and moment,

$$\begin{aligned} \Sigma F_x &= P_g - P_s = 0; P_g = P_s = P \\ \Sigma M &= M_s + M_g - d_{gs} P = 0; P = \frac{M_s + M_g}{d_{gs}} \end{aligned} \quad (1)$$

The moments required to produce the curvature of radius r are:

$$M_g = \frac{E_g I_g}{r} \quad (2)$$

$$M_s = \frac{E_s I_s}{r} \quad (3)$$

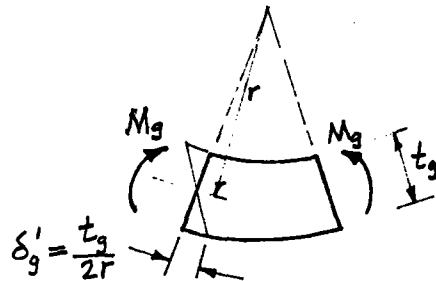
Substituting these moments in equation (1),

$$P = \frac{E_g I_g + E_s I_s}{d_{gs} r} \quad (4)$$

At the bond line, the elongation of the glass per unit length is:

$$\epsilon_g = \alpha_g \Delta T + \frac{P}{E_g A_g} + \frac{t_g}{2r} \quad (\text{in/in}), \quad (5)$$

where $(\alpha_g \Delta T)$ is the elongation due to a change of temperature ΔT , $(P/E_g A_g)$ is the elongation due to the force P , and $(t_g/2r)$ is the elongation due to the bending moment M_g , as shown below:



Similarly, the change of length (per unit length of the steel stiffener) of the steel at the bond line is:

$$\epsilon_s = \alpha_s \Delta T - \frac{P}{E_s A_s} - \frac{h_s}{r} \quad (6)$$

Geometric compatibility requires these two elongations to be equal. Therefore equating (5) and (6) gives:

$$\alpha_g \Delta T + \frac{P}{E_g A_g} + \frac{t_g}{2r} = \alpha_s \Delta T - \frac{P}{E_s A_s} - \frac{h_s}{r}$$

Rearranging, and collecting like terms,

$$\Delta T(\alpha_g - \alpha_s) + P\left(\frac{1}{E_g A_g} + \frac{1}{E_s A_s}\right) = -\frac{1}{r}\left(\frac{t_g}{2} + h_s\right) \quad (7)$$

Recognizing that $d_{gs} = \frac{t_g}{2} + h_s$,

and substituting for P from equation (4) in (7) gives:

$$\Delta T(\alpha_g - \alpha_s) + \left[\frac{E_g I_g + E_s I_s}{d_{gs} r}\right] \left[\frac{1}{E_g A_g} + \frac{1}{E_s A_s}\right] + \frac{d_{gs}}{r} = 0$$

$$\text{Let } K = \left[\frac{E_g I_g + E_s I_s}{d_{gs}}\right] \left[\frac{1}{E_g A_g} + \frac{1}{E_s A_s}\right] + d_{gs}$$

$$\text{Then, } \Delta T(\alpha_g - \alpha_s) + \frac{K}{r} = 0$$

$$\text{or, } \Delta T(\alpha_s - \alpha_g) = \frac{K}{r}$$

$$\text{Therefore, } r = \frac{K}{\Delta T(\alpha_s - \alpha_g)}$$

Now, from Figure E-1, the change of slope can be calculated from the following equation:

$$\theta = \frac{\delta}{2r} ,$$

and the stresses can be calculated using equations (1), (2), and (3) and substituting into the equation for combined axial and bending stresses.

The stress on the outer glass face is,

$$\sigma_g^{\text{outer}} = \left[\frac{P}{A_g} - \frac{E_g t_g}{2r} \right] \quad (8)$$

The stress on the inner glass face is,

$$\sigma_g^{\text{inner}} = \left[\frac{P}{A_g} + \frac{E_g t_g}{2r} \right] \quad (9)$$

This technique was verified by comparing calculated deflections with those measured in a test, and by comparing calculated stresses with those calculated by NASTRAN (NASA STRuctural ANalysis Program).

A laminated glass panel measuring 85 by 114 inches, with three hat-section stringers bonded to the glass in the long direction, was first heated to a temperature change of 38°F above room temperature (at which it was bonded). Then, it was cooled to a temperature change of 35°F below room temperature. Measurement of the panel deflections for each condition were made along the length of the panel.

The section properties of the panel and the thermal deflections were calculated using this technique. The good agreement between these calculated deflections and those measured in the test can be seen in Figure E-2.

The NASTRAN program was also used to model the stiffened panel in greater detail. Stresses were calculated at each point in the structure for a

temperature change of +29°F. The maximum glass tensile stress was predicted by NASTRAN to be 60 psi, and the maximum glass compressive stress was 20 psi.

Using this method,

$$K = 1.441$$

$$r = \frac{K}{\Delta T(\alpha_s - \alpha_g)} = \frac{1.441}{29 (1.98) 10^{-6}} = 25,100 \text{ in.}$$

$$M_g = \frac{E_g I_g}{r} = \frac{10 \times 10^6 \times 0.001302}{25,100} = 0.52 \text{ in-lb/in.}$$

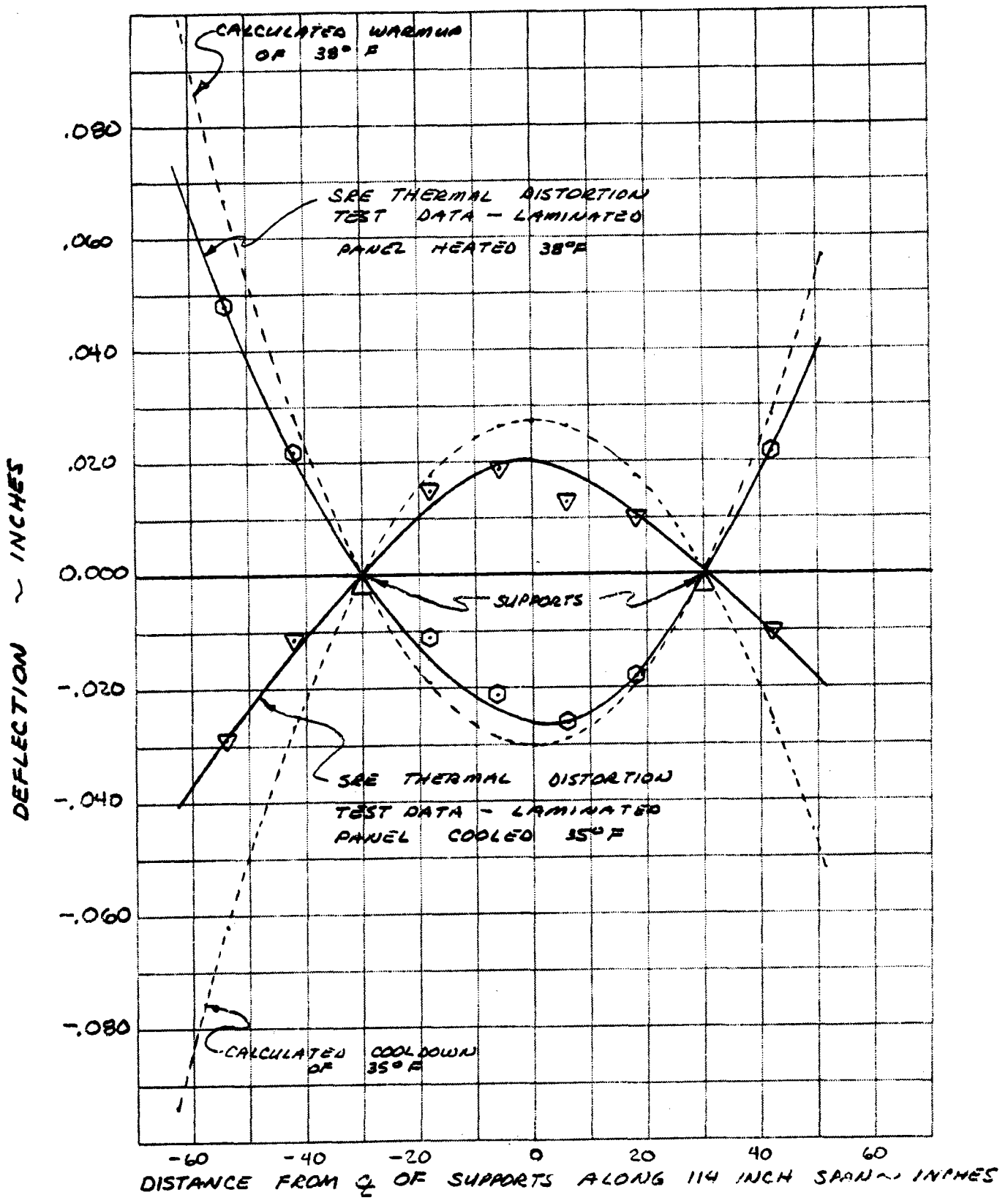
$$M_s = \frac{E_s I_s}{r} = \frac{29 \times 10^6 \times 0.004755}{25,100} = 5.50 \text{ in-lb/in.}$$

$$p = \frac{M_g + M_s}{d_{gs}} = \frac{0.52 + 5.50}{0.94} = 6.4 \text{ lb/in.}$$

$$\sigma_g^{\text{inner}} = \frac{p}{A_g} + \frac{E_g t g}{2r} = \frac{6.4}{.25} + \frac{10 \times 10^6 (.25)}{2(25,100)} = 26 + 50 = 76 \text{ psi}$$

$$\sigma_g^{\text{outer}} = \frac{p}{A_g} - \frac{E_g t g}{2r} = \frac{6.4}{.25} - \frac{10 \times 10^6 (.25)}{2(25,100)} = 26 - 50 = -24 \text{ psi}$$

Thus the results of this method yield slightly conservative stresses and deflections.



COMPARISON OF SRE LAMINATED PANEL THERMAL DISTORTION TEST DATA AND CALCULATED DEFLECTION

FIGURE E-2

APPENDIX F

EXAMPLE OF COMPUTERIZED OPTIMUM

REPAIR LEVEL ANALYSIS

Appendix F

EXAMPLE OF COMPUTERIZED OPTIMUM REPAIR LEVEL ANALYSIS

This appendix presents an actual output of the Optimum Repair Level Analysis (ORLA) computer. The computer analysis of the azimuth drive assembly is given to provide a better understanding of the results. The relative costs for each of the support options for the azimuth drive assembly are shown on Sheet 2 of 12. (Columns titled DEPOT Repair and INTR Repair are equivalent to Solar Program designations of off-site and on-site repair, respectively) A clear-cut decision for on-site (INTR) repair is indicated by the subtotal cost of \$1,028,339. The sensitivity tests make it possible to examine the impact on life-cycle cost of varying the indicated input values; if a factor is found to be critical (i.e., a variation results in selecting a different repair option), the source of that factor should be reexamined for validity and/or may indicate an area for potential maintenance cost reduction. All values indicated are relative and should not be construed as life-cycle costs.

PASS NR 1 PROTOTYPE HELIOSTAT COMMERCIAL SITE

LIFCY 360
 PCTOS 0,000
 NHRPM 275
 NWPDB 100
 NARDB 6

5 REPAIRABLE ITEM(S) WILL BE ANALYSED

ITEM NR 1 DRIVE ASSEMBLY AZIMJTH

575.00 DOLLARS

CW 0 POUNDS (RE-USABLE CNTR (FIGHT))
 NULBS 461.0 POUNDS (WEIGHT OF RFR ITEM)
 NUPWS 180 (QUALITY PER NHA)
 PCTON 1,000 (OPERATE TO FLT.HR.RATIO)

1 FAILURE MODES WILL BE ANALYZED

MODE NR 1 ASSEMBLY FAILURE PASS 1 ITEM 1

| | | |
|---|---|--------|
| F | MEAN TIME BETWEEN REPAIR----- | 340136 |
| A | MAN-HOURS REQUIRED TO REPAIR----- | 5.5 |
| I | NR PAGES DEPOT LEVEL TECH DATA----- | 10.0 |
| L | NR PAGES INT,LEVEL TECH DATA----- | 10.0 |
| | TRAINING RATE--PER MAN-WEEK----- | 500.0 |
| | MAN-WEEKS OF TRAINING(DEPOT LEVEL)----- | 1.0 |
| M | MAN-WEEKS OF TRAINING(INT.LEVEL)----- | 1.0 |
| O | INT.LEVEL SPECIAL AGE COST----- | 7500. |
| D | INT.LEVEL FACILITIES COST----- | 15000. |
| E | DEPOT LEVEL SPECIAL AGE COST----- | 7500. |
| | DEPOT LEVEL FACILITIES COST----- | 15000. |
| D | REPAIR PARTS COST PER REPAIR----- | 95.0 |
| A | NEW ASSEMBLIES INTRODUCED----- | 3 |
| T | NEW PARTS INTRODUCED----- | 14 |
| A | WEIGHT OF INT,LEVEL SPECIAL AGE----- | 500 |
| | WEIGHT OF REPAIR PARTS PER REPAIR----- | 32.0 |
| | NUMBER OF LINE ITEMS TO STOCK----- | 17 |
| | NUMBER OF AUTOMATIC TEST STEPS----- | 0 |
| | MEAN TIME TO AUTOMATICALLY TEST----- | 0.00 |
| | COST INT,LEVEL AGE,HIGH MTRD----- | 7500. |
| | COST INT,LEVEL AGE,LOW MTRD----- | 7500. |
| | COST DEPOT LEVEL AGE,HIGH MTRD----- | 7500. |
| | COST DEPOT LEVEL AGE,LOW MTRD----- | 7500. |

OPTIMUM REPAIR LEVEL ANALYSIS OF DRIVE ASSEMBLY AZIMUTH

PASS 1 ITEM 1 MODE 1 ASSEMBLY FAILURE

| COST ELEMENTS | DEPOT REPAIR | INTR. REPAIR | DISCARD |
|-------------------|--------------------|--------------------|--------------------|
| SPARES | \$ 16150. | \$ 1088. | \$ 3012471. |
| SAFETY STOCK | 4184. | | |
| SUPPLY ADMIN | 0. | 9180. | |
| PART INTRODUCTION | 1758. | 1758. | |
| REPAIR PARTS | 477713. | 497713. | |
| PKING + SHIPPING | 2536792. | 88272. | 1265105. |
| AGE | 1250. | 7500. | |
| FACILITIES | 2500. | 15000. | |
| LABOR | 447208. | 402545. | |
| TRAINING | 325. | 4850. | |
| TECHNICAL DATA | 433. | 433. | |
| SUB-TOTAL | \$ 3508513. | \$ 1028339. | \$ 4277576. |

SENSITIVITY TESTS

| | | | |
|--------------------|-------------|-------------|-------------|
| + .50 X MTBD | \$ 2342265. | \$ 698796. | \$ 2653143. |
| - .50 X MTBD | \$ 7010760. | \$ 2017956. | \$ 8555153. |
| + .50 X REPAIR MH | \$ 3732117. | \$ 1229611. | \$ ----- |
| - .50 X REPAIR MH | \$ 3284919. | \$ 827066. | \$ ----- |
| + .50 X TRAINING | \$ 3509676. | \$ 1030764. | \$ ----- |
| - .50 X TRAINING | \$ 3508351. | \$ 1025914. | \$ ----- |
| + .50 X UNIT COST | \$ 3767537. | \$ 1277739. | \$ 5783612. |
| - .50 X UNIT COST | \$ 3249490. | \$ 778939. | \$ 2771341. |
| + .50 X AGE COST | \$ 3509138. | \$ 1032089. | \$ ----- |
| - .50 X AGE COST | \$ 3507888. | \$ 1024589. | \$ ----- |
| + .25 X FLEET SIZE | \$ 4384075. | \$ 1275743. | \$ 5346970. |
| - .25 X FLEET SIZE | \$ 2632952. | \$ 780935. | \$ 3208182. |
| + .21 X UTIL. RATE | \$ 4243985. | \$ 1236158. | \$ 5175867. |
| - .21 X UTIL. RATE | \$ 2773042. | \$ 820519. | \$ 3379285. |

ITEM NR 2 JACK ASSEMBLY TRACKING

198.00 DOLLARS

CW 0 POUNDS (RE-USABLE CNTR WEIGHT)
 NULBS 60.0 POUNDS (WEIGHT OF RPR ITEM)
 NUPKS 180 (QUANTITY PER NHA)
 PCTON 1,000 (OPERATE TO FLT.HR.RATIO)

1 FAILURE MODES WILL BE ANALYZED

MODE NR 1 ASSEMBLY FAILURE PASS 1 ITEM 2

| | | |
|---|---|--------|
| F | MEAN TIME BETWEEN REPAIR----- | 366300 |
| A | MAN-HOURS REQUIRED TO REPAIR----- | 3.0 |
| I | NR PAGES DEPOT LEVEL TECH DATA----- | 10.0 |
| L | NR PAGES INT,LEVEL TECH DATA----- | 10.0 |
| | TRAINING RATE--PER MAN-WEEK----- | 500.0 |
| | MAN-WEEKS OF TRAINING(DEPOT LEVEL)----- | .5 |
| M | MAN-WEEKS OF TRAINING(INT,LEVEL)----- | .5 |
| O | INT.LEVEL SPECIAL AGE COST----- | 2500. |
| D | INT.LEVEL FACILITIES COST----- | 7500. |
| E | DEPOT LEVEL SPECIAL AGE COST----- | 2500. |
| | DEPOT LEVEL FACILITIES COST----- | 7500. |
| D | REPAIR PARTS COST PER REPAIR----- | 45.0 |
| A | NEW ASSEMBLIES INTRODUCED----- | 1 |
| T | NEW PARTS INTRODUCED----- | 14 |
| A | WEIGHT OF INT,LEVEL SPECIAL AGE----- | 200 |
| | WEIGHT OF REPAIR PARTS PER REPAIR----- | 12.0 |
| | NUMBER OF LINE ITEMS TO STOCK----- | 15 |
| | NUMBER OF AUTOMATIC TEST STEPS----- | 0 |
| | MEAN TIME TO AUTOMATICALLY TEST----- | 0.00 |
| | COST INT,LEVEL AGE,HIGH MTBD----- | 2500. |
| | COST INT,LEVEL AGE,LOW MTBD----- | 2500. |
| | COST DEPOT LEVEL AGE,HIGH MTRD----- | 2500. |
| | COST DEPOT LEVEL AGE,LCW MTRD----- | 2500. |

OPTIMUM REPAIR LEVEL ANALYSIS OF JACK ASSEMBLY TRACKING

| PASS 1 | ITEM 2 | MODE 1 | ASSEMBLY FAILURE | | |
|-------------------|--------|--------------|------------------|---------|-------------|
| COST ELEMENTS | | DEPGT REPAIR | INTR. REPAIR | DISCARD | |
| SPARES | \$ | 5164. | \$ | 348. | \$ 963243. |
| SAFETY STOCK | | 1339. | | | |
| SUPPLY ADMIN | | 0. | | 8100. | |
| PART INTRODUCTION | | 1460. | | 1460. | |
| REPAIR PARTS | | 218919. | | 218919. | |
| PKING + SHIPPING | | 306609. | | 30629. | 152895. |
| AGE | | 417. | | 2500. | |
| FACILITIES | | 1250. | | 7500. | |
| LABOR | | 226509. | | 203886. | |
| TRAINING | | 163. | | 2425. | |
| TECHNICAL DATA | | 433. | | 433. | |
| SUB-TOTAL | \$ | 762261. | \$ | 476200. | \$ 1116138. |

| SENSITIVITY TESTS | | | | | |
|--------------------|----|----------|----|---------|-------------|
| + .50 X MTBD | \$ | 509667. | \$ | 325091. | \$ 744464. |
| - .50 X MTBD | \$ | 1520799. | \$ | 929982. | \$ 2232276. |
| + .50 X REPAIR MH | \$ | 875515. | \$ | 578144. | \$----- |
| - .50 X REPAIR MH | \$ | 649006. | \$ | 374257. | \$----- |
| + .50 X TRAINING | \$ | 762342. | \$ | 477413. | \$----- |
| - .50 X TRAINING | \$ | 762179. | \$ | 474988. | \$----- |
| + .50 X UNIT COST | \$ | 874971. | \$ | 585834. | \$ 1597760. |
| - .50 X UNIT COST | \$ | 649550. | \$ | 366567. | \$ 634516. |
| + .50 X AGE COST | \$ | 762469. | \$ | 477450. | \$----- |
| - .50 X AGE COST | \$ | 762052. | \$ | 474950. | \$----- |
| + .25 X FLEET SIZE | \$ | 951893. | \$ | 589646. | \$ 1395172. |
| - .25 X FLEET SIZE | \$ | 572626. | \$ | 362755. | \$ 837103. |
| + .21 X UTIL, RATE | \$ | 921554. | \$ | 571495. | \$ 1350527. |
| - .21 X UTIL, RATE | \$ | 602968. | \$ | 380906. | \$ 881749. |

ITEM NR 3 DRIVE MOTOR AZIMUTH

70.00 DOLLARS

| | | |
|-------|-------------|---------------------------|
| CW | 0 POUNDS | (RE-usable CNTR WEIGHT) |
| NULBS | 17.0 POUNDS | (WEIGHT OF RPR ITEM) |
| NUPHS | 180 | (QUANTITY PER NHA) |
| PCTON | 1.000 | (OPERATE TO FLT.HR.RATIO) |

1 FAILURE MODES WILL BE ANALYZED

MODE NR 1 ASSEMBLY FAILURE PASS 1 ITEM 3

| | | |
|---|---|--------|
| F | MEAN TIME BETWEEN REPAIR----- | 295858 |
| A | MAN-HOURS REQUIRED TO REPAIR----- | 2.5 |
| I | NR PAGES DEPOT LEVEL TECH DATA----- | 10.0 |
| L | NR PAGES INT,LEVEL TECH DATA----- | 10.0 |
| | TRAINING RATE--PER MAN-WEEK----- | 500.0 |
| | MAN-WEEKS OF TRAINING(DEPOT LEVEL)----- | .5 |
| | MAN-WEEKS OF TRAINING(INT,LEVEL)----- | .5 |
| M | INT.LEVEL SPECIAL AGE COST----- | 2500. |
| O | INT.LEVEL FACILITIES COST----- | 5625. |
| D | DEPOT LEVEL SPECIAL AGE COST----- | 2500. |
| E | DEPOT LEVEL FACILITIES COST----- | 5625. |
| D | REPAIR PARTS COST PER REPAIR----- | 10.0 |
| A | NEW ASSEMBLIES INTRODUCED----- | 1 |
| T | NEW PARTS INTRODUCED----- | 8 |
| A | WEIGHT OF INT,LEVEL SPECIAL AGE----- | 200 |
| | WEIGHT OF REPAIR PARTS PER REPAIR----- | 3.0 |
| | NUMBER OF LINE ITEMS TO STOCK----- | 9 |
| | NUMBER OF AUTOMATIC TEST STEPS----- | 0 |
| | MEAN TIME TO AUTOMATICALLY TEST----- | 6.00 |
| | COST INT,LEVEL AGE,HIGH MTBD----- | 2500. |
| | COST INT,LEVEL AGE,LOW MTBD----- | 2500. |
| | COST DEPOT LEVEL AGE,HIGH MTBD----- | 2500. |
| | COST DEPOT LEVEL AGE,LOW MTBD----- | 2500. |

OPTIMUM REPAIR LEVEL ANALYSIS OF DRIVE MOTOR AZIMUTH

PASS 1 ITEM 3 MODE 1 ASSEMBLY FAILURE

| COST ELEMENTS | DEPOT REPAIR | INTR. REPAIR | DISCARD |
|-------------------|-------------------|-------------------|-------------------|
| SPARES | \$ 2260. | \$ 152. | \$ 421621. |
| SAFETY STOCK | 585. | | |
| SUPPLY ADMIN | 0. | 4860. | |
| PART INTRODUCTION | 855. | 855. | |
| REPAIR PARTS | 60232. | 60232. | |
| PKING + SHIPPING | 107555. | 9484. | 53634. |
| AGE | 417. | 2500. | |
| FACILITIES | 939. | 5625. | |
| LABOR | 233699. | 210359. | |
| TRAINING | 163. | 2425. | |
| TECHNICAL DATA | 433. | 433. | |
| SUB-TOTAL | \$ 407138. | \$ 296925. | \$ 475256. |

SENSITIVITY TESTS

| | | | |
|--------------------------------|------------|------------|------------|
| + .50 X MTBD | \$ 272495. | \$ 203610. | \$ 316996. |
| - .50 X MTBD | \$ 811470. | \$ 577152. | \$ 950511. |
| + .50 X REPAIR MH | \$ 523987. | \$ 402104. | \$ ----- |
| - .50 X REPAIR MH | \$ 292288. | \$ 191746. | \$ ----- |
| + .50 X TRAINING | \$ 407219. | \$ 298138. | \$ ----- |
| - .50 X TRAINING | \$ 407056. | \$ 295713. | \$ ----- |
| + .50 X UNIT COST | \$ 439676. | \$ 327117. | \$ 686066. |
| - .50 X UNIT COST | \$ 375599. | \$ 266733. | \$ 264445. |
| + .50 X AGE COST | \$ 407346. | \$ 298175. | \$ ----- |
| - .50 X AGE COST | \$ 406929. | \$ 295675. | \$ ----- |
| + .25 X FLEET SIZE | \$ 509221. | \$ 366982. | \$ 594070. |
| - .25 X FLEET SIZE | \$ 306054. | \$ 226868. | \$ 356442. |
| + .21 X UTIL ₁ RATE | \$ 492047. | \$ 355773. | \$ 575059. |
| - .21 X UTIL ₁ RATE | \$ 322228. | \$ 238077. | \$ 375452. |

ITEM NR 4 DRIVE MOTOR (LEVATION)

75.00 DOLLARS

| | | |
|-------|-------------|--------------------------|
| CW | 0 POUNDS | (RE-USABLE CNTR WEIGHT) |
| NULBS | 18.0 POUNDS | (WEIGHT OF RPR ITEM) |
| NUPWS | 180 | (QUANTITY PER NHA) |
| PCTON | 1.000 | (OPEATE TO FLT.IP.RATIO) |

1 FAILURE MODES WILL BE ANALYZED

MODE NR 1 ASSEMBLY FAILURE PASS 1 ITEM 4

| | | |
|---|---|--------|
| F | MEAN TIME BETWEEN REPAIR----- | 295858 |
| A | MAN-HOURS REQUIRED TO REPAIR----- | 2.5 |
| I | NR PAGES DEPOT LEVEL TECH DATA----- | 10.0 |
| L | NR PAGES INT,LEVEL TECH DATA----- | 10.0 |
| | TRAINING RATE--PER MAN-WEEK----- | 500.0 |
| | MAN-WEEKS OF TRAINING(DEPOT LEVEL)----- | .5 |
| | MAN-WEEKS OF TRAINING(INT,LEVEL)----- | .5 |
| M | INT,LEVEL SPECIAL AGE COST----- | 2500. |
| O | INT,LEVEL FACILITIES COST----- | 5625. |
| D | DEPOT LEVEL SPECIAL AGE COST----- | 2500. |
| E | DEPOT LEVEL FACILITIES COST----- | 5625. |
| D | REPAIR PARTS COST PER REPAIR----- | 10.0 |
| A | NEW ASSEMBLIES INTRODUCED----- | 1 |
| T | NEW PARTS INTRODUCED----- | 8 |
| A | WEIGHT OF INT,LEVEL SPECIAL AGE----- | 200 |
| | WEIGHT OF REPAIR PARTS PER REPAIR----- | 3.0 |
| | NUMBER OF LINE ITEMS TO STOCK----- | 9 |
| | NUMBER OF AUTOMATIC TEST STEPS----- | 0 |
| | MEAN TIME TO AUTOMATICALLY TEST----- | 0.00 |
| | COST INT,LEVEL AGE,HIGH MTBD----- | 2500. |
| | COST INT,LEVEL AGE,LOW MTBD----- | 2500. |
| | COST DEPOT LEVEL AGE,HIGH MTBD----- | 2500. |
| | COST DEPOT LEVEL AGE,LOW MTBD----- | 2500. |

OPTIMUM REPAIR LEVEL ANALYSIS OF DRIVE MOTOR ELEVATION

PASS 1 ITEM 4 MODE 1 ASSEMBLY FAILURE

| COST ELEMENTS | DEPOT REPAIR | INTR. REPAIR | DISCARD |
|--------------------------------|-------------------|-------------------|-------------------|
| SPARES | \$ 2422. | \$ 163. | \$ 451737. |
| SAFETY STOCK | 627. | | |
| SUPPLY ADMIN | 0. | 4860. | |
| PART INTRODUCTION | 855. | 855. | |
| REPAIR PARTS | 60232. | 60232. | |
| PKING + SHIPPING | 113893. | 9485. | 56789. |
| AGE | 417. | 2500. | |
| FACILITIES | 938. | 5625. | |
| LABOR | 233699. | 210359. | |
| TRAINING | 163. | 2425. | |
| TECHNICAL DATA | 433. | 433. | |
| SUB-TOTAL | \$ 413668. | \$ 296937. | \$ 508526. |
| SENSITIVITY TESTS | | | |
| + .50 X MTRD | \$ 276850. | \$ 203618. | \$ 339187. |
| - .50 X MTRD | \$ 824530. | \$ 577176. | \$ 1017053. |
| + .50 X REPAIR MH | \$ 530517. | \$ 402116. | \$ ----- |
| - .50 X REPAIR MH | \$ 296815. | \$ 191758. | \$ ----- |
| + .50 X TRAINING | \$ 413749. | \$ 298150. | \$ ----- |
| - .50 X TRAINING | \$ 413586. | \$ 295725. | \$ ----- |
| + .50 X UNIT COST | \$ 445308. | \$ 327134. | \$ 734395. |
| - .50 X UNIT COST | \$ 382027. | \$ 266740. | \$ 282658. |
| + .50 X AGE COST | \$ 413876. | \$ 298187. | \$ ----- |
| - .50 X AGE COST | \$ 413459. | \$ 295687. | \$ ----- |
| + .25 X FLEET SIZE | \$ 516383. | \$ 366997. | \$ 635658. |
| - .25 X FLEET SIZE | \$ 310952. | \$ 226877. | \$ 381395. |
| + .21 X UTIL ₁ RATE | \$ 499949. | \$ 355787. | \$ 615317. |
| - .21 X UTIL ₁ RATE | \$ 327387. | \$ 238087. | \$ 401736. |

ITEM NR 5 HELIOSTAT CONTROL ELECTRONICS

98.00 DOLLARS

| | | |
|-------|------------|---------------------------|
| CW | 0 POUNDS | (RE-USABLE CTR WEIGHT) |
| NULBS | 2.0 POUNDS | (WEIGHT OF RFR ITEM) |
| NUPHS | 1%0 | (QUANTITY PER MHA) |
| PCTON | 1.000 | (OPEATE TO FLT.I.R.RATIC) |

1 FAILURE MODES WILL BE ANALYZED

MODE NR 1 CIRCUIT CARD FAILURE PASS 1 ITEM 5

| | | |
|---|---|--------|
| F | MEAN TIME BETWEEN REPAIR----- | 606060 |
| A | MAN-HOURS REQUIRED TO REPAIR----- | 3.5 |
| I | NR PAGES DEPOT LEVEL TECH DATA----- | 15.0 |
| L | NR PAGES INT.LEVEL TECH DATA----- | 15.0 |
| | TRAINING RATE--PER MAN-WEEK----- | 500.0 |
| | MAN-WEEKS OF TRAINING(DEPOT LEVEL)----- | 1.0 |
| | MAN-WEEKS OF TRAINING(INT.LEVEL)----- | 1.0 |
| M | INT.LEVEL SPECIAL AGE COST----- | 25000. |
| O | INT.LEVEL FACILITIES COST----- | 7500. |
| D | DEPOT LEVEL SPECIAL AGE COST----- | 25000. |
| E | DEPOT LEVEL FACILITIES COST----- | 7500. |
| | REPAIR PARTS COST PER REPAIR----- | 15.0 |
| D | NEW ASSEMBLIES INTRODUCED----- | 1 |
| A | NEW PARTS INTRODUCED----- | 10 |
| T | WEIGHT OF INT.LEVEL SPECIAL AGE----- | 300 |
| A | WEIGHT OF REPAIR PARTS PER REPAIR----- | .5 |
| | NUMBER OF LINE ITEMS TO STOCK----- | 11 |
| | NUMBER OF AUTOMATIC TEST STEPS----- | 0 |
| | MEAN TIME TO AUTOMATICALLY TEST----- | 0.00 |
| | COST INT.LEVEL AGE,HIGH MTRD----- | 25000. |
| | COST INT.LEVEL AGE,LOW MTRD----- | 25000. |
| | COST DEPOT LEVEL AGE,HIGH MTRD----- | 25000. |
| | COST DEPOT LEVEL AGE,LOW MTRD----- | 25000. |

OPTIMUM REPAIR LEVEL ANALYSIS OF HELIOSTAT CONTROL ELECTRONICS

PASS 1 IIEH 5 MODE 1 CIRCUIT CARD FAILURE

| COST ELEMENTS | DEPCT REPAIR | INTR. REPAIR | DISCARD |
|--------------------|--------------|--------------|------------|
| SPARES | \$ 1545. | \$ 104. | \$ 206150. |
| SAFETY STOCK | 400. | | |
| SUPPLY ADMIN | 0. | 5940. | |
| PART INTRODUCTION | 1057. | 1057. | |
| REPAIR PARTS | 44105. | 44105. | |
| PKING + SHIPPING | 6177. | 771. | 3060. |
| AGE | 4167. | 25000. | |
| FACILITIES | 1250. | 7500. | |
| LABOR | 159717. | 143766. | |
| TRAINING | 325. | 4850. | |
| TECHNICAL DATA | 650. | 650. | |
| SUB-TOTAL | \$ 219392. | \$ 233742. | \$ 291230. |
| SENSITIVITY TESTS | | | |
| + .50 X MTBD | \$ 141815. | \$ 170890. | \$ 194250. |
| - .50 X MTBD | \$ 431336. | \$ 422488. | \$ 582460. |
| + .50 X REPAIR MH | \$ 299251. | \$ 305626. | \$ ----- |
| - .50 X REPAIR MH | \$ 139534. | \$ 161859. | \$ ----- |
| + .50 X TRAINING | \$ 219555. | \$ 236167. | \$ ----- |
| - .50 X TRAINING | \$ 219230. | \$ 231317. | \$ ----- |
| + .50 X UNIT COST | \$ 242417. | \$ 255847. | \$ 435305. |
| - .50 X UNIT COST | \$ 195367. | \$ 211638. | \$ 147155. |
| + .50 X AGE COST | \$ 221476. | \$ 246242. | \$ ----- |
| - .50 X AGE COST | \$ 217309. | \$ 221242. | \$ ----- |
| + .25 X FLEET SIZE | \$ 272378. | \$ 280929. | \$ 364037. |
| - .25 X FLEET SIZE | \$ 166406. | \$ 186556. | \$ 216422. |
| + .21 X UTIL, RATE | \$ 263900. | \$ 273379. | \$ 352388. |
| - .21 X UTIL, RATE | \$ 174884. | \$ 194106. | \$ 230072. |

CW 0 POUNDS (RE-USABLE CKTR WEIGHT)
 NULBS 2.0 POUNDS (WEIGHT OF PPR ITEM)
 NUPHS 114 (QUANTITY PER NHA)
 PCTON 1.000 (UPELATE TO FLT.I.R.RATIO)

1 FAILURE MODES WILL BE ANALYZED

MODE NR 1 CIRCUIT CARD FAILURE PASS 2 ITEM 2

| | | |
|---|---|--------|
| F | MEAN TIME BETWEEN REPAIR----- | 412372 |
| A | MAN-HOURS REQUIRED TO REPAIR----- | 3.5 |
| I | NR PAGES DEPOT LEVEL TECH DATA----- | 15.0 |
| L | NR PAGES INT,LEVEL TECH DATA----- | 15.0 |
| | TRAINING RATE--PER MAN-WEEK----- | 500.0 |
| | MAN-WEEKS OF TRAINING(DEPOT LEVEL)----- | 1.0 |
| | MAN-WEEKS OF TRAINING(INT.LEVEL)----- | 1.0 |
| M | INT.LEVEL SPECIAL AGE COST----- | 100. |
| O | INT.LEVEL FACILITIES COST----- | 0. |
| D | DEPOT LEVEL SPECIAL AGE COST----- | 100. |
| E | DEPOT LEVEL FACILITIES COST----- | 0. |
| D | REPAIR PARTS COST PER REPAIR----- | 13.0 |
| A | NEW ASSEMBLIES INTRODUCED----- | 1 |
| T | NEW PARTS INTRODUCED----- | 12 |
| A | WEIGHT OF INT,LEVEL SPECIAL AGE----- | 0 |
| | WEIGHT OF RPAIR PARTS PER REPAIR----- | .5 |
| | NUMBER OF LINE ITEMS TO STOCK----- | 13 |
| | NUMBER OF AUTOMATIC TEST STEPS----- | 0 |
| | MEAN TIME TO AUTOMATICALLY TEST----- | 0.00 |
| | COST INT,LEVEL AGE,HIGH MTBD----- | 100. |
| | COST INT,LEVEL AGE,LOW MTBD----- | 100. |
| | COST DEPOT LEVEL AGE,HIGH MTBD----- | 100. |
| | COST DEPOT LEVEL AGE,LOW MTBD----- | 100. |

OPTIMUM REPAIR LEVEL ANALYSIS OF DATA DISTRIBUTION INTERFACE

| PASS 2 ITEM 2 | | MODE 1 | CIRCUIT CARD FAILURE | | |
|--------------------------------|----|--------------|----------------------|---------|----------|
| COST ELEMENTS | | DEPOT REPAIR | INTR, REPAIR | DISCARD | |
| SPARES | \$ | 19, | \$ | 1, | \$ 3421, |
| SAFETY STOCK | | 5, | | | |
| SUPPLY ADMIN | | 0, | | 7020, | |
| PART INTRODUCTION | | 1258, | | 1258, | |
| REPAIR PARTS | | 356, | | 356, | |
| PKING + SHIPPING | | 57, | | 7, | 29, |
| AGE | | 17, | | 100, | |
| FACILITIES | | 0, | | 0, | |
| LABOR | | 1487, | | 1336, | |
| TRAINING | | 325, | | 4850, | |
| TECHNICAL DATA | | 650, | | 650, | |
| SUB-TOTAL | \$ | 4173, | \$ | 15581, | \$ 3450. |
| SENSITIVITY TESTS | | | | | |
| + .50 X MTBD | \$ | 3533, | \$ | 15014, | \$ 2301. |
| - .50 X MTBD | \$ | 6096, | \$ | 17283, | \$ 6899. |
| + .50 X REPAIR MH | \$ | 4916, | \$ | 16250, | \$----- |
| - .50 X REPAIR MH | \$ | 3430, | \$ | 14912, | \$----- |
| + .50 X TRAINING | \$ | 4336, | \$ | 16006, | \$----- |
| - .50 X TRAINING | \$ | 4011, | \$ | 13156, | \$----- |
| + .50 X UNIT COST | \$ | 4362, | \$ | 15759, | \$ 5160. |
| - .50 X UNIT COST | \$ | 3984, | \$ | 15402, | \$ 1739. |
| + .50 X AGE COST | \$ | 4181, | \$ | 15631, | \$----- |
| - .50 X AGE COST | \$ | 4165, | \$ | 15531, | \$----- |
| + .25 X FLEET SIZE | \$ | 4654, | \$ | 16006, | \$ 4312. |
| - .25 X FLEET SIZE | \$ | 3692, | \$ | 15155, | \$ 2587. |
| + .21 X UTIL ₁ RATE | \$ | 4577, | \$ | 15938, | \$ 4174. |
| - .21 X UTIL ₁ RATE | \$ | 3769, | \$ | 15223, | \$ 2725. |

APPENDIX G

LOGISTIC SUPPORT ANALYSIS WORK SHEETS

Appendix G
LOGISTIC SUPPORT ANALYSIS WORK SHEETS

These work sheets are the means of collecting maintenance-related data in a usable form for all the logistics and maintenance-related analyses of the Prototype Heliostat.

LOGISTICS SUPPORT ANALYSIS WORKSHEETS

Item Name: DRIVE ASSY, AZIMUTH System: PROTOTYPE HELIOSTAT
 Weight: 461 LBS Repair Decision: ON-SITE
 Prelim Cost Est: \$575.00 Method: ORLA MODEL
 Qty: 18,000/SITE MTBF: 340,136 Sys MTTR: 4.0
 R&R MHRS: 19.2 Repair MHRS: 5.5

Description:

The Azimuth Drive Assembly supports the reflector structure and provides the means for producing azimuth rotation for solar tracking, emergency slewing, and routine positioning for stowage and maintenance. The drive train includes a heliocon gear input reducer and a harmonic drive output stage which provides an overall gear reduction of 39,200:1.

Maintenance Concept:

The complete assembly is removed and replaced upon component failure. Bench repair of removed assemblies is accomplished by replacement of defective gear train components. The harmonic drive section is lubricated by heavy duty oil and the input reduction gear cavity is packed with grease. Scheduled servicing/lubrication is not planned. General area/ corrosion control inspection will include verification that grease and oil seals are not leaking.

Support Equipment:

Replacement of the drive assembly requires a mobile crane to hoist and remove the reflector support structure and a forklift to remove and replace the drive assembly. Hoisting can be accomplished with universal slings.

Bench repair requires a portable or overhead hoist and a holding fixture to support assembly/disassembly, a means verifying input/output torque, and standard precision mechanical inspection tools for checking wear tolerances and backlash.

Facilities:

No special facilities are required. Bench area floor space of approximately 400 ft² should be adequate.

NOTE: MTBF = mean time between failures
 MTTR = mean time to repair
 R&R = remove and replace

LOGISTICS SUPPORT ANALYSIS WORKSHEETS

Item Name: JACK ASSEMBLY, TRACKING/STOWAGE System: PROTOTYPE HELIOSTAT
 Weight: 60 LBS Repair Decision: ON-SITE
 Prelim Cost Est: \$198.00 Method: ORLA MODEL
 Qty: 36,000/SITE MTBF: 366,300 Sys MTTR: 2.2
 R&R MHRS: 4.4 Repair MHRS: 3.0

Description:

The Jack Assembly is a ball screw, translating tube configuration which requires no backlash adjustment. The design includes a single stage input gear reduction. An integral drive motor mount is provided and the input pinion is on the drive motor shaft. The tracking and stowage jack assemblies are interchangeable.

Maintenance Concept:

The Jack Assembly is removed and replaced upon component failure. Bench repair of removed assemblies is accomplished by replacement of defective components. Scheduled lubrication is not planned; however, the condition of grease seals will be verified as part of general area/corrosion control inspections. Evidence of loss of grease or entry of moisture/contaminants will initiate corrective maintenance.

Support Equipment:

A restraining device or safety link is required to prevent rotation of the reflector structure during replacement of either tracking or stowage jack. Bench repair requires a holding fixture, a means for checking input torque versus output, and standard precision mechanical inspection tools for checking wear tolerances.

Facilities:

No special facilities are required. Bench area floor space of approximately 200 ft² should be adequate.

LOGISTICS SUPPORT ANALYSIS WORKSHEETS

Item Name: DRIVE MOTOR, AZIMUTH System: PROTOTYPE HELIOSTAT
 Weight: 17 LBS Repair Decision: ON-SITE
 Prelim Cost Est: \$70.00 Method: ORLA MODEL
 Qty: 18,000/SITE MTBF: 295,858 Sys MTTR: 1.7
 R&R MHRS: 3.4 Repair MHRS: 2.5

Description:

The Azimuth Drive Motor is mounted on the drive assembly housing and provides the power for azimuth tracking. The Line Replaceable Unit (LRU) includes the motor, the drive electronics components, and the incremental encoder.

Maintenance Concept:

The Drive Motor Assembly is removed and replaced upon component failure. Bench repair of removed assemblies is accomplished by replacement of the incremental encoder, drive electronics, and motor components. Motor bearings are permanently lubricated and no scheduled maintenance is required.

Support Equipment:

Replacement of the motor assembly does not require any special tools or equipment. Bench repair requires a controlled input power source and a means of measuring output torque and RPM. A holding fixture, common tools and standard test equipment are required for disassembly/assembly and verification of incremental encoder operation.

Facilities:

No special facilities are required. Bench area floor space of approximately 150 ft² should be adequate.

LOGISTICS SUPPORT ANALYSIS WORKSHEETS

Item Name: DRIVE MOTOR ELEVATION/STOWAGE System: PROTOTYPE HELIOSTAT
 Weight: 18 LBS Repair Decision: ON-SITE
 Prelim Cost Est: \$75.00 Method: ORLA MODEL
 Qty: 36,000/SITE MTBF: 295,858 Sys MTTR: 1.9
 R&R MHRS: 3.8 Repair MHRS: 2.5

Description:

The Elevation and Storage Drive Motors are mounted on the tracking and storage jack assemblies, respectively. The motors are interchangeable. The Line Replaceable Unit (LRU) includes the motor, the motor controller components and the incremental encoder.

Maintenance Concept:

The Drive Motor Assembly is removed and replaced upon component failure. Bench repair of removed assemblies is accomplished by replacement of the incremental encoder, motor controller and motor components. Motor bearings are permanently lubricated and no scheduled maintenance is required.

Support Equipment:

Replacement of the motor assembly does not require any special tools or equipment. Bench repair requires a controlled input power source and a means of measuring output torque and RPM. A holding fixture, common tools, and standard test equipment are required for disassembly/assembly and verification of incremental coder operation. Bench support equipment is also utilized for azimuth drive motor repair.

Facilities:

No special facilities are required. Bench area floor space is shared with azimuth drive motor repair area.

LOGISTICS SUPPORT ANALYSIS WORKSHEETS

Item Name: HELIOSTAT J-BOX System: PROTOTYPE HELIOSTAT
 Weight: 10 LBS Repair Decision: ON-LINE
 Prelim Cost Est: \$47.00 Method: TASK ANALYSIS
 Qty: 18,000/SITE MTBF: 862,069 Sys MTTR: 1.6
 R&R MHRS: - Repair MHRS: 3.2

Description:

The Heliostat J-Box is a dust and waterproof electrical junction box, located near the base of the pedestal, which houses the terminal strips and circuit breaker for terminating/interconnecting the field power and data cables with the heliostat power and data wiring.

Maintenance Concept:

Replacement of the J-Box is not anticipated, except for major physical damage. The box is repaired in-place by replacement of electrical components or weather seals.

Support Equipment:

No special equipment required.

Facilities:

None required.

LOGISTICS SUPPORT ANALYSIS WORKSHEETS

Item Name: HELIOSTAT CONTROL ELECTRONICS System: PROTOTYPE HELIOSTAT
 Weight: 1 LB Repair Decision: OFF-SITE
 Prelim Cost Est: \$98.00 Method: ORLA MODEL
 Qty: 18,000/SITE MTBF: 606,060 Sys MTTR: 1.3
 R&R MHRS: 2.6 Repair MHRS: 3.5

Description:

The Heliostat Control Electronics respond to heliostat array controller commands and calculate positioning commands for heliostat movement. The microprocessor based circuitry is contained on a circuit card installed in an electronic J-box located on the azimuth drive assembly housing. The J-box cover is easily removable for access to the circuit card which is a 4" by 5" two-layer board with conformal coating for moisture protection.

Maintenance Concept:

The circuit card is removed and replaced upon component failure. Fault detection and isolation is accomplished by operational indications, heliostat array software routines, and the mobile test van. Bench repair is accomplished by replacement of defective components.

Support Equipment:

Replacement does not require any special tools or equipment other than the mobile test van. Bench repair requires a circuit card test station and an electronic bench repair and inspection station.

Facilities:

No special facilities required. Bench area floor space of approximately 200 ft² should be adequate.

LOGISTICS SUPPORT ANALYSIS WORKSHEETS

Item Name: HELIOSTAT POWER/DATA CABLES System: PROTOTYPE HELIOSTAT
 Weight: - Repair Decision: ON-LINE
 Prelim Cost Est: - Method: TASK ANALYSIS
 Qty: 5/HELIOSTAT MTBF: 9,090,909 Sys MTRR: 1.8
 R&R MHRS: - Repair MHRS: 3.6

Description:

The Power/Data Cables carry the three-phase power and data for control of the heliostat drive motors and include the cables from the pedestal J-box through the hollow harmonic drive shaft to the heliostat electronics J-box and from the electronics J-box to the three drive motors. Data transmission between the J-boxes is by fiber optics. All other cables are electrical.

Maintenance Concept:

The Heliostat Cables are repaired in-place by standard electrical and optical fiber repair methods and replacement terminals and ion connectors. Procurement of spare cable assemblies is not planned. In the event repair is not economical due to major damage, a complete cable assembly can be fabricated from bulk wire/optical fiber and spare cable terminations.

Support Equipment:

No special support equipment required. Repair accomplished by standard electrical and optical fiber repair tools and test equipment.

Facilities:

None required.

LOGISTICS SUPPORT ANALYSIS WORKSHEETS

Item Name: DATA DISTRIBUTION INTERFACE (DDI) System: PROTOTYPE HELIOSTAT
 Weight: 1 LB Repair Decision: DISCARD
 Prelim Cost Est: \$125.00 Method: ORLA MODEL
 Qty: 57/SITE MTBF: 206,186 Sys MTTR: 1.6
 R&R MHRS: 3.2 Repair MHRS: (3.5)

Description:

The DDI Electronics provides the communications data interface between the heliostat array controller and the heliostat controller. Two identical microprocessor based logic networks (two 4" by 5" two-layer circuit boards) are installed in a J-box, located at the power transformer/power distribution panel sites, to provide communications redundancy in the event one channel fails.

Maintenance Concept:

The DDI circuit cards are replaced upon component failure. Fault detection and isolation is accomplished by operational indications, heliostat array software routines, and the mobile test van. Bench repair is accomplished by replacement of defective components.

Support Equipment:

Replacement does not require any special tools or equipment other than the mobile test van. Bench repair requires a circuit card test station and an electronic bench repair and inspection station.

Facilities:

No special facilities required. Bench area floor space of approximately 200 ft² should be adequate.

Item Name: POWER TRANSFORMER System: PROTOTYPE HELIOSTAT
 Weight: 2,600 LBS Repair Decision: OFF-SITE
 Prelim Cost Est: \$6,150.00 Method: TASK ANALYSIS
 Qty: 57/SITE MTBF: 500,000 Sys MTTR: 2.4
 R&R MHRS: 8.3 Repair MHRS: *

Description:

Power for heliostat operation is distributed through a system of 57 transformers rated at 225 KVA with 4160 volt primary and 480/277 volt secondary windings. Each transformer supplies power to 12 to 16 groups of heliostats by branch circuits which feed approximately 24 heliostats each.

Maintenance Concept:

The Power Transformer is removed and replaced for internal electrical failure. Units removed for failure are surveyed for extent of damage and dispositioned for salvage and/or rebuilt at the manufacturer's facility or specialized repair area.

Support Equipment:

Removal and replacement of the transformer requires use of a forklift or mobile crane and universal hoisting slings.

Facilities:

Manufacturer's facility.

*Scrap/salvage if labor and materials exceed 65 percent of unit cost.

LOGISTICS SUPPORT ANALYSIS WORKSHEETS

Item Name: POWER DISTRIBUTION PANEL System: PROTOTYPE HELIOSTAT
 Weight: - Repair Decision: ON-LINE
 Prelim Cost Est: - Method: TASK ANALYSIS
 Qty: 57/SITE MTBF: 66,667 Sys MTR: 1.6
 R&R MHRS: - Repair MHRS: 3.2

Description:

The Power Distribution Panel is a 480 volt three-phase load center containing a 100 amp main circuit breaker and 12 to 16 branch circuit breakers of 40 amps each.

Maintenance Concept:

The Power Distribution Panels are repaired in-place by replacement of circuit breakers.

Support Equipment:

No special support equipment required. Repair is accomplished using common tools and test equipment.

Facilities:

None required.

LOGISTICS SUPPORT ANALYSIS WORKSHEETS

Item Name: FIELD POWER/DATA CABLES System: PROTOTYPE HELIOSTAT
 Weight: - Repair Decision: ON-LINE
 Prelim Cost Est: - Method: TASK ANALYSIS
 Qty: 18,063/SITE MTBF: 4,545,454 Sys MTTR: 3.5
 R&R MHRS: - Repair MHRS: 7.0

Description:

The Field Power/Data Distribution Network includes the primary cable runs from the power house to the power transformers and data distribution interfaces and secondary runs from these points to the heliostats. The primary cables contain three conductor copper cables and two circuit fiber optic cables within the same jacket. The secondary cables contain the power conductors and a single fiber optic circuit. The cables are direct buried.

Maintenance Concept:

The Field Power/Data Cables are repaired in-place by standard electrical and optical fiber repair methods and replacement of terminals and/or connectors. Procurement of spare cable assemblies is not planned. In the event repair is not economical due to major damage, a complete cable assembly can be fabricated from bulk cable and spare cable terminations.

Support Equipment:

No special support equipment required. Repair accomplished by standard electrical and optical fiber repair tools and test equipment.

Facilities:

None required.

LOGISTICS SUPPORT ANALYSIS WORKSHEETS

Item Name: PEDESTAL System: PROTOTYPE HELIOSTAT
 Weight: - Repair Decision: ON-LINE
 Prelim Cost Est: - Method: TASK ANALYSIS
 Qty: 18,000/SITE MTBF: 9,090,909 Sys MTTR: 1.0
 R&R MHRS: - Repair MHRS: 2.0

Description:

The Pedestal is fabricated of 24 inch diameter spiral welded steel pipe with a wall thickness of 0.1046 inch and is 125 inches long. The lower 48 inches of length is expanded to produce a slight taper (0.14 inch diameter per foot) to obtain a slip-joint attachment with the foundation on installation. The pedestal is hot-dip galvanized after fabrication.

Maintenance Concept:

Repair in-place utilizing standard structural repair processes.

Support Equipment:

No special support equipment required.

Facilities:

None required.

LOGISTICS SUPPORT ANALYSIS WORKSHEETS

Item Name: REFLECTOR STRUCTURE System: PROTOTYPE HELIOSTAT
 Weight: 1,300 LBS Repair Decision: ON-LINE
 Prelim Cost Est: - Method: TASK ANALYSIS
 Qty: 18,000/SITE MTBF: 8,333,333 Sys MTRR: 1.5
 R&R MHRS: - Repair MHRS: 3.0

Description:

The Reflector Support structure is fabricated from galvanized steel sheet in two sections which bolt to a tubular center beam attached to the drive unit assembly. The structure supports each reflector mirror by a pair of hat-section stringers which are bonded to the glass when the reflector is assembled. Six reflector mirrors are installed in each support structure section or a total of twelve per heliostat.

Maintenance Concept:

The Reflector Structure is repaired in-place utilizing standard structural repair processes.

Support Equipment:

No special support equipment required.

Facilities:

None required.

LOGISTICS SUPPORT ANALYSIS WORKSHEETS

Item Name: MIRROR MODULE System: PROTOTYPE HELIOSTAT
 Weight: 147 LBS Repair Decision: DISCARD
 Prelim Cost Est: - Method: TASK ANALYSIS
 Qty: 216,000/SITE MTBF: 10,000,000 Sys MTTR: 2.0
 R&R MHRS: 5.0 Repair MHRS: -

Description:

Each mirror module measures 48 by 132 inches and is made up of laminated glass. The front sheet is a .060 inch thick pane of fusion glass which is mirrored on its inner surface. The back sheet is 3/16 inch float glass bonded to the front glass with polyurethane adhesive.

Maintenance Concept:

The Reflector Panels are removed, replaced and discarded upon failure. Minor cracks may be repaired in place by adhesive bonding of a mirror patch on the front of the mirror module.

Support Equipment:

Removal and replacement requires a mobile crane and a mirror handling and hoisting sling.

Facilities:

None required.

LOGISTICS SUPPORT ANALYSIS WORKSHEETS

Item Name: HELIOSTAT ARRAY CONTROLLER System: PROTOTYPE HELIOSTAT
 Weight: - Repair Decision: SERVICE CONTRACT
 Prelim Cost Est: - Method: TASK ANALYSIS
 Qty: 1 MTBF: TBD Sys MTTR: TBD
 R&R MHS: _____ Repair MHS: _____

Description:

The HelioStat Array Controller (HAC) is located in the MCS building and provides the interface between MCS and the collector field. The HAC and backup will consist of two off-the-shelf commercially available mini-computers with support peripheral and interfacing equipment. The hardware includes the operation console consisting of a keyboard, cathode ray tube, and control panel; a control processing unit; a storage unit; field interface; MCS interface, and a time pickup unit.

Maintenance Concept:

It is expected that the HAC will have interchangeability with MCS central processing units and other components, and will be maintained as a subsystem/group. At this time, the baseline maintenance concept is assumed to be via a commercial service contract.

Support Equipment:

Furnished by service contraction.

Facilities:

No special maintenance facilities required.

* U.S. GOVERNMENT PRINTING OFFICE: 1979 .640 .092/ 610

G-17